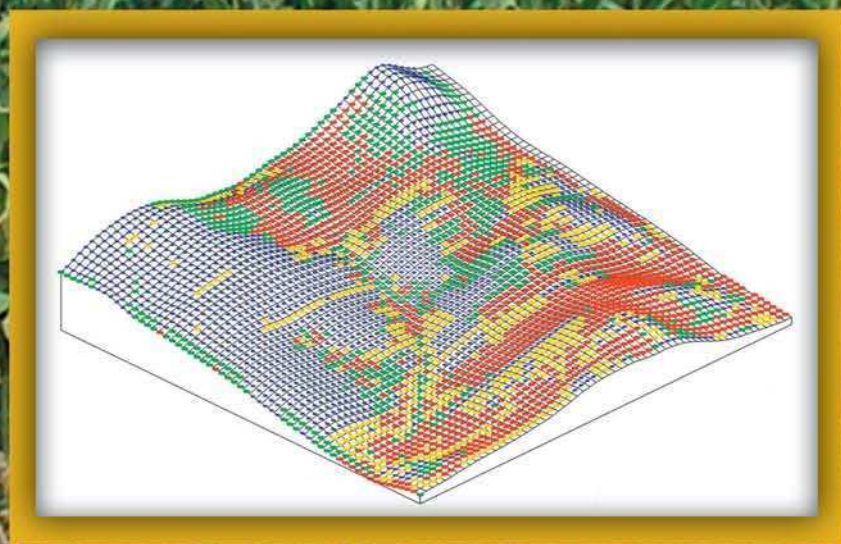


GIS Applications in Agriculture

Edited by
Francis J. Pierce
David Clay



GIS APPLICATIONS IN AGRICULTURE SERIES

GIS Applications in Agriculture

GIS Applications in Agriculture

Edited by
Francis J. Pierce
David Clay

GIS APPLICATIONS IN AGRICULTURE SERIES



CRC Press
Taylor & Francis Group
Boca Raton London New York

CRC Press is an imprint of the
Taylor & Francis Group, an informa business

CRC Press
Taylor & Francis Group
6000 Broken Sound Parkway NW, Suite 300
Boca Raton, FL 33487-2742

© 2007 by Taylor & Francis Group, LLC
CRC Press is an imprint of Taylor & Francis Group, an Informa business

No claim to original U.S. Government works
Printed in the United States of America on acid-free paper
10 9 8 7 6 5 4 3 2 1

International Standard Book Number-10: 0-8493-7526-6 (Hardcover)
International Standard Book Number-13: 978-0-8493-7526-2 (Hardcover)

This book contains information obtained from authentic and highly regarded sources. Reprint material is quoted with permission, and sources are indicated. A wide variety of references are listed. Reasonable efforts have been made to publish reliable data and information, but the author and the publisher cannot assume responsibility for the validity of all materials or for the consequences of their use.

No part of this book may be reprinted, reproduced, transmitted, or utilized in any form by an electronic, mechanical, or other means, now known or hereafter invented, including photocopying, microfilming, and recording, or in any information storage or retrieval system, without written permission from the publishers.

For permission to photocopy or use material electronically from this work, please access www.copyright.com (<http://www.copyright.com/>) or contact the Copyright Clearance Center, Inc. (CCC) 222 Rosewood Drive, Danvers, MA 01923, 978-750-8400. CCC is a not-for-profit organization that provides licenses and registration for a variety of users. For organizations that have been granted a photocopy license by the CCC, a separate system of payment has been arranged.

Trademark Notice: Product or corporate names may be trademarks or registered trademarks, and are used only for identification and explanation without intent to infringe.

Library of Congress Cataloging-in-Publication Data

Pierce, F. J. (Francis J.)
GIS applications in agriculture / Francis J. Pierce and David Clay.
p. cm. -- (GIS applications for agriculture)
Includes bibliographical references and index.
ISBN-13: 978-0-8493-7526-2 (alk. paper)
ISBN-10: 0-8493-7526-6 (alk. paper)
1. Geographic information systems. 2. Agricultural mapping. 3.
Agriculture--Data processing. 4. Agriculture--Remote sensing. I. Clay, David
(David E.) II. Title. III. Series.

G70.212.P54 2007
630.2085--dc22

2006025884

Visit the Taylor & Francis Web site at
<http://www.taylorandfrancis.com>
and the CRC Press Web site at
<http://www.crcpress.com>

Preface

Agriculture is a business sector ideally suited for the application of Geographic Information Systems (GIS) because it is natural resource based, requires the movement, distribution, and/or utilization of large quantities of products, goods, and services, and is increasingly required to record details of its business operations from the field to the marketplace. Nearly all agricultural data has some form of spatial component, and a GIS allows you to visualize information that might otherwise be difficult to interpret. The value of GIS to agriculture continually increases as advances in technology accelerate the need and opportunities for the acquisition, management, and analysis of spatial data on the farm and throughout the agriculture value chain.

As a technology, GIS has greatly advanced from its initial use in the 1960s by cartographers who wanted to adopt computer techniques in map-making to the versatile toolkit it is today. The GIS toolkit available today has evolved largely by innovations created in one application of GIS being shared and built upon in subsequent applications. Thus, GIS users, by sharing their innovations and applications formally and informally, were very important to the development of the GIS tools available today. Sharing applications and innovations among users remains an important aspect of GIS both within and across disciplines and business sectors.

Those who use GIS in agriculture recognize that the potential application of GIS in agriculture is large. However, the GIS user community in production agriculture is rather small compared to other business sectors. There is a lack of formal opportunities to share applications and innovations of GIS specifically focused on agriculture. To support and advance the use of GIS in agriculture, our intent was to develop a book series to provide a venue for users to share their applications and innovations of GIS in agriculture. The book series is titled *GIS Applications for Agriculture* and will be published and distributed by CRC Press. Books in this series will be published periodically as need and resources allow. The primary audience for this book series is current users of GIS in an agricultural context including researchers, educators, government agencies, private firms, consultants, and growers. The intent is for the infusion of these agricultural applications into standard GIS publications and formal and informal education programs within and external to agriculture.

This book is the first in a proposed series of books focusing on relevant applications of GIS for agriculture that will address a range of topics and audiences. It includes 10 chapters with an accompanying CD that provide examples of GIS applications primarily associated with precision agriculture, with one (Chapter 1) dealing with a regional water quality problem. Most chapters provide data and software programs that enable readers to recreate the specific application as part of a formal or informal learning experience in GIS. Ideas for future volumes in the

GIS Applications for Agriculture series are welcome. Proposals for new volumes can be submitted either to Dr. Pierce or directly to CRC Press.

As editors, we would like to thank those who contributed to the idea of this book series, particularly Max Crandall, and for those who helped organize this first volume, Pierre Robert, Harold Reetz, Jr., and Matthew Yen. We thank all reviewers, particularly Cheryl Reese and Pedro Andrade-Sanchez, whose assistance was invaluable. We thank John Sulzycki of CRC Press for his efforts in gaining approval for this book series.

The Editors

Francis J. Pierce, Ph.D., has served since 2000 as director of the Center for Precision Agricultural Systems (CPAS) at Washington State University (WSU) located at the Irrigated Agriculture Research and Extension Center in Prosser, Washington. He holds a joint appointment as professor in the Departments of Crop and Soil Sciences and Biological Systems Engineering at WSU. Before that he was professor of soil science in the Department of Crop and Soil Sciences at Michigan State University, East Lansing, Michigan, from 1984 to 2000. He has M.S. and Ph.D. degrees in soil science from the University of Minnesota and a B.S. in geology from the State University of New York at Brockport. His major fields of interest have included soil management particularly as it relates to conservation tillage and soil and water quality and has been extensively involved in many aspects of precision agriculture since 1991. His current research at CPAS is focused on the development of wireless sensor networks and remote, real-time monitoring and control systems for production agriculture as well as the assessment and management of spatial variability in agricultural systems. Books he co-edited include *Soil Management for Sustainability* published by the Soil and Water Conservation Society; *Advances in Soil and Water Conservation* published by Sleeping Bear Press, Inc.; and *The State of Site-Specific Management* published by the American Society of Agronomy. He also co-authored the CRC Press book *Contemporary Statistical Models for the Plant and Soil Sciences* with Oliver Schabenberger. Dr. Pierce is a recipient of the USDA Distinguished Service Award, is founding member of the North Central Regional Research Committee on Site-Specific Management, and has served on a number of national committees and review panels. He is a member of the American Society of Agronomy, Soil Science Society of America, the Soil and Water Conservation Society, and the American Society of Agricultural and Biological Engineers.

David E. Clay, Ph.D., is a professor of soil science at South Dakota State University where he has teaching and research responsibilities. He received his B.S. degree from the University of Wisconsin in 1976, a M.S. degree in soil fertility from the University of Idaho in 1984, and a Ph.D. in soil biochemistry from the University of Minnesota in 1988. Dr. Clay has published over 100 scientific articles and has served on the editorial boards for the *Agronomy Journal* and the *Site-Specific Management Guidelines*. Dr. Clay is an active member of the honorary societies Sigma Xi and Gamma Sigma Delta, and he has served as chairman of the Agricultural Systems division in the American Society of Agronomy.

Contributors

Viacheslav I. Adamchuk

Biological System Engineering
Department
University of Nebraska
Lincoln, Nebraska

James Alfonso

U.S. Fish & Wildlife Service
Devils Lake, North Dakota

Pedro Andrade-Sanchez

Center for Precision Agricultural
Systems
Washington State University
Prosser, Washington

R. Bobbitt

GeoSpatial Experts
Thornton, Colorado

C. Gregg Carlson

South Dakota State University
Brookings, South Dakota

Florence Cassel S.

Center for Irrigation Technology
California State University Fresno
Fresno, California

Jiyul Chang

Geographic Information Science Center
of Excellence
South Dakota State University
Brookings, South Dakota

David E. Clay

Plant Science Department
South Dakota State University
Brookings, South Dakota

Sharon A. Clay

Plant Science Department
South Dakota State University
Brookings, South Dakota

David W. Franzen

North Dakota State University
Fargo, North Dakota

N. Kitchen

USDA-ARS
University of Missouri
Columbia, Missouri

Jonathan Kleinjan

Plant Science Department
South Dakota State University
Brookings, South Dakota

T.G. Mueller

Department of Plant and Soil Sciences
University of Kentucky
Lexington, Kentucky

T.S. Murrell

Potash & Phosphate Institute (PPI)
Woodbury, Minnesota

H.F. Reetz, Jr.

Foundation for Agronomic Research
Monticello, Illinois

Q.B. Rund

PAQ Interactive, Inc.
Monticello, Illinois

Bruce Seelig

Western Plains Consulting
Bismarck, North Dakota

Shrinivasa K. Upadhyaya

Department of Biological and
Agricultural Engineering
University of California Davis
Davis, California

Chenguang Wang

Statistics Department
University of Florida
Gainesville, Florida

Philip Westra

Department of Bioagricultural Sciences
and Pest Management
Colorado State University
Fort Collins, Colorado

Lori J. Wiles

USDA-ARS, Water Management
Research Unit
Fort Collins, Colorado

Contents

Chapter 1

Application of GIS to Integrated Pest Management on U.S. Fish and
Wildlife Service Land..... 1
Bruce Seelig and James Alfonso

Chapter 2

Nitrogen Management in Sugar Beet Using Remote Sensing and GIS..... 35
David W. Franzen

Chapter 3

Using Historical Management to Reduce Soil Sampling Errors..... 49
David E. Clay, N. Kitchen, C. Gregg Carlson, Jonathan Kleinjan, and Jiyul Chang

Chapter 4

Developing Productivity Zones from Multiple Years of Yield Monitor Data..... 65
Jonathan Kleinjan, David E. Clay, C. Gregg Carlson, and Sharon A. Clay

Chapter 5

Site-Specific Weed Management in Growers' Fields: Predictions from
Hand-Drawn Maps..... 81
Lori J. Wiles, R. Bobbitt, and Philip Westra

Chapter 6

Map Quality Assessment for Site-Specific Fertility Management..... 103
T.G. Mueller

Chapter 7

Gleaning More Information from Yield Data 121
T.S. Murrell, Q.B. Rund and H.F. Reetz, Jr.

Chapter 8

Soil Salinity Mapping Using ArcGIS 141
Florence Cassel S.

Chapter 9

Using GIS and On-the-Go Soil Strength Sensing Technology for
Variable-Depth Tillage Assessment..... 163
Pedro Andrade-Sanchez and Shrinivasa K. Upadhyaya

Chapter 10

Collocating Multiple Self-Generated Data Layers 185
Viacheslav I. Adamchuk and Chenguang Wang

Index 197

1 Application of GIS to Integrated Pest Management on U.S. Fish and Wildlife Service Land

Bruce Seelig and James Alfonso

CONTENTS

1.1 Executive Summary.....	1
1.2 Introduction	2
1.3 Methods	4
1.4 Results	11
1.4.1 Soils Data.....	12
1.4.2 Land-use Data.....	19
1.4.3 Proximity Data.....	20
1.4.4 Pesticide Application/Properties.....	22
1.4.5 Summation of Delivery Potential Factors.....	22
1.5 Conclusions	28
References.....	32

1.1 EXECUTIVE SUMMARY

The U.S. Fish & Wildlife Service (USFWS) has observed a steady reduction in the quality of wildlife habitat due to invasive and noxious weeds in North Dakota. They have taken the first steps in instituting an integrated pest management (IPM) strategy to restore habitat that has been damaged by invasive species. While herbicide application is part of their IPM strategy, the USFWS recognizes that the positive environmental impacts from improved habitat could be outweighed by the negative impacts of pesticide contamination to water resources. Therefore, they also include a systematic assessment of potential pesticide contamination of water resources in their IPM strategy.

A geographic information system (GIS) was used to develop an assessment of potential contamination of water resources on land managed for waterfowl production in the Devils Lake area of North Dakota. The results of the water resource assessments are intended as the first level of information for a pesticide management

decision tree. Pesticide management in areas with high potential to deliver pesticides to water resources will be managed differently than areas of low potential. The application of the assessment methodology to the IPM strategy was first tested in Ramsey County, North Dakota. Earlier methodologies used to assess for potential delivery of pesticides to water resources in North Dakota were adapted to the Ramsey County study. Critical factors that contribute to pesticide fate and translocation in the environment were determined through access to databases of countywide extent. GIS was used to import, manipulate, and summarize the data so that potential pesticide contamination to water resources could be displayed for all areas in Ramsey County. These results were then available for geographic comparison with wildlife habitat areas and incorporation into USFWS IPM strategy. The scope of this paper is limited to the surface water analysis.

Six factors were used to determine the potential delivery of pesticides to surface water resources as follows: soil erodibility, frequency of flooding, runoff potential, land use, proximity to major streams and/or lakes, and pesticide application/properties. These factors were selected based on their observed effects on contaminant transport. Accessibility of data to measure the value of each factor was also a consideration.

The first step in a county analysis for potential pesticide delivery to surface water is acquiring the appropriate tools and databases. Image Analyst, Spatial Analyst, and Soil Data Viewer extensions to ArcView 3.2 (ESRI, Redlands, California) are required. In addition, other tools that allow the user to clip grids, modify grids, and change coordinate systems are also needed. The databases required for this analysis are the Natural Resources Conservation Service Soil Survey Geographic (NRCS SSURGO), North Dakota Department of Transportation Geographic Information Systems (NDDOT GIS), and North Dakota office of the Agricultural Statistics Service (NDASS) Land-use Image. Once users acquire the GIS tools listed above, they may import the soils, geography, and land use for Ramsey County, and begin the analysis.

The results of the analysis provide a view of potential pesticide delivery to surface water resources over a relatively large area. Ramsey County has an area of approximately 1,311 square miles, or 839,040 acres. Data that help evaluate factors of demonstrated importance with respect to pesticide transport and fate were successfully acquired. The results show that these factors could be systematically integrated to provide comparative information important to resource planning decisions. The strength of the analysis lies in the extent and resolution of the databases used. Information regarding potential pesticide delivery can be compared over an area of approximately 1 million acres or between fields as small as 5 acres.

1.2 INTRODUCTION

The Devils Lake Wetland Management Complex is part of the U.S. Fish & Wildlife Service (USFWS) system in the heart of the Prairie Pothole Region. It is an eight-county area in northeastern North Dakota with cultivated agriculture as the dominant land use. Although a wide range of crops are grown, small grains are dominant. Prior to cultivation the native plant community was prairie grassland. The wetlands

of this management complex are used in spring and summer for nesting and feeding by local waterfowl, and hundreds of thousands of migrating waterfowl use these wetlands during spring and fall. The USFWS manages over 200,000 acres of land throughout the eight-county area as waterfowl production areas (WPA), national wildlife refuges, easement refuges, game preserves, and wetland easements.

Influx of nonindigenous plant species (weeds) is one of the most important wildlife management issues, second only to habitat loss. These species contribute to decreased biological diversity of ecosystems with negative impacts to water, energy, nutrient cycles, productivity, and biomass.¹ In grassland systems weeds now account for 13–30% of the plant community. The USFWS recognizes that the quality of wildlife habitat has been reduced by the presence of invasive and noxious weeds on land in the Devils Lake Wetland Complex. They have taken the first steps in instituting an integrated pest management (IPM) strategy to restore habitat that has been damaged by invasive species.

Herbicide application is one of the tools that will be used within the IPM strategy adopted for the Devils Lake Wetland Management Complex. The USFWS recognizes that the positive environmental impacts from improved habitat could be outweighed by the negative impacts of pesticide contamination to water resources. Included in its IPM strategy is a systematic assessment of potential pesticide contamination of water resources in the complex. The results of the assessment will be used within the context of a decision tree, to determine the management alternatives or if further study is required.

Ramsey County was the first in the Devils Lake Wetland Management Complex to test the application of the assessment methodology to the IPM strategy. The methodology used to assess aquifer sensitivity to pesticides² and potential delivery of pesticides to surface water³ was modified for the Ramsey County assessment. Values for critical factors that contribute to pesticide fate and translocation in the environment were determined through access to databases of countywide extent. GIS was used to import, manipulate, and summarize the data so that potential pesticide contamination to water resources could be displayed for all areas in Ramsey County. These results were then available for geographic comparison with wildlife habitat areas and incorporation into USFWS IPM strategy. Methods and results will only be presented for the surface water analysis.

Pesticides are entrained in runoff water in two forms, soluble species and adsorbed species.^{4–7} As runoff water moves over the surface soil it interacts with the surface both physically and chemically. The depth of interaction influences the amount of pesticide that moves off-site, and varies under different circumstances.⁸ Despite the variability, a 4-inch depth of interaction is often used to estimate edge-of-field losses of contaminants.^{7,9} These losses include pesticides dissolved in the runoff water and pesticides adsorbed to suspended sediment transported by the runoff.

The availability of pesticides to translocation by runoff is strongly influenced by the characteristics of application, formulation, and chemistry.^{4,6,7,10–12} Increased knowledge of these factors has improved the accuracy of predicting edge-of-field losses of pesticides. However, many investigations show that substantial reductions in pesticide concentrations occur between the edge-of-field and streams and lakes.^{10,13–15}

Wauchope's¹⁰ work defined a general pattern of pesticide loss from cropland. He concluded that on average 1% of the total foliar-applied organochlorine insecticides was lost to surface runoff. However, this family of insecticides is no longer used. He also estimated for pesticides with wettable powder formulations, such as the triazine herbicides, annual runoff losses would be about 2% of the total applied on land with less than 10% slope, and about 5% of the total applied on land with greater than 10% slope. Non-organochlorine insecticides, incorporated pesticides, and all other herbicides were estimated to have losses of about 0.5% of the total applied.

1.3 METHODS

Predicting where and when pesticide use may cause damaging concentrations in surface water environments depends on knowledge of local conditions and processes that rule pesticide fate. Research and study have helped to demonstrate the complexity of pesticide contamination, but have also identified certain critical elements that are regularly found to influence surface water contamination. Systematic assessment of these elements cannot predict the exact nature of contamination at any given place for any given time without a large risk of error. However, systematic assessment can estimate ordered results that may be used to prioritize management decisions that attempt to address surface water protection.

Six factors were used to determine the potential delivery of pesticides to surface water resources as follows: soil erodibility, frequency of flooding, runoff potential, land use, proximity to major streams and/or lakes, and pesticide application/properties. These factors were selected based on their observed effects on contaminant transport. Accessibility of data to measure the value of each factor was also a consideration. The criteria used to rate each of these factors are discussed in detail below.

Soil erodibility is an important indicator of the potential for transport of pesticides with sediment. In general, erosion control has been demonstrated to reduce the total load of agricultural chemicals that leave cropped fields.¹⁶⁻¹⁸ The large majority of residual pesticides are adsorbed to soil materials, particularly organic matter. When these soil materials are detached and translocated due to the erosion process, pesticides are also translocated. Although the adsorbed form of a pesticide is not as mobile or active as the soluble form, it is a source of slow-release to the environment. Soils with characteristics that allow greater erodibility have greater potential to allow translocation of adsorbed pesticides. The soil k factor is an indicator of surface erodibility, and ranges from low (0.02–0.2) to intermediate (0.2–0.4) to high (0.4–0.69). In Ramsey County, soil erodibility ranged from low to intermediate. The k factor for the dominant condition for each soil mapping unit was extracted from the NRCS SSURGO database for Ramsey County.¹⁹ Values of 3, 2, and 1 were assigned to the “high,” “intermediate,” and “low” potential categories, respectively.

Flooding affects the translocation of pesticides to water resources. SCS staff²⁰ and Hornsby²¹ adjusted upward potential pesticide losses in surface runoff from soils that have greater occurrences of flooding. Flooding may remove large quantities of

pesticides in solution or adsorbed to sediments in a single event.²⁰ Soils are rated according to their frequency of flooding. Soils that are frequently flooded have a high potential for pesticide transport compared to those that never flood. The frequency of soil flooding was extracted from the NRCS SSURGO database for Ramsey County.¹⁹ Flooding was determined for the dominant soil in each mapping unit. Values of 3, 2, and 1 were assigned to “common,” “occasional,” and “rare to never” flooding categories, respectively.

Runoff is an important soil factor to the translocation of pesticides both as soluble and sediment phases. It is largely influenced by the soil permeability and slope. When water reaches the soil surface as a liquid it must evaporate, infiltrate, or run off.²² Horton²³ defined infiltration as the entry of water through the soil surface. The rate at which water can enter the soil is influenced by many factors such as surface cover, vegetation canopy, surface crusting, rainfall energy, slope, and surface texture. The maximum infiltration capacity generally occurs at the beginning of a storm, and decreases rapidly due to changes in the surface caused by water movement. When the rate of precipitation exceeds the infiltration rate, water accumulates as surface storage, and when the capacity of the surface storage is exceeded, runoff occurs.²² A positive correlation exists between the slope of land surface (vertical distance/horizontal distance) and the amount of runoff and eroded sediment.^{16,24,25} Hornsby,²¹ Goss and Wauchope,²⁶ and Goss²⁷ recognized the need to adjust potential losses of pesticides upward for soils on steeper slopes.

The runoff class for a soil is determined by the layer of minimum saturated hydraulic conductivity (K_{sat}) within the upper meter (Table 1.1). If the lowest K_{sat} occurs in the layer above 0.5 m, this value is used to estimate runoff. However, if the lowest K_{sat} is in the 0.5–1.0 m layer, the runoff estimate is reduced by one class. Runoff class ranges from “negligible,” where permeability is high and slope is low, to “very high,” where permeability is very low to impermeable and slope is high (Table 1.2).²⁸ Soil permeability for the dominant soil and slope for the dominant condition of each soil mapping unit were extracted from the NRCS SSURGO database for Ramsey County.¹⁹ The runoff class was determined for the dominant soil in each mapping unit. Values of 5, 3, 2, and 1 were assigned to the “very high” and “high,” “medium” and “low,” “very low” and “negligible” runoff categories, respectively. Further classification grouped classes “negligible,” “very low,” and

TABLE 1.1
NRCS K_{sat} categories and ranges of values

NRCS K_{sat} Category	K_{sat} (μ /sec)
Impermeable	0–0.01
Very slow	0.01–0.42
Slow	0.42–1.4
Moderately slow	1.4–4
Moderate	4–14
Moderately rapid	14–42
Rapid	42–141
Very rapid	141–705

TABLE 1.2
NRCS surface runoff classes index

Slope (%)	Permeability Class					
	Rapid & Very Rapid	Moderately Rapid	Moderate	Moderately Slow	Slow	Very Slow & Impermeable
Concave	Negligible	Negligible	Negligible	Negligible	Negligible	Negligible
< 1	Negligible	Negligible	Negligible	Low	Medium	High
1–5	Negligible	Very low	Low	Medium	High	Very high
5–10	Very low	Low	Medium	High	Very high	Very high
10–20	Very low	Low	Medium	High	Very high	Very high
≥ 20	Low	Medium	High	Very high	Very high	Very high

Source: Soil Survey Staff, National soil survey handbook, Title 430-VI., NRCS, USDA, U.S. Gov. Printing Office, Washington, D.C., 1998.

“low” into a single “low” potential delivery class and classes “very high” and “high” into a single “high” potential delivery class. The resulting three classes—low, medium and high—are used in our analysis.

Land use affects pesticide translocation. Human manipulation of surface cover has significant impacts on water infiltration, runoff, and erosion. In general, surface cover with healthy plant growth improves water infiltration, reduces runoff, and protects the soil surface from erosion losses. Tillage that leaves the soil surface unprotected during erosive periods causes profound increases in runoff and erosion losses from fields.^{25,29,30} Compared to conventional tillage systems, sediment losses are much smaller for reduced tillage or no tillage.^{17,31} Tillage is indirectly related to surface water quality due to its impact on the delivery of runoff and eroded sediment to streams and lakes.³²

In the northern Great Plains, the practice of summer fallowing has been a regular component of many cropping rotations.³³ Fallowing ensures that a portion of the farm will yield a crop because of the soil NO_3 and water that is carried over from the fallow (unplanted) year to spring planting of the following year. Although this practice lowers the risk of a complete crop failure, it also has serious negative effects on surface water resources due to increased sediment translocation via water movement. Summer fallow maintained through the application of regular tillage leaves the soil surface with little protection during the erosive periods of the year, and contributes to excessive runoff of water and sediments. When developing the universal soil loss equation, Wischmeier and Smith²⁵ used erosion losses from clean-tilled continuous fallow as the baseline to compare all other forms of management and cover. With respect to soil erosion, it is the worst-case scenario.

Wischmeier and Smith²⁵ showed that erosion from cultivated soils is dependent on many factors. The type of crop and management of its residue play an important role in controlling erosion. Wischmeier's³⁴ work with the universal soil loss equation demonstrated that bare tilled fields and permanent vegetation were on opposite ends of the spectrum with respect to erosion. Because the type of crop grown influences

the factors that control runoff and erosion, cropping patterns and land use are linked to water quality.^{24,25} Various land-use practices allow a range of water quality impacts due to different characteristics of vegetative growth.

Land use was placed into five broad categories based on surface cover. Urban use and summer fallow have high potential to contribute to pesticide losses due to lack of adequate surface cover. Row crops consisting of corn (*Zea mays* L.), sunflowers (*Helianthus pumilus*), soybeans (*Glycine max* L. Merr.), dry beans (*Phaseolus vulgaris*), and potatoes (*Solanum tuberosum*) have a somewhat high potential. Small-grain crops such as wheat (*Triticum aestivum* L.), barley (*Hordeum vulgare*), and other types of crops that form a dense canopy quickly have an intermediate potential. Pasture, rangeland, and hay crops that have continual surface cover are rated as somewhat low potential. Forest or wooded areas have the least disturbed surface cover and have low potential.

The 2001 NDASS land-use database³⁵ was used to identify and delineate the five categories of surface cover. Values of 5, 4, 3, 2, and 1 were assigned to the “high,” “somewhat high,” “intermediate,” “somewhat low,” and “low” surface cover categories, respectively.

Proximity of specific areas to streams and lakes influences the potential for delivery of contaminants from these locations. Runoff is not the same from all areas of a watershed, and usually large areas yield no runoff or sediment.³⁶ During runoff-producing events, areas contributing water to the channel expand outward from the stream with increasing duration of the event.³⁷ This hydrologic phenomenon is responsible for the most regular runoff production being from areas close to stream channels; this is particularly true in drier climates. Stewart et al.¹⁶ recognized proximity of cropped fields to surface water resources as a critical factor in determining acceptable levels of soil loss from fields. As the density of the network of surface drains increases so does the amount of sediment delivered to streams.³⁶

Concentrations of pesticides in receiving streams have been shown in many studies to be orders of magnitude smaller than pesticide concentrations in runoff leaving field edges.^{4,7,14,15,38} During transport, pesticide concentrations are rapidly attenuated by mechanisms of dilution, deposition and trapping of sediments, adsorption to channel materials, and pesticide degradation.⁷ After leaving the field edge, the distance that runoff water must travel before reaching a stream or lake has a significant impact on the total loading to streams or lakes.¹² In most studies herbicide residues fall below detectable limits in waters a few hundred yards below sprayed areas.^{4,12} Rhode et al.¹³ found that nearly 90% of the trifluralin in runoff leaving a field was removed in a waterway 24 m long. Similar results were reported for 2,4-D.

The longer the time and distance of transport, the greater the opportunity for pesticide attenuation to occur; therefore, the proximity of a receiving water body to the source of pesticide runoff is a factor that must be determined. Areas within 250 feet of a water resource have a high potential for contaminant delivery. Areas 250–500 feet from a water resource have intermediate potential for contaminant delivery. Areas >500 feet from a water resource have low potential for contaminant delivery.

The location of streams was extracted from the ND DOT GIS database.³⁹ The location of surface water bodies was extracted from the ND DOT GIS, the NRCS

SSURGO, and NDASS land-use databases. Buffers of 250 and 500 feet were delineated around streams and lakes. Values of 3, 2, and 1 were assigned to the “high,” “intermediate,” and “low” proximity categories, respectively. The USFWS plans to apply a similar buffering protocol to wetlands identified in the National Wetlands Inventory, but this was beyond the scope of this project.

Pesticide application/properties affect the mobility and availability of pesticides. This factor is a combination of (1) pesticide formulation and application characteristics, (2) pesticide affinity for soil materials, and (3) pesticide affinity to water.

Pesticide formulation-application has been shown to have significant effects on the translocation of various pesticides (Table 1.3). Wauchope¹⁰ concluded after extensive review of research results that long-term pesticide losses can be grouped into three broad categories based on formulation and application: (1) wettable powders, (2) foliar-applied organochlorine insecticides, and (3) non-organochlorine insecticides, incorporated pesticides, and all other herbicides. He estimated annual edge-of-field losses of 2–5%, 1%, and 0.5%, respectively, of the total pesticide applied within these three categories. He theorized that wettable powder formulations leave a dust coating on the soil surface upon evaporation that is easily entrained in runoff water. Arsenical and cationic pesticides, such as Paraquat, may also be prone to losses via dust entrainment in surface runoff.

Wauchope¹⁰ determined by comparing many study results a trend in pesticide concentrations from edge-of-field runoff related to modes of application and pesticide formulation. Pesticide concentrations in edge-of-field runoff occurred in the following pattern among five pesticide application-formulation categories: incorporated emulsions or granules < insoluble pesticides applied as emulsions to soil surface or crop foliage < soluble pesticides applied as solutions to soil surface < < wettable powders applied to soil surface < soluble pesticides applied to crop foliage.

Pesticide affinity to soil materials is used to determine the potential for pesticide runoff to occur in the sediment phase. Hornsby,²¹ Goss and Wauchope,²⁶ and Goss²⁷ demonstrated that pesticide contamination could be addressed systematically by combining selected pesticide and soil properties. Pesticide solubility, half-life ($T_{1/2}$), and organic carbon adsorption (K_{oc}) are used to determine potential runoff in the sediment phase (Table 1.4). Pesticide affinity to water is also characterized by a combination of $T_{1/2}$, K_{oc} , and solubility (Table 1.5). A composite pesticide mobility

TABLE 1.3
Pesticide mobility rating based on application and formulation

Pesticide Application/Formula	Delivery Potential Category	Delivery Potential Value
All other formulation and application combinations	Low	1
Soluble pesticides (>100,000 mg/l) applied to plant foliage	High	3
Wettable powders applied to soil surface	High	3

TABLE 1.4
Pesticide mobility rating based on affinity to soil materials

Pesticide Properties	Delivery Potential Category	Delivery Potential Value
$T_{1/2} \leq 1$ day or $T_{1/2} \leq 2$ days and $K_{oc} \leq 500$ or $T_{1/2} \leq 4$ days and $K_{oc} \leq 900$ and solubility ≥ 0.5 mg/l or $T_{1/2} \leq 40$ days and $K_{oc} \leq 500$ and solubility ≥ 0.5 mg/l or $T_{1/2} \leq 40$ days and $K_{oc} \leq 900$ and solubility ≥ 2 mg/l	Low	1
Pesticides that do not meet the High or Low criteria	Intermediate	2
$T_{1/2} \geq 40$ days and $K_{oc} \geq 1000$ or $T_{1/2} \geq 40$ days and $K_{oc} \geq 500$ and solubility ≤ 0.5 mg/l	High	3

Source: Goss D.W., Screening procedure for soils and pesticides for potential water quality impacts, Weed Tech., 6, 701, 1992.

TABLE 1.5
Pesticide mobility rating based on affinity to water

Pesticide Properties	Delivery Potential Category	Delivery Potential Value
$K_{oc} \geq 100,000$ or $K_{oc} \geq 1000$ and $T_{1/2} \leq 1$ day or solubility < 0.5 mg/l and $T_{1/2} < 35$ days	Low	1
Pesticides that do not meet the High or Low criteria	Intermediate	2
Solubility ≥ 1 mg/l and $T_{1/2} > 35$ days and $K_{oc} < 100,000$ mg/l or solubility ≥ 10 mg/l but < 100 mg/l and $K_{oc} \leq 700$	High	3

Source: Goss D.W. and Wauchope, R.D., The SCS/ARS/CES pesticide properties database: II Using it with soils data in a screening procedure. In Pesticides in the next decade: the challenges ahead, Weigmann, D.L., Ed., Proc. 3rd National Research Conf. on Pesticides, 8-9 November 1990, Virginia WRRC and Polytechnic Institute and State University, Blacksburg, VA., 1990, 471.

rating is arrived at by summing the values from the three categories discussed above (Table 1.6).

Overall potential for pesticide delivery to surface water was determined by summing the six factors. The values for the summation ranged from 6 to 20. These values were grouped into three potential pesticide delivery categories: (1) high (16-20), (2) intermediate (11-15), and (3) low (6-10).

The GIS program ArcView 3.2 was used to import, manipulate, and summarize the data. Soils information from Ramsey County SSURGO database¹⁹ was extracted as shapefiles using the Soil Dataviewer 3.0 extension⁴⁰ to ArcView 3.2. The SSURGO files were downloaded from the NRCS website <http://www.ncgc.nrcs.usda.gov/products/datasets/ssurgo/>. Clicking on Soil Data Mart will bring up the web page <http://soil-datamart.nrcs.usda.gov/>. At this website, the user will enter the state and county, in consecutive screens, and lastly select Select Survey Area to obtain data files. Follow

TABLE 1.6
Composite pesticide mobility rating for pesticides used by the USFWS in the Devils Lake Management Complex

Pesticide	Composite Delivery Potential Category (Value)	Delivery Potential Value
2,4-D acid	Low (4)	1
2,4-D amine	Intermediate (6)	2
2,4-D ester	Low (4)	1
Arsenal (Imazapyr amine)	High (8)	3
Arsenal (Imazapyr acid)	Intermediate (6)	2
Assure II (quizalofop)	Intermediate (6)	2
Curtail (Clopyralid amine)	Low (4)	1
Curtail (2,4-D amine)	Intermediate (6)	2
Harmony extra XP (Thifensulfuron methyl)	Low (4)	2
Harmony extra XP (Tribenuro methyl)	Low (4)	2
MCPA dimethyl salt	Intermediate (7)	2
MCPA ester	Intermediate (5)	2
Plateau (Imazapic)	Intermediate (6)	2
Poast (Sethoxydim)	Low (4)	1
Redeem (Triclopyr amine)	Intermediate (6)	2
Redeem (Clopyralid amine)	Low (4)	1
Roundup (glyphosate)	High (9)	3
Transline (Clopyralid amine)	Low (4)	1

the instructions on this page to download. Soil data for the area may also be downloaded from <http://websoilsurvey.nrcs.usda.gov/app/WebSoilSurvey.aspx>. The Soil Data Viewer 3.0 extension may be downloaded at the NRCS website <http://www.itc.nrcs.usda.gov/soildataviewer/updates.htm>. Computers with Windows XP Professional (Microsoft Corp., Redmond, Washington) are compatible with Soil Data Viewer 4.0, which also may be downloaded from the NRCS site mentioned above. The shapefiles were converted to raster (grid) format with coordinates expressed in meters, UTM 83 Zone 14 projection, and a resolution of 30 m × 30 m pixels.

The land-use data for North Dakota were imported into ArcView 3.2 as an image projected in UTM 83 Zone 14 with a resolution of 30 m × 30 m pixels. The image was clipped using a shapefile of Ramsey County in UTM 83 Zone 14 coordinates. The clipped image of Ramsey County was converted to a grid with the same resolution as the image using the Spatial Analyst extension.

The buffer function in ArcView 3.2 was used to create shapefiles of two zones of equal width, 0–250 ft and 250–500 ft, around streams imported from the ND DOT GIS database. The buffer function was also used to create similar zones of the same width around areas of water that were imported from three different databases (ND DOT, NRCS SSURGO, and 2001 NDASS land-use image). The water features from each of the three databases were converted to separate shapefiles and then merged into a single shapefile. This shapefile was then buffered and a new shapefile created that delineated the two zones of 250-ft width around lakes. The shapefiles of stream

and lake buffers were merged into a single buffer shapefile that was converted into a grid projected as UTM 83 Zone 14 with 30×30 m resolution.

For this analysis the pesticide application/properties factor is applied as a constant throughout the county. In other words, the analysis assumes that the pesticide in question is applied everywhere at the same rate. This results in three different potential pesticide contamination maps (each map assuming application of either a high, intermediate, or low value for the pesticide application/properties factor). A grid with coordinates expressed in meters, UTM 83 Zone 14 projection, and a resolution of $30 \text{ m} \times 30 \text{ m}$ pixels was created for each of the three mobility categories. The Ramsey County boundary imported from the ND DOT GIS database was used as the template to create the three pesticide application/properties grids.

Each data grid was reclassified as needed into the appropriate potential delivery categories. These grid themes were subsequently used in the summation process to determine overall potential for delivery of pesticides to surface water resources. The three summed grid layers were filtered using the Remove Noise function in the Grid Generalization extension to ArcView 3.2. This step eliminated areas less than 5 acres.

A separate map layer was prepared from each factor layer delineating only areas of high potential. This was done by selecting the high-potential categories from the five grid coverages (somewhat high was also selected from the land-use grid) and then converting to a shapefile. Displaying the overall potential grid with the high-potential shapefiles helps to explain to resource managers the reasons for landscape variations in delivery potential of pesticides to water resources. The factor layers with high potential are designed to become visible only at a scale of 1:30,000 or larger.

Data for Ramsey County highways, towns, sections, townships, county roads, and county boundary were imported from the ND DOT GIS database³⁹ as unprojected shapefiles. Data from the National Wetlands Inventory were downloaded as UTM 83 Zone 14 projected coordinates for Ramsey County from the website <http://www.fws.gov/nwi/>. (The following site is an additional resource for locating wetlands data: <http://nmviewogc.cr.usgs.gov/viewer.htm>.) Using ArcView 3.2, the 36 quad sheets with wetland delineations for Ramsey County were merged into a composite wetland layer. This layer was reprojected to decimal degree coordinates before further use. Wetland methods and techniques of wetland management used by the USFWS depend on the major wetland categories: (1) lacustrine, (2) riverine, (3) temporary, (4) seasonal, and (5) semi-permanent. Wetland management zones were created by querying the wetland layer for each of these major types and creating a new shapefile for each category.

1.4 RESULTS

The first step in a county analysis for potential pesticide delivery to surface water is acquiring the appropriate tools and databases. Image Analyst, Spatial Analyst, and Soil Data Viewer extensions to ArcView 3.2 are required. In addition, other tools that allow the user to clip grids, modify grids, and change coordinate systems are also needed. The databases required for this analysis are the NRCS SSURGO,

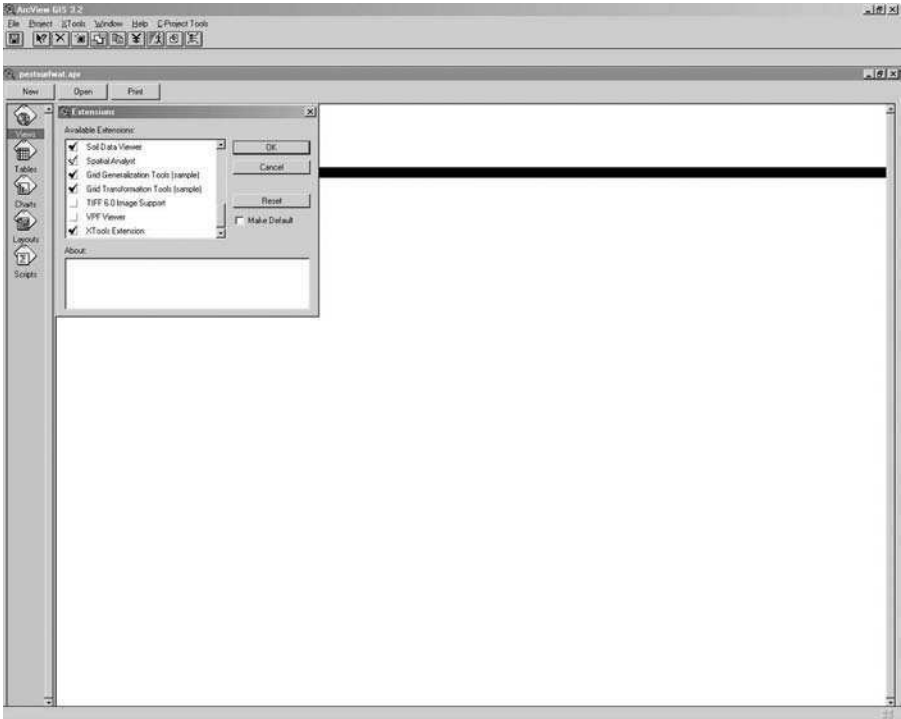


FIGURE 1.1 Window to select the appropriate ArcGIS extensions.

NDDOT GIS, and NDASS Land-use Image. Once the user acquires the GIS tools listed above, they may import the soils, geography, and land use for Ramsey County and begin the analysis.

ArcView 3.2 is opened and the extensions mentioned previously are turned on (Figure 1.1). Select **Properties** in the drop-down menu under **View** in the top tool bar. Change the projection to **UTM 83 Zone 14** with meters as the map units.

1.4.1 SOILS DATA

Add the Ramsey County geographic data from the ND DOT GIS database to the view (Figure 1.2). Add the Ramsey County soils data (*Nd071_a.shp*) from the SSURGO database to the view. The **Soil Data Viewer** can now be used to create the soil properties layers required for the assessment analysis. Activate the Ramsey County soils shapefile and click the **Soil Data Viewer** button in the top menu (Figure 1.3a). The **Soil Data Viewer** will open.

Select the **Options** tab and browse to the *access template.mdb* file (Figure 1.3b). This file comes with the Soil Data Viewer download. It is a clean template that is required for each SSURGO project. Each time a new SSURGO project is begun, the *access template.mdb* file must be copied and pasted into the project folder. The use of Soil Data Viewer will change the template in that project folder, thereby making it unusable for any other soils project. Select the **Description** tab and in the

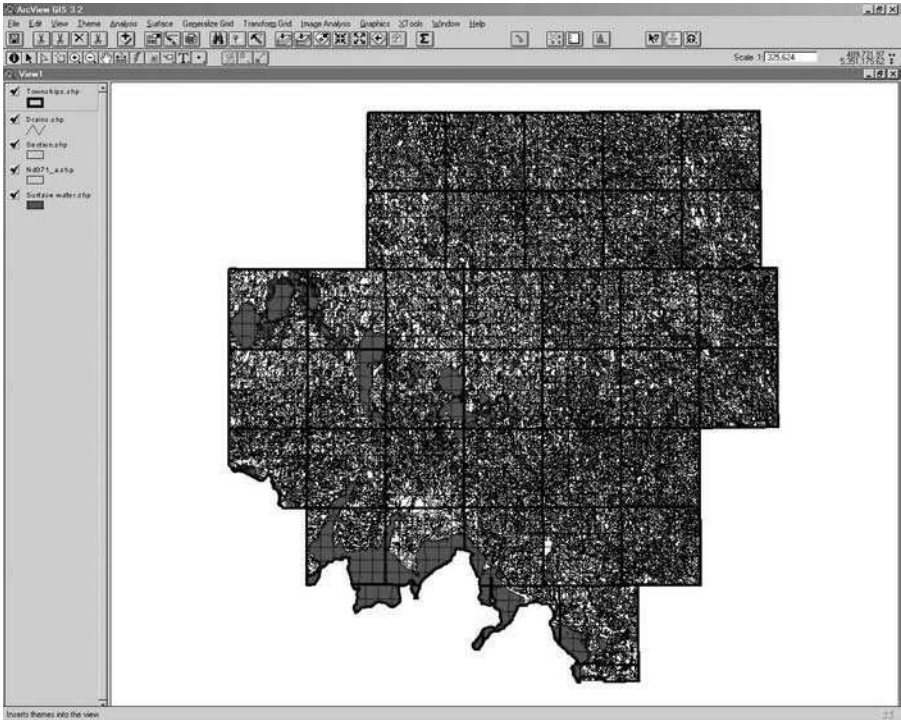


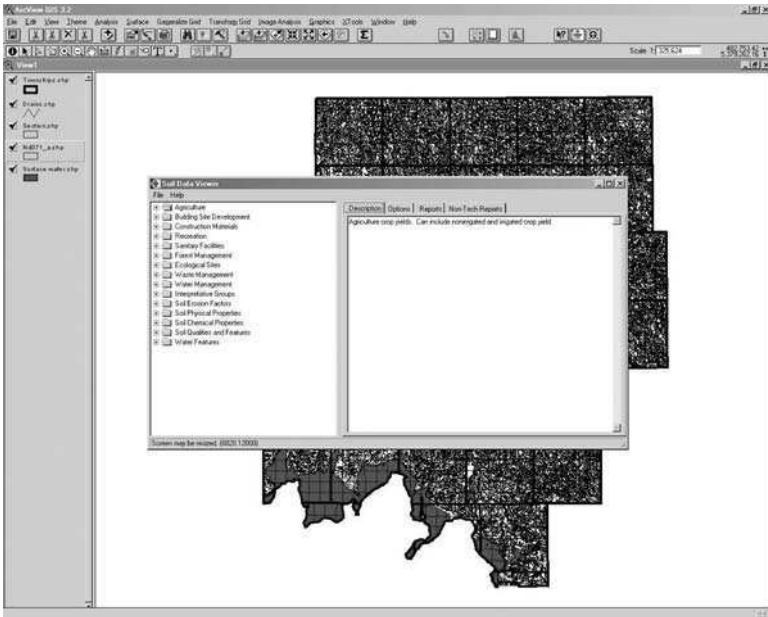
FIGURE 1.2 View of Ramsey County geographic data from the “ND DOT GIS” data base and soils data (Nd071_a.shp) from the SSURGO database.

left-hand view expand the **Soil Erosion Factor** folder. Select the *K-factor-whole soil* file. Now go back to the **Options** tab. In the **Data Filter Option** window scroll to **Dominant Condition**. Then click the **Produce Map** button.

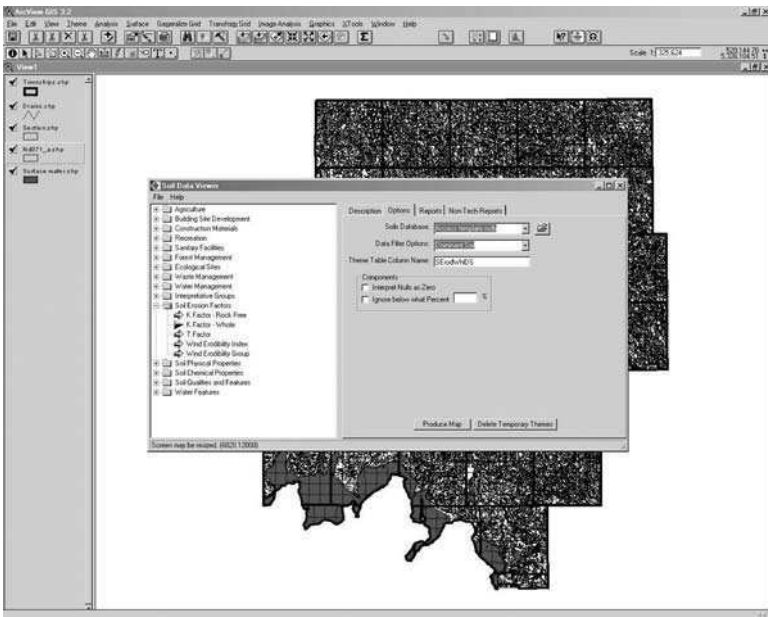
Add the theme, *Ramseybnd.shp* to the view (Figure 1.3c). Select the pull-down menu under **Theme** in the top toolbar and scroll to **convert to a grid**. In the following pop-up window, name the file and place in the temp directory by default. In the next pop-up window set the **grid extent** the same as *Ramseybnd.shp* and the **cell size as 30 m**. In the **conversion field** window select **SErodWhIDS** for cell values.

Reclassify the new grid layer into the three potential delivery categories as previously defined (Figure 1.4a). This is done by selecting the pull-down menu under **Analysis** in the top toolbar and scrolling to **Reclassify**. In the pop-up menu go the **classification field** window and scroll to **s_value**. Then change the values to reflect the three potential delivery categories for the K-factor (Table 1.7, Figure 1.4b). The same procedure is used to create the flooding delivery potential grid (Table 1.8, Figure 1.5).

Determining the potential delivery for the runoff factor is more complicated because the runoff class is not directly available from SSURGO database. Runoff class must be determined by considering both soil permeability and slope, which are available from the SSURGO database. As explained previously, minimum permeability (K_{sat}) must be determined in both the upper and lower 50 cm of soil. Using

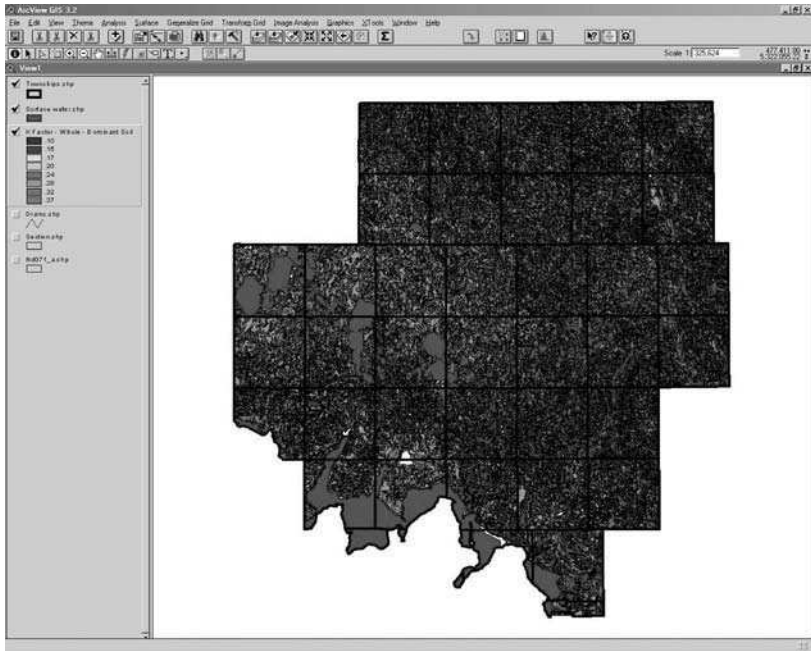


(a)



(b)

FIGURE 1.3 The “Soil Data Viewer” window used to create soil properties layers in the background Ramsey County view. (a) The “description” tab on the right is used to explain the file contents selected in the window on the left. (b) The “option” tab on the left allows the user to set summary parameters for soil data selected from the files in the left window. (c) A new map is generated for the selected soil property and displayed in the Ramsey County view.

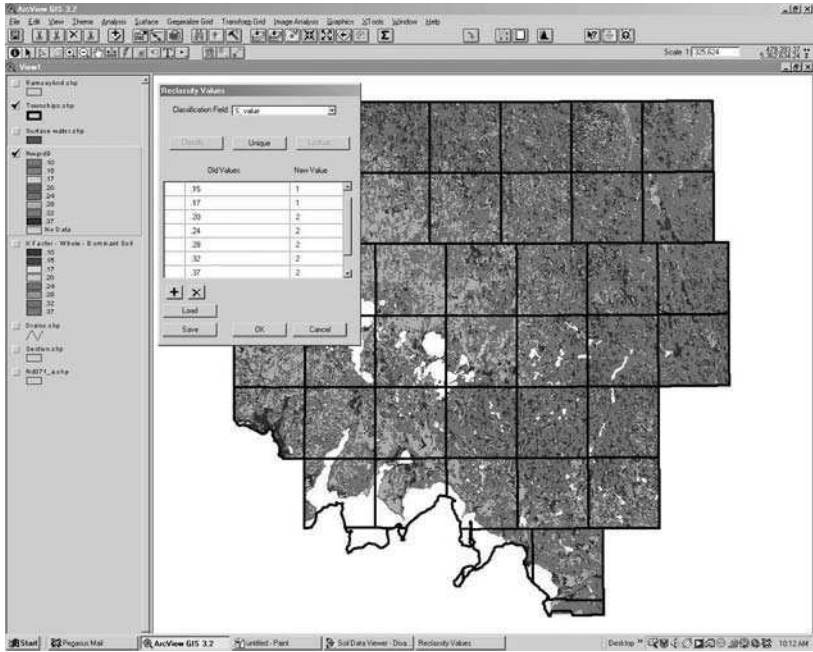


(c)

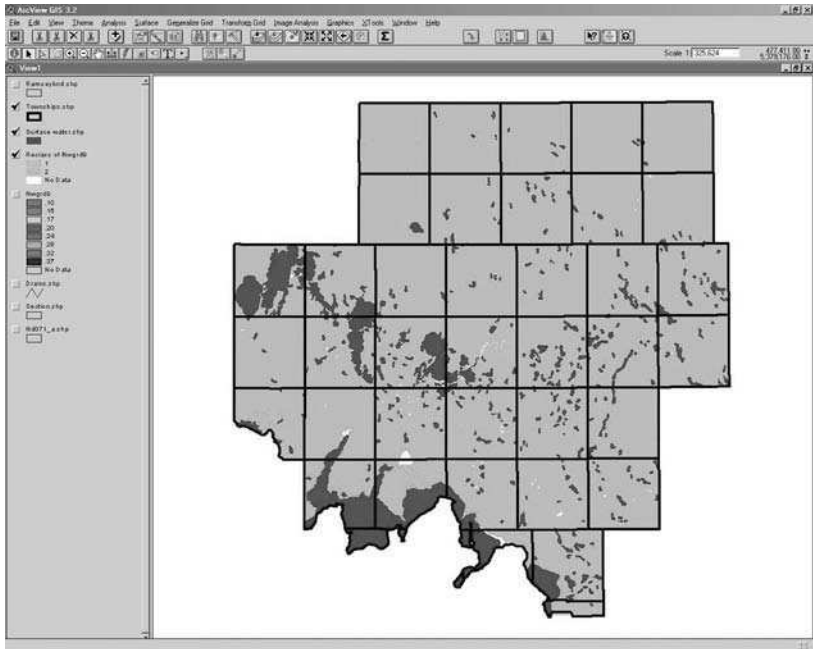
FIGURE 1.3 (continued)

the **Soil Data Viewer** extension, the same initial steps as discussed above are followed to select the options for permeability class in the **soil physical properties** folder. In the **option** window (Figure 1.6a), select for the slowest permeability in the 0 to 150 cm of the dominant soil. **Do not produce a map.** Select the **Report** tab and in the **report** window select **all records** and **preview report**. The report is previewed in your word processor (Figure 1.6b). The preview is printed for subsequent use in the runoff class determination. The above procedure is repeated to determine the minimum permeability in the 150–300-cm soil depth. Slope information is determined similarly by selecting the options for **representative slope** in the **Soil Qualities and Features** folder. In the **option** window, the dominant condition is selected. Then follow the same steps previously outlined to generate a report.

The three tables generated are used to determine the runoff class as defined previously. The results of the runoff class determination are recorded in a spreadsheet and saved as a database file (.dbf) or delimited text file (.txt) that is imported into the ArcView project by adding in the **table view**. The runoff table (*runoff.dbf* provided with other data files) is then joined to the attribute table for the SSURGO soils map (*Nd071_a.shp*) using the **map unit symbol** as the common feature. A runoff class map is created from the shapefile, *Nd071_a.shp*, by changing the legend to the runoff feature. This is saved as a grid and reclassified into the appropriate potential delivery categories following the steps previously outlined (Table 1.9, Figure 1.6c).



(a)



(b)

FIGURE 1.4 Reclassification of a new grid layer into the three potential pesticide delivery categories based on soil erodibility (k-factor). (a) The “reclassify values” window is used to change and regroup grid values into 3 categories. (b) A map with the regrouped categories is displayed.

TABLE 1.7
Potential pesticide delivery based on soil erodibility (k-factor)

k-factor	Potential Delivery Category	Potential Delivery Value
0.02–0.2	Low	1
0.2–0.4	Intermediate	2
0.4–0.69	High	3

TABLE 1.8
Potential pesticide delivery based on soil flooding frequency

Flooding Frequency	Potential Delivery Category	Potential Delivery Value
Never to rare	Low	1
Occasional	Intermediate	2
Common to frequent	High	3

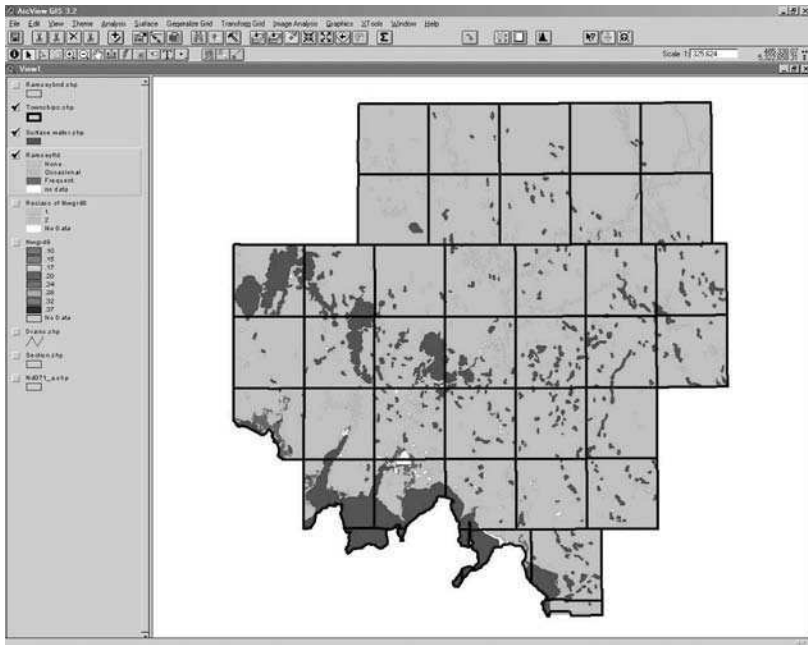
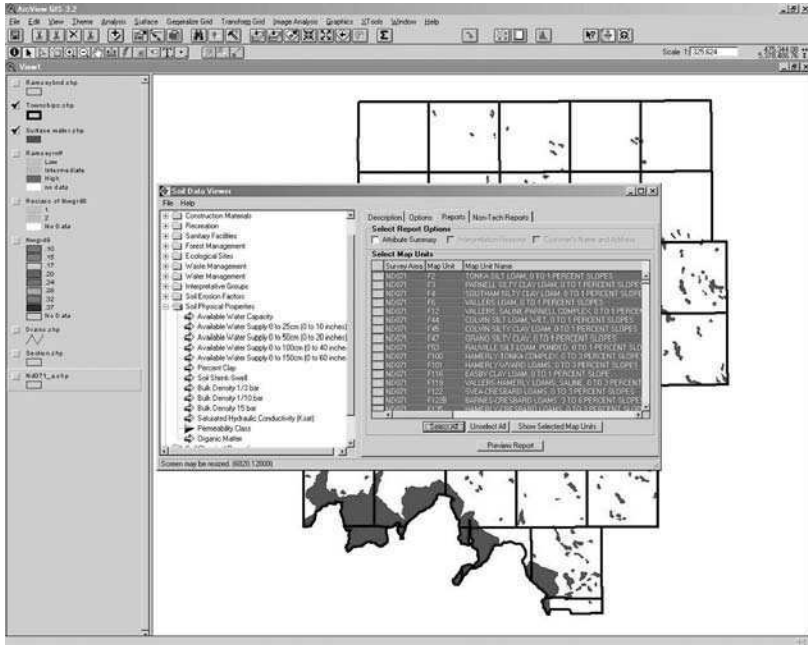
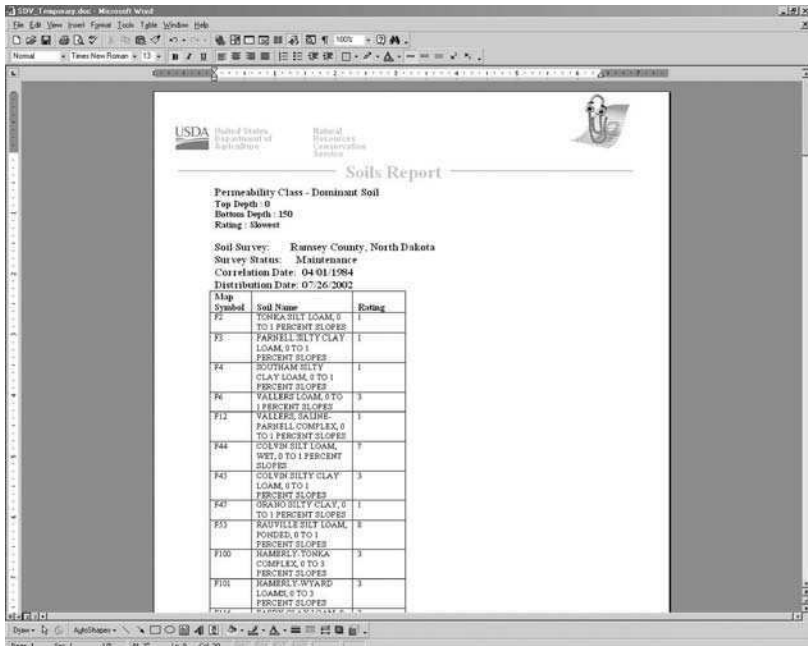


FIGURE 1.5 Reclassification of a new grid layer into the three potential pesticide delivery categories based on soil flooding frequency.



(a)



(b)

FIGURE 1.6 Reclassification of a new grid layer into the three potential pesticide delivery categories based on soil runoff. (a) The “option” job is used to organize the soils’ data by permeability. (b) The “report” tab is used to display the permeability class by mapping unit. (c) The soil reclassified runoff class data is displayed as a map of potential pesticide delivery.

nearest-neighbor technique to include only areas of approximately 5 acres or greater. In the pull-down menu (Figure 1.7a) under **Generalize Grid** in the top menu, select **remove noise**. In the pop-up-window type in 23 cells in the cell count window. The new land-use grid created is used in the summary process.

Unfortunately summer fallow and idle land were included in the same land-use unit in the NDASS database. Idle land includes CRP acreages. In terms of surface cover, the CRP acreage would have been better combined with pasture and rangeland. The result is that summer fallow acreage is overestimated, which causes an overestimation of potential delivery of pesticides to surface water resources in some areas (Table 1.10, Figure 1.7b).

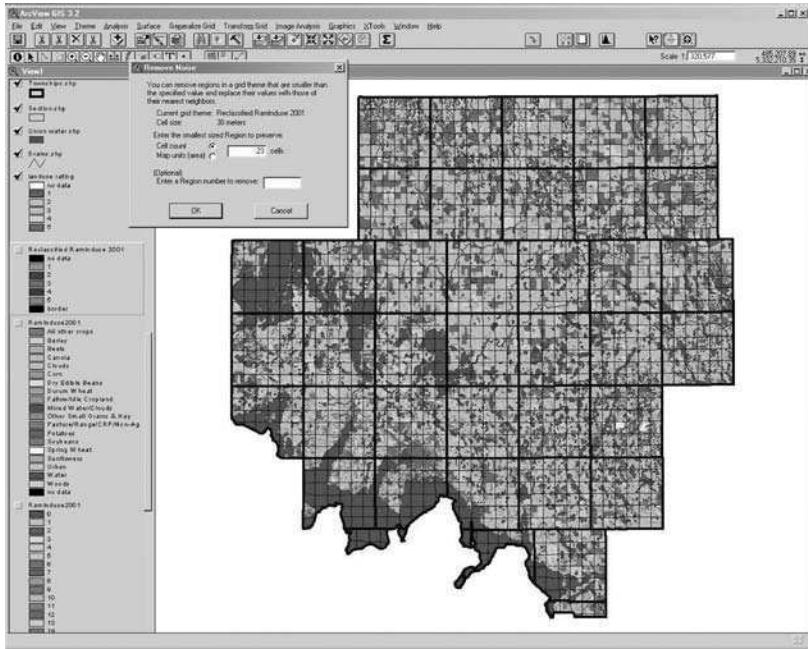
1.4.3 PROXIMITY DATA

Streams are buffered by activating the stream theme (*drain.shp*) imported from the ND DOT database. Select the pull-down menu (Figure 1.8a) under **Theme** in the top tool bar and scroll to **create buffer**. In the pop-up window select **features of a theme** and scroll to *Drains.shp*. In the next window select **at a specific distance** and type in **250**. In the **Distance Units are** window, scroll to **Feet**. In the next window select **yes** to dissolve barriers between buffers. Finish by naming a new theme and saving in the project folder.

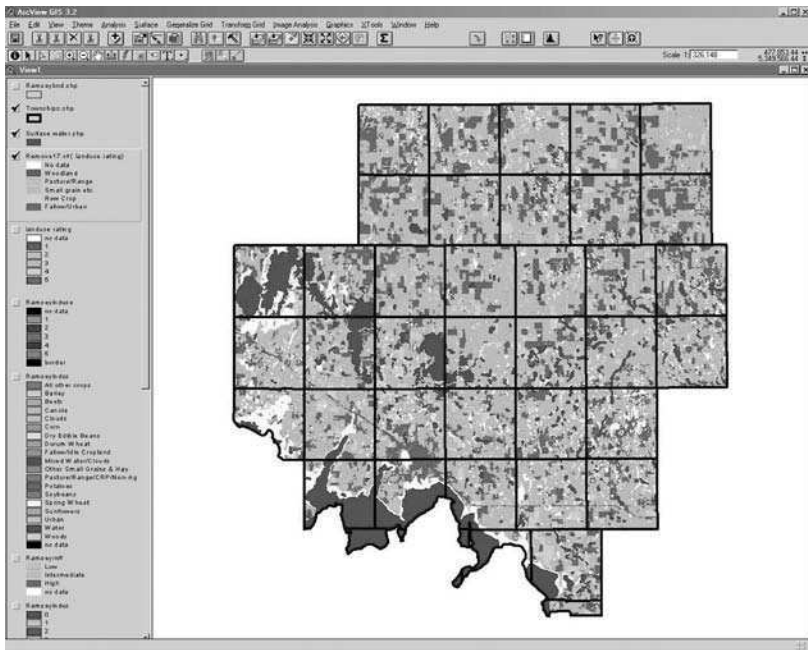
A similar procedure is used to buffer around the lakes. Combining the water features from the ND DOT, NRCS SSURGO, and NDASS land-use databases using the **X-tools** extension creates the lakes theme. First, a shapefile from the water feature in each of the three themes must be created by selection and creation of a new theme (provided with other data files as *surfacewater.shp*, *nrcswater.shp* and *ndasswater.shp*) (Figure 1.8b). Then select the **X-tools** pull-down menu in the top tool bar and scroll to **merge themes**. In the pop-up windows that subsequently appear, the appropriate shapefiles to be merged are selected. The merged theme is named *all water.shp* (provided in the data files for the project). Go back to the **X-tools** pull-down menu and select **convert shape to graphics**. In the pop-up window that appears select *all water.shp*. Go to the **Edit** pull-down menu in the top tool bar and select **all graphics**. Go back to the **Edit** pull-down menu and select **union graphics** (Figure 1.8c). Go back to the **X-tools** pull-down menu and select **convert graphics to shapes**. In the subsequent pop-up windows, highlight **1 graphic polygon** and name the new shapefile *union all water*.

Activate the **union all water** theme and scroll to **create buffers** in the pull-down menu under **theme** in the top tool bar. Follow the same steps as outlined for the stream buffers, except after the **dissolve buffer** step, an additional step is taken to select **create buffers so they are outside the polygons**. You should have created four different shapefiles of buffers (one for each of the two different buffer distances around streams and around lakes).

The shapefiles for 250-ft buffers around streams and lakes are **merged**, **unioned** as graphics, and **saved** as a composite 250-ft buffer, *union 250 buffer.shp*, using the same protocol as described previously. The same steps are followed to create a composite 500-ft buffer, *union 500 buffer.shp*, around streams and lakes. The buffers



(a)



(b)

FIGURE 1.7 Reclassification of a new grid layer into the three potential pesticide delivery categories based on land use. (a) The “remove noise” window is used to group cells from the land-use map in the background into areas no smaller than 5 acres. (b) The regrouped land-use map displayed is a better depiction of actual areas.

TABLE 1.10
Potential pesticide delivery based on land use

Land-use Category	Potential Delivery Category	Potential Delivery Value
Woodland	Low	1
Pasture, rangeland, hayland	Somewhat low	2
Small grains and other crops that form a dense canopy quickly	Intermediate	3
Row crops	Somewhat high	4
Urban, summer fallow	High	5

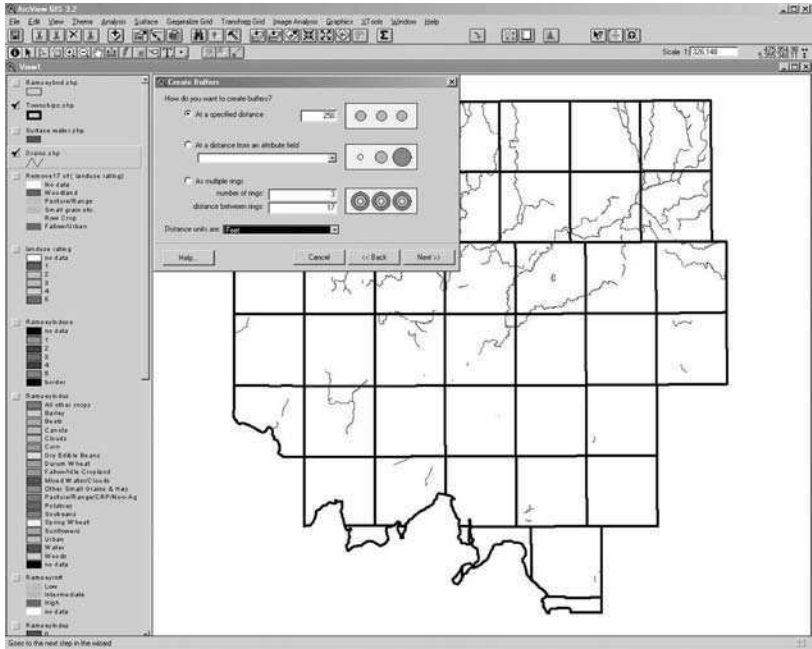
are created in this way so that odd overlapping areas created when merging stream and lake buffers can be eliminated. You may scroll to **erase features** in the pull-down menu under **X-tools** in the top tool bar. In the following windows, select the composite 500-ft buffer shapefile as the theme with the **features to be erased** and the 250-ft shapefile as the **erase theme**. Then use the **X-tools** extension to **merge** the erased theme with the 250-ft buffer theme. Create a grid from the merged buffer theme using the same protocol described previously for grid creation. This grid is reclassified into the appropriate delivery potential categories (Table 1.11, Figure 1.8d).

1.4.4 PESTICIDE APPLICATION/PROPERTIES

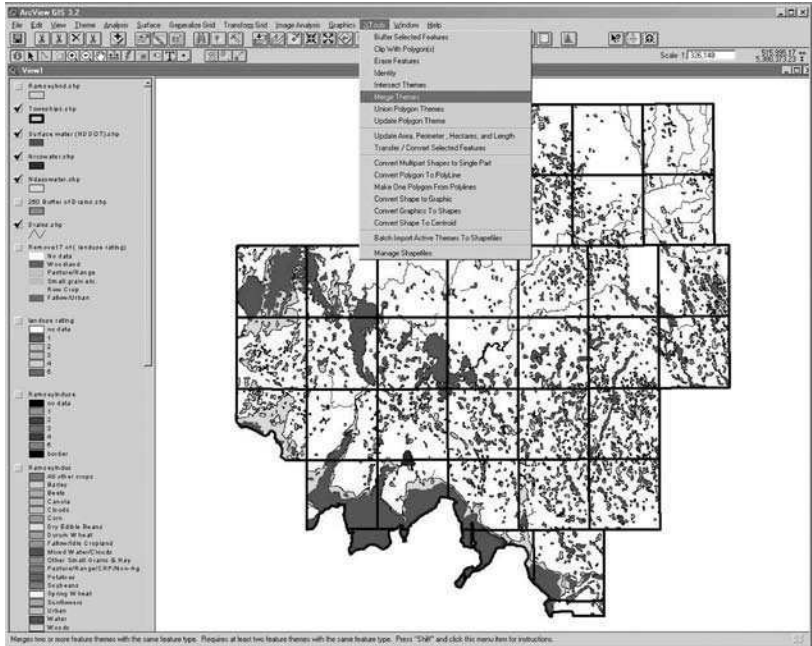
For this analysis the pesticide application/properties factor is applied as a constant throughout the county. In other words the analysis assumes that the pesticide in question is applied everywhere at the same rate. This results in three different potential pesticide contamination maps because each has a different pesticide application/properties delivery potential (high, intermediate, or low) (Table 1.12). Use the Ramsey County boundary file (*Ramseybnd.shp*) to create three grids with 30×30 m pixels. Each grid is reclassified to a single unique value for one of the three potential delivery categories (Figure 1.9).

1.4.5 SUMMATION OF DELIVERY POTENTIAL FACTORS

The map calculator function in the Spatial Analyst extension sums the six potential delivery factors. In the pull-down menu under **Analysis** in the upper tool bar, scroll to **map calculator** (Figure 1.10). Expand the window that appears to the full screen to set up the calculation for summation. Go to the **Layers** window and double click on the first factor theme to be included in the calculation. Then click the **+** button. Go back to the **Layers** window and select the next factor theme. Continue this process until all factor themes have been entered into the equation, remembering that only one of the pesticide application/properties themes should be used. Then click on the **evaluate** button. The calculation is repeated for each of the three pesticide application/properties themes (Figure 1.11a,b,c). The result is three different summation themes for potential pesticide delivery (Table 1.13). Each of these

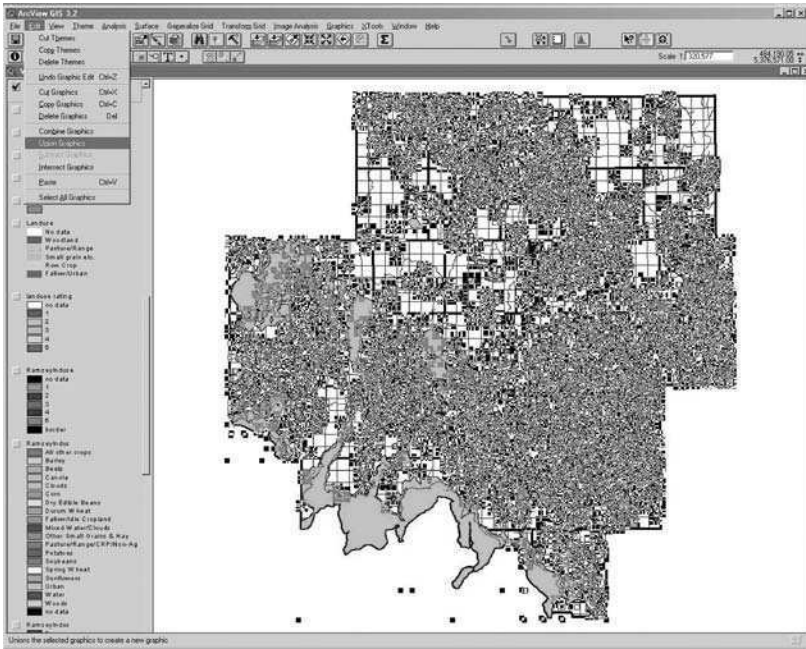


(a)

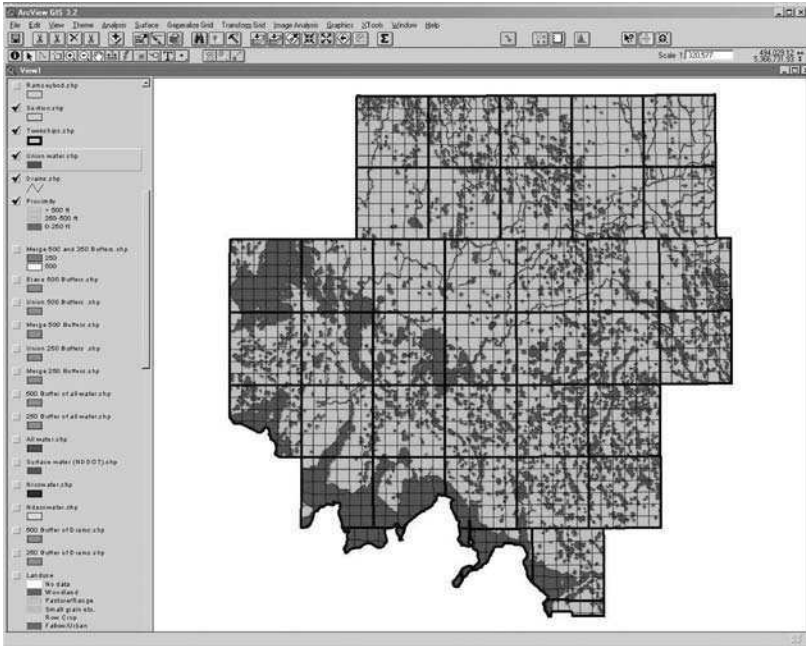


(b)

FIGURE 1.8 Reclassification of a new grid layer into the three potential pesticide delivery categories based on proximity to water bodies. (a) The stream theme in the background is buffered using the “create buffer” window. (b) The different water themes displayed in the background are combined using the “merge theme” function. (c) Graphics of the merged water theme (background) are selected and unioned. (d) The final step merges the composite 250 ft. and 500 ft. buffers, streams and lakes into a single shapefile.



(c)



(d)

FIGURE 1.8 (continued)

TABLE 1.11
Potential pesticide delivery based on proximity

Distance to Water Resource	Potential Delivery Category	Potential Delivery Value
> 500 ft	Low	1
250–500 ft	Intermediate	2
0–250 ft	High	3

TABLE 1.12
Potential pesticide delivery based on chemical/physical properties and mode of application

Pesticide Property/Application Score	Potential Delivery Category	Potential Delivery Value
3–4	Low	1
5–7	Intermediate	2
8–9	High	3

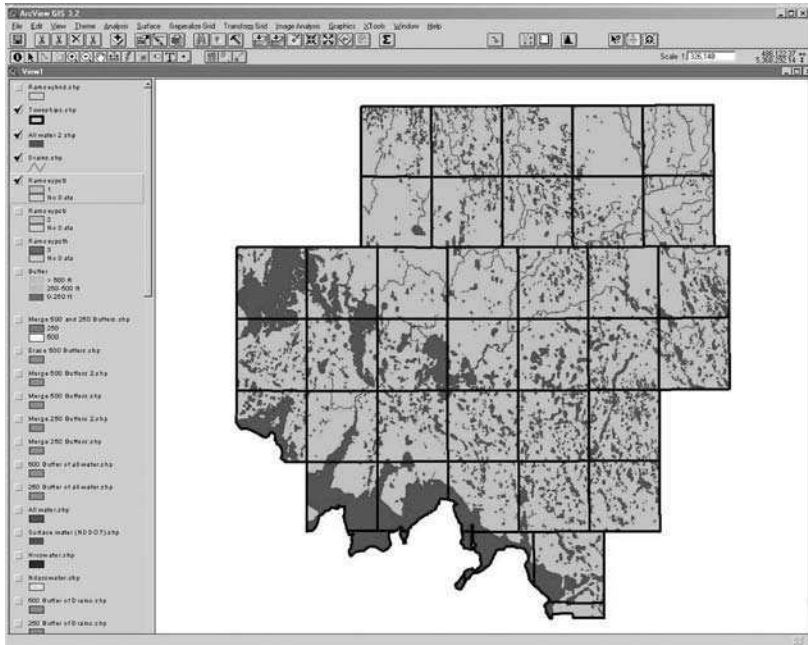


FIGURE 1.9 Reclassification of a new grid layer into the three potential pesticide delivery categories based on pesticide chemical/physical properties.

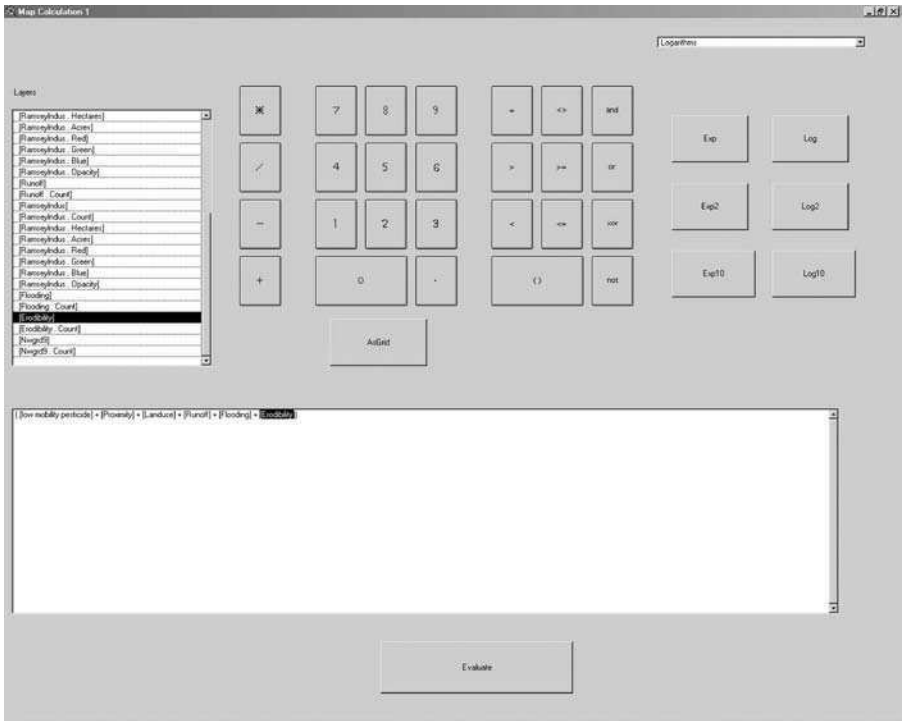
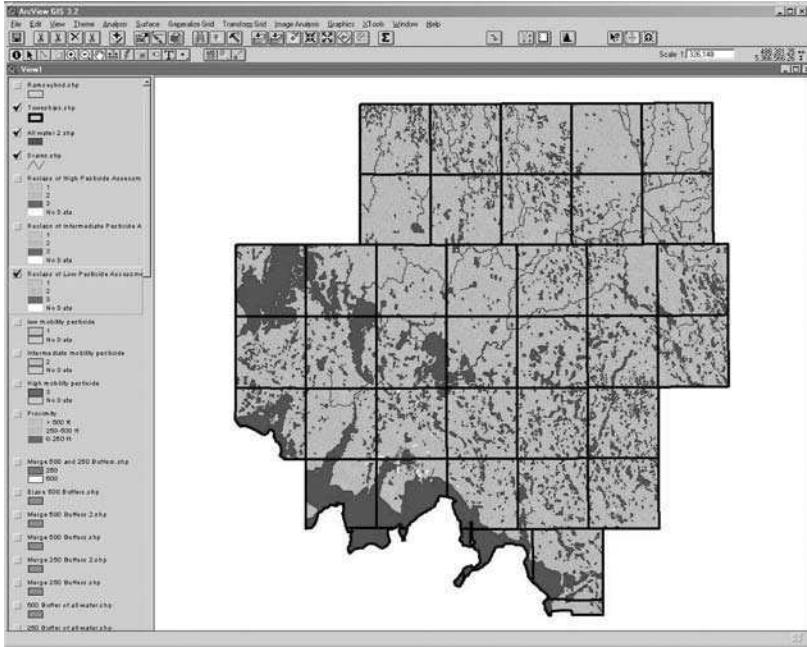


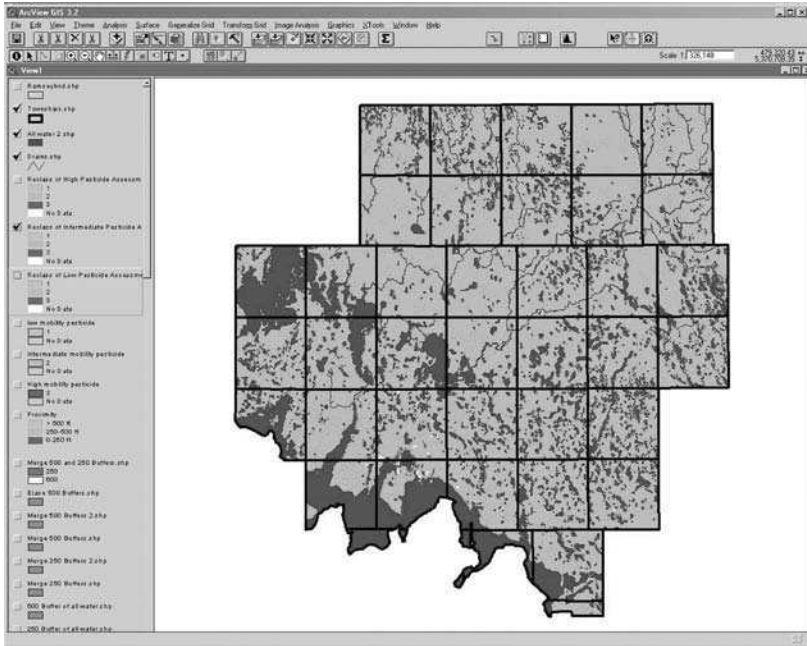
FIGURE 1.10 Reclassification of a new grid layer based on summation of all six factors using the map calculator function in the Spatial Analyst extension.

themes is reclassified into the appropriate categories using the methods discussed previously.

Open the table for the **runoff** grid and select the **high** record. Close the table and select **convert to shapefile** in the pull-down menu under **Theme** in the top tool bar. Double click on the new theme in the legend. In the **legend editor** window that appears (Figure 1.12a), double click the colored box. In the window that appears select the **fill palette** button and change to a transparent box with a black pattern and apply. In the pull-down menu under **Theme** in the top tool bar select **properties**. On the left side of the window that appears, scroll to the **display** icon and click. In the following window (Figure 1.12b) that appears, type in **60000** in the **maximum scale** window. This will ensure that this shapefile will not appear at smaller scales. Follow the same protocol to create shapefiles with transparent patterns for the “high” category of the other delivery potential grids (Figure 1.12c). It should be noted that when grids are converted to shapefiles, angular polygons unlike the square pixels result. The original square shapes can be retained, if the grids are resampled on a pixel size 1/3 the size of the original using the Grid Transformation extension.

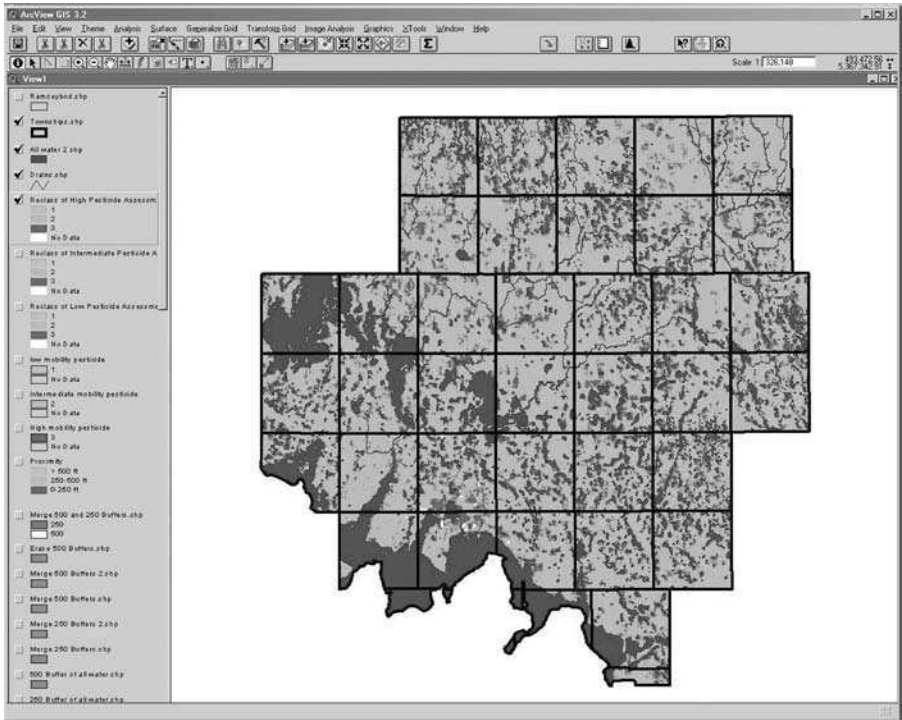


(a)



(b)

FIGURE 1.11 Layers of overall potential pesticide delivery based on summation of all six factors. (a) low potential, (b) intermediate potential, and (c) high potential.



(c)

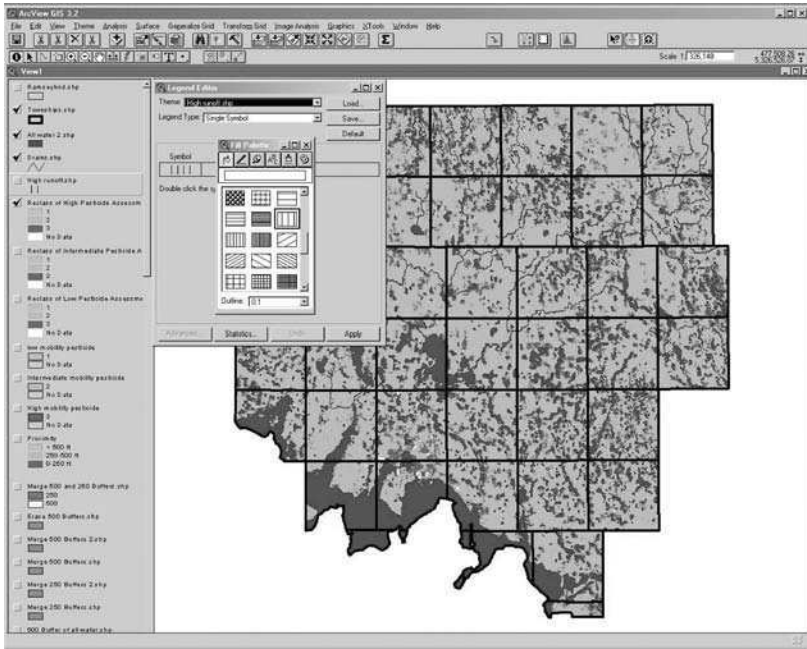
FIGURE 1.11 (continued)

TABLE 1.13
Overall potential pesticide delivery based on summation of all six factors

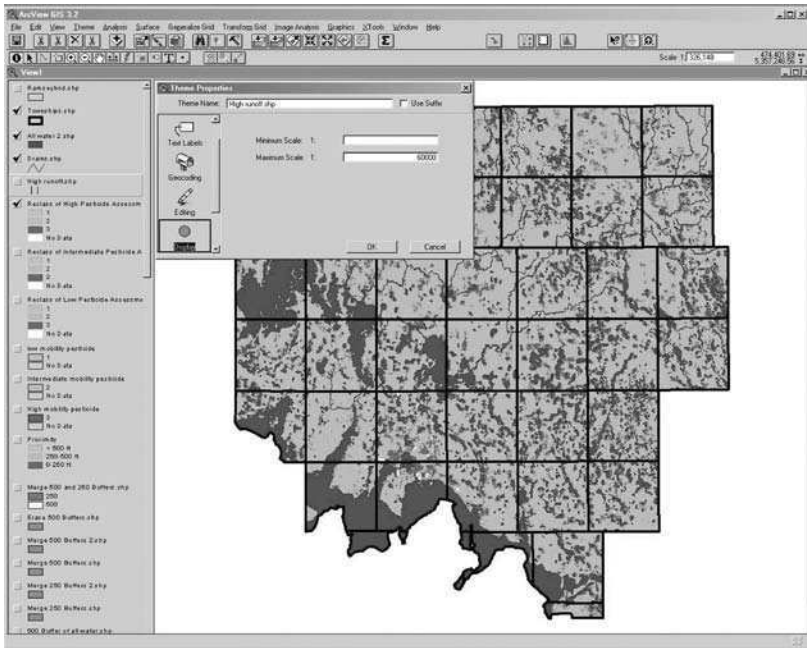
Summation Value	Potential Delivery Category	Potential Delivery Value
6–10	Low	1
11–15	Intermediate	2
16–20	High	3

1.5 CONCLUSIONS

The results of the analysis provide a view of potential pesticide delivery to surface water resources over a relatively large area. Ramsey County has an area of approximately 1,311 square miles or 839,040 acres. Data that help evaluate factors of demonstrated importance with respect to pesticide transport and fate were successfully acquired. The results show that these factors could be systematically integrated to provide comparative information important to resource planning decisions. The strength of the analysis lies in the extent and resolution of the databases used.

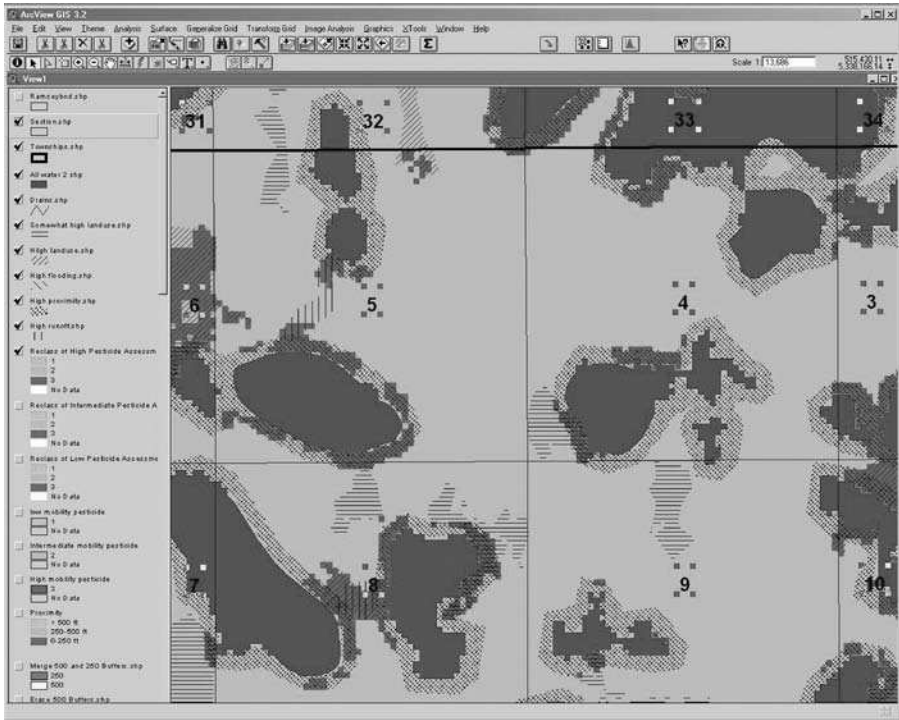


(a)



(b)

FIGURE 1.12 Creating a shapefile from the high potential soil runoff grid layer. (a) A transparent fill is selected in the legend editor so that the high potential factors can be overlaid. (b) The theme properties' window is used to set a maximum scale to prevent map clutter at small scales. (c) High factor potential themes, each with a different transparent pattern, may be displayed together.



(c)

FIGURE 1.12 (continued)

Information regarding potential pesticide delivery can be compared over an area of approximately 1 million acres or between fields as small as 5 acres.

The power of the assessment is further demonstrated when displayed with other geographic databases such as the National Wetland Inventory (provided with the data files for the project), streams and lakes, or areas of human activity. Areal relationships between these different themes are important to the development of resource management plans, particularly during the initial phases. Whether the area is several hundred thousand acres or a cropped field of a few acres, consideration of these results will make subsequent decisions related to pesticide management more effective.

There are limitations to the assessment that need some discussion. Previously mentioned were the summer fallow interpretation and grid/shapefile incongruity problems. The summer fallow problem may be overcome in future NDASS land-use images by applying slightly different cataloging methodology during image processing. As mentioned earlier, grid resampling will solve the grid/shapefile incongruity problem.

Areas of “no data” do present a significant challenge to planning in those specific locations. The soils factor and land-use coverages contain areas of “no data” and are labeled as such. Some of the soil mapping units simply were not populated with

data for certain characteristics. There is no solution to this problem. One must take what one gets from the SSURGO download. The land-use database has areas of clouds and water that cannot be assigned a delivery potential value; therefore, they are represented as “no data.” A solution to this problem is the application of statistical smoothing techniques, such as the “neighborhood statistics” function in the Spatial Analyst extension. Smoothing results in a more complete indication of land use in areas covered by clouds, but may be somewhat misleading where land-use values were extended to areas of water. Smoothed values assigned to areas of water are not appropriate; however, displaying the water theme with precedence over the delivery potential themes solves this problem.

The “no data” problem is carried forward when the map calculator sums the factor layers. This means that if just one factor layer has areas of “no data,” these areas will not receive a summed value. Pixels originally with no data received a mean value based on pixel values in the surrounding neighborhood. Most discrepancies in the land-use layer should disappear when the water layer is applied to the view.

The edges of the map layers appear to be shifted approximately 30 m in some places. This is a problem associated with data clipping, conversion, and differences between vector and raster (grid) formats. Slight edge shifts may occur when grids are created or clipped using polygons (vector) of slightly different spatial extent. In addition, when a grid format is created from a vector format, the pixels created will not fall exactly on the vector boundaries. The larger the pixels, the greater the potential shift or difference with other layers. Following a consistent procedure when creating data layers helps to minimize the shift between layers. All factor layers except the land-use layer can be overlaid with an exact fit on the edges. However, because the land-use layer must be used to calculate the overall delivery layer, the overall delivery layer also does not agree exactly with the other layers. The land-use layer differs from all other layers in its original format. The land-use layer was imported as an image, whereas all other data layers were either imported or created as shapefiles. This probably explains much of the shift in the final layers.

Finally, the assessment process and results should not be viewed as an attempt to predict pesticide loading to water resources. The determination of potential delivery of pesticides is just that, a relative estimate of potential. The factors used to estimate the potential are based on knowledge gained from scientific studies. The methodology outlined here inventories those factors and places a relative value on their importance. However, it was never intended that values would be measured for inclusion in a calculation that would attempt to model environmental processes. The results of the assessment are a good method to help resource managers decide where and when the application of process models is warranted. For instance, USFWS plans to apply the US EPA GENEEC model in areas where the surface water assessment indicates that two or more factors have high potential to deliver pesticides. In a similar step, the application of the US EPA SCI-GROW model is planned for areas where the aquifer assessment (not shown) indicates that two or more factors have high potential to contribute pesticides to groundwater.

REFERENCES

1. Mac, M.J., et al., Status and trends of the nation's biological resources, 2 vols, U.S. Dept. Int., USGS, Reston, VA., 1998.
2. Seelig, B.D., An assessment system for potential groundwater contamination from agricultural pesticide use in North Dakota, ER-18, Extension Service, North Dakota State University, Fargo, ND, 1994.
3. Seelig, B.D., Protecting surface water from pesticide contamination in North Dakota—recommendations for assessment and management, ER-37, Extension Service, North Dakota State University, Fargo, ND, 1998.
4. Caro, J.H., Pesticides in agricultural runoff, in *Control of Water Pollution from Cropland, Vol. II — An Overview*, U.S. Dept. of Ag, ARS, and U.S. Envir. Prot. Agency, Rep. No. ARS-H-5-2 and EPA-600/2-75-026b, U.S. Gov. Printing Office, Washington, D.C., 1976, 91.
5. Dean, J.D., Potency factors and loading functions for predicting agricultural nonpoint source pollution, in *Agricultural Management and Water Quality*, Schaller, F.W. and Bailey, G.W., Eds., Iowa State University Press, Ames, IA, 1983, 155.
6. Rao, P.S.C. et al., Retention and transformations of pesticides in relation to nonpoint source pollution from croplands, in *Agricultural Management and Water Quality*, Schaller, F.W. and Bailey, G.W., Eds., Iowa State University Press, Ames, IA, 1983, 126.
7. Leonard, R.A., Movement of pesticides into surface waters, in *Pesticides in the Soil Environment: Processes, Impacts, and Modeling*, Cheng, H.H., Ed., SSSA Book Series: 2. Soil Sci. Soc. Am. Inc., Madison, WI, 1990, 303.
8. Gaynor, J.D., MacTavish, D.C., and Findlay, W.I., Atrazine and metolachlor loss in surface and subsurface runoff from tillage treatments in corn, *J. Environ. Qual.*, 24, 246, 1995.
9. Knisel, W.G., Foster, G.R., and Leonard, R.A., CREAMS: a system for evaluating management practices, in *Agricultural Management and Water Quality*, Schaller, F.W. and Bailey, G.W., Eds., Iowa State University Press, Ames, IA, 1983, 178.
10. Wauchope, R.D., The pesticide content of surface water draining from agricultural fields — a review, *J. Environ. Qual.*, 7, 459, 1978.
11. Baker, J.L. and Johnson, H.P., Evaluating the effectiveness of BMPs from field studies, in *Agricultural Management and Water Quality*, Schaller, F.W. and Bailey, G.W., Eds., Iowa State University Press, Ames, IA, 1983, 281.
12. Christensen, B. et al., BMPs for water quality — best management practices to reduce runoff of pesticides into surface water: a review and analysis of supporting research, WQBMP1-0993-.25K, Cons. Tech. Info. Center, West Lafayette, IN, 1993.
13. Rhode, W.A. et al., Trifluralin movement in runoff from a small agricultural watershed, *J. Environ. Qual.*, 9, 37, 1980.
14. Wu, T.L., Correll, D.L., and Remenapp, H.E.H., Herbicide runoff from experimental watersheds, *J. Environ. Qual.*, 12, 330, 1983.
15. Ng, H.Y.F. et al., Dissipation and loss of atrazine and metolachlor in surface and subsurface drain water: a case study, *Water Res.*, 29, 2309, 1995.
16. Stewart, B.A. et al., in *Control of Water Pollution from Cropland, Vol. II — An Overview*, U.S. Dept. of Ag, ARS, and U.S. Envir. Prot. Agency, Rep. No. ARS-H-5-2 and EPA-600/2-75-026b, U.S. Gov. Printing Office, Washington, D.C., 1976, 91.
17. Beyerlein, D.C. and Donigian, A.S., Modeling soil and water conservation practices, in *Best management practices for agriculture and silviculture*, Loehr, R.C., Haith, D.A., Walter, M.F., and Martin, C.S., Eds., Proc. 1978 Cornell Agricultural Waste Management Conference, Ann Arbor Science Publishers, Inc., Ann Arbor, MI, 1979, 687.

18. Shoemaker, C.A. and Harris, M.O., The effectiveness of SWCPs in comparison with other methods for reducing pesticide pollution, in *Effectiveness of Soil and Water Conservation Practices for Pollution Control*, Haith, D.A. and Loehr, R.C., Eds., EPA-600/3-79-106, 1979, 206.
19. NRCS, Soil survey geographic database for Ramsey County, North Dakota, USDA-Natural Resources Conservation Service, Fort Worth, TX, 2002.
20. SCS Staff, Soil/pesticide interaction rankings for pesticide leaching and surface loss, Nat. Bull. No. 430-1-4. USDA Soil Conservation Service, Washington, D.C., 1991.
21. Hornsby, A.G., Site-specific pesticide recommendations: the final step in environmental impact prevention, *Weed Tech.*, 6, 736, 1992.
22. Branson, F.A., Gifford, G.F., and Owen, J.R., Rangeland hydrology. Soc. Range Man., Range Sci. Series, No. 1, Belke Printing Co., Denver, CO, 1975.
23. Horton, R.E., The role of infiltration in the hydrologic cycle, *Am. Geophys. Union Trans.*, 14, 446, 1933.
24. Wischmeier, W.H., Cropland erosion and sedimentation, in *Control of Water Pollution from Cropland, Vol. II – An Overview*, U.S. Dept. of Ag, ARS, and U.S. Envir. Prot. Agency, Rep. No. ARS-H-5-2 and EPA-600/2-75-026b, U.S. Gov. Printing Office, Washington, D.C., 1976, 31.
25. Wischmeier, D.A. and Smith, D.D., Predicting rainfall erosion losses — a guide to conservation planning, *USDA, Ag. Hndbk. 537*, Science and Education Admin., U.S. Gov. Print. Office, Washington, D.C., 1978.
26. Goss, D.W. and Wauchope, R.D., The SCS/ARS/CES pesticide properties database: II Using it with soils data in a screening procedure, in *Pesticides in the Next Decade: The Challenges Ahead*, Weigmann, D.L., Ed., *Proc. 3rd National Research Conf. on Pesticides 8–9 November 1990*, Virginia WRRC and Polytechnic Institute and State University, Blacksburg, VA, 1990, 471.
27. Goss, D.W., Screening procedure for soils and pesticides for potential water quality impacts, *Weed Tech.*, 6, 701, 1992.
28. Soil Survey Staff, National soil survey handbook, *Title 430-VI*, NRCS, USDA, U.S. Gov. Printing Office, Washington, D.C., 1998.
29. Roose, E.J. and Masson, F.X., Consequences of heavy mechanization and new rotation on runoff and on loessial soil degradation in northern France, in *Soil Erosion and Conservation*, Il-Swaify, S.A., Moldenhauer, W.C., and Lo, A., Eds., *Proc. "Malama 'Aina '83," International Conf. on Soil Erosion and Conservation*, 16–22 January, 1983, Honolulu, Hawaii, SCSA, Ankeny, IA, 1985, 24.
30. Wicherek, S.P. and Bernard, C., Assessment of soil movements in a watershed from Cs-137 data and conventional measurements (example: the Parisian Basin), *Catena*, 25, 141, 1995.
31. Sharpley, A.N. and Smith, S.J., Wheat tillage and water quality in the Southern Plains, *Soil Tillage Res.*, 30, 33, 1994.
32. Coote, D.R., MacDonald, E.M., and DeHaan, R., Relationships between agricultural land and water quality, in *Best management Practices for Agriculture and Silviculture*, Loehr, R.C., Haith, D.A., Walter, M.F., and Martin, C.S., Eds., *Proc. 1978 Cornell Agricultural Waste Management Conference*, Ann Arbor Science Publishers, Inc., Ann Arbor, MI, 1979, 79.
33. NDASS Staff, North Dakota agricultural statistics 1998, *Ag. Statistics No. 67*, North Dakota State University, Fargo, ND, 1998.
34. Wischmeier, W.H., Estimating the soil loss equation's cover and management factor for undisturbed areas, in *Present and Prospective Technology for Predicting Sediment Yield and Sources*, ARS-S-40, Ag. Res. Ser., USDA, 1975, 118.

35. NDASS, USDA/NASS Cropland Data Layer for North Dakota, North Dakota Agricultural Statistics Service, Fargo, ND, 2001.
36. Campbell, I.A, The partial area concept and its application to the problem of sediment source areas, in *Soil Erosion and Conservation*, Il-Swaify, S.A., Moldenhauer, W.C., and Lo, A., Eds., *Proc. "Malama 'Aina '83," International Conf. on Soil Erosion and Conservation*, 16–22 January, 1983, Honolulu, Hawaii, SCSA, Ankeny, IA, 1985, 128.
37. Satterlund, D.R., *Wildland Watershed Management*, The Ronald Press Co., New York, 1972.
38. Baker, J.L. et al., Nutrient and pesticide movement from field to stream: a field study, in *Proc. 1978 Cornell Agricultural Waste Management Conference*, Loehr, R.C., Haith, D.A., Walter, M.F., and Martin, C.S., Eds., Ann Arbor Science Publishers, Inc., Ann Arbor, MI, 1979, 213.
39. NDDOT, State of North Dakota GIS base map data–1.1a, North Dakota Department of Transportation, Bismarck, ND, 2001.
40. NRCS-ITC, Customer service toolkit soil data viewer, USDA-NRCS, Information Tech. Center, Fort Collins, CO, 2001.

2 Nitrogen Management in Sugar Beet Using Remote Sensing and GIS

David W. Franzen

CONTENTS

2.1 Executive Summary.....	35
2.2 Introduction	36
2.3 Methods	38
2.4 Results	40
2.4.1 Using Satellite Images and GIS to Help Solve Sugar Beet Production Problems	41
2.4.2 Use of a Ground-Based Sensor to Delineate N Management Zones from Sugar Beet Tops	44
2.5 Summary.....	47
Acknowledgments.....	47
References.....	47

2.1 EXECUTIVE SUMMARY

One of the most successful early applications of remote sensing and geographic information systems (GIS) in agriculture has been in improving sugar beet (*Beta vulgaris*) nitrogen management. Sugar beet is a crop that leaves much of the nitrogen it takes up during the growing season in the field at harvest. A portion of that nitrogen can be credited against the supplemental fertilizer nitrogen required by the following crop. Satellite imagery can be used to delineate areas within sugar beet fields where higher or lower nitrogen credits can be applied to the subsequent crop. The amount of nitrogen credits for subsequent crops is directly related to green reflectance of the sugar beet's canopy. Recent research using a ground-based active sensor has shown promise through finer image resolution and the opportunity for more timely imagery acquisition.

2.2 INTRODUCTION

Sugar beet is a foreign crop to many people, although most people in the United States eat the fruits of its production regularly — sugar. Where sugar beet is grown for seed production, it is a biennial crop, grown to full maturity over two years. However, if sugar beet is grown for sugar processing, it is an annual crop; sown in the spring and harvested in the fall. At harvest, there are two components that are important: the green, leafy tops, and the sugar storage component of the root (Figure 2.1).

Sugar beet cannot be grown everywhere. The presence of rocks is not good for harvest or processing. A more important component of production is the local availability of sugar beet processing facilities. Without processing plants nearby, sugar beet production would not be profitable. Transportation costs can rapidly



FIGURE 2.1 Sugar beet in the month of September, showing harvestable beet, taproot, and tops.

consume the value of the product. Conversely, if nearby growers decided not to grow sugar beets, the factories would be in financial trouble, since transportation costs to move more distant production into the factory would make production costs prohibitive. Consequently, there has been a close relationship between sugar beet processors and growers. In some areas, such as the Red River Valley in Minnesota and North Dakota, the relationship has been especially strong due to the development of grower cooperatives.

Early in the development of the sugar beet industry, researchers found that there was a unique relationship between nitrogen (N) fertilizer application and sugar beet production. As N fertilizer rates increased, sugar yields decreased.¹ During sugar beet refining, the nitrogenous impurities within the root also increase the cost of processing. Growers are therefore encouraged not to over-fertilize with N.

Sugar beets can use N from fertilizer as well as from residual N in the soil. In the 1970s, the concept of using soil sampling and nitrate analysis of soil as an approach to manage residual N was proposed.² In a very short time, soil sampling for N management in sugar beets was widespread in the Red River Valley of Minnesota and North Dakota.³

Sugar beet harvest is unique compared to most other crops grown in the United States. In some cultures, sugar beet tops are harvested and removed from the field as a livestock feed before or at root harvest. However, in the United States, the sugar beet tops are removed using a defoliator (Figure 2.2) that cuts the tops off along with a very small part of the root crown and distributes the beaten-up leaves on the soil surface. The lifter (Figure 2.2), which immediately follows the defoliator, lifts the beets from the ground to a truck for shipment to the processor. Distribution of nutrients at sugar beet harvest is different than production of cereal grain and oilseed crops, where most of the plant nutrients move to the grain and seed. When grain and oilseed is harvested, most of the plant nutrients are also removed. In sugar beets, many nutrients, including N, remain in the foliage.

The concept of treating sugar beet tops as a green manure was first reported in France.⁴ The results of this study showed that sugar beet tops provided significant N to the subsequent crop and should be treated as a green manure crop — a crop that is grown partially to maturity, but is terminated before harvest and all the nutrients returned to the soil for use by the next crop. Organic farmers often use this principle to provide N and other nutrients to subsequent crops to limit the use of commercial fertilizers.

The color of leaves at harvest is related to the amount of N contained within the plant.⁵⁻⁹ Yellow sugar beet tops at harvest suggest that the leaves contain low levels of N, while green tops suggest that the plants contain a substantial amount of N. Leaf color can be used as a basis for N credits from sugar beet. For yellow leaves, no N credit is provided, while for dark green leaves, a credit of 90 kg ha⁻¹ is provided. Remote sensing can be used to assess plant color.

Low-cost LANDSAT data can be purchased by sugar cooperatives. LANDSAT data have a pixel size of approximately 30 m. These data can be processed to produce a number of different products. One of the most popular is the N Difference Vegetation Index (NDVI) ((red-NIR)/(red + NIR)). The imagery that is most useful for assessing residual N is collected between August and October. Imagery closer to

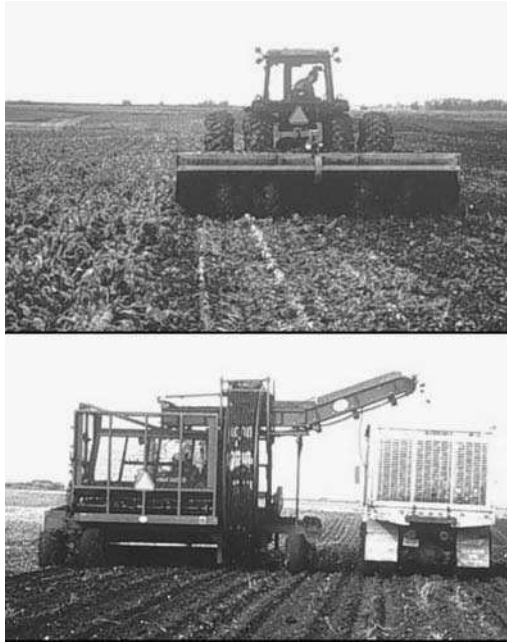


FIGURE 2.2 Sugar beet defoliator (top) is used within hours of harvest by the sugar beet lifter (bottom).

harvest is preferred, but due to possible interference by cloud cover, imagery obtained earlier in the summer can be used to increase the chance of a successful image in any given area.

When the agricultural consultants (agriculturalists) of the sugar cooperatives receive the images from the imagery provider, the agriculturalists visit a few farms in each view and determine whether the NDVI measurement in the image is related to green, yellow-green, or yellow. This relationship is then transferred to other fields in the area. The NDVI values within each image are then classified based on that ground-truthed relationship using ArcView (ESRI, Redlands, California) software. The fields are classified into three to five zones based on the established ground-truth relationship between sugar beet top color and the image NDVI values. From these zones of N credits, a fertilizer-spread map is developed using SGIS® (SOILTEQ, Minnetonka, Minnesota) software, which is ArcView-based.

Although about 30% of Red River Valley sugar beet growers in 2005 utilized this zone N credit technique, the development of maps and N credits is still somewhat subjective. The following discussion provides an outline of how the current management recommendations are developed and how a ground-based active sensor can be used.

2.3 METHODS

The development of zones in a GIS package such as ArcView or in a non-GIS software such as Surfer® (Golden Software, Golden, Colorado) is subjective, and

in terms of imagery, not very easy. If the data came to the user in a raw form as a text (.txt) file, either program would handle it well. If the data came to the user as an image, the image must first be converted to a .txt file and then imported into the GIS program. The user can then select data intervals for the imagery that might be useful and rely on the software to develop a certain number of zones that fit the base criteria in what is called “unsupervised classification,” or the user can manipulate the data intervals within the GIS software to fit a view that makes sense when compared with other data including topography, yield maps, electrical conductivity, or previous year imagery. In the Red River Valley, much of the zone development is conducted by agriculturalists who are familiar with the farm and grower, so the activity of zone development is mostly a “supervised” classification, using the image viewing software developed by the supplier (AgriImaGIS, Inc. Maddock, North Dakota).

When one data layer, such as imagery, is used to develop zones, classification is usually chosen as a method to accomplish the task. Classification means that the data values (in imagery, the colors or hues are in values from 1 to 256) are divided into categories or classes. The classification method can vary depending on the experiences and preferences of the user. Common choices for single data layers within ArcView are equal spacing, Jenks¹⁰ natural breaks, and some multiple of standard deviation. The equal spacing choice would be appropriate for data that is equally distributed within the histogram of data. Standard deviation is a more statistical approach with normally distributed data. Jenks natural breaks is a procedure that groups data into classes that are relatively separate of the other classes, relying on the natural grouping of the data instead of a more subjective division.¹⁰

When an image is added to the ArcView screen, the file name of the image appears on a file column to the left of the main screen. Under the file name will be a red, green, and blue box. By left-clicking on any box, a small window will open with **Visible** checked. By left-clicking the **Visible** option of the red box, the check is removed and the image assumes the properties of only the green and blue boxes. This operation is reversible, so if the user wants to see the red layer again, the **Visible** command is simply rechecked. Sometimes the red-green-blue image is appropriate to work with, while in other images, one or two of the three layers is most representative of differences in the field. Once the proper choice is made, the image can be exported as a tag image file format (.tif) file by right clicking the file name in the column to the left of the viewing area and then choosing **Data > Export Data** in the choices that appear sequentially. Sometimes the .tif file created in this manner is not usable in other formats; one way to ensure a useful .tif file after creating the .tif in the manner already described, is to go to **File > Export Map**, then save as a .tif under the previously used file name.

To classify an image within ArcView, either the raw numeric data or the numeric data generated from the image through another program are required. Classification of imagery within Surfer also must be conducted using numeric data. It is possible to import a .tif file into Surfer, but it can then only be viewed, and cannot be classified in that format. One program that has been used to generate these numeric data is Noesys Transform[®] (Fortner Software LLC, Sterling, Virginia). An 8-bit .tif file can be opened in Transform, which then opens a numeric matrix of the user’s choice of

designated columns and rows containing the raw data originally used to make the image. Without further manipulation, the numeric data can only be exported as an ASCII text matrix, which is not usable in GIS formats. However, using the “xyz1” macro, from the **Transform** toolbar, the data can be transformed from matrix to x, y, and z columns. The resulting file can be saved as .txt and imported into both Excel® (Microsoft Corporation, Redmond, Washington) or Surfer. The “xyz1” macro does not automatically appear as a macro choice. However, the “xyz1” macro code is imbedded in the macro archives and can be copied and pasted into an active macro by following the instructions within the program.

Classification of numeric data within ArcView is relatively easy and meaningful, as long as the classification results correspond to the user’s knowledge of the field. Sometimes variability in the data is low, and if the data are not enhanced in some way, or the classification criteria are not fine enough, ArcView will not automatically search for the criteria required to provide more than two or three classes. In some relatively flat Red River Valley fields, for example, instead of recording feet or meters, use of inches or centimeters is necessary to provide enough numeric range for ArcView to function well. Another trick is to not use the default number for standard deviation, but use a fraction of it. If the results are still not satisfactory, a program such as Surfer might be better suited. Within Surfer, the user can dictate as many classes as are required. In addition, the composition of the classes can be orchestrated by choosing the range of each class, which is very difficult to do within ArcView. The resulting map can be exported out of Surfer as a .tif and imported into ArcView through the **add data** tool bar option. The resulting image can then be registered using the corner georeferences of the data.

Another possible way to delineate zones from imagery alone is through the ArcView companion program ERDAS Imagine® (Leica Geosystems Group, Norcross, Georgia). Within ArcView, display a .tif image. In the **file** bar to the left of the screen, left click on the file name of the image. Choose **Data**, then **Export Data**. Within the three choices is the **Image (.img)** file. Choose the image option and the correct path to save the data. Once the .img file is created, it can be opened or manipulated using Imagine software. To create classes in the image, left click on the **Classifier** icon in the **Imagine** toolbar at the top of the viewing screen. Choose **Unsupervised classification** from the choices of items within the Classifier column. Once the Unsupervised classification window is opened, enter the image (.img) file that will be classified, and create the output file and signature file that will go with the final classification. Under the **Initializing options** button, one can choose the range of standard deviation on which the classification will be based. Also, the number of classes can be chosen in the space designated **classes**. The output file will have an .img extension, so it will be readable in both Imagine and ArcView.

2.4 RESULTS

Two examples are provided to illustrate the use of remote sensing and GIS to define N management zones based on sensing N content of sugar beet tops. The first example describes the mapping of N management zones for wheat (*Triticum aestivum* L.) in St. Thomas, North Dakota, based on remotely sensed N content of sugar

beet tops, and the second example describes the use of a ground-based sensor compared to satellite imagery for zone delineation of N credits following sugar beet in Crookston, Minnesota.

2.4.1 USING SATELLITE IMAGES AND GIS TO HELP SOLVE SUGAR BEET PRODUCTION PROBLEMS

The crop rotation at the St. Thomas, North Dakota, site was sugar beet followed by wheat followed by potato (*Solanum tuberosum*) then back to sugar beet.¹¹ This is a highly profitable rotation, but in this field the sugar beets were suffering from high yield with low sugar content, resulting in much lower sugar payments than growers in different areas with different rotations. Although the logical cause of low sugar and high yield would be high residual soil N levels, the site had low soil N levels down to four-foot depths, and nothing out of the ordinary was observed. The decision was made to sample sugar beet tops for N content to assess this as a source of the observed problem.

Four fields 16–20 ha in size were soil-sampled to a 2-m depth in a 0.2-ha grid in the fall of each year of a four-year study. Sugar beet tops ranged from light to very dark green as illustrated for one field in Figure 2.3. A 3-m length of row within

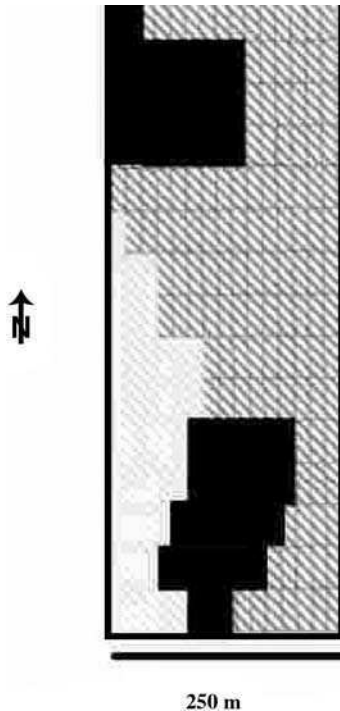


FIGURE 2.3 Fertilizer application map for the field in Figure 2.4 created using classification of an image to delineate zones, and soil nitrate data to finalize the nitrogen rates. The final zones were hand-drawn, scanned, and geo-registered for use by an applicator. Each hue would receive a different nitrogen rate.

each grid was harvested for root yield and top yield in the sugar beet years. Nitrogen

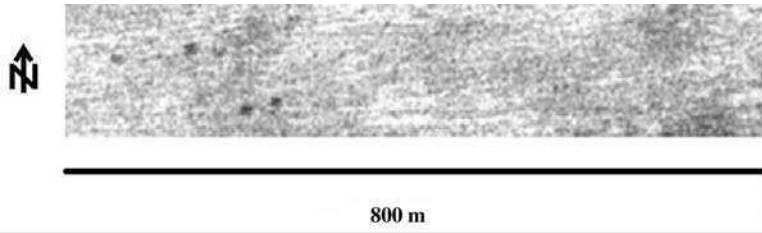


FIGURE 2.4 Aerial photography in August of a sugar beet field showing darker, more robust areas with more N and biomass than lighter areas.

in the sugar beet tops ranged from 112 kg ha⁻¹ to 448 kg ha⁻¹. A Landsat 5 NDVI satellite image for one sugar beet field showed a range of hue differences corresponding to a range of low to high vigor, while an aerial photograph for the same field showed a range from no growth due to excessive water to high vigor in the darkest areas (Figure 2.4). The aerial image has three advantages over the NDVI satellite image. First, the aerial image has a much finer resolution than the LANDSAT data. Second, since the relationship between sugar beet top N credit to subsequent crops is based on the level of greenness of the canopy, ground-truth information is much more critical in the NDVI image than in the true-color photograph. Third, areas within the field of poor growth and thin stands are clearly identifiable in the aerial image. These areas are not clearly identifiable in the satellite (NDVI) image.

In this example, early in the use of remote sensing of sugar beet tops, GIS was only used at the last step to develop the application map for N fertilizer to the subsequent wheat (*Triticum aestivum L.*) crop. Today, GIS is more easily used to remove subjectivity in delineating the fertilizer management zones from imagery. In this case, N fertilizer management zones were delineated by hand drawing around areas with similar greenness and vigor. The satellite and aerial imagery did not match exactly, and aerial imagery was weighted more than the satellite imagery. The resulting N fertilizer application map (Figure 2.5 shows that N credits ranged from 0 (168 kg N ha⁻¹ rate to wheat) to 78 kg N ha⁻¹ (90 kg N ha⁻¹ to wheat). The farmer applied N fertilizer in the spring as anhydrous ammonia using an applicator equipped with a variable rate controller.

The result of the variable N application showed no wheat yield differences between zones where large and small N credits were given (Table 2.1), suggesting that the N credits given to the zones were appropriate. If too great a credit had been given, yields would have been lower at the lower N rates. Since this study, sugar beet quality in the fields has dramatically improved as a result of using imagery to identify sugar beet tops with excessive N and reducing N rates accordingly to the subsequent crop. This practice has also helped to reduce residual N levels when the rotation again is planted back to sugar beets. The zones identified during the sugar beet year have also been found to correspond to areas of related residual soil N levels throughout the rotation.¹¹ The zones delineated during the sugar beet year are

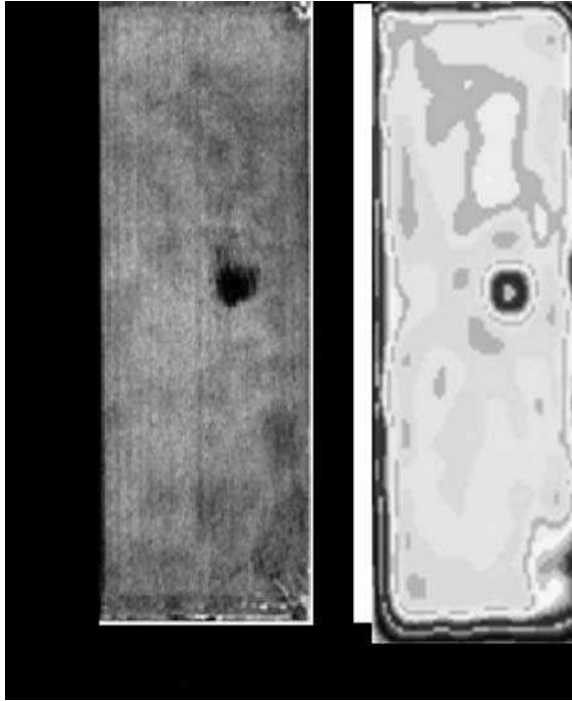


FIGURE 2.5 Sugar beet images from a single field obtained using aerial photography (left) and satellite imagery (right). The satellite imagery has been processed using viewer software that interpolates the raw image data and groups the data into classes. The raw data in the satellite image still exist within the GIS database, and can be further manipulated into different numbers of classes using different methods.

TABLE 2.1
Wheat yield differences between zones in a field near St. Thomas, North Dakota, that received various N credits from anticipated sugar beet top N contributions from the previous fall

Zone	Wheat Yield, kg ha ⁻¹
168 kg N ha ⁻¹	3790
112 kg N ha ⁻¹	3823
90 kg N ha ⁻¹	3695
Significance at P <0.05	none

therefore used to identify soil-sampling zones after wheat and potatoes (*solanum tuberosum L.*), resulting in improved N application rates throughout the fields in the off-sugar beet and sugar beet growing years.

In practice, GIS is an important component in the practical application of the relationship between sugar beet canopy color and N credits to subsequent crops. American Crystal Sugar Cooperative agricultural consultants obtain satellite imagery during July through early September. These images are transferred through GIS to hand-held PDAs and used by agriculturalists to visit certain fields and establish a basic relationship between the NDVI in the images and greenness in those fields. The fields are then divided by the grower into three to five zones of N credits for the following crop. The fertilizer-spread map is produced by transferring GIS information contained in the PDA to an appropriate software program containing the N application rates for each zone. American Crystal Sugar Cooperative reported that about 30% of their grower acreage used sugar beet canopy tops in 2005 to reduce fertilizer N levels to subsequent crops. A survey of grower use patterns shows an economic advantage for growers using these same zones as a basis for residual nitrate N soil sampling prior to growing sugar beets in a field.

2.4.2 USE OF A GROUND-BASED SENSOR TO DELINEATE N MANAGEMENT ZONES FROM SUGAR BEET TOPS

In 2002, a study was conducted in a 16-ha sugar beet field near Crookston, Minnesota. Measurements of canopy NDVI were calculated from spectral reflectance of sugar beet tops obtained using a Greenseeker[®] (NTech Industries Inc., Ukiah, California) handheld sensor and compared plant biomass, height, and N content of sugar beet tops. In 2003, NDVI in two sugar beet fields was mapped using the Greenseeker sensor, and results were compared to NDVI obtained with satellite imagery.

The Greenseeker sensor emits both near-infrared and red light that is used to calculate NDVI. Because the reception of the light back into the sensor would vary depending on the distance of the emitter and the object, only the ratio of infrared and red light, in terms of NDVI, is recorded. The ratio cancels out the distance term, so that as long as the emitter is within 0.5 to 0.75 m of the object, there is no variance with distance. Because this is an active light source and only the emitted light is analyzed as it is reflected from the object, this sensor can be used under a range of ambient conditions occurring at night, in the daylight, or under clouds, with no difference in the reflected reading. These characteristics give the Greenseeker an advantage over satellite or aerial imagery because these technologies are based on passive light that is reflected or emitted by the objects of interest. Oklahoma State University maintains an excellent website (www.dasnr.okstate.edu/nitrogen_use) that details the development of this sensor. The sensor obtains several readings per second and compiles them in a spreadsheet database for ease of use.

In 2002, on the day of harvest, a 16-ha sugar beet field was divided into 0.1-ha grids. A length of 3-m of row within each grid was sensed with the ground-based sensor, measured for canopy height using a meter stick, then roots and tops were harvested, weighed, and analyzed for nutrient content. Canopy height measurements were conducted on the areas surveyed. The correlations between NDVI and canopy dry matter content, N content (% N), and total N (lb N/acre) were relatively low ($r < 0.55$), but all comparisons were significantly correlated (Table 2.2). However, when the NDVI readings were multiplied by the canopy height, the correlation values

TABLE 2.2
Comparison of dry matter, N content (% N), and total N (lb N/acre) of sugar beet tops with ground-based NDVI and NDVI multiplied by canopy height at Crookston, Minnesota, 2002

Property	NDVI	NDVI × Canopy Height
	Correlation Coefficient (r)	
Dry matter	0.40	0.69
N concentration	0.55	0.81
Total N	0.51	0.57

increased. Although early in the season NDVI has been shown to be highly correlated with biomass, later in the season when leaves cover other leaves and leaf area completely covers the soil, NDVI readings become saturated and differences in more robust canopies are difficult or impossible to measure.¹² It seems that NDVI without a correction is more a two-dimensional measure of plant biomass than a volume measurement. By correcting for volume with a height measurement, the value of the NDVI measurement is enhanced (Table 2.2). Studies conducted on corn in Nebraska have supported the use of green NDVI for higher correlation to crop N content. The green NDVI measurements are a better indication of N status in larger crops, and do not saturate at later plant growth stages as seems evident with red-NDVI measurements. Height measurement in corn using red-NDVI helps improve the N and red-NDVI relationship.¹²

In 2003, the Greenseeker sensor was mounted on a sugar beet defoliator and modified so that a GPS reading would be associated with the sensor readings. Satellite images of the fields were also obtained in August and again in October just prior to harvest. Much finer detail is provided in the ground-based sensor image compared with the satellite image (Figure 2.6). Areas of about 8.4 m² are represented by the ground-based image compared with 84 m² for the satellite image. An advantage of the satellite imagery is the area along the west side of the bottom image, which seems to indicate less vigorous canopy compared to the satellite image. This area was affected by dust on sugar beet leaves from a north-south gravel road. In the satellite image, there was either no dust present, the image was not affected by dust, or the resolution was so large that the dust was inconsequential.

There also appears to be a timing difference between the field images in Figure 2.6. The satellite image was obtained in August, while the ground-based image was obtained the day of harvest in October. The ground-based image clearly shows large differences in NDVI between parts of the field, particularly between the north and the south. In the satellite image, taken two months before the ground-based image, little difference between the north and south is evident. It is likely that the sugar beet plants were still adequately fertilized by the residual soil N in August. However, as residual N levels were further depleted, canopy differences were detected in September and October.

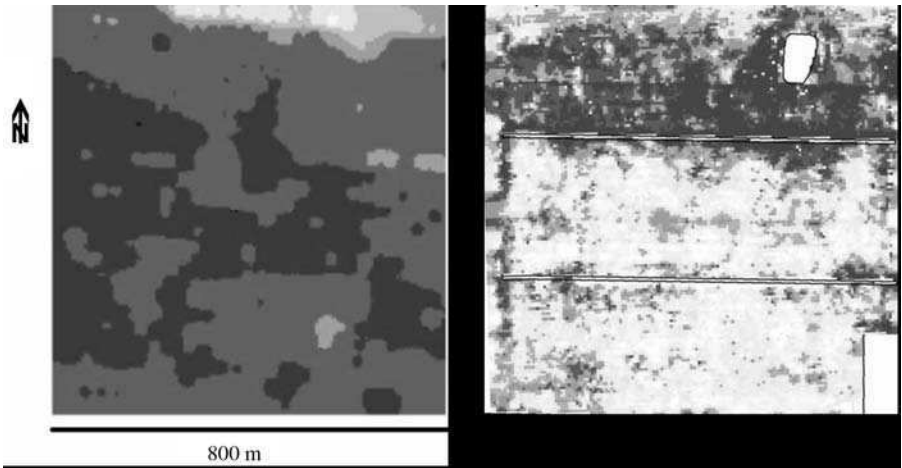


FIGURE 2.6 A satellite image (left) of a sugar beet field near Crookston, Minnesota, taken in August, compared with data from the Greenseeker® ground-based active sensor (right) at harvest in October. Each dataset was classified into at least five classes. Darker tones are an indication of higher N credits for the subsequent crop. (Images courtesy of Gary Wagner, Climax, MN.)

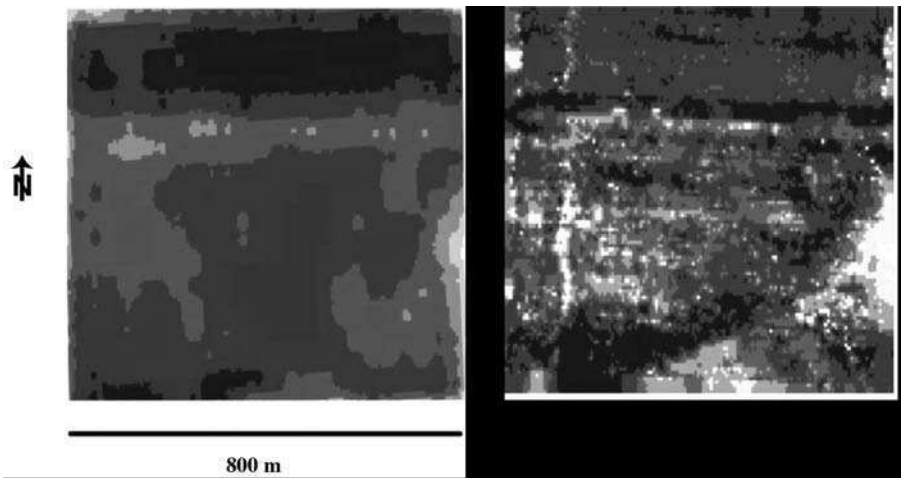


FIGURE 2.7 Satellite image (left) of a field near Crookston, Minnesota, compared with classified image of Greenseeker® ground-based sensor data (right).

In a second field, there is a sharp, curved boundary in the southeast part of the field in the ground-based image (Figure 2.7). The satellite image only roughly defined this area. The satellite image defined a more vigorous area in the north, similar to the pattern of the ground-based sensor. General patterns of vigor were expressed by the satellite image, but finer detail was available from the ground-based sensor.

2.5 SUMMARY

Sugar beet canopy images are being used to reduce N application rates to crops that immediately follow sugar beet in rotations. Aerial photographs appear to be most related to the developed relationship between sugar beet canopy color and the amount of N to credit subsequent crops. However, satellite NDVI images are much more easily and economically obtained. Use of GIS has made the application of this relationship practical for large numbers of growers and acreage. Use of ground-truth to establish a general relationship between sugar beet canopy color with relative greenness is an important component of this process. GIS aids in locating specific areas of vigor/greenness during ground-truth, and transfer of this spatial information to be used in an N fertilizer variable-rate application map.

The N credit zone map is also being used as a template for residual nitrate soil sampling throughout the rotation. Use of these zones to direct soil sampling has resulted in lower residual soil N levels when the field is again seeded to sugar beets, which increases the likelihood of high sugar beet quality and grower profitability.

Use of a ground-based sensor appears to be promising in the development of the sugar beet canopy greenness and N availability relationship. Ground-based sensors can be used the day of harvest, in contrast to images obtained sometimes months before the canopies are actually returned to the soil. Ground-based sensors also measure a much smaller resolution, resulting in better definition of N credit zones. Measurement of canopy height increased the relationship between NDVI readings and N content with the ground-based sensor. Use of GIS will be very useful in the application of ground-based imagery to variable-rate N application.

ACKNOWLEDGMENTS

Most of this work was funded by the Sugarbeet Research and Education Board of Minnesota and North Dakota. Additional funding was supplied by EPA-319 grants and through the North Dakota office of USDA-NRCS.

REFERENCES

1. Headden, W.P., Deterioration in the quality of sugarbeets due to nitrates formed in the soil, *Col. Agr. Exp. Sta. Bull.*, 183, 179, 1912.
2. Giles, J.F., Reuss, J.O., and Ludwick, A.E., Prediction of nitrogen status of sugarbeets by soil analysis, *Agron. J.*, 67, 454, 1975.
3. Moraghan, J.T., Sugar production and soil nitrate, in *1979 Sugarbeet Research and Extension Reports*, Sugarbeet Research and Education Board of Minnesota and North Dakota, 10, 1980, 119.
4. Crohain, A. and Rixhon, L., Practical fertilizer value of sugarbeet tops (La valeur fertilisante pratique des feuilles et collets de betterave sucriere), *Bull. Rech. Agron. Gembloux*, 2, 397, 1967.
5. Moraghan, J.T. and Smith, L.J., Nitrogen in sugarbeet tops and the growth of a subsequent wheat crop, *Agron. J.*, 88, 521, 1996.

6. Moraghan, J.T. et al., Canopy reflectance and GPS technology in relation to sugar production, in *1996 Sugarbeet Research and Extension Reports*, Sugarbeet Research and Education Board of Minnesota and North Dakota, 27, 1997, 121.
7. Moraghan, J.T., Testing a new precision farming technique involving sugarbeet tops in growers fields, in *1997 Sugarbeet Research and Extension Reports*, Sugarbeet Research and Education Board of Minnesota and North Dakota, 28, 1998, 120.
8. Moraghan, J.T., A successful application of a new precision farming technique by a sugarbeet grower, in *1998 Sugarbeet Research and Extension Reports*, Sugarbeet Research and Education Board of Minnesota and North Dakota. 29, 1999, 120.
9. Sims, A.L., Moraghan, J.T., and Smith, L.J., Spring wheat response to fertilizer nitrogen following a sugar beet crop varying in canopy color, *Prec. Agric.*, 3, 283, 2002.
10. Jenks, G.F. and Coulton, M.R., *International Yearbook of Cartography*, 3, 119, 1963.
11. Franzen, D.W. et al., Summary of four years of research on poor quality sugarbeets in a sugarbeet, spring wheat, potato rotation, in *2001 Sugarbeet Research and Extension Reports*, Sugarbeet Research and Education Board of Minnesota and North Dakota, 32, 2002, 152.
12. Shanahan, J., personal communication, 2004.

3 Using Historical Management to Reduce Soil Sampling Errors

David E. Clay, N. Kitchen, C. Gregg Carlson, Jonathan Kleinjan, and Jiyul Chang

CONTENTS

3.1 Executive Summary.....	49
3.2 Introduction	50
3.3 Methods	50
3.4 Results	51
3.4.1 Impacts of Homesteads and Other Human Factors on Nutrient Variability.....	51
3.4.2 GIS Application	53
3.4.3 Summary Effects of Humans on Nutrient Variability.....	62
3.5 Summary.....	62
Acknowledgments.....	63
References.....	63

3.1 EXECUTIVE SUMMARY

Many of the small farms that dotted the countryside a hundred years ago had enclosures where horses, cows, and hogs were kept. The remnants from these enclosures impact soil properties today. Management that occurred on these farms 50 or even 100 years ago influences our ability to collect representative soil samples. Aerial photographs stored by USDA Farm Services Agronomy offices provide clues to past management. The objectives of this chapter are to (1) demonstrate the importance of considering the impact of human activities on collecting representative soil samples and (2) provide a data set that can be used as a GIS application for testing these concepts. The data set consists of data collected from a grid-soil-sampled field located in South Dakota. Historical aerial photographs provide a view of prior uses of the land. A comparison between prior uses and current soil nutrient concentrations showed that when considering immobile soil nutrients like P and K, farmers and agricultural consultants need to realize that fields maintain a memory. Old homesteads should be sampled separately from the rest of the field. Other human-induced factors that should be considered include fence lines and rotational

sequence. Isolating areas impacted by historical management prior to soil sampling is paramount for developing reliable crop nutrient plans. Including samples from old homesteads may compromise the resulting fertilizer recommendation. Although not directly considered in this chapter, it is important to point out that soil properties, such as landscape position, pH, drainage, and soil texture, which are not directly impacted by man, also influence soil variability and soil test results.

3.2 INTRODUCTION

Most fertilizer recommendation programs contain the crucial steps of collecting representative soil samples, accurate and precise laboratory analysis, and using a well-calibrated fertilizer recommendation model to estimate fertilizer recommendations. It is often assumed that collecting a soil sample is trivial. This is not so. Obtaining accurate and representative soil samples is the basis for soils-based fertilizer recommendations.

A representative soil sample is one that adequately portrays the nutrient content of the area sampled. There are several excellent papers that review various aspects of soil sampling protocols.¹⁻¹⁴ These papers recommend that (1) soil sampling protocols should consider how the fertilizer is applied, (2) at least 12 to 20 cores should be combined into a single sample, and (3) individual samples should be collected from sub-field areas where differential management occurred. As a rule, the difficulty of obtaining a representative sample increases with variability. Fertilizing highly variable fields based on a single composite sample can result in substantial areas that are under-fertilized and other areas that are over-fertilized.

Clay et al.¹¹ proposed four specific guidelines for soil sampling fields impacted by prior management. First, crop producers need to keep track of where fertilizers containing immobile nutrients are band applied. Band application can cause small-scale variability for many years. To avoid over-sampling fertilizer bands, sampling protocols for fields with residual bands should be followed. Second, sample areas where animals were confined separately from the rest of the field. Third, whenever possible avoid soil sampling guess rows (i.e., edge rows of planter passes). Fourth, recommendations are improved by including at least 15 to 20 individual cores in a composite sample. Failure to follow these guidelines can increase the probability of inaccurate fertilizer recommendations. This chapter demonstrates the impacts of human activities on soil nutrient variability and provides exercises for calculating sampling requirements for $\text{NO}_3\text{-N}$ (nitrate-N) and soil test P and K.

3.3 METHODS

Grid soil samples were collected from fields located in South Dakota and Missouri. Soil samples from the 0–6 inch depth in all fields were collected from at least a 200 by 200 foot grid. Samples from South Dakota were analyzed for $\text{NO}_3\text{-N}$, Olsen-P, and ammonium acetate extractable-K,¹¹ while samples from Missouri were analyzed for Bray-1 extractable-P and ammonium acetate extractable-K.¹⁴ Results from soil test analysis were used to develop fertilizer recommendations for N, P, and K. The

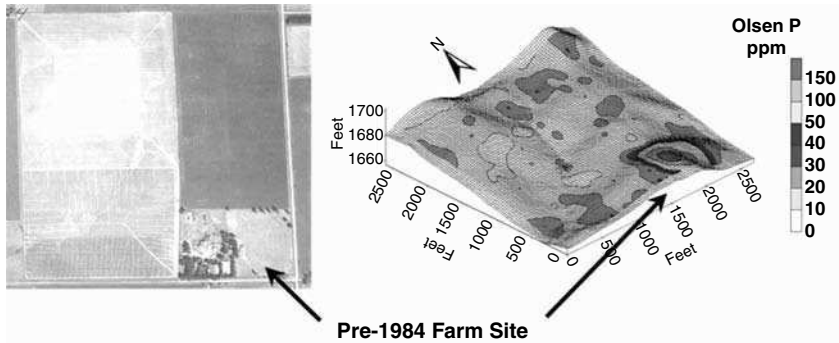


FIGURE 3.1 Aerial images collected from a South Dakota field in 1956 and a soil P contour map based on soil samples collected in 1997. Current images show that the farmsite has been removed from the field. The aerial image collected in 1956 was obtained from the USDA-NRCS.

South Dakota fields were located in the eastern side of the state while the Missouri field was located in the north-central part of the state. Parent materials in the South Dakota sites were glacial till or loess while at the Missouri site the soil was a well-weathered loess with a pronounced clay pan. Elevation and apparent electrical conductivity surveys were conducted in all fields.¹⁵⁻¹⁷ Historical aerial photographs were obtained from the USDA Farm Service Agency offices. These photographs were used to identify a number of different features including field boundaries, locations of home sites, and the location of animal confinement areas. Figures 3.1 and 3.2 show examples of these photographs. Historical aerial photographs were georeferenced and the boundaries for historical management zones identified in ArcView (ESRI, Redland, California). Based on this classification, data sets for the different management zones were developed.

Composite soil sampling requirement (n) was calculated using the equation

$$n = t^2 s^2 / D^2 \quad (3.1)$$

where t is the value associated with a specific probability level (P) and degrees of freedom (df) ($1.28, = 0.20, df = \infty$), s is the standard deviation, and D is the desired confidence interval.¹⁸ The mean and standard deviation were both calculated using Microsoft Excel (Microsoft Corp., Redmond, Washington).

3.4 RESULTS

3.4.1 IMPACTS OF HOMESTEADS AND OTHER HUMAN FACTORS ON NUTRIENT VARIABILITY

Sampling protocols that consider historical management are important, particularly in fields where farm animals were wintered or fed. Soil samples taken within these

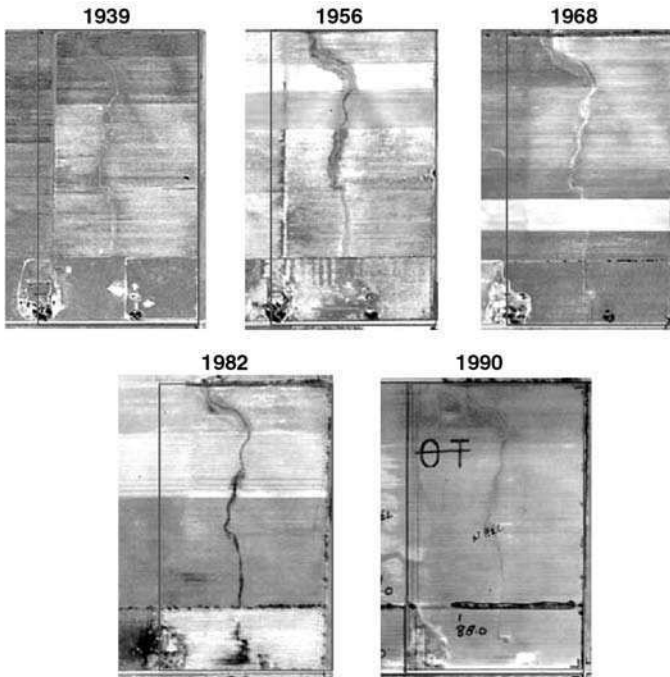


FIGURE 3.2 A sequence of aerial images collected between 1939 and 1990 from a Missouri field.

areas may have elevated P and K levels for decades after the animals have been removed. For example, a survey of 13 grid-soil-sampled fields in South Dakota showed that excluding the old farmsteads from the composite sample reduced the sampling error (smaller confidence interval) and soil test P level (Table 3.1). These results were attributed to very high soil nutrient concentrations in the area of the old homesteads (Figure 3.1).

Most fields have experienced new management strategies over time that are not consistent with current management (Figures 3.1 and 3.2). Over the years, field sizes, farming direction, locations of fences, rotations, and fertility programs can change. It is difficult to provide guidance on which historical management practices should be considered and which ones can be ignored. Assessments need to be conducted on a field-by-field basis. Prior to 1960, in much of the U.S. Midwest, field sizes were typically 16 ha or less. Aerial photographs clearly show that, over time, large fields have been produced by combining small fields (Figure 3.2). Based on historical rotations, fields can be separated into different management zones (Figure 3.3).

Understanding historical changes in management is important because row crops often received more fertilizer and lime than pastures, and manure was typically applied to fields close to the farmstead. Yield depression from soil compaction can be seen in some aerial photos and is associated with livestock paths, and machinery

TABLE 3.1
The influence of excluding the old farmstead on the 80% confidence interval (CI) associated on the soil test P results

Location	Site #	Soil Test P		CI, 50 Cores	
		Farmstead		Farmstead	
		Included	Excluded	Included	Excluded
		ppm	ppm	ppm	ppm
South Dakota	1	23	17	9.64	3.63
	2	32	16	22.24	3.29
	3	21	16	8.80	2.12
	4	42	20	16.43	6.55
	5	7	6	1.64	0.55
	6	7	7	1.45	1.10
	7	10	6	4.45	0.77
	8	40	27	11.08	5.17
	9	10	7	3.29	1.45
	10	13	12	2.79	2.19
	11	21	18	5.45	5.20
	12	16	12	6.02	4.62
Missouri	13	14	12	3.15	1.73

traffic between adjacent small fields. Soil erosion that results from many years of tillage influences topsoil depth and water holding capacity. Human-induced effects have a lasting impact on soil characteristics.

Prior to subdividing fields, a manager needs to ask the question, is the value of the spatial information that will be collected worth the cost of data collection? The cost of the information must be balanced with reduced yields associated with under fertilizing a given area of a field and the higher fertilizer costs associated with over fertilizing other areas of the field. In the field shown in Figure 3.3, subdividing the field based on historical sequence showed that the soil test results for the whole field, area-A, area-B, area-C, and area-D were 12, 10, 8, 11, and 20 ppm Bray-P, respectively. These results show that based on the Missouri P recommendations, the P recommendation for area B should be increased, while the recommendation for area D should be decreased.

3.4.2 GIS APPLICATION

The grid soils data from the South Dakota field were collected from a 100 × 200-ft grid. This data set is on the CD accompanying this book, labeled as *Chapter 3 nutrient data*. The file contains two data sets, each on a different sheet. One sheet is labeled “with homestead” and the other is labeled “without homestead.” The data set labeled “with homestead” contains 369 points and the data set labeled “without

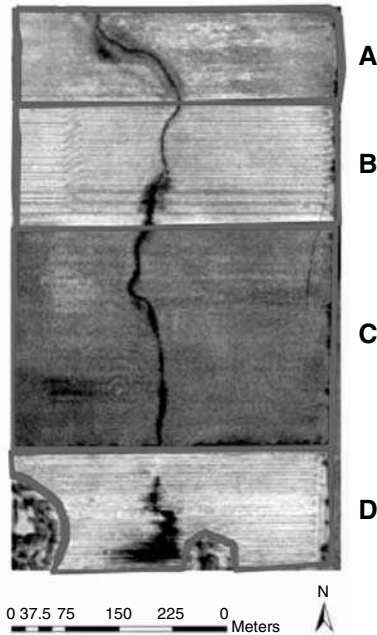


FIGURE 3.3 A 1982 aerial photo showing how polygons were drawn around four areas with different historical management practices. Two farmstead areas on the south end of the field were removed and the field divided as it was cropped in 1982.

homestead” contains 352 data points. The data set labeled “with homestead” contains all the data points in the field, while the data points from the homestead were removed from the “without homestead” data set. Columns in the data set represent relative (not actual) latitude and longitude values, elevation values as measured with a survey-grade global positioning system, the amount of $\text{NO}_3\text{-N}$ (lbs N acre^{-1}) contained in the surface 2 ft, the concentration (ppm) of Olsen P and ammonium acetate extractable K in the surface 6 inches, and pH, measured in water, for the surface 6 inches.

Exercise 1: In this exercise a correlation analysis will be conducted with Excel. The purpose is to evaluate relationships between the measured soil parameters. Correlation analysis is accomplished by (1) selecting **Tools, Data Analysis, and Correlation** on the menu bar (note: if your program does not have Data Analysis program under Tools it will need to be loaded from the Excel program disk to complete this example); (2) highlight all the cells from C4 to G372 with the mouse and click OK. The resulting table shows the strength of the linear relationship between the parameter in the data set (Table 3.2). Data in the table are called correlation coefficients, which are often reported as r values. Correlation coefficients have values that range from -1 to 1 . A value of one represents a perfect positive relationship, a negative one value represents a perfect negative relationship, while a value of zero represents no relationship. The relatively high correlation coefficient ($r = 0.68$) between P and

TABLE 3.2
Correlation matrix developed in Microsoft Excel. The data set used in this analysis was Chapter 3 nutrient data/with homestead.

	Elevation	Nitrate	P	K	pH
Elevation	1				
Nitrate	-0.06	1			
P	-0.21	0.31	1		
K	-0.02	0.20	0.69	1	
pH	-0.41	0.11	0.33	0.20	1

K suggest that locations with high P have high K. The negative relationship between elevation and pH suggests that areas with high elevation have low pH. Similar analysis should be conducted on the data set without the homestead.

Questions: What are the differences between the two data sets? Why is the apparent relationship between P and K weaker in the “without homestead” than the “with homestead” data set?

Answer: The old homestead had very high P and K concentrations. Removing these points from the data set weakened the apparent relationship between P and K. This analysis suggests that the old homestead still impacts the measured soil parameters. Soil pH and elevation were negatively correlated in both data sets. Removing the old homestead points from the data set had little effect on the resulting correlation coefficient. The negative relationship was the result of high pH values being generally found in footslope areas while low pH values were found in summit/shoulder areas. This spatial pattern was the result of water leaching salts, including calcium carbonate (lime), from summit/shoulder areas. In footslope areas, calcium carbonate was transported from the groundwater to surface soil with capillary water. Lime is a material that is added to low pH soils to increase the soil pH value.

Exercise 2: In this exercise the influence of the old homestead on nutrient variability will be explored. This information is used to assess sampling requirements as calculated in Equation 3.1. In the “with homestead” data set, type **=stdev(D4:D372)** in cell D373, and then copy this value to cells E373, F373, and G373. The value in cell D373 should be 22.85. This value represents the standard deviation of the column of numbers. The variance is then determined by squaring this value. In cell D374 type **=(1.28^2)*D373^2/5^2**.

This expression is the Excel version of Equation 3.1. The value of 1.28 is the t value associated with a probability of 80% (= 0.10) and a very large number of degrees of freedom (df = number of observation – 1, or 369 – 1). D373 is the standard deviation described above, and 5 is the desired confidence interval. The ^2 symbol squares the value. This equation then can be copied to cell E374, F374, and G374. For these other parameters a different D (desired confidence interval) may be desired.

For $\text{NO}_3\text{-N}$, values in D373 and D374 are 22.85 and 34.23. The value of 34 indicates that 34 individual cores should be combined into a single sample, in order for the mean composite sample to be within 5 lb N acre⁻¹ 80% of the time. The influence of the old homestead on nutrient variability is assessed by comparing the standard deviations or the variances of the data sets with and without the homestead.

Questions: How did the old homestead influence the soil $\text{NO}_3\text{-N}$, P, K, and pH standard deviations? Which nutrient had the highest sampling requirement? How did the desired confidence interval influence the composite core sampling requirement?

Answer: The homestead has a large influence on the P and K standard deviations and a relatively small impact on $\text{NO}_3\text{-N}$ and pH standard deviations. These results were attributed to the relatively immobile nutrients (P and K) sticking to the soil (applied to soil with manure from animal enclosures located near the homestead) while the mobile nutrient ($\text{NO}_3\text{-N}$) is soluble and did not stick to the soil matrix. The sampling requirement was dependent on the desired confidence; decreasing the desired confidence interval increased the sampling requirement.

Exercise 3: The data provided in the data set can be used to develop topographic relief maps and nutrient contour maps. A number of different software applications can be used to accomplish this task. The P nutrient contour map overlaid on an elevation map is shown in Figure 3.1. Similar maps should be developed for $\text{NO}_3\text{-N}$, K, and pH.

Question: How are the maps for the different nutrients different? To see the spatial variation of soil nutrients, the ArcView program can be used to develop 2-D or 3-D contour maps using spatial data sets.

Answer: The following provides detailed information for developing a 3-D soil test-K contour map using ArcView 3.3, which includes Spatial Analyst 1.1 and 3D Analyst 1.1 extensions.

This exercise is accomplished by following the series of steps below. The spatial data set used in this exercise is *chapter 3 nutrient data* on the CD accompanying this book.

Step 1: Open the data file with the Excel program. The Excel file format must be converted to tab delimited text (.txt) file format. The text file should have one head row at the top of the data. The head row should not include dashes, commas, periods, or spaces. In the data file, the top two rows must be removed and the head of the fourth column ($\text{NO}_3\text{-TOTAL}$) needs to be changed to NO_3_TOTAL in the “with homestead” data. Modify the “without homestead” data the same way. Save them as two text files (*with*

homestead and *without homestead*) on your hard drive (you need to save these files in a separate folder for this exercise).

Step 2: Open ArcView 3.3. To activate Spatial Analyst and 3D Analyst extensions, in the **Project** window, go to **File** in the menu bar and click **Extensions**. In the **Extensions** dialog box, check the boxes for 3D Analyst and Spatial Analyst and click OK. Now, you are ready to use ArcView. In the **Project** window, open the text file by clicking on **Project/Add Table** in the menu bar and find the text file from Step 1. In the **Add Table** dialog box, make sure that List Files of Type is Delimited Text [*.txt], choose the text file, and click OK. When the table is open, the table window can be closed. For further steps, save this project as a GIS_Exercise by selecting **Save Project As** under **File** in the menu bar. Then the name of project box changes from *Untitled* to *gis_exercise.apr* (Figure 3.4).

Step 3: Open the **View** window by clicking **New** in the GIS exercise project box. To open point data, in the **View** window, select **View** in the menu bar and click **Add Event Theme**. In the **Add Event Theme** dialog box, choose the file name (*chapter 3 nutrient data.txt*), X (Long_m), and Y (Lat_m) variables by clicking the buttons on the right of each option. Now you can see a point theme name on the left of the **View** window. Check the box in

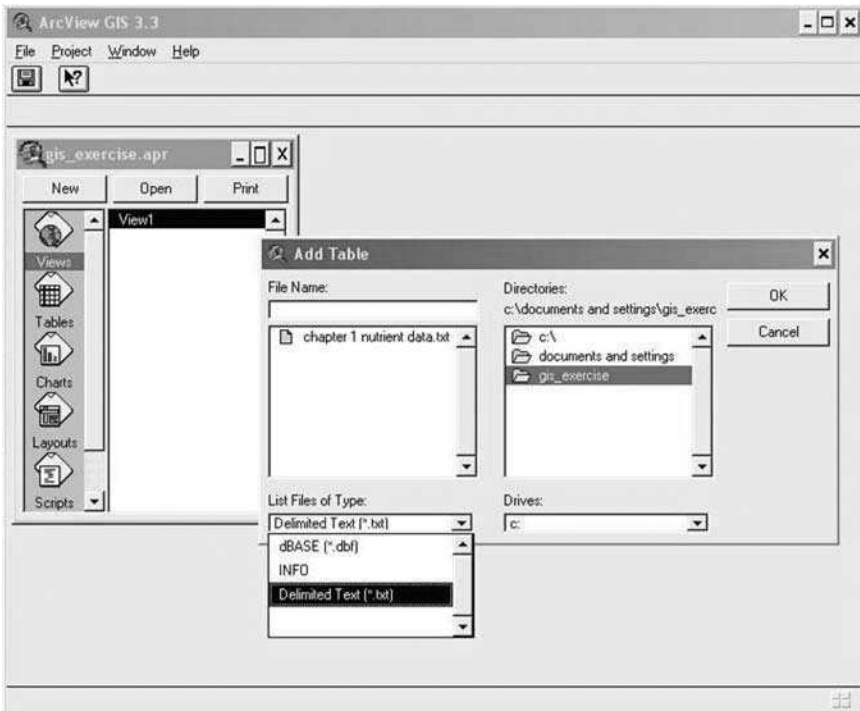


FIGURE 3.4 ArcView 3.3 screen after step 2.

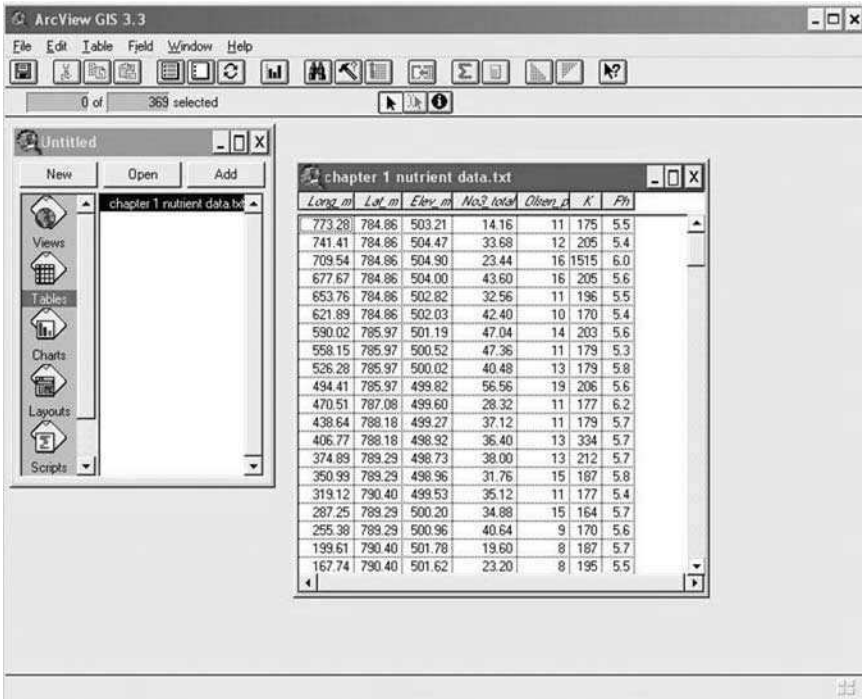


FIGURE 3.5 ArcView Screen after step 3.

front of the theme name, then the point data is displayed in the **View** window (Figure 3.5).

Step 4: To create a 2-D contour map, go to **Surface** in the menu bar and click **Interpolate Grid**. Make sure that the point theme name is activated (when you click the theme name once, a box appears around the theme name). In the **Output Grid Specification** dialog box, choose **Same As chapter 3 nutrient data.txt** in **Output Grid Extension** option and click OK (Figure 3.6). Other options (Output Grid Cell Size, Number of Rows, and Number of Columns) could be changed, but the default creates general contour maps. Increasing Output Grid Cell Size decreases the Number of Rows and Number of Columns, and generates a rough contour map. In the **Interpolate Surface** dialog box, choose IDW (inverse weight distance) for **Method** and K for **Z Value Field** by clicking the buttons and choosing **Nearest Neighbor** (Figure 3.7). Other options (No. of Neighbors, Power, and Barriers) could also be changed, but the default creates general contour maps. You can see the new surface theme name (*Surface from chapter 3 nutrient data.txt*) on the left of the **View** window (Figure 3.8). Check the box in front of the theme name, then the contour map is displayed in the **View** window.

Step 5: To create a 3-D contour map using the elevation data, create an elevation contour map following Step 4. Choose elevation data (*Elev_m*)

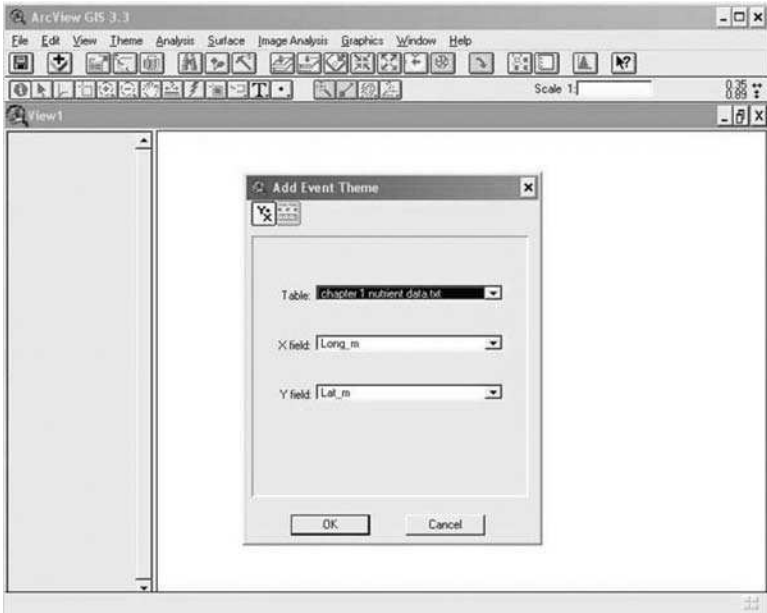


FIGURE 3.6 ArcView 3.3 screen before clicking OK in step 4.

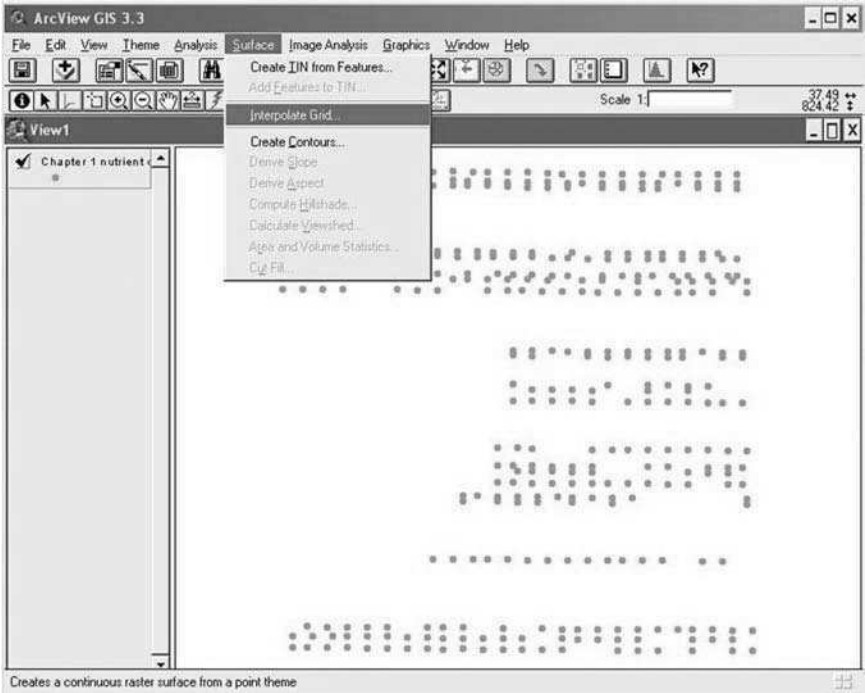


FIGURE 3.7 ArcView 3.3 screen when interpolated grid is selected in step 4.

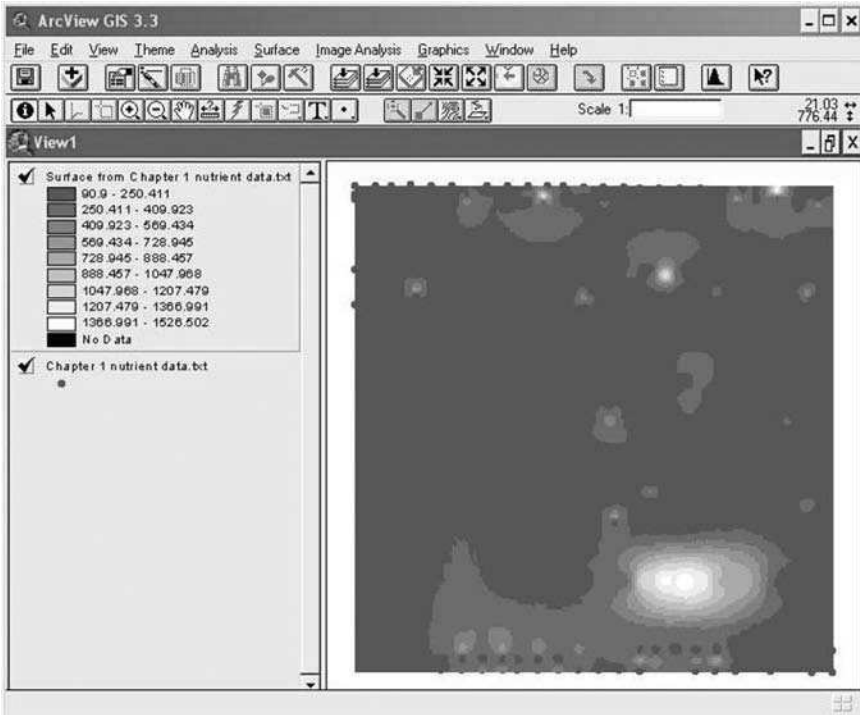


FIGURE 3.8 ArcView screen at the completion of step 4.

for the **Z Value Field** in the **Interpolate Surface** dialog box to develop a surface map. You can see the new surface theme name (*Surface from chapter 3 nutrient data.txt*) on the left of the **View** window. The name of the theme is the same as the surface theme of K, but the range of classes is different. After developing the elevation surface map, go to **Theme** in the menu bar and click **Convert Grid to TIN**. Make sure that the elevation surface theme name is activated. In the **Convert Grid to TIN** dialog box, keep the deflate value for a general TIN map. When you increase this value, you get a denser TIN map. Save the file in the folder created in the **Output TIN Name** dialog box (you can save the file with any name, but in this exercise the file name is *elev*). You can see the new TIN theme name (*Elev*) on the left of the **View** window. Check the box in front of the TIN name and the TIN map is displayed in the **View** window (Figure 3.9).

Step 6: To show the 3-D map, go to **View** in the menu bar and click **3D Scene**. Make sure that only the K surface theme is checked (remove checks from other theme names). In the **3D Theme** dialog box, choose **Theme** and click OK. Now the **3D Scene** window is open and the soil test-K contour map is displayed. You can change the background color from black to white to see the map more clearly. Go to **3D Scene** in the menu bar and click **Properties**. In the **3D Scene Properties** dialog box, click **Select** in the **Background Color** option, choose color, click OK, and click OK once

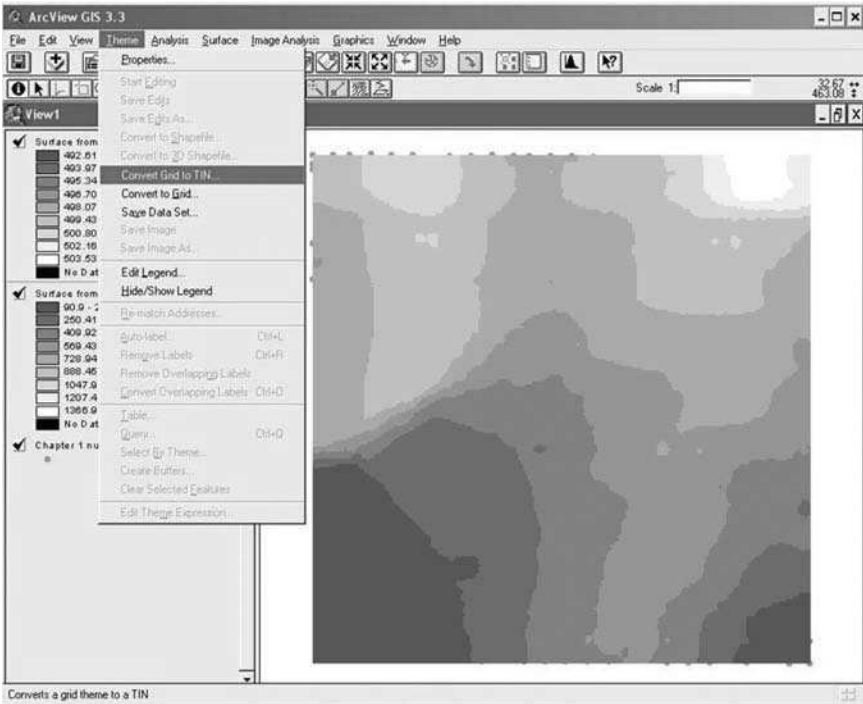


FIGURE 3.9 ArcView 3.3 screen showing the 2-D elevation map

more. To superimpose the soil test-K contour map on the topography map, go to **Theme** in the menu bar and click **3D Properties**. In the **3D Theme Properties** dialog box, check **Surface in Assign Base Heights By**, choose the *elevation.tin* file created, and click OK. (If you do not find the *elevation.tin* file in the list, click the **open file** icon at **Surface** option. In the **Get Source** dialog box, choose TIN in **Source Types**, find the *elevation.tin* file from the folder, and click OK. You can see the *elevation.tin* file from the list of **Surface**. Now, choose the TIN file.) Increase the value Z Factor to make more relief on the 3-D map. In this exercise, when you change the Z Factor to 20, landscapes can be seen; click OK at the bottom (Figure 3.10). After closing the dialog box, the map will disappear from the window, then click the **Zoom to Full Extent** icon at the top of the **3D Scene** window. Now the 3-D soil test-K contour map superimposed on the topography map can be seen. The 3-D map can be moved in any direction: put the cursor on the 3-D map, left-click and hold and move. This exercise should be repeated for $\text{NO}_3\text{-N}$.

Answer: For the relatively immobile nutrients (P and K) their concentrations were very high in the old homestead (Figures 3.1 and 3.10). This was not the case for the mobile nutrient ($\text{NO}_3\text{-N}$). Landscape differences were

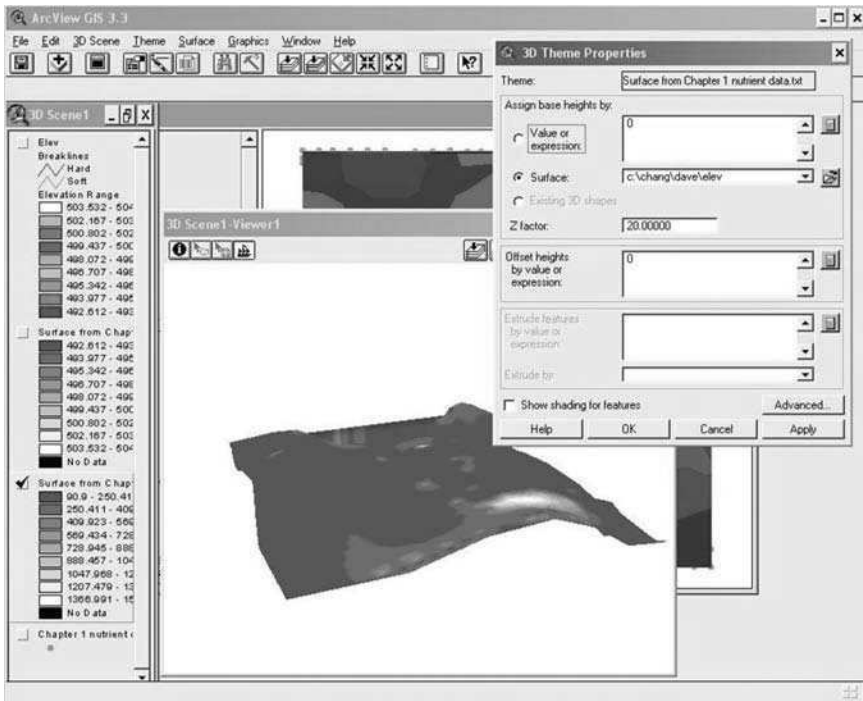


FIGURE 3.10 ArcView 3.3 screen showing the soil test K values superimposed on the topography map.

apparent for soil pH. However, landscape differences were not apparent for P, K, and $\text{NO}_3\text{-N}$.

3.4.3 SUMMARY EFFECTS OF HUMANS ON NUTRIENT VARIABILITY

The above example and exercises show that nutrient variability and the confidence interval of composite samples by nutrient are influenced by old homesteads. Nutrients that are more likely to be sorbed (K and P) on soil are more likely to be elevated in soil collected from old homestead areas than anions ($\text{NO}_3\text{-N}$) that leach. This example shows that (1) the first step in collecting reliable soil samples for fertilizer recommendation is to identify and sample old farmsteads separately from the rest of the field; (2) it is difficult to obtain representative soil samples if samples from old home sites are included in the composite sample; and (3) if samples from these areas are combined with other field areas, the fertilizer recommendation may be compromised.

3.5 SUMMARY

A consequence of increasing farm and equipment sizes is homestead removal. For example, in Brookings County, South Dakota, a random survey of 384 quarter sections in aerial photographs collected in 1950 and 1990 showed that the number

of quarter sections with building sites decreased from 218 to 180 over the 40 years. The location of the farmsteads removed from fields was not random but was directly related to land productivity. The higher the land productivity, the more likely the farmstead was removed. Given the number of management changes that have occurred in production fields over the past 100 years, it is difficult to provide step-by-step guidance for developing sampling protocols that account for historical management. When considering immobile soil nutrients like P and K, farmers and agricultural consultants need to realize that fields maintain a memory. Old homesteads should be sampled separately from the rest of the field. Other human-induced factors that should be considered include fence lines and rotational sequence. Isolating areas impacted by historical management prior to soil sampling is paramount for developing reliable crop nutrient plans. A first step in all sampling protocols is to identify old homesteads and sample them separately from the rest of the field. Including these samples in the composite sample may compromise the resulting recommendation. Although not directly considered in this paper, it is important to point out that soil properties, such as landscape position, pH, drainage, and soil texture, which are not directly impacted by man, also influence soil variability and soil test results.

ACKNOWLEDGMENTS

Support for research presented in this chapter was provided by United Soybean Board, North Central Soybean Board, South Dakota Corn Utilization Council, South Dakota Soybean Research and Promotion Council, Upper Midwest Aerospace Consortium (UMAC) NASA, and USDA-CSREES Grout 2004–51130–02248. Mention of trade names or commercial products in this chapter is solely for the purpose of providing specific information and does not imply recommendation or endorsement by the U.S. Department of Agriculture.

REFERENCES

1. Kitchen, N.R., Havlin, J.L., and Westfall, D.G., Soil sampling under no-till banded phosphorus, *Soil Sci. Soc. Am. J.*, 54, 1661, 1990.
2. Blackmer, A.M. et al., Estimating nitrogen needs for corn by soil testing, *PM 1381* Iowa State University Extension, Ames, Iowa, 50011, 1991.
3. Buchholz, D.D., How to get a good soil sample, Missouri agricultural publication g09110, University of Missouri, 1993. Available online at <http://muextension.sim-mouri.edu/splo/agguides/soil/g09110.htm>. Accessed 5/6/02.
4. Skopp, J., Kachman, S.D., and Hergert, G.W., Comparison of procedures for estimating sampling numbers, *Commun. Soil Sci. Plant Anal.* 26, 2559, 1995.
5. Clay, D.E. et al., Soil sampling strategies for estimating residual nitrogen. *J. Prod. Agri.*, 10, 446, 1997.
6. Franzen, D. and Cihacek, L.J., Soil sampling as a basis for fertilizer application, NDSU Extension Service, SD 990, 1998. Available online at <http://www.sbreb.org/brochures/soilsampling/soilsamp.htm>. Accessed 5/6/02.

7. Franzen, D., Site-specific farming — #2 soil sampling and variable-rate fertilizer application, North Dakota State University, 1999. Available online at <http://www.ext.nodak.edu/extpubs/plantsci/soilfert/sf1176-2.htm>. Accessed 5/6/02.
8. Fleming, K.L., Westfall, D.G., and Wiens, D.W., Field testing of management zones for VRT, SSMG-21, in *Site Specific Management Guidelines*, Potash and Phosphate Institute, 1999. Available online at <http://www.ppi-far.org/ssmg>.
9. Franzen, D.W. and Kitchen, N.R., Developing management zones to target nitrogen applications, SSMG-5, in *Site Specific Management Guidelines*, Potash and Phosphate Institute, 1999. Available online at <http://www.ppi-far.org/ssmg>.
10. Ferguson, R.B. and Hergert, G.W., Soil sampling for precision agriculture. Univ. Neb. Exten. EC 154, 2000. Available online at <http://www.ianr.unr.unl.edu/pubs/soil/ec154/ec154.html>. Accessed 5/6/02.
11. Clay, D.E. et al., Collecting representative soil samples for N and P fertilizer recommendations, *Crop Manag.* doi:10.1094/CM-2002-12XX-01-MA, 2002. Available online at <http://www.plantmanagementnetwork.org/pub/cm/management/np/>.
12. Chang, J. et al., Different techniques to identify management zones impact nitrogen and phosphorus sampling variability, *Agron. J.*, 95, 1550, 2003.
13. Clay, D.E., Carlson, C.G., and Chang, J., Identifying the “best” approach to identify nutrient management zones: a South Dakota example, in *Site Specific Management Guidelines*, SSMG-41, Potash and Phosphate Institute, Norcross, GA, 2004. Available online at <http://www.ppi-far.org/ssmg>.
14. Brown, J.R. and Rodriguez, R.R., Soil testing in Missouri: a guide for conducting soil tests, in *Missouri. Exten. Cir. 923*, Univ. of Missouri Extension Division, Columbia, Missouri, 1983.
15. Johansen, D.P., et al., Vertical accuracy of two differential corrected global positioning systems, *J. Soil Water Con.*, 56, 198, 2001.
16. Lund, E.D., Christy, C.D., and Drummond, P.E., Practical applications of soil electrical conductivity mapping, in *Precision Agriculture '99- Proc. of the 2nd Eur. Conf. on Precision Agriculture, Odense Congress Centre, Denmark, 11–15 July 1999*, Stafford, J.V., Ed., SCI, Sheffield, UK, 1999, 771.
17. Kitchen, N.R. et al., Soil electrical conductivity and topography related to yield for three contrasting soil-crop systems, *Agron. J.*, 95, 483, 2003.
18. Stein, C., A two sample test for a linear hypothesis whose power is independent of the variance, *Ann. Math. Stat.*, 16, 243, 1945.

4 Developing Productivity Zones from Multiple Years of Yield Monitor Data

*Jonathan Kleinjan, David E. Clay,
C. Gregg Carlson, and Sharon A. Clay*

CONTENTS

4.1 Executive Summary.....	65
4.2 Introduction	66
4.3 Methods	66
4.3.1 Background.....	66
4.3.2 Cleaning Yield Monitor Data	67
4.3.3 Gridding Data	67
4.3.4 Statistical Calculations.....	67
4.3.5 Identifying Productivity Zones.....	69
4.3.6 Calculating Zone Impacts on Yield Variability	74
4.4 Results and Discussion.....	74
4.5 Conclusions	76
4.6 Exercise: Mapping Productivity Zones.....	77
4.6.1 Overview	77
4.6.2 File Formats	77
4.6.3 Mapping Productivity Zones	77
Acknowledgments.....	78
References.....	78

4.1 EXECUTIVE SUMMARY

The advent of relatively inexpensive and accurate global positioning systems along with combine yield monitors has provided the opportunity for agricultural producers to instantaneously record and map crop yields while harvesting. Yield is the ultimate integrator of landscape and climatic variability and therefore should provide useful information for identifying management zones. However, due to year-to-year cli-

matic variation, it is difficult to identify useful management zones based on a single year's yield map. Increasing the number of years used to define zones may be a solution to this problem. This chapter demonstrates a technique to define a type of management zone known as a productivity zone based on multiple years of yield monitor data and discusses the percentage of yield variability explained by the zones. The procedure to identify productivity zones involves removing erroneous data or "cleaning" the yield data sets, creating common grid cells across years, and calculating yield and standard deviation maps. "Average" maps created from multiple years of yield monitor data may be used to determine yield goals and fertilizer recommendations, while standard deviation maps may be used to identify areas requiring corrective management. The yield variability in productivity zones that incorporated both standard deviation and average yield data was, on average, 43% lower than total field variability over four years.

4.2 INTRODUCTION

Producers who have been collecting yield monitor data for multiple years have begun to ask "How can we use our yield data to improve management?" These data sets may be combined to define a type of management zone known as a productivity zone. There are at least two different approaches proposed for identifying productivity zones. The first approach is to calculate the impact of zone boundaries on fertilizer recommendations. Chang et al.¹ reported that landscape-specific yield goals, combined with grid-cell sampling, can be used to improve N and P fertilizer recommendations by 35% and 59%, respectively. This approach requires that a model be used to calculate fertilizer recommendations and that extensive soil sampling be conducted to define initial soil conditions. A second approach is to determine the impact of productivity zones on yield variability.²⁻⁵ This approach assumes that the best zone delineation method minimizes yield variability. For example, Fridgen et al.⁴ reported that management zones based on elevation reduced yield variability by 80%. The objectives of this chapter are to present a case study demonstrating an approach for determining productivity zones in a 160-acre field located in eastern South Dakota, to provide a georeferenced, cleaned, and gridded yield monitor data set for multiple crop years (1996, 1998, 2000, 2002), and to provide an exercise in mapping productivity zones using ArcView[®] software (ESRI, Redlands, California).

4.3 METHODS

4.3.1 BACKGROUND

The field used in this case study is located in east-central South Dakota. The crop rotation at the site is corn (*Zea mays* L.) followed by soybean (*Glycine max* L. Merr.). The corn yield data collected in 1996, 1998, 2000, and 2002 were used in this example. Fertilizers and pesticides were applied as needed. Tillage methods have been either no-tillage (1996 and 1998) or strip-tillage (2000 and 2002). Average yields in 1996, 1998, 2000, and 2002 were 103, 167, 141, and 92 bu ac⁻¹, respec-

tively. Low yields in 1996 were due to cool and very wet conditions while low yields in 2002 were due to caused severe lodging caused by strong winds.

4.3.2 CLEANING YIELD MONITOR DATA

In order to be confident about yield information, it is necessary to remove erroneous data points.^{5,6} Yield monitor data sets normally contain values that are incorrect. For example, erroneous data can be collected when harvest swaths are not the full header width, the combine's speed is rapidly changing, or at points near the end rows. Cleaning the data removes problem values and can improve the ability to explain yield variability. From a visual perspective, removing erroneous data may have little impact upon the appearance of yield maps. However, from an analytical perspective, removing erroneous data may have a significant impact upon our ability to compare the data to other information layers within a decision support system. Cleaning yield monitor data is necessary for accurate management decisions. Programs available for cleaning yield monitor data are Field Analyst, available at <http://plantsci.sdstate.edu/precisionfarm/paper/publicationSoftware.aspx>, and DM-Comp Software (Chapter 10) Yield Editor 1.00, available at www.fse.missouri.edu/ars/decision_aids.htm. Field Analyst and Yield Editor 1.00 can clean either AgLeader® (AgLeader, Chicago, Illinois) advanced file or Greenstar® (Deere, & Company, Moline, Illinois) text file formats. Field analyst is included under the Chapter 4 directory on the CD accompanying this book.

4.3.3 GRIDGING DATA

To analyze multiple years of data, it is necessary to convert the yield data to a common coordinate system because yield monitor data recorded from the same field for multiple years do not necessarily have the same coordinates. One technique to accomplish this task is to identify grid cells. Field Analyst converts multiple years of yield data to a common grid-cell format by (1) calculating the maximum and minimum latitude and longitude for a field, (2) selecting a desired grid-cell size, and (3) determining the average yields for each grid cell. This case study used a grid-cell size of 45 × 45 feet. This corresponds to three times the combine header width (15 ft.). A 45 × 45-foot grid-cell size results in over 3400 grid cells in a 160-acre field. The assigned grid-cell values are the average of all yield data that fall within the boundaries of the grid cell. A sample data set produced by Field Analyst is shown in Table 4.1. This sample data set is included with this case study. For each grid cell, Field Analyst calculates a cell designation (Row #, Column #), the latitude and longitude coordinates in decimal degrees, feet, and meters (to the center of the grid cell), the number of yield measurements, and average yield value within each grid cell.

4.3.4 STATISTICAL CALCULATIONS

To calculate the standard deviation for a given grid cell, it may be necessary to convert yields from different crops to a common scale. Converting yields to a common scale allows yields of corn, soybeans, wheat, or any other crop to be directly

TABLE 4.1
A portion of a Field Analyst output file with grid-cell locations, counts, and average yields for four years of corn yield data

Row _No	Column _No	Longitude	Long_ Feet	Latitude	Lat_ Feet	Counts	Elevation (feet)	Counts	Corn96 Counts	Corn98 Counts	Corn00 Counts	Corn02 Counts			
1	1	-96.66	22.50	44.22	22.50	15	1660.48	9	111.35	9	176.87	15	151.40	9	110.72
1	2	-96.66	22.50	44.22	67.50	14	1660.68	26	112.98	10	176.25	8	156.60	10	95.43
1	3	-96.66	22.50	44.22	112.50	13	1660.28	20	107.71	13	217.89	10	155.27	8	89.88
1	4	-96.66	22.50	44.22	157.50	5	1659.72	5	114.23	2	212.60	6	153.29	3	106.48
1	5	-96.66	22.50	44.23	202.50	7	1659.09	20	115.57	16	204.69	9	165.56	12	112.79
1	6	-96.66	22.50	44.23	247.50	6	1658.46	3	109.43	2	216.24	4	186.51	2	110.30
1	7	-96.66	22.50	44.23	292.50	7	1657.81	28	140.38	15	207.91	15	183.71	15	105.00
1	8	-96.66	22.50	44.23	337.50	7	1657.15	22	97.93	2	226.14	14	184.03	15	103.47
1	9	-96.66	22.50	44.23	382.50	7	1657.23	28	125.86	11	222.65	14	186.52	14	103.47
1	10	-96.66	22.50	44.23	427.50	7	1657.64	21	136.68	11	216.81	14	170.89	18	110.49
1	11	-96.66	22.50	44.23	472.50	6	1658.07	20	126.84	11	215.48	14	164.53	19	143.61
1	12	-96.66	22.50	44.23	517.50	8	1658.42	25	121.93	15	213.91	15	169.01	17	143.04
1	13	-96.66	22.50	44.23	562.50	7	1658.82	18	124.45	15	219.43	14	170.19	18	145.65
1	14	-96.66	22.50	44.23	607.50	8	1659.24	15	124.60	13	212.76	15	172.22	19	144.38
1	15	-96.66	22.50	44.23	652.50	7	1659.63	15	121.23	11	193.17	15	163.22	17	135.32
1	16	-96.66	22.50	44.23	697.50	7	1660.06	21	110.04	16	183.88	16	145.64	16	124.54
1	17	-96.66	22.50	44.23	742.50	7	1660.55	21	112.05	15	174.86	12	148.57	18	123.39
1	18	-96.66	22.50	44.23	787.50	8	1661.10	20	119.06	14	165.14	15	142.10	17	120.78
1	19	-96.66	22.50	44.23	832.50	7	1661.73	19	101.52	13	144.55	14	123.04	18	104.58

compared. It is important to point out that this normalization process is not necessary for all types of analysis. For example, in this study, only corn yield data were used and therefore, normalization is not required. An in-depth discussion of normalization methods is beyond the scope of this chapter. Basic statistics, such as multiple year average yields, standard deviations, and the coefficients of variation (CV) can be calculated on the grid-cell output file using spreadsheet software. An example of a calculated statistics file is shown in Table 4.2. Using Excel, average yield is calculated in cell J2 using the formula `=AVERAGE(F2:I2)`, standard deviation in cell K2 is calculated by `=STDEV(F2:I2)`, and the CV is calculated in cell L2 using the equation $(K2/J2)*100$. After typing these formulas, the data set is completed by filling in each column.

4.3.5 IDENTIFYING PRODUCTIVITY ZONES

Productivity zones based on the average yield and standard deviation values can be identified using several approaches. First, average yield values can be used to identify areas of low, medium, and high production. These areas can be identified by cluster analysis, producer preferences, and natural boundaries.^{1,7-9} This case study used average yields, standard deviations, coefficients of variation, and a combination of average yield and standard deviation to identify productivity zones. In the average yield approach, arbitrary yield values based on producer preference were chosen as the boundaries between each of three zones. Each of the zones encompassed 30–40% of the field area. Low producing areas had average yields of less than 119 bu ac⁻¹, medium producing areas had average yields ranging from 119–132 bu ac⁻¹, and high producing areas had average yields greater than 132 bu ac⁻¹ (Figure 4.1).

Productivity zones based on standard deviation were separated into three zones. Areas with low variability had standard deviations of less than 31.5 bu ac⁻¹, areas with medium variability had standard deviations between 31.5 and 42.5 bu ac⁻¹, and areas with high variability had standard deviations greater than 42.5 bu ac⁻¹ (Figure 4.2).

Productivity zones based on the coefficient of variation (CV) were also separated into three zones. In this case study, areas with a low CV had values less than 25%, medium areas had values ranging from 25 to 33%, and high CV areas had values greater than 33% (Figure 4.3).

In the final approach, both yield and standard deviation data are used to identify four different productivity zones. In this case study, yields were split into two categories, above and below the average yield. Standard deviations were also split into two categories, above and below the average standard deviation. Combining these categories resulted in four productivity zones with the following characteristics: (1) high yield, high deviation, (2) low yield, high deviation, (3) high yield, low deviation, and (4) low yield, low deviation (Figure 4.4).

Three new columns in the data set are needed for this classification. The first column (M) is used to classify yield into (1) above or (2) below average categories. This is accomplished by typing the formula `=IF(J2>125.74,1,2)` in cell M2 (note: the field average yield is 125.74 bu ac⁻¹). The second column (N) is used to classify variability into two categories, (1) above or (3) below the average standard deviation

TABLE 4.2
A portion of a summary file with elevation, seasonal and average yields, standard deviations, and coefficients of variation for four years of corn yield data

Row_No	Column_No	Long_Feet	Lat_Feet	Elevation (ft)	Corn96	Corn98	Corn00	Corn02	Average Yield (bu/ac)	Standard Deviation (bu/ac)	Coefficient of Variation (%)
1	1	22.50	22.50	1660.48	111.35	176.87	151.40	110.72	137.59	32.38	23.53
1	2	22.50	67.50	1660.68	112.98	176.25	156.60	95.43	135.32	37.50	27.71
1	3	22.50	112.50	1660.28	107.71	217.89	155.27	89.88	142.69	57.23	40.11
1	4	22.50	157.50	1659.72	114.23	212.60	153.29	106.48	146.65	48.51	33.08
1	5	22.50	202.50	1659.09	115.57	204.69	165.56	112.79	149.65	43.98	29.39
1	6	22.50	247.50	1658.46	109.43	216.24	186.51	110.30	155.62	54.21	34.84
1	7	22.50	292.50	1657.81	140.38	207.91	183.71	105.00	159.25	45.70	28.70
1	8	22.50	337.50	1657.15	97.93	226.14	184.03	103.47	152.89	62.71	41.02
1	9	22.50	382.50	1657.23	125.86	222.65	186.52	103.47	159.62	54.74	34.29
1	10	22.50	427.50	1657.64	136.68	216.81	170.89	110.49	158.72	45.95	28.95
1	11	22.50	472.50	1658.07	126.84	215.48	164.53	143.61	162.62	38.47	23.66
1	12	22.50	517.50	1658.42	121.93	213.91	169.01	143.04	161.97	39.62	24.46
1	13	22.50	562.50	1658.82	124.45	219.43	170.19	145.65	164.93	40.86	24.77
1	14	22.50	607.50	1659.24	124.60	212.76	172.22	144.38	163.49	38.22	23.38
1	15	22.50	652.50	1659.63	121.23	193.17	163.22	135.32	153.23	31.83	20.77
1	16	22.50	697.50	1660.06	110.04	183.88	145.64	124.54	141.02	32.09	22.76
1	17	22.50	742.50	1660.55	112.05	174.86	148.57	123.39	139.72	27.96	20.01
1	18	22.50	787.50	1661.10	119.06	165.14	142.10	120.78	136.77	21.62	15.81
1	19	22.50	832.50	1661.73	101.52	144.55	123.04	104.58	118.42	19.84	16.75

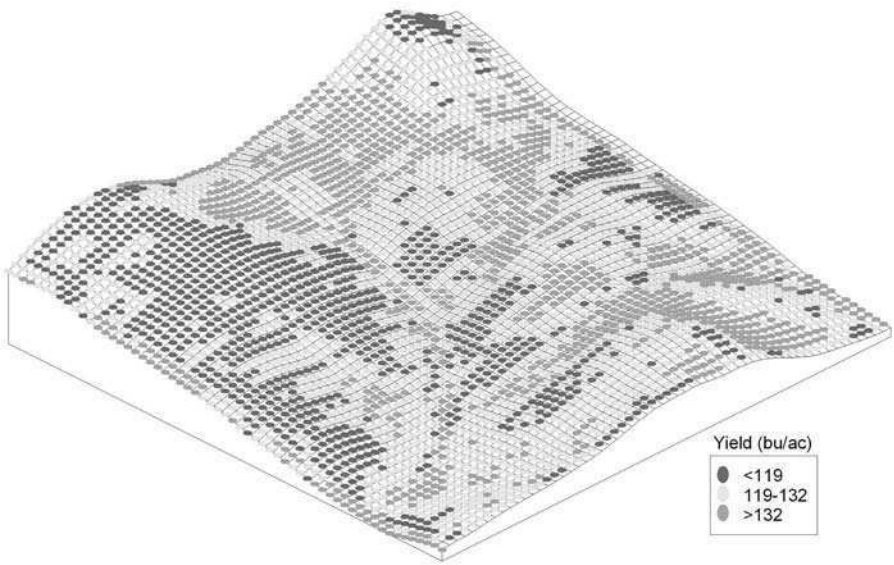


FIGURE 4.1 Topography overlaid with average yield zones.

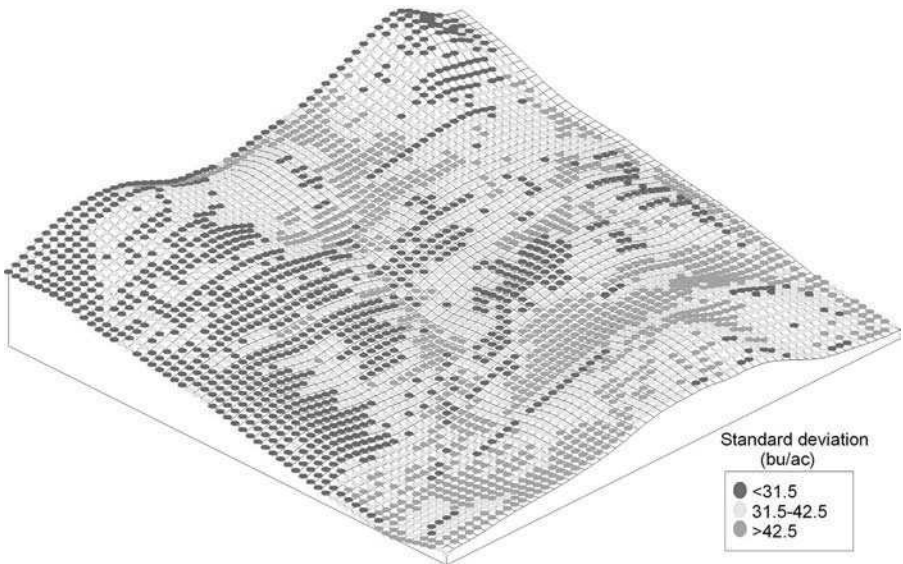


FIGURE 4.2 Topography overlaid with standard deviation zones.

value. This can be accomplished by typing the formula **=IF(K2>36.85,1,3)** in cell N2 (note: the field average standard deviation is 36.85). When adding the yield and variability categories together, the numbers combine to create four unique zone values. This is accomplished by entering the formula **=M2+N2** in cell O2. Columns need to be filled down to complete calculations for the entire data set. Grid cells

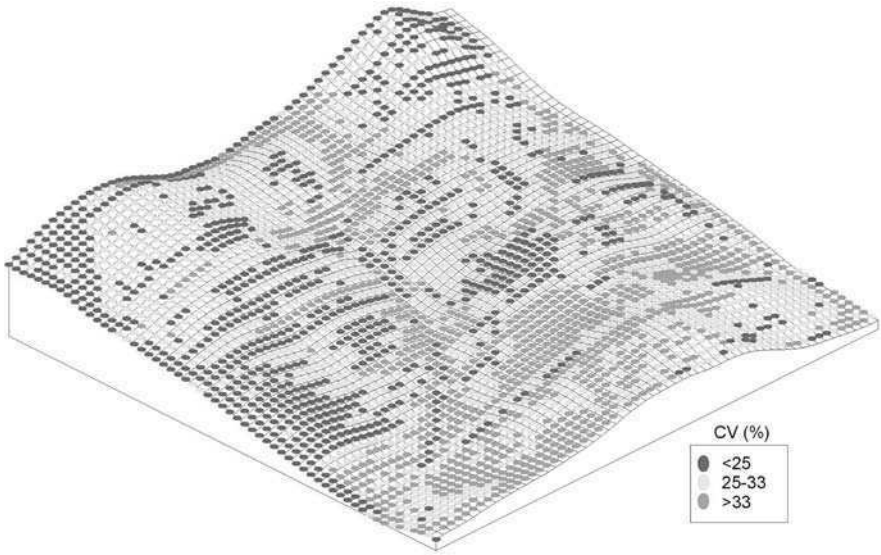


FIGURE 4.3 Topography overlaid with coefficient of variation (CV) zones.

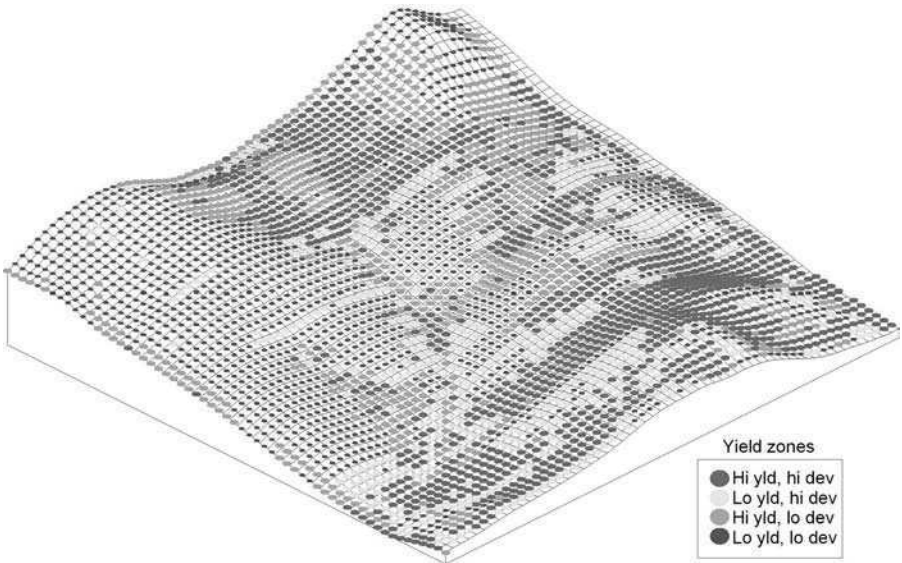


FIGURE 4.4 Topography overlaid with combination average yield and standard deviation zones.

with a combined yield and variability value of 2, 3, 4, and 5 are categorized as high yield and high deviation, low yield and high deviation, high yield and low deviation, and low yield and low deviation, respectively. These functions can be performed in any spreadsheet software package. An example of this data set is shown in Table 4.3.

TABLE 4.3
A portion of a summary file showing the yield, deviation, and combination zones as calculated by the spreadsheet

Long Feet	Lat Feet	Elevation (ft)	Corn96	Corn98	Corn00	Corn02	Average Yield (bu/ac)	Standard Deviation (bu/ac)	Coefficient of Variation (%)	Yield Zone	Deviation Zone	Combination Zone
22.50	22.50	1660.48	111.35	176.87	151.40	110.72	137.59	32.38	23.53	1.00	3.00	4.00
22.50	67.50	1660.68	112.98	176.25	156.60	95.43	135.32	37.50	27.71	1.00	1.00	2.00
22.50	112.50	1660.28	107.71	217.89	155.27	89.88	142.69	57.23	40.11	1.00	1.00	2.00
22.50	157.50	1659.72	114.23	212.60	153.29	106.48	146.65	48.51	33.08	1.00	1.00	2.00
22.50	202.50	1659.09	115.57	204.69	165.56	112.79	149.65	43.98	29.39	1.00	1.00	2.00
22.50	247.50	1658.46	109.43	216.24	186.51	110.30	155.62	54.21	34.84	1.00	1.00	2.00
22.50	292.50	1657.81	140.38	207.91	183.71	105.00	159.25	45.70	28.70	1.00	1.00	2.00
22.50	337.50	1657.15	97.93	226.14	184.03	103.47	152.89	62.71	41.02	1.00	1.00	2.00
22.50	382.50	1657.23	125.86	222.65	186.52	103.47	159.62	54.74	34.29	1.00	1.00	2.00
22.50	427.50	1657.64	136.68	216.81	170.89	110.49	158.72	45.95	28.95	1.00	1.00	2.00
22.50	472.50	1658.07	126.84	215.48	164.53	143.61	162.62	38.47	23.66	1.00	1.00	2.00
22.50	517.50	1658.42	121.93	213.91	169.01	143.04	161.97	39.62	24.46	1.00	1.00	2.00
22.50	562.50	1658.82	124.45	219.43	170.19	145.65	164.93	40.86	24.77	1.00	1.00	2.00
22.50	607.50	1659.24	124.60	212.76	172.22	144.38	163.49	38.22	23.38	1.00	1.00	2.00
22.50	652.50	1659.63	121.23	193.17	163.22	135.32	153.23	31.83	20.77	1.00	3.00	4.00
22.50	697.50	1660.06	110.04	183.88	145.64	124.54	141.02	32.09	22.76	1.00	3.00	4.00
22.50	742.50	1660.55	112.05	174.86	148.57	123.39	139.72	27.96	20.01	1.00	3.00	4.00
22.50	787.50	1661.10	119.06	165.14	142.10	120.78	136.77	21.62	15.81	1.00	3.00	4.00
22.50	832.50	1661.73	101.52	144.55	123.04	104.58	118.42	19.84	16.75	2.00	3.00	5.00

The data set provided with this case-study can be imported into ArcView or an alternative geographic information systems software package for data viewing, interpretation, and development of shapefiles for export to variable-rate equipment.

4.3.6 CALCULATING ZONE IMPACTS ON YIELD VARIABILITY

Yield variability reductions are calculated with the equation

$$\%variance\ reduction = 100 \times \left[1 - \frac{s_{pz}^2}{s_{field}^2} \right] \quad (4.1)$$

where s_{pz}^2 is the pooled variance of all productivity zones and s_{field}^2 is the variance of the entire field.⁸ Pooled variance (s_{pz}^2) is calculated with the equation

$$s_{pz}^2 = \frac{\sum (n_i - 1)s_i^2}{N - z} \quad (4.2)$$

where n_i is the number of points in each zone, s_i^2 is the variance of each zone, N is the total number of points in all zones and z is the number of zones.¹⁰ Field variance (s_{field}^2) is calculated with the equation

$$s_{field}^2 = \frac{\sum (x_i - \bar{x})^2}{(n - 1)} \quad (4.3)$$

where x_i are the yield values of each data point, \bar{x} is the field average yield, and n is the number of data points in the field.¹⁰ The yield variability reduction calculations are accomplished by (1) calculating the variance for the entire field (Equation 4.3), (2) sorting the data based on the various productivity zones, (3) calculating the variance for each zone (Equation 4.3), (4) calculating the pooled variance values for each method of zone delineation (Equation 4.2), and (5) calculating the percent reduction in variance (Equation 4.1). The reductions in yield variability for each year using the different productivity zone delineation methods can be seen in Table 4.4.

4.4 RESULTS AND DISCUSSION

The four different approaches used to characterize multiple-year yield data had both similarities and differences (Table 4.4). Production zones created from average yields separated the field into areas with low, medium, and high yields. Low yields were observed in the summit or shoulder landscape positions, medium yields were generally observed in the backslope positions, and high yields often were found in footslope or toeslope positions. In eastern South Dakota, where moisture is often

TABLE 4.4
Impact of the four methods to identify productivity zones on the percent reduction in yield variation when compared to whole field variability

Year	Method of Productivity Zone Delineation – % Reduction in Yield Variation			
	Average Yields	Standard Deviations	Coefficient of Variation	Average + Standard Deviation
1996	7	16	29	26
1998	53	49	27	63
2000	48	37	18	54
2002	20	0	4	18
All years	32	28	22	43

the limiting factor for crop production, average yields are generally correlated to landscape position. However, this approach does not take into consideration the extremes in variability that may occur on a temporal basis. Areas of high production in one year may have limited production in a different year with different weather conditions. Production zones based solely on yield will improve as additional years are added to the data set. Average yield zones can help producers to set production goals for different field areas and vary inputs to account for the expected differences in production.

To improve management, it is necessary to examine the standard deviation of individual grid-cell yields over time. Areas with low standard deviation, typically were summit, shoulder, and backslope. Areas with an average or medium standard deviation are typically located in transition areas, which also occur in backslopes. Toeslope and footslope areas may have a high standard deviation because these areas can have both very high and very low yields, depending on climatic conditions. Areas with high standard deviation may require additional management. For example, in toeslope areas, tile drainage can be installed to remove excess water. By understanding within-field variability, producers may be better able to manage this variability and increase production.

The coefficient of variation is another way to delineate zones based on variability. However, the CV also takes the field average yields into account. Basically, the CV measures the variability in the values in a population relative to the magnitude of the population mean.¹⁰ The zones created with CV values are similar to those created by standard deviations.

In order to gain a better understanding of how the average yields and standard deviations in a field interact, it may be necessary to define zones taking both measures into account. In the example field, areas with both high yields and high standard deviations were found in footslope areas that have occasional problems with excess moisture. These areas produce high yields in dry years and low to average yields in wet years. Approximately 32% of the field areas fit into this category. These areas are good candidates for installing tile drainage. Selecting yield goals for these areas is difficult due to the large variability. In relatively dry years these areas can produce yields in excess of 200 bu ac⁻¹, while in very wet years, yields can be as low as

0 bu ac⁻¹. The areas with low yields and high deviations are typically toeslope areas that are extremely wet or in compacted regions surrounding wet field areas. The yields are usually low due to excess water or compaction and only produce high yields when conditions are ideal. Producers may try to control variability in these areas by limiting compaction, using drainage methods, or planting extremely low areas to grass waterways. Areas of the field with high yields and low deviations are typically backslope areas that have adequate soil moisture but are not prone to flooding. Producers may wish to increase inputs in these areas, as agronomists report that nutrient depletion often occurs in areas of consistently high production. Finally, the areas of the field with low yields and low deviations are typically summit or shoulder positions with limited soil moisture. These areas may also be eroded with low organic matter contents and limited production capabilities. Producers may wish to cut back inputs in these areas to increase efficiency. Agronomists often report that due to several years of low yields and correspondingly low crop removal rates, nutrients have accumulated in these areas.

A notable trend occurred for all types of production zone delineation processes. Yield variability (s^2_{field}) was increased by extremely wet conditions in 1996 and decreased by a severe windstorm during pollination in 2002. In years with extremely high or low variability (s^2_{field}), zones based on average values of yield and standard deviation will not perform as well. All methods examined did a better job of explaining yield variability in the years 1998 and 2000, when yield patterns were close to “average” (Table 4.4). There is one exception to this statement. In 1996, when variability was high, the CV approach was the best, reducing yield variability by 29%. However, the zone delineation method that most consistently explained variability was the combination average and standard deviation approach. Over all years, this method reduced yield variability by an average of 43%. The amount of variability reduced was much higher, 63% and 54% in the more “average” years of 1998 and 2000, respectively. The method based on average yields reduced variability by an average of 32%. This approach also performed better in the years 1998 and 2000, reducing yield variability by 53% and 48%, respectively. The standard deviation approach reduced variability by an average of 28% and performed the best in years 1998 and 2000, reducing variability by 49% and 37%, respectively. Finally, the production zones based on CV reduced variability by an average of 22%. This approach performed best in 1996 and 1998, reducing variability by 29% and 27%, respectively.

4.5 CONCLUSIONS

There are several ways to use yield data to analyze yield trends both spatially and temporally. Production zones will become more accurate with time as more and more growing seasons are added into a field database. Different maps can be used for different purposes. Average yield maps can be used to define yield goals. However, in areas with high standard deviations, care must be used when using average values. Standard deviation maps are very useful in identifying areas requiring corrective treatments. By comparing yield and standard deviation maps, the costs associated with not implementing a corrective treatment can be determined. For

example, if a 10-acre area in a footslope area has excess water 1 year out of 10 resulting in a 90% yield loss, the loss from that year would be \$4,500 (10 acres @ 180 bu ac⁻¹ loss @ \$2.50 bu⁻¹). This scenario occurred in 1996 in the example field provided with this case study. In this case study, the best method for explaining yield variability in fields was using a combination of average yields and standard deviation to delineate productivity zones. Due to the variability present in any agricultural production system, it is up to producers to analyze and interpret the different zones created for each field and determine how management decisions can be altered to increase production efficiency.

4.6 EXERCISE: MAPPING PRODUCTIVITY ZONES

4.6.1 OVERVIEW

Any GIS package may be used to map the data generated by Field Analyst. In this exercise, ArcView will be used to plot productivity zones. This program may be used to create shapefiles from Field Analyst data to drive variable rate applications.

4.6.2 FILE FORMATS

ArcView uses either text files (.txt) or database files (.dbf). Files may be converted to this format using Excel or most other spreadsheet programs. Note: If using GPS coordinates, latitude and longitude values must be specifically designated to have six decimal places.

4.6.3 MAPPING PRODUCTIVITY ZONES

This section outlines the process used to map productivity zones. To begin, open the ArcView 3.3 software program.

1. As the program starts, a window will pop up asking whether or not to add a new view. Select **with a new view** and click OK. When the dialogue box asking **would you like to add new data to the view** appears, click **No**.
2. In the **Untitled** window, click on the **Tables** icon and then click **Add**. A window entitled **Add Table** should appear, allowing navigation to the *datafile.dbf* file supplied with this exercise.
3. After selecting the *datafile.dbf* file, click OK. *Remember to select (.dbf) as the file type in ArcView.* The data table should appear in a new window.
4. Next the data from the table will be added to the view. First, click on the **View1** window to make it active. From the toolbar at the top of the screen, select **View** and then **Add Event Theme**.
5. A window entitled **Add Event Theme** appears. Make sure the **X field** reads Long_feet and the **Y field** reads Lat_feet. Click OK to continue.
6. A *datafile.dbf* theme should appear in the **View1** window. Click on the check box to the left of the theme name to make the map visible. These are the grid points used for productivity zone delineation.

7. In order to see the productivity zones, data points need classification. To do this, double-click on the box surrounding the *datafile.dbf* theme name. The **Legend Editor** window should appear.
8. From the **Legend Type** pulldown menu, select **Unique value**.
9. In this exercise the combination zones will be mapped. Select **Combination zones** from the **Values Field** pull-down menu and then click **Apply**. The **Legend Editor** window can now either be closed or minimized.
10. The map should now show four color levels representing the different zones. For zone interpretations, refer back to earlier discussion in the “Identifying productivity zones” section.
11. To change the type of zones on the map, simply reopen the **Legend Editor** window, change the zone type in the **Values Field** pulldown menu, and click **Apply**.

ACKNOWLEDGMENTS

Funding was provided by the South Dakota Soybean Research and Promotion Council, Upper Midwest Aerospace Consortium (UMAC) the United Soybean Board, NASA, the North Central Soybean Research Program, the South Dakota Agricultural Experiment Station, and USDA-CREES Grant 2004 51/30-02248.

REFERENCES

1. Chang, J. et al., Defining yield goals and management zones to minimize yield and nitrogen and phosphorus fertilizer recommendation errors, *Agron. J.*, 96, 825, 2004.
2. Bakhsh, A. et al., Spatio-temporal analysis of yield variability for a corn-soybean field in Iowa, *Trans. ASAE*, 43, 31, 2000.
3. Diker, K. et al., Frequency analysis of yield for delineating management zones, in *Proceeding of the 6th International Conference on Precision Agriculture, July 14–17, 2002*, Robert, P.C. et al., Eds., Bloomington, MN. ASA-CSSA-SSSA, Madison, WI, 2002.
4. Fridgen, J.J., Kitchen, N.R., and Sudduth K.A., Variability of soil and landscape attributes within sub-field management zones, in *Proceeding of the 5th International Conference on Precision Agriculture, July 16–19, 2000. Bloomington, MN*, Robert, P.C. et al., Eds., ASA-CSSA-SSSA, Madison, WI, 2000.
5. Blackmore, S. and Moore, M., Remedial correction of yield map data, *Prec. Agric.*, 1, 53, 1999.
6. Thylen, L. and Algerbo, P.A., An expert filter removing erroneous yield data, in *Proceeding of the 5th International Conference on Precision Agriculture, July 16–19, 2000. Bloomington, MN*, Robert, P.C. et al., Eds., ASA-CSSA-SSSA, Madison, WI, 2000.
7. Fleming, K.L., Westfall, D.G., and Wiens, D.W., Field testing management zones for VRT, in *Site-Specific Management Guideline*, SSMG-21. PPI-FAR, Norcross, GA, 1999. Available online at www.ppi-ppic.org.

8. Kitchen, N. et al., Procedures for evaluation unsupervised classification to derive management zones, in *Proceeding of the 6th International Conference on Precision Agriculture, July 14–17, 2002*, Robert, P.C. et al., Eds., Bloomington, MN, ASA-CSSA-SSSA, Madison, WI, 2002.
9. Walker, T. et al., Defining and managing yield zones for rice and soybeans — a case study, *Better Crops with Plant Food*, 88, 10, 2004.
10. Rao, P.V., *Statistical Research Methods in the Life Sciences*, Brooks/Cole Publishing Co., Pacific Grove, CA, 1998.

5 Site-Specific Weed Management in Growers' Fields: Predictions from Hand-Drawn Maps

Lori J. Wiles, R. Bobbitt, and Philip Westra

CONTENTS

5.1 Executive Summary.....	81
5.2 Introduction	82
5.2.1 Site-Specific Strategies for Weed Management.....	83
5.2.2 Variability in the Benefits of Site-Specific Weed Management.....	83
5.3 Overview of the WeedSite Program.....	84
5.4 Evaluating Site-Specific Weed Management	85
5.4.1 Creating a Scenario.....	85
5.4.2 Identifying Polygons.....	88
5.4.3 Predicting Outcomes for Simulation Polygons.....	88
5.4.4 Decision Algorithms	88
5.4.5 Viewing Results	89
5.5 Examples with Maps Drawn by Agricultural Consultants.....	90
5.5.1 Predictions: What We Know	92
5.5.2 Predictions: What We Are Learning.....	93
5.6 Limitations: Accuracy and Speed	96
5.7 Conclusions	96
Acknowledgment	99
References.....	99

5.1 EXECUTIVE SUMMARY

Herbicide use may be reduced 30–80% without impacting crop yield with site-specific weed management. Herbicide use is varied within a field to match the variation in the weed population. However, growers will not adopt this strategy until they are confident that the reduction in herbicide and other benefits of site-specific weed management will justify the cost of implementation and future weed control

will not be compromised. Predicting the outcome of site-specific weed management is difficult because benefits vary with the composition and spatial distribution of the weed population, possible herbicide treatments, and the resolution of variable management. WeedSite software was developed so growers could investigate the potential benefits of postemergence site-specific weed management in irrigated corn specifically for their weed populations and implementation of site-specific weed management. Users choose the resolution of patch spraying and may divide a field into management units. Georeferenced weed maps and GIS software are not needed. Net gain from site-specific weed management, area of the field not treated, herbicide use and cost, yield loss from weed competition, and weeds left in the field are all calculated from hand-drawn weed maps and results can be mapped. We think WeedSite can be useful for educating growers, agricultural consultants, and students about the potential benefits of postemergence site-specific weed management in irrigated corn in addition to published field experiments. Evaluations are consistent with what is known about variation in the benefits of site-specific weed management. Predictions from hand-drawn maps will be less accurate than predictions from field experiments but more germane. General features of spatial distributions may be more representative and users choose the weed species present, the resolution of management, and the candidate herbicides.

5.2 INTRODUCTION

Weeds grow in patches of varying size, shape, and composition within fields¹⁻⁵ yet herbicide treatments are usually selected based on the “average” weed population and applied uniformly across a field. Site-specific weed management (SSWM) may reduce herbicide use while still achieving appropriate and economical control.⁶ This is a strategy of varying weed management within a field to match the variation of the species and density of the weed population. Herbicide use may be reduced because herbicide is applied only where the benefits exceed the costs. Further, control may be more cost effective and future weed problems minimized because the type and rate of herbicide can be varied for local weed populations within the field.

Growers are aware of the spatial variability of weed populations in their fields and many practice simple strategies of site-specific weed management with post-emergence herbicides such as spraying field edges with a different herbicide or higher rate than the rest of the field.⁷ However, few practice the potentially more valuable SSWM with the technology of precision agriculture. Even if a grower already has the technology and knowledge, SSWM may still be more expensive and require more time than uniform management. Using SSWM requires the grower to map the weed population in a field, make many rather than a single management decision for a field, and prescribe the varying management in a format for the site-specific technology used. Also, growers are concerned that additional weeds left untreated in the field may lead to more serious weed problems in the future. Growers need to know that the reduction in herbicide use and other benefits will exceed the costs and that future weed control will not be compromised before investing in the technology, learning the new skills, and committing the additional time needed for site-specific weed management.

5.2.1 SITE-SPECIFIC STRATEGIES FOR WEED MANAGEMENT

One approach to site-specific weed management is to map weed populations in the field and then divide the field into subunits with the herbicide application for each selected according to the average weed population indicated on the map for each subunit.⁸ In this scenario, herbicides are applied uniformly in subunits. For the patch spraying strategy of SSWM, subunits may be cells of a sprayer grid with the width and length of cells determined by the size and technology of the sprayer (patch or variable rate) that will be used.⁹ Cell width is the length of the boom or smaller if sections of the boom or individual nozzles can be operated independently. The length of a sprayer grid cell is determined by how quickly herbicide application can be varied with the sprayer.¹⁰ Subunits of a field, called management units, can be either the smallest area that a grower can manage independently¹¹ or an area that a grower needs to manage independently based on the variability of the weed population.¹² For growers without global positioning systems (GPS) and patch or variable rate sprayers, management units can be easily identified areas such as a pass of the sprayer or half of a field.

The choice of management for each sprayer grid cell or management unit may be spray or no spray, the typical concept of patch spraying, or applying one of several herbicides or herbicide mixtures for the most cost-effective control of different types of weeds such as annuals and perennials.¹³ Alternatively, a grower may spray the entire field with a single herbicide, but vary the rate depending on the density of the weed population.¹⁴ Growers may prefer this latter approach to leaving areas of the field unsprayed to minimize the risk of seed production from uncontrolled weeds.

5.2.2 VARIABILITY IN THE BENEFITS OF SITE-SPECIFIC WEED MANAGEMENT

Herbicide use may be reduced by 90% or more with SSWM with reductions of 40–70% common in research studies.^{9,15–21} However, reductions are not consistent. For example, in one study of site-specific compared to uniform weed management, herbicide use was reduced 98% in one corn field but only 11.5% in a nearby field.²¹ Net gain from site-specific weed management of wild oat (*Avena fatua* L.) varied from \$3.19 to \$19.98 ha⁻¹ in four fields of dryland spring wheat.²²

The benefit of SSWM in a particular field is difficult to predict because herbicide use with SSWM varies with the size, shape, arrangement, and species composition of patches and the site-specific strategy used.^{11,23,24} In general, the benefit of site-specific management increases with the patchiness of the weed population because more of a field can be left untreated.^{6,25} Also, herbicide use is minimized with smaller management units and sprayer cells because more cells or units will be weed-free.^{24,26} For patch spraying (on/off), the actual reduction depends on the weed-free area at the spatial resolution of the patch sprayer.²⁴ Weed species present^{11,13} and the choice of herbicides²³ also influence the benefits of SSWM because control with a herbicide and the ability to compete with the crop varies among weed species. The economic benefit of SSWM will be greatest with the more expensive herbicides,¹¹ but will vary with the yield potential and selling price of the crop.

With the observed variability of herbicide use and economic and other benefits with SSWM in research studies, and the many potential reasons for the variability, growers need estimates for the composition and distributions of weed populations in their fields and the site-specific strategies that can potentially fit their needs. For these reasons, we developed a computer program for growers and agricultural consultants to explore the potential benefits of different strategies of SSWM in their irrigated corn fields.

5.3 OVERVIEW OF THE WEEDSITE PROGRAM

Our objective was to develop an easy-to-use computer program (WeedSite) that growers and agricultural consultants in Colorado, USA, can use to investigate the potential benefits of site-specific, postemergence weed management in their irrigated corn fields. Our goal was education rather than recommendations and our targeted audience included growers and agricultural consultants who do not own site-specific technology and may not even be familiar with site-specific weed management. To meet this objective, our most important requirements were that georeferenced field or weed data and GIS software would not be needed. Also, we wanted software distribution to be free to reach the most potential users.

Most growers and agricultural consultants are aware of variation in the spatial distribution of weeds in their corn fields. Few draw maps, but most make management decisions based on their perceptions of the distribution and many will readily draw a weed map if asked.⁷ The program we developed does not require georeferenced weed maps. Instead, uniform and site-specific weed management are evaluated based on hand-drawn weed maps.

The program has three modules: (1) a GIS interface, (2) a simulation model for predicting biological and economic outcomes of weed management, and (3) decision algorithms that identify the optimal site-specific management from the predicted outcomes for the weed populations in the field. Each component of the program performs an essential task for determining the optimal uniform or site-specific weed management. These tasks are completed sequentially with the results of a task completed by one module written to a database to be retrieved by the next module.

WeedSite was developed for the Windows environment using Microsoft Visual Basic 6.0[®] (Microsoft Corporation, Redmond, Washington, USA) and MapObjects LT 2.0[®] (ESRI, Redlands, California, USA). MapObjects LT is a Windows ActiveX[®] (Microsoft Corporation, Redmond, Washington, USA) software control that provides extensive GIS interface tools for map display, analysis, drawing, querying, and navigation, and there are no royalties for distribution of programs developed using this software. Custom programming was necessary for functions not included in MapObjects LT such as map legends. Model parameters and users' scenarios and results are stored in Microsoft Access 2000 databases[®] (Microsoft Corporation, Redmond, Washington, USA) and maps are stored as ESRI shapefiles.

Because the MapObjects LT software does not include tools for calculating the intersections of polygons (weed patches, management units, etc.), vector polygons representing weed patches, management units, and sprayer grid cells are converted

to a raster data set for analysis. This allows finite and discrete calculations for the area of intersection of different layers. The raster size is based on a database parameter that represents the length and width of a raster cell and can be changed by users. Length and width of sprayer grids are limited to multiples of this parameter. Areas of the intersections that need to be identified for an evaluation are calculated by finding the number of raster cells that intersect the derived polygons and then multiplying that number by the area of a raster grid cell.

5.4 EVALUATING SITE-SPECIFIC WEED MANAGEMENT

WeedSite evaluates uniform and SSWM strategies for a set of tactics specified in a model database and a scenario. A tactic is no control, an application of one or more herbicides at a specified rate, or a sequential application of herbicides. A scenario is the set of field, weed population, production, and strategy information specified by the user. Strategies are uniform management and different methods of implementing site-specific management (Table 5.1). Site-specific strategies are patch spraying with one or two tactics; user-defined management units with the model or the user selecting the tactic for each unit; and an estimate of maximum benefit from site-specific weed management.

5.4.1 CREATING A SCENARIO

The user creates maps and specifies information of a scenario through a single screen of the GIS interface. The minimum information needed for a scenario is a field map, a weed map and a sprayer grid, and production and economic information (Figure 5.1). A scenario may also include management units, plus tactics for the management units, and the user may choose to evaluate just a subset of tactics of the program (Figure 5.1).

TABLE 5.1
Site-specific strategies differ by the type of management polygons and method for selecting optimal tactic or tactics

Strategy	Management Polygons	Method for Selecting Optimal Tactics
Uniform management	Field	One tactic for the field
Maximum benefit	Unique weed populations	One tactic for each unique weed population
Patch spraying with one tactic	Sprayer grid cells	One tactic or no control for each cell
Patch spraying with two tactics	Sprayer grid cells	One of two tactics or no control for each cell
Management units	User-defined subunits of the field	One tactic for each management unit
Grower management	User-defined subunits of the field	User selects a tactic for each management unit

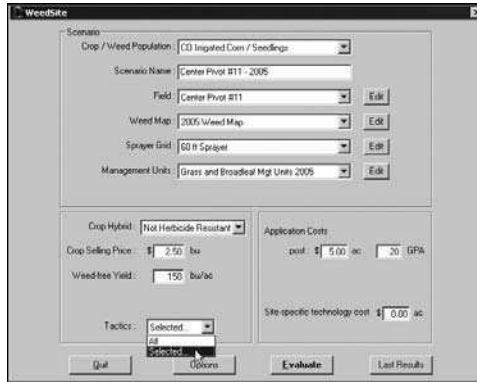


FIGURE 5.1 WeedSite users create scenarios that include maps, production information, and choice of tactics for an evaluation.

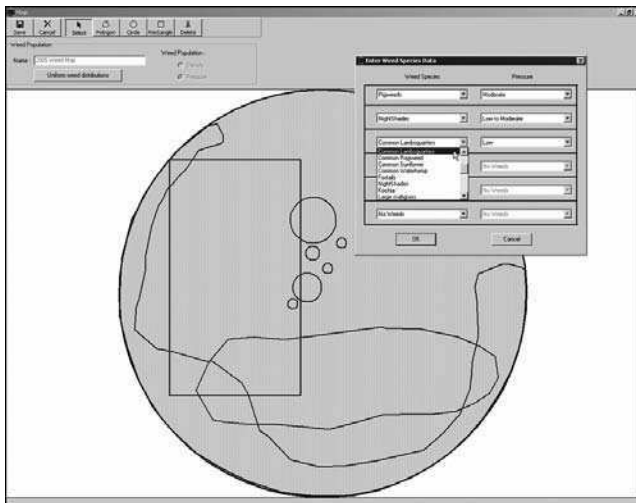


FIGURE 5.2 Users draw weed maps and may use density or pressure to describe the weed population, include up to six weed species in a patch, and specify weeds that are uniformly distributed through the field.

Fields, weed patches, and management units can be circles, rectangles, or any shape drawn by the user with a GIS polygon tool (Figure 5.2). Populations in a weed patch may include up to six weed species and are described as density [weeds per 100 ft (30.5 m) of row] for each weed species or by choosing from a list of pressure ratings (Figure 5.2). English units are used in the program since these are most appropriate for the intended audience. Pressure ratings indicate expected percent crop yield loss and a pressure rating is converted to density for each weed species based on the competitiveness of the weed species. Weed patches can overlap. For these areas, weed presence is the higher density or weed pressure for a species that is included in more than one of the overlapping patches. Besides weed patches,

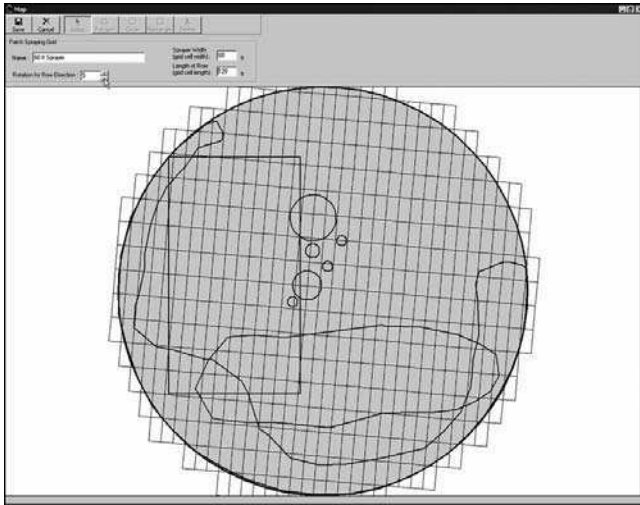


FIGURE 5.3 Sprayer grids of various sizes and orientation relative to the field can be generated with WeedSite.

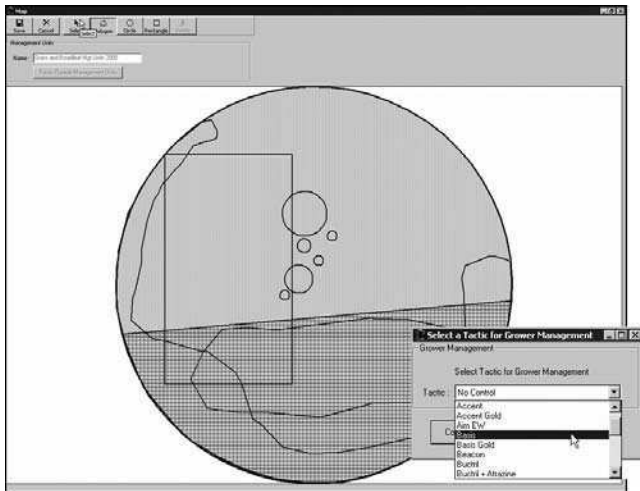


FIGURE 5.4 A field can be divided into management units that do not overlap and the user can choose to specify the tactic for each unit.

up to six weed species that are uniformly distributed throughout a field may be specified.

Different sprayer grids can be created to compare SSWM with various variable rate or patch sprayers. The user selects the length and width of sprayer grid cells and the angle for orientation of the grid relative to the field (Figure 5.3). Management units, like weed patches, can be circles, rectangles, or polygons but cannot overlap (Figure 5.4). For the site-specific strategy of grower management, the user chooses a tactic for each management unit (Figure 5.4).

5.4.2 IDENTIFYING POLYGONS

The first step of an evaluation is identifying weed, management, and simulation polygons of a scenario. Weed polygons are weed patches that do not overlap with other patches and polygons created by overlapping patches. The area of the field without patches is also defined as a weed polygon. Management polygons are the entire field (uniform management), weed polygons (maximum benefit), sprayer grid cells (patch spraying with one or two tactics), and the management units drawn by the user plus any area of the field not included in management units (management units and grower management) (Table 5.1). Simulation polygons are intersections of weed polygons with management polygons. These are the fundamental units for simulating the outcome of management and calculations of the decision algorithms.

5.4.3 PREDICTING OUTCOMES FOR SIMULATION POLYGONS

The second step in an evaluation is simulating biological and economic outcomes for each simulation polygon for all possible tactics or the set of tactics selected by the user. The simulation model in WeedSite is a modified version of an existing weed management decision model, GWM/WEEDCAM,^{27,28} with herbicide databases updated with information from the Colorado²⁹ and Nebraska³⁰ weed management guides. Outcomes predicted for each simulation polygon/tactic combination are herbicide use (active ingredient), cost of herbicide, weed escapes, crop yield loss from competition with weed escapes, and gross margin. Gross margin (GM) is the value of the crop calculated from the user's prediction of crop price (P_c) and expected yield with no weeds (Y_{nw}) minus the simulated yield loss from weeds not controlled by the tactic (Y_w). Percent yield loss depends on percent control with the tactic, density and estimated competitiveness of the different species of the weed population, and a relationship between weed density and crop yield loss. It is assumed that the weeds emerge with the crop and are controlled at the optimal time. All results are calculated per unit area (acre). GWM/WEEDCAM has been evaluated on 50 farms in a 4-year study in eastern Colorado.³¹ The model is also suitable for corn production in the panhandle of Nebraska.

5.4.4 DECISION ALGORITHMS

The tactics are specified for the grower management strategy. Decision algorithms for the other strategies all identify the tactic that optimizes gross margin for a field, but differ by the number of tactics for optimal management and which simulation polygons must have the same tactic (Table 5.1). For example, the same tactic must be specified for all simulation polygons within a management unit or sprayer grid cell. Gross margin for a field is the weighted sum of the gross margin for each simulation polygon with the proportion of the area of the field of a simulation polygon as the weight. Optimal management may be one tactic to as many tactics as the number of unique weed populations (maximum benefit) or management units

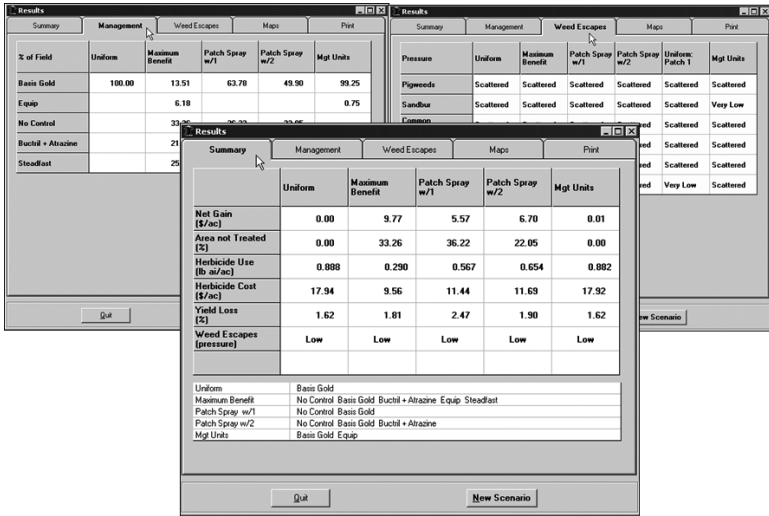


FIGURE 5.5 WeedSite generates tables of results that include net gain from site-specific weed management, outcomes related to herbicide use, and crop yield loss (summary tab), area of the field for each tactic (management tab), and weeds left in the field (weed escapes tab), and the scenario and tables can be printed (print tab).

in a field (Table 5.1). Gross margin for grower management is calculated in the same method as the other strategies, but with the tactics specified.

Herbicide use, weeds not controlled, and yield loss from competition with uncontrolled weeds are calculated for the field for a management strategy with the same method as gross margin. We also calculate net gain from SSWM for easier comparison among the site-specific strategies and with the optimal uniform management. This is the gross margin with optimal management for a site-specific strategy minus the gross margin for the optimal uniform strategy and the site-specific technology cost. A net gain greater than zero indicates net return is greater with site-specific than uniform management.

5.4.5 VIEWING RESULTS

Net gain from SSWM, optimal tactics, herbicide use, area of the field treated, crop yield, and weeds escaping control in the field are displayed in tables on the **Summary**, **Management**, and **Weed Escapes** tabs of the results screen of the GIS interface (Figure 5.5). However, differences among the site-specific strategies and why these occurred can best be understood by viewing maps. Spatial variability of the information in the tables can be displayed on the **Maps** tab for each management strategy (Figure 5.6). The user can print the scenario, results tables, and maps from the **Print** tab or copy maps to the Windows clipboard (Figure 5.6).

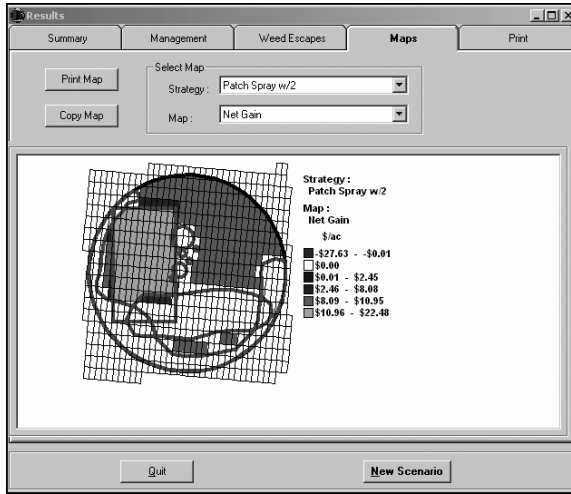


FIGURE 5.6 Predicted results of uniform and site-specific weed management can be mapped for a better understanding of the outcomes of site-specific weed management.

5.5 EXAMPLES WITH MAPS DRAWN BY AGRICULTURAL CONSULTANTS

Use of WeedSite is illustrated with maps drawn by agricultural consultants during interviews about how they make weed management decisions.⁷ The maps were digitized by the authors and are shown in Figures 5.7 and 5.8 with the uniformly distributed species and the weed polygons, and the species in each, identified. Weed species included in the maps were *Echinochloa crus-galli* (L.) Beauv., *Cenchrus longispinus* (Hack.) Fern., *Salsola tragus* L., *Kochia scoparia* (L.) Schrad., *Amaranthus retroflexus* L., *Chenopodium album* L., *Solanum physalifolium* Rusby, *Cirsium arvense* (L.) Scop., and *Setaria viridis* (L.) Beauv.

The interviews were conducted before WeedSite was developed so we did not have all the information needed for an evaluation. Consequently, the authors chose the field size (30.4 ha), crop yield (10 T ha⁻¹), crop price (\$168.25 kg⁻¹), two sprayer grids (6 × 18 m and 12 × 36 m), and two management units for both fields. Grower management was not included in the evaluations. The larger spraying grid and management units for the fields are shown in Figures 5.9 and 5.10. Management units were selected to be a primarily grass unit and a primarily broadleaf unit. Tactics in the WeedSite database are 24 herbicides and herbicide mixtures that are commonly used by corn growers in Colorado. We did the evaluations with all the tactics in the database and with the five least expensive tactics excluded to illustrate the effect of herbicide cost on the benefits of SSWM. The cost of these tactics was \$3.71 to \$15.10 ha⁻¹ and the cost of the remaining tactics was \$24.00 to \$80.28 ha⁻¹. No control was also simulated. No site-specific technology cost was included since this information is not yet available. Without this cost, net gain can be interpreted as the maximum amount that can be spent on SSWM if the objective is to maximize profit.

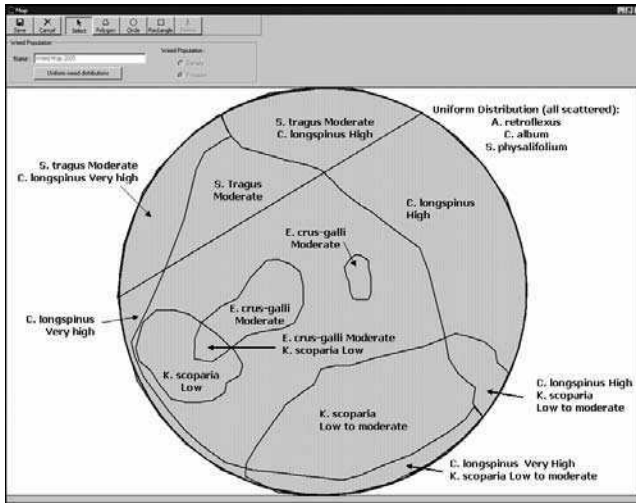


FIGURE 5.7 Weed map of Field A drawn by an agricultural consultant with weed species in each weed polygon and uniformly distributed throughout the field identified.

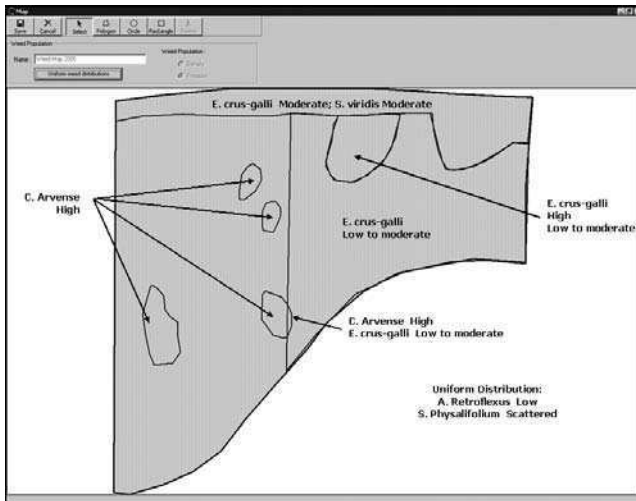


FIGURE 5.8 Weed map of Field B drawn by an agricultural consultant with weed species in each weed polygon and uniformly distributed throughout the field identified.

The predicted outcomes of site-specific and uniform weed management for the agricultural consultants' hand-drawn maps illustrate both well-established and emerging principles of the benefits of site-specific weed management.

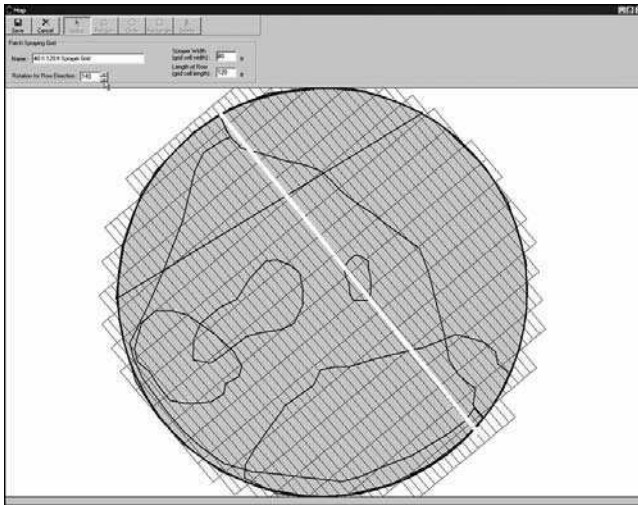


FIGURE 5.9 The two management units, indicated by the white line dividing the field, and the 12×36 m sprayer grid for Field A.

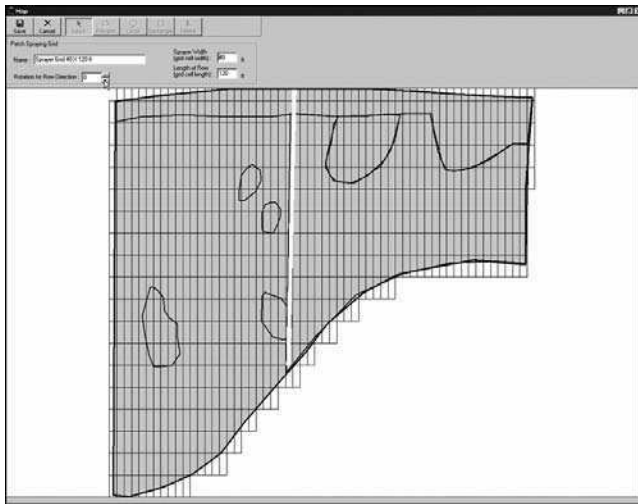


FIGURE 5.10 The two management units, indicated by the white line dividing the field, and the 12×36 m sprayer grid for Field B.

5.5.1 PREDICTIONS: WHAT WE KNOW

Benefits of patch spraying compared to uniform management predicted from the hand-drawn maps were generally consistent with published results. Herbicide use and cost, and area of the field treated were reduced; economic gain was small; and slightly more weeds were left in the field (indicated by greater crop yield loss

and more weed escapes) for the patch spraying with one-tactic strategies (Tables 5.2 and 5.3). Three of the four effects were predicted for the patch spraying with two-tactic strategies. Herbicide use has been typically reduced 30–80% in research studies.^{9,15–21} For these maps, recommended herbicide use was reduced by 32–43% with the patch spraying strategies for Field A and 41–54% with patch spraying with one tactic for both sets of tactics and patch spraying with two tactics with the most expensive tactics for Field B. Cost of the herbicide and area of application was reduced in all cases. Yield loss from weeds left in the field increased by up to 1.3% with the patch spraying strategies. The maximum yield loss was 3.6% (patch spraying with one tactic, all tactics, Field A). Net gain from patch spraying compared to uniform weed management was \$6.57 to \$19.29 ha⁻¹ for field A and \$3.38 to \$17.76 ha⁻¹ for Field B.

The benefits of patch spraying typically increase with finer resolution of management^{24,26} and the predicted outcomes illustrate this effect. Herbicide use and cost, and area of application were smaller with the finer grid (6 × 18 m) for both of the patch spraying strategies and both sets of tactics (Tables 5.2 and 5.3). Yield loss was the same or increased with grid size. However, decreasing sprayer grid size by half increased net gain by at most \$2.84 ha⁻¹ (patch spraying with one tactic, most expensive tactics, Field A). The smallest increase was \$0.07 ha⁻¹ (patch spraying with two tactics, all tactics, Field A). The effect of grid size for patch spraying would likely be larger with much smaller weed patches than drawn in these maps.

The results also illustrate the observed or expected influence of weed population on the value of SSWM. The value of site-specific management increases with weed-free area in a field^{6,25} and is thought to be more valuable with higher density and greater aggregation of weed populations.⁶ The maps did not include any weed-free areas, but weed pressure was higher for Field A than Field B. The expected yield loss with no control was 9.8% for Field A and 7.7% for Field B (data not shown). The estimated maximum net gain of SSWM was \$9.06 ha⁻¹ (all tactics) and \$5.43 (most expensive tactics) greater for Field A than for Field B (Tables 5.2 and 5.3). Net gain also increased with weed pressure for all but two of the patch spraying tactics, but the herbicide-related benefits were lower for Field A than Field B. An exception is herbicide use for patch spraying with two tactics when all tactics are considered

The value of SSWM is expected to be greater with more expensive herbicides. Maximum benefit increased \$9.88 ha⁻¹ for Field A and \$13.51 ha⁻¹ for Field B when the five least expensive tactics were excluded from possible tactics (Tables 5.2 and 5.3). Net gain for all patch spraying and management unit strategies showed the expected increase in net gain with more expensive tactics. The increase was smaller for Field B with the lower weed pressure except with management units. Changes in the herbicide-related outcomes were inconsistent.

5.5.2 PREDICTIONS: WHAT WE ARE LEARNING

Predictions for SSWM based on these maps illustrate benefits of SSWM that are not widely recognized. First, site-specific management at a very coarse resolution (management units) may be valuable. Net gain from implementing SSWM with

TABLE 5.2
Predicted outcomes for site-specific and uniform weed management in Field A for a scenario with all possible tactics and a scenario with the five least expensive tactics excluded

	Uniform Application	Maximum Benefit of Site-Specific ^a	Site-Specific Strategy						Management Units
			Patch Spraying			Patch Spraying			
			One Tactic			Two Tactics			
			6 × 18 m	12 × 36 m	6 × 18 m	12 × 36 m	6 × 18 m	12 × 36 m	
			All Tactics						
Net gain (\$ ha ⁻¹)	—	\$14.25	\$7.93	\$6.57	\$12.28	\$10.40	\$0.00		
Area of application (% of field)	100%	71%	57%	64%	76%	82%	100%		
Herbicide use (kg ai ha ⁻¹)	0.017	0.142	0.010	0.011	0.010	0.011	0.017		
Cost of herbicide (\$ ha ⁻¹)	\$14.65	\$13.76	\$8.35	\$9.34	\$9.09	\$9.90	\$14.65		
Yield loss (%)	3.0%	2.1%	3.6%	3.5%	2.7%	2.8%	3.0%		
			Most Expensive Tactics^b						
Net gain (\$ ha ⁻¹)	—	\$24.13	\$16.60	\$13.76	\$19.29	\$16.55	\$0.02		
Area of application (% of field)	100%	67%	57%	64%	72%	78%	100%		
Herbicide use (kg ai ha ⁻¹)	0.995	0.325	0.568	0.636	0.676	0.733	0.989		
Cost of herbicide (\$ ha ⁻¹)	\$44.31	\$23.61	\$25.27	\$28.26	\$26.95	\$28.87	\$44.26		
Yield loss (%)	1.67%	1.8%	2.6%	2.5%	1.9%	1.9%	1.6%		

^aMaximum benefit from site-specific weed management is estimated with the optimal tactic selected for each unique local weed population in the field.

^bFive herbicide or herbicide mixtures that cost \$3.71 to \$15.00 ha⁻¹ were excluded as possible tactics.

ai = active ingredient

TABLE 5.3
Predicted outcomes for site-specific and uniform weed management in Field B with for a scenario with all possible tactics and a scenario with the five least expensive tactics excluded

	Uniform Application	Maximum Benefit of Site-Specific ^a	Site-Specific Strategy					Management Units
			Patch Spraying		Patch Spraying			
			One Tactic	Two Tactics	6 × 18 m	12 × 36 m	6 × 18 m	
Net gain (\$ ha ⁻¹)	—	\$5.19	\$3.58	\$3.38	\$4.42	\$4.35	\$0.00	
Area of application (% of field)	100%	100%	53%	56%	53%	56%	100%	
Herbicide use (kg ai ha ⁻¹)	0.017	0.036	0.009	0.010	0.043	0.059	0.017	
Cost of herbicide (\$ ha ⁻¹)	\$14.65	\$10.32	\$7.83	\$8.23	\$7.24	\$7.36	\$14.65	
Yield loss (%)	1.5%	1.4%	2.6%	2.5%	2.6%	2.5%	1.5%	
			All Tactics					
			Most Expensive Tactics^b					
Net gain (\$ ha ⁻¹)	—	\$18.70	\$16.06	\$15.24	\$17.76	\$17.07	\$12.77	
Area of application (% of field)	100%	50%	53%	48%	53%	56%	42%	
Herbicide use (kg ai ha ⁻¹)	0.039	0.020	0.021	0.018	0.022	0.024	0.015	
Cost of herbicide (\$ ha ⁻¹)	\$39.10	\$19.24	\$20.87	\$17.89	\$20.35	\$21.24	\$16.50	
Yield loss (%)	1.5%	2.3%	2.5%	2.8%	2.2%	2.2%	3.4%	

^aMaximum benefit from site-specific weed management is estimated with the optimal tactic selected for each unique local weed population in the field.

^bFive herbicide or herbicide mixtures that cost \$3.71 to \$15.00 ha⁻¹ were excluded as possible tactics.

ai = active ingredient

the two management units selected by the authors was \$12.77 ha⁻¹ with the most expensive herbicides in Field B. This was more than half of estimated maximum benefit of site-specific management (Table 5.3). The management units strategy was not valuable for any other case, but may have been with more than two management units.

Multiple tactics may be a valuable site-specific strategy,¹³ but research on SSWM with multiple tactics in the field is rare besides variable rate of a single herbicide. Adding a second tactic to patch spraying increased net gain from site-specific management by an average of \$0.84 to 4.35 ha⁻¹. Two to four tactics were recommended in the three cases for which yield loss was less with site-specific rather than uniform management (maximum benefit, all tactics, both fields and patch spraying with two tactics, all tactics, Field A). The value of yield loss prevented was \$0.38 to \$3.38 ha⁻¹. In one case, the benefit of SSWM was more cost-effective control of weeds rather than reduced herbicide use (Tables 5.4 and 5.5). Herbicide use was greater, but yield loss and herbicide cost were reduced in the case of the maximum benefit with all tactics in Field A.

5.6 LIMITATIONS: ACCURACY AND SPEED

WeedSite users will understand that the usefulness of their evaluations will depend on the accuracy of the weed maps they draw. They also should be aware that the detail of the map will influence accuracy of the evaluations. For example, the value of SSWM would likely be underestimated if the user chooses to draw a big patch to represent a scattered group of small patches. Underestimation will depend on the size of the small patches relative to the area of the single big patch, raster cell size, and the grid for patch spraying. Besides the error in evaluations due to the inaccuracy and lack of detail of maps, there will be error from predicting outcomes of weed management with a simple simulation model given the many interacting factors influencing the choice and outcomes of management. However, the relationships between the benefits from SSWM and weed distribution, number of tactics that can be used, and management resolution will likely still be demonstrated.

The greatest limitation of WeedSite as a tool to evaluate SSWM is the time required for an evaluation. Users can increase raster cell size for faster, but less accurate evaluations. Evaluations would be faster and likely more accurate with an analysis of polygon intersections rather than the raster-based calculations of polygon size. A web-based version of WeedSite would overcome this limitation because there are libraries of GIS functions for Visual Basic code that calculate polygon intersections and we could eliminate the use of raster cells. Royalties charged for distribution of these libraries would not be a problem with a web-based version since we would not be distributing the program.

5.7 CONCLUSIONS

We think WeedSite can be a useful tool to help growers, agricultural consultants, and students learn about the potential benefits of SSWM in irrigated corn and how

TABLE 5.4
Tactics recommended for site-specific and uniform weed management in Field A for a scenario with all possible tactics and a scenario with the five least expensive tactics excluded

Tactic	Uniform Application	Maximum Benefit of Site-Specific ^a	Site-Specific Strategy						Management Units
			Patch Spraying			Patch Spraying			
			One Tactic			Two Tactics			
			6 × 18 m	12 × 36 m	6 × 18 m	12 × 36 m	12 × 36 m	12 × 36 m	
Percentage of Field									
All Tactics									
No Control	—	29%	43%	36%	24%	17%	—	—	
17 g ha ⁻¹ rimsulfuron + 6 g ha ⁻¹ thifensulfuron	100%	27%	57%	64%	50%	55%	100%	100%	
7 g ha ⁻¹ carfentrazone-ethyl	—	26%	—	—	27%	28%	—	—	
878 g ha ⁻¹ imisulfuron + 131 g ha ⁻¹ nicosulfuron + 852 g ha ⁻¹ atrazine	—	13%	—	—	—	—	—	—	
34 g ha ⁻¹ foramsulfuron + 2 g ha ⁻¹ iodosulfuron-methyl-sodium	—	5%	—	—	—	—	—	—	
Most Expensive Tactics ^b									
No Control	—	33%	43%	36%	28%	22%	—	—	
878 g ha ⁻¹ rimsulfuron + 131 g ha ⁻¹ nicosulfuron + 852 g ha ⁻¹ atrazine	100%	14%	57%	64%	48%	50%	100%	100%	
34 g ha ⁻¹ foramsulfuron + 2 g ha ⁻¹ iodosulfuron-methyl-sodium	—	6%	—	—	—	—	—	—	
841 g ha ⁻¹ bromoxynil + 561 g ha ⁻¹ atrazine	—	21%	—	—	24%	28%	—	—	
39 g ha ⁻¹ nicosulfuron + 13 g ha ⁻¹ rimsulfuron	—	26%	—	—	—	—	—	—	

^aMaximum benefit from site-specific weed management is estimated with the optimal tactic selected for each unique local weed population in the field.

^bFive herbicide or herbicide mixtures that cost \$3.71 to \$15.00 ha⁻¹ were excluded as possible tactics.

TABLE 5.5
Tactics recommended for site-specific and uniform weed management in Field B for a scenario with all possible tactics and a scenario with the five least expensive tactics excluded

Tactic	Uniform Application	Maximum Benefit of Site-Specific ^a	Site-Specific Strategy				Management Units
			Patch Spraying		Patch Spraying		
			One Tactic	Two Tactics	One Tactic	Two Tactics	
	6 × 18 m	12 × 36 m	6 × 18 m	12 × 36 m			
Percentage of Field							
All Tactics							
No Control	—	—	47%	44%	47%	44%	—
645 g ha ⁻¹ 2,4 D Amine	—	4%	—	—	—	8%	—
7 g ha ⁻¹ carfentrazone-ethyl	—	50%	—	—	5%	—	—
878 g ha ⁻¹ rimsulfuron + 131 g ha ⁻¹ nicosulfuron + 852 g ha ⁻¹ atrazine	100%	46%	53%	56%	48%	48%	100%
Most Expensive Tactics ^b							
No control	—	50%	47%	52%	46%	44%	58%
105 g ha ⁻¹ mesotrione	—	4%	—	—	6%	8%	—
34 g ha ⁻¹ foramsulfuron + 2 g ha ⁻¹ iodosulfuron-methyl-sodium	—	46%	—	—	48%	48%	42%
37 g ha ⁻¹ foramsulfuron	—	—	—	48%	—	—	—
26 g ha ⁻¹ nicosulfuron + 13 g ha ⁻¹ rimsulfuron	100%	—	53%	—	—	—	—

^aMaximum benefit from site-specific weed management is estimated with the optimal tactic selected for each unique local weed population in the field.

^bFive herbicide or herbicide mixtures that cost \$3.71 to \$15.00 ha⁻¹ were excluded as possible tactics.

the benefits can vary from field to field and with the strategy for implementing site-specific weed management. We acknowledge the inaccuracy of hand-drawn weed maps but our examples show that much of what is known about variability of benefits of SSWM can be demonstrated. Also, the benefits of SSWM with multiple tactics or situations for which herbicide use is not reduced, but control is more cost-effective, may be difficult to predict without a tool such as WeedSite. Hand-drawn maps are usually the only information about weed distribution available for growers' fields. These maps are reasonable because WeedSite is for education rather than recommendations.

Hand-drawn weed maps may be more representative than field experiments of the weed species and distributions in a user's field. The best feature of WeedSite, however, may be that users can investigate the benefits of site-specific weed management for how they would do it. For example, a herbicide application is recommended according to the concept of economic threshold³² in WeedSite and many field experiments.^{6,8,9,13,21,27,31} However, we know from discussions with growers and agricultural consultants that herbicides may be selected for many reasons other than cost-effectiveness, such as maximum weed control, guarantees on performance, herbicides on sale, herbicides they already have, and personal preference. Also, a grower may want to treat an area of a field with a very low weed population. To accommodate these choices, we included the options of choosing just some of the tactics for an evaluation (Figure 5.1) and selecting the tactic for each management unit (Figure 5.4). With the strategy of grower management, users can choose the whole field as a management unit and specify a particular tactic to compare site-specific outcomes with a uniform herbicide application they choose. Users also choose the resolution of patch spraying and may draw any number of management units of various sizes and shapes.

WeedSite can be downloaded for free from the USDA-ARS website <http://arsag-software.ars.usda.gov/> and is also provided in the CD included with this book under the Chapter 5 directory. The decision model of WeedSite is structured to be modified for different row crops or regional variation in outcomes or tactics of weed management by changing values in databases.²⁸ We chose parameters to give the same result the postemergence weed management component of the decision model Weed-CAM.³¹ Contact the authors for information on the database structure.

ACKNOWLEDGMENT

This research was partially funded by the U.S. Environmental Protection Agency, Region 8, Denver, Colorado. Mention of a trade name or proprietary product does not constitute a guarantee or warranty by the U.S. Department of Agriculture and does not imply approval to the exclusion of other products that may be suitable.

REFERENCES

1. Cardina, J., Johnson, G.A., and Sparrow, D.H., The nature and consequence of weed spatial distribution, *Weed Sci.*, 45, 364, 1997.

2. Colbach, N., Forcella, F., and Johnson, G.A., Spatial and temporal stability of weed populations over five years, *Weed Sci.*, 48, 366, 2000.
3. Johnson, G.A., Mortensen, D.A., and Gotway, C.A., Spatial and temporal analysis of weed seedling populations using geostatistics, *Weed Sci.*, 44, 704, 1996.
4. Wiles, L.J. and Schweizer, E.E., Spatial dependence of weed seed banks and strategies for sampling, *Weed Sci.*, 50, 595, 2002.
5. Wyse-Pester, D.Y., Wiles, L.J., and Westra, P., Infestation and spatial dependence of weed seedling and mature weed populations in corn, *Weed Sci.*, 50, 54, 2002.
6. Oriade, C.A., King, R.P., Forcella, F., and Gunsolus, J.L., A bioeconomic analysis of site-specific weed management for weed control, *Rev. Agric. Econ.*, 18, 523–535, 1996.
7. Wiles, L.J., Canner, S.R., and Bosley, D.B., Talking about weed pressure: an interview survey of farmer and crop consultant descriptions of weed density level, *Proc. West. Weed Sci. Soc.*, 51, 117, 1998.
8. Nordbo, E., Christensen, S., Kristensen, K., and Walter, A.M., Patch spraying of weeds in cereal crops, *Aspects Appl. Biol.*, 40, 325, 1994.
9. Brown, R.B. and Steckler, J.-P.G.A., Prescription maps of spatially-variable herbicide application in no-till corn, *Trans. Am. Soc. Agric. Eng.*, 38, 1659, 1995.
10. Paice, M.E.R., Miller, P.C.H., and Day, W., Control requirements for spatially selective herbicide sprayers, *Comp. Electr. Agric.*, 14, 163, 1996.
11. Johnson, G.A., Cardina, J., and Mortensen, D.A., Site-specific weed management: current and future directions, in *Site-Specific Management for Agricultural Systems*, Robert, P.C., Rust, R.H., and Larson, W.E., Eds., American Society of Agronomy, Madison, WI, 131, 1997.
12. Mulla, D.J., Mapping and managing spatial patterns in soil fertility and crop yield, in *Site-Specific Crop Management*, Robert, P.C., Rust, R.H., and Larson, W.E., Eds., American Society of Agronomy, Madison, WI, 15, 1993.
13. Medlin, C.R. and Shaw, D.R., Economic comparison of broadcast and site-specific herbicide application in nontransgenic and glyphosate-tolerant *Glycine max*, *Weed Sci.*, 48, 652, 2000.
14. Paice, M.E.R. and Day, W., Using computer simulation to compare patch spraying strategies, in *Precision Agriculture '97*, Stafford, J.V., Ed., Bios Scientific Publishers Limited, Oxford, UK, 421, 1997.
15. Colliver, C.T., Maxwell, B.D., Tyler, D.A., Roberts, D.W., and Long, D.S., Georeferencing wild oat infestations in small grains: accuracy and efficiency of three weed survey techniques, in *Precision Agriculture*, Robert, P.C., Rust, R.H., and Larson, W.E., Eds., American Society of Agronomy, Madison, WI, 453, 1996.
16. Gerhards, R., Wyse-Pester, D.Y., Mortensen, D.A., and Johnson, G., Characterizing spatial stability of weed populations using interpolated maps, *Weed Sci.* 45, 108, 1997.
17. Green, H.M., Vencill, W.K., Kvien, C.K., Boydell, B.C., and Pocknee, S., Precision management of spatially variable weeds, in *Precision Agriculture '97*, Stafford, J.V., Ed., Bios Scientific Publishers Limited, Oxford, UK, 983, 1997.
18. Heisel, T., Christensen, S., and Walter, A.M., Weed managing model for patch spraying in cereal, in *Precision Agriculture*, Robert, P.C., Rust, R.H., and Larson, W.E., Eds., American Society of Agronomy, Madison, WI, 999, 1996.
19. Heisel, T., Christensen, S., and Walter, A.M., Validation of weed patch spraying in spring barley — a preliminary trial, in *Precision Agriculture '97*, Stafford, J.V., Ed., Bios Scientific Publishers Limited, Oxford, UK, 879, 1997.

20. Rew, L.J., Cussans, G.W., Muggleston, M.A., and Miller, P.C.H., A technique for mapping the spatial distribution of *Elymus repens*, with estimates of potential herbicide usage from patch spraying, *Weed Res.*, 36, 283, 1996.
21. Williams II, M.M. and Mortensen, D.A., Crop/weed outcomes from site-specific and uniform soil-applied herbicide applications, *Prec. Agric.*, 2, 377, 2001.
22. Luschei, E.C., Van Wychen, L.R., Maxwell, B.D., Bussan, A.J., Buschena, D., and Goodman, D., Implementing and conducting on-farm weed research with the use of GPS, *Weed Sci.* 49, 536, 2001.
23. Christensen, S., Walter, A.M., and Heisel, T., The patch treatment of weeds in cereals, *Brighton Crop Protection Conference – Weeds*, British Crop Protection Council, Farnham, UK, 591, 1999.
24. Wallinga, J., Groeneveld, R.W.M., and Lotz, L.A.P., Measures that describe weed spatial patterns at different levels of resolution and their applications for patch spraying of weeds, *Weed Res.*, 38, 351, 1998.
25. Van Wychen, L.R., Bussan, A.J., and Maxwell, B.D., Accuracy and cost effectiveness of GPS-assisted wild oat mapping in spring cereal crops, *Weed Sci.*, 50, 129, 2002.
26. Rew, L.J., Miller, P.C.H., and Paice, M.E.R., The importance of patch mapping resolution for sprayer control, *Aspects Appl. Biol.*, 48, 49, 1997.
27. Lybecker, D.W., Schweizer, E.E., and Westra, P., Computer decision aid for managing weeds in irrigated corn, in *Agricultural Research to Protect Water Quality*, Soil and Water Conservation Society, Minneapolis, MN, 295, 1993.
28. Wiles, L.J., King, R.P., Schweizer, E.E., Lybecker, D.W., and Swinton, S.M., GWM: General weed management model, *Agric. Systems*, 50, 355, 1996.
29. Beck, K.G., McDonald, S.K., Nissen, S.J., Oman, C.C., and Westra, P.H., 2004 *Colorado Weed Management Guide for Field and Vegetable Crops*, Publication XCM-205, Colorado State University Cooperative Extension Service, Fort Collins, CO, 2004.
30. Gaussoin, R.E., Kappler, B.F., Klein, R.N., Knezevic, S.Z., Lyon, D.J., Martin, A.R., Roeth, F.W., Wicks, G.A., and Wilson, R.G., 2005 *Weed Management Guide*, Publication EC04-130-D, University of Nebraska Cooperative Extension, Lincoln, NE, 2005.
31. Lybecker, D.W., Schweizer, E.E., and King, R.P., Weed management decisions in corn based on bioeconomic modeling, *Weed Sci.*, 39, 124, 1991.
32. Coble, H.D. and Mortensen, D.A., The threshold concept and its application to weed science, *Weed Technol.*, 6, 191, 1992.

6 Map Quality Assessment for Site-Specific Fertility Management

T.G. Mueller

CONTENTS

6.1	Executive Summary	103
6.2	Introduction	104
6.3	Materials and Methods.....	105
6.4	Results	108
6.5	Summary and Conclusions	110
6.6	GIS Application.....	111
	Acknowledgment	115
	References.....	119

6.1 EXECUTIVE SUMMARY

Maps of soil and crop properties must be of adequate quality for site-specific fertility management to be effective. Therefore, managers should consider assessing map quality in test fields before adopting site-specific fertility management for an entire farm. The objective of this study was to demonstrate how map quality assessment methods could be applied to the site-specific management of a central Kentucky field. Ordinary kriging, inverse distance weighted (IDW), radial basis function, and polynomial interpolation procedures were applied to two soil fertility data sets (200- and 300-ft regular grids) from a central Kentucky field. Validation and cross-validation analyses generated substantially different results. Global and local polynomial interpolation procedures produced maps of unreliable quality. Ordinary kriging, IDW interpolation, and radial basis interpolation produced similar maps. Maps obtained using 300-ft grids were generally of poor quality. Substantial improvements occurred only for P soil test values and P fertilizer recommendations with the more intensive 200-ft sampling grids.

6.2 INTRODUCTION

A fundamental assumption of site-specific fertility management is that economically optimum application rates of lime, P, and K are adequately known across agricultural fields.¹ To estimate these rates, soil samples obtained from around individual grid points or within zones are composited. The composite samples are then sent to a laboratory for chemical analyses and algorithms are used to determine fertilizer recommendations. With grid sampling, soil properties and fertilizer recommendation maps are created with stochastic (e.g., ordinary kriging) and deterministic (e.g., inverse distance weighted, radial basis function, and polynomial) interpolation procedures (see Johnston et al.² for more details regarding interpolation techniques). The zone sampling approach involves assigning the test results to the zones from which the subsamples were collected.

The quality of fertility and fertilizer recommendation maps is generally not questioned. However, maps created with commonly used sampling and interpolation procedures have been found to be of marginal to poor quality in some studies.³⁻⁵ Therefore, managers should evaluate map quality at test sites prior to whole-farm adoption of site-specific P, K, and lime management.

Map quality can be evaluated by comparing predicted and observed soil properties. Predicted and measured values can be determined either with *validation* or *cross-validation* analyses. Validation analysis involves the collection of an independent data set and comparing estimated and measured values for each validation point. Others⁶ have referred to *validation* analysis as “jackknife analysis.” Because validation involves the collection of an additional data set, assessing map quality with this approach is potentially very costly. *Cross-validation* is often used for map quality assessment because it requires virtually no additional effort or resources. It involves removing an observation from a prediction data set. Next, the reduced data set is used to generate a prediction at the location of the point that had been removed. Then, the data point is added back to the data set. This process is repeated for all observations in the data set. Unfortunately, cross-validation may do a poor job at predicting map errors for data collected on regular grids.³ However, a recent study demonstrated that this method performed well for unaligned grids.⁵

Validation and cross-validation can be used to assess map quality with plots of predicted versus measured values or maps of residuals. Quantitative measurements include estimates of map error (e.g., the mean absolute error, mean squared error, and bias) and measures of map goodness (e.g., correlation between predicted and measured values, prediction efficiency).

In some cases, cross-validation has been used to select interpolation procedures⁷⁻¹⁰ although this is generally not recommended.¹¹⁻¹⁵ Current versions of ArcGIS (ESRI, Redlands, California) allow interpolation parameters to be selected with a cross-validation error minimization procedure. One study evaluated the use of cross-validation errors for optimizing IDW interpolation but found that this approach was generally inferior to simply using distance exponent values between 1.5 and 2.0.¹⁶

Below we will demonstrate the application of map quality assessment techniques for the site-specific management of a field in the Outer Bluegrass Region of central Kentucky. Data from a previously published study⁴ were used for these analyses.

6.3 MATERIALS AND METHODS

This study was conducted in a field located in the Outer Bluegrass physiographic region of Kentucky (38°132 N, 85°2740 W). It had been in a no-till 2-year corn- (*Zea mays* L.) wheat- (*Triticum aestivum* L.)-double-crop soybean- (*Glycine max* L. Merr.) rotation for more than 15 years. The soils were primarily derived from limestone residuum overlain by loess.

Soil samples obtained from points on a 100-ft regular grid by Mueller et al.⁴ were used in this analysis. From this data set, one 200-ft (n = 144) and one 300-ft grid (n = 68) subsets were extracted (Figure 6.1) with n indicating the total number of sampling points. In addition to these grids, validation samples were obtained randomly within regular grids (n = 70) (Figure 6.1). At each grid point, five sub-samples (one at the grid point and four within a 23-ft radius) were obtained using a 2.1-cm-diameter core to a depth of 8 in and these samples were combined to form a composite at each grid or sample point. Soils were air dried at 77°F and ground to pass a 2-mm sieve. Standard soil analyses were conducted by the soil testing laboratory at the Department of Regulatory Services, University of Kentucky. Analyses included pH (1:1 soil:water mixture), Shoemaker-McLean-Pratt buffer pH,¹⁷ P, K, Ca, and Mg (Mehlich III extractable¹⁸). Soil test P and K are reported in pounds per acre and P and K recommendations are reported in pounds of P₂O₅ or K₂O fertilizer per acre. Tri-state fertilizer recommendations¹⁹ for lime were calculated to adjust the pH to 6.4. The University of Kentucky¹⁸ recommendations for P and K were used.

The 200-ft grid data were explored using the Histogram, Normal Q-Qplot, and Trend Analysis tools available with the ArcGIS Geostatistical Analyst. Lognormal or Box-Cox transformations were performed for all variables with the exception of the lime, P, and K recommendations.

Interpolations (inverse distance weighted interpolation, global polynomial interpolation, local polynomial interpolation, radial basis function, and ordinary kriging) were conducted using the Geostatistical Wizard that is found on the Geostatistical Analyst tool bar. Theoretical details and methods for using these interpolation procedures have been described by Johnston et al.² The 200-ft and 300-ft data sets were used for prediction and the validation data set was used for validation analysis. The radial basis functions included the completely regularized spline, spline with tension, multiquadric, inverse multiquadric, and thin plate spline procedures. Interpolations were conducted with IDW for power values between 1.0 and 5.0. Interpolations were conducted with optimal power values for IDW and optimal parameter values for the radial basis functions. The software employs cross-validation to determine these optimal values. The search radii were set to 400 ft for the 200-ft grid data set and to 800 ft for the 300-ft data set.

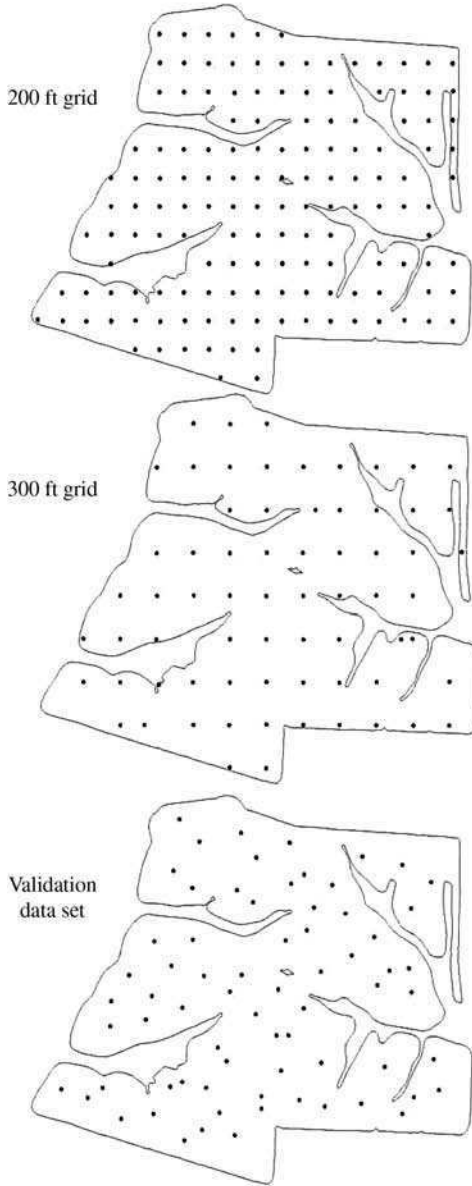


FIGURE 6.1 Soil data sets.

Prediction errors were calculated with validation and cross-validation analyses. The mean provided by geostatistical analysis is referred to as bias and the RMSE is the square root of the mean square error (MSE).

The predicted and measured values were used to calculate various measures of map quality. The MSE was the sum of accuracy and precision. It is defined in Equation 6.1.

$$\text{MSE} = \text{Accuracy} + \text{Precision} = \frac{1}{n_v} \sum_{i=1}^{n_v} v_i^2 \quad (6.1)$$

where v_i was the difference between the predicted and the observed values at location i ($i = 1, \dots, n_v$), and n_v was the number of validation or cross-validation points. Accuracy (the square of bias) is defined in Equation 6.2.

$$\text{Accuracy} = (\text{Bias})^2 = \left(\frac{1}{n_v} \sum_{i=1}^{n_v} v_i \right)^2 \quad (6.2)$$

Precision (the variance of the residuals) is defined in Equation 6.3.

$$\text{Precision} = \frac{1}{n_v} \sum_{i=1}^{n_v} (v_i - \bar{v})^2 \quad (6.3)$$

where \bar{v} represents the mean of the residuals.

A one-tailed t-test used to test for bias is defined in Equation 6.4.

$$t = \frac{\text{bias}}{\text{precision} / \sqrt{n_v}} \quad (6.4)$$

where $df = n_v - 1$.

Prediction efficiency is defined in Equation 6.5.

$$\text{Prediction efficiency (\%)} = 100 \left(\text{MSE}_{\text{field average}} - \text{MSE} \right) \left(\text{MSE}_{\text{field average}} \right)^{-1} \quad (6.5)$$

where $\text{MSE}_{\text{field average}}$ was the MSE obtained by using the field average values (obtained from the 200-ft grid data sets) as an estimate for all validation data points.

6.4 RESULTS

The histograms for soil test pH and buffer pH were bell shaped and points fell along the reference in the QQ plots. This result indicated that these variables did not deviate substantially from normality. However, P and K soil test values were positively skewed and P, K, and lime recommendation values deviated moderately to severely from normality. A log transformation of P improved the shape of this distribution. A Box-Cox transformation with negative parameter values was more appropriate for soil test K. However, lime, P, and K recommendations could not be normalized with ArcGIS. The shapes of these distributions were important to consider because kriging is not optimal if the data are not Gaussian.^{2,12}

The trends were relatively minor for the pH, buffer pH, and lime data. However, there were some spatial trends for P and K soil test value and fertilizer recommendations. Spatial trends are important because they are the basis for global and local polynomial interpolation and are used to make decisions about stationarity assumptions.

For unbiased estimates with normally distributed residuals, RMSE values can be meaningfully compared with standard deviations of the raw data. Further, 68%, 95%, and 99% of the mapped values would be expected to be plus or minus one, two, or three RMSEs from the predicted values, respectively. Only pH was both unbiased and had normally distributed residuals. Since the RMSE values for pH were greater than the standard deviations (Table 6.1), the interpolated values were more effective predictors of soil pH than the field average values.

Prediction efficiencies and correlation values indicated that kriged predictions of soil test P and P fertilizer recommendation were substantially better than interpolated values of pH, buffer pH, test K, lime recommendation, and K recommendation. Prediction efficiency is a standard measure of map quality and reflects the reduction in interpolation error relative to errors that would occur with a field average prediction. While correlation values are frequently used to assess map quality, they reflect only the scatter of the residuals about the regression between predicted and measured values. They do not reflect the scatter about the one-to-one line. While nonlinearity, non-normality, heterogeneous error variances, and spatially dependent errors can impact the significance tests, the correlation values will still be legitimate indicators of the strength of the linear relationship. Unfortunately, the relationship between prediction efficiency values and correlation between predicted and measured values appears to be nonlinear (Figure 6.2). Therefore, it is difficult to compare predictions from different studies that use these different measures of goodness.

The residuals generally did not align well along the one-to-one lines of the plots of predicted versus measured for the 200-ft (Figure 6.3) and 300-ft (Figure 6.4) grid data sets. With the exception of soil test P, increasing sampling intensity from a 300- to 200-ft grid did not dramatically improve the quality of the maps. While in most studies map quality is evaluated quantitatively, plots of predicted versus measured should always be examined before adopting a system of sampling and interpolation.

Prediction efficiency calculated with cross-validation did not relate well with prediction efficiency determined using validation analysis (Figure 6.5), which is consistent with the findings of Mueller et al.³ Brouder et al.⁵ found better relation-

TABLE 6.1
Statistics for the residuals for ordinary kriging and standard deviation of the raw data

	Bias		RMSE		Standard Deviation		Prediction Efficiency		Correlation		
	200-ft	300-ft	200-ft	300-ft	200-ft	300-ft	200-ft	300-ft	200-ft	300-ft	
pH	-0.0456	-0.0346	0.299	0.304	0.337	0.37	15.7	13.1	0.40	0.37	
Buffer pH	-0.0273 *	-0.0319 *	0.135	0.146	0.158	0.19	20.1	6.9	0.45	0.36	
P	6.47	10.6	**	18.9	25.3	33.8	35.0	58.9	26.2	0.79	0.60
K	-8.37	-7.49		64.4	66.8	57.8	64.4	8.3	1.1	0.30	0.19
Lime recommendation	0.250	0.324	*	1.15	1.22	1.23	1.49	18.0	7.4	0.43	0.37
P recommendation	-3.47	-6.64	*	21.5	25.5	33.8	32.4	59.2	42.4	0.77	0.68
K recommendation	2.41	2.81		27.5	28.3	26.9	28.2	6.9	1.5	0.27	0.20

*, ** bias values significantly different from zero at P > 0.05 and 0.01.

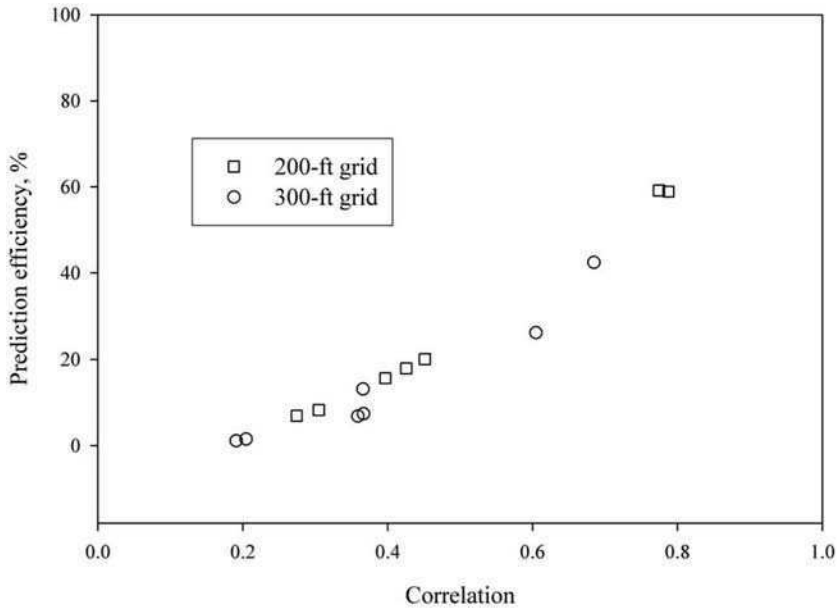


FIGURE 6.2 Prediction efficiency versus correlation between predicted and measured values for the 200- and 300-ft grid data.

ships but they did not use a validation data set with points that were randomly distributed in space. Rather, the validation points were grid points that were not being used for the interpolations in question. Additionally, they used unaligned grids for their prediction data sets whereas regular grids were used by Mueller et al.³ and in this study.

For five data sets across Kentucky (including the one used in this study), Mueller et al.¹⁶ found that when cross-validation was used to optimize IDW interpolations, prediction efficiencies were not as large as they would have been if a distance exponent between 1.5 and 2.0 had been used as demonstrated here in Figure 6.6. For regular grids, cross-validation should not be used to optimize the distance exponent value for IDW interpolation. Considering the findings of Brouder et al.,⁵ this practice might be appropriate for data collected on irregular grids.

The performance of ordinary kriging for soil test P (Figure 6.7) was not substantially better than that of IDW (Figure 6.6), polynomial, or radial basis interpolation (Figure 6.8). Although P was log normally distributed and there were spatial trends, log normal ordinary kriging and trend removal did not substantially improve prediction quality.

6.5 SUMMARY AND CONCLUSIONS

Quantitative and qualitative methods are necessary for effectively evaluating map quality. However, only validation analysis should be used to evaluate the quality of

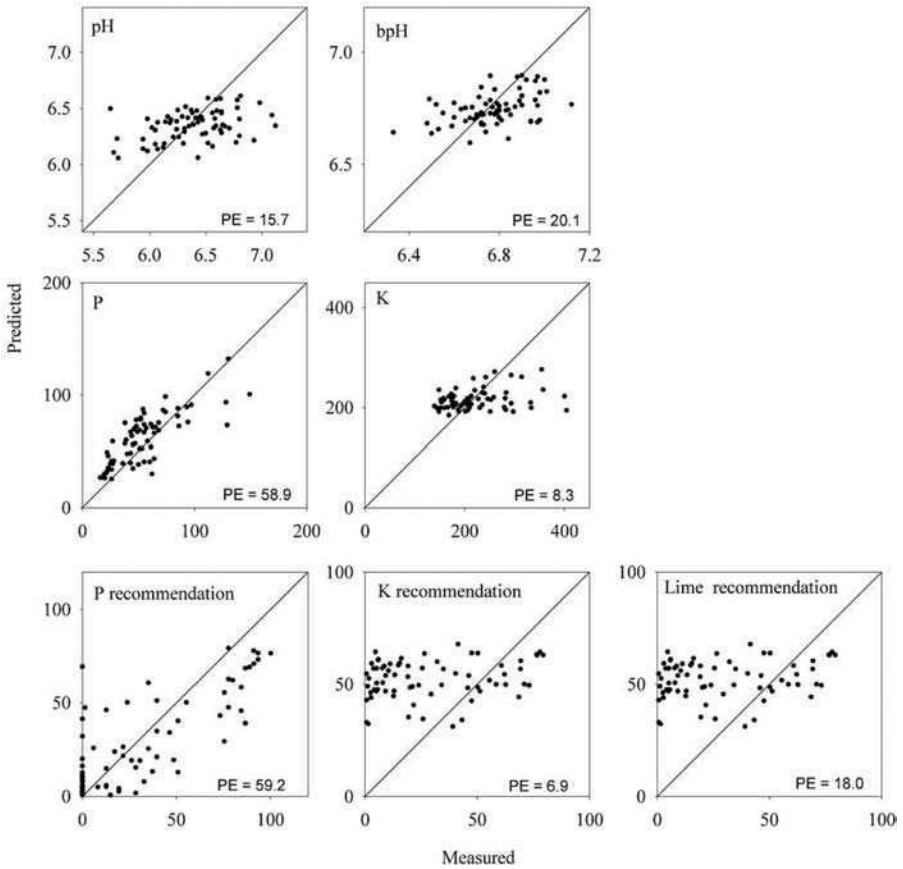


FIGURE 6.3 Predicted versus measured values for the 200-ft grid data set.

maps created with data collected on regular grids because cross-validation may lead to incorrect decisions regarding site-specific management practices.

In this study, map quality assessment methods were used to determine that log normal kriging and spatial trend removal did not necessarily produce maps of greater quality. Further, it was observed that ordinary kriging, IDW interpolation, and radial basis functions generally yielded maps of similar quality. Polynomial interpolation methods produced maps of inconsistent quality. Finally, maps created with 300-ft grids generally produced maps of marginal quality. Increasing sampling intensity to 200-ft grids only substantially improved prediction quality for soil test P and P fertilizer recommendations.

6.6 GIS APPLICATION

To complete this exercise, you must have ArcGIS 9.X and the Geostatistical Analyst extension installed. To enable the extension, begin by clicking on **tools** and then **extensions**. Make sure that Geostatistical Analyst is checked. Click close. Next,

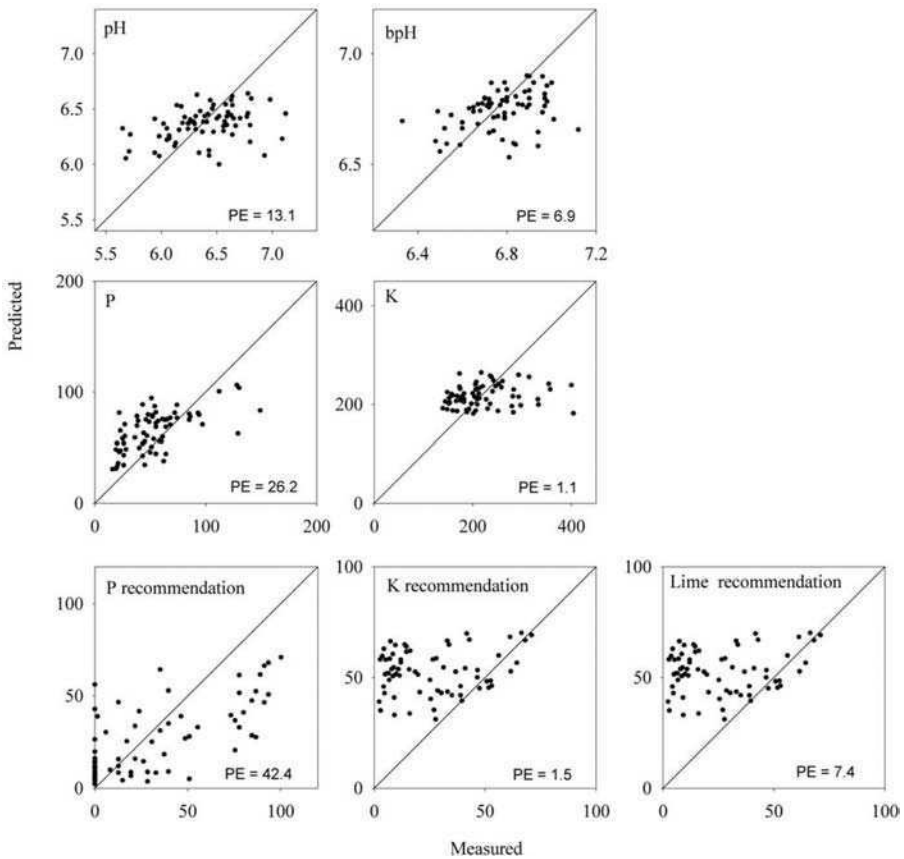


FIGURE 6.4 Predicted versus measured values for the 300-ft grid data set.

right click on the tool bar at the top of the screen. Then check the **Geostatistical Analyst** tool bar if it is not checked already. Repeat to turn on the **3D Analyst** if it is not already available. You will also need to open the geodatabase *soils data.mdb* from the CD that came with this book. Add the data from *Soils data.mdb* provided on the CD into an empty ArcMap project. This includes the *fl6* boundary file and the *XYField16_200* and *XYField16_Val* data files. The data have been projected into Kentucky State Plane (NAD_1983_StatePlane_Kentucky_North_FIPS_1601_Feet).

Click on the **Geostatistical Analyst** button on the tool bar and choose **Explore Data** and then select either **Histogram** or **Normal QQ Plot**. Figure 6.9 demonstrates how the QQ plots can be used to detect deviations from normality and to test the transformed values. See Johnston et al.² for more details on the use of these procedures.

Trend analysis can also be easily conducted with ArcGIS. Click on the **Geostatistical Analyst** button. Select **Explore Data** and then **Trend analysis**. Observe in the example provided in Figure 6.10 that the trends for soil test P were clearly visible in the east-west (green line) and north-south (blue line) directions. The green

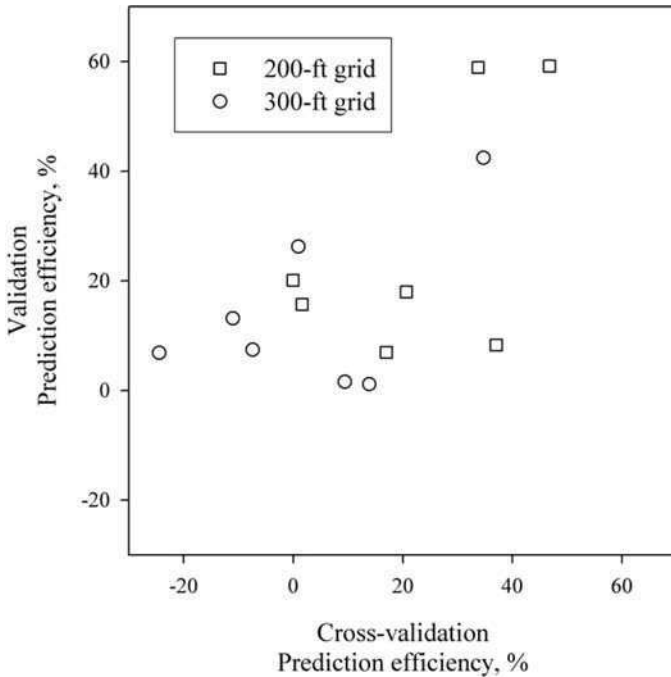


FIGURE 6.5 Prediction efficiency determined with validation analysis versus prediction efficiency versus cross-validation analysis.

and blue dots projected on the side of the graph represented the substantial scatter about the trend lines in a particular direction.

Click on the **Geostatistical Analyst** button and then click on the **Geostatistical Wizard** button. Under **data set 1**, click on *XYField16_200* (this is a 200-foot grid) and under **attribute** click on pH. Check the box next to the word **Validation**. A check should appear. Under **Input data**, click on *XYField16_val* (this is the validation data set) and set **attribute** to pH. Under **Methods**, make sure Inverse Distance Weighting (IDW) is selected. Click **next**. Note that the power is set to 2, which is the default because many people use IDW with the distance exponent equal to 2. Click **Optimize Power Value**. Note that the optimum power is 1.96 (based on cross validation). Note that the default Major and Minor Semiaxis are set to 1055. These define the geometry of the search neighborhood. Change these numbers to 400. Click on **optimize power** again. Notice that the optimal power is now 1.60. Click **Finish**. Click OK.

Note that the interpolated map does not follow the field boundaries. You can improve the map’s appearance by changing some settings. Right click on **Layers** and click on **Properties**. Click on the **data frame** tab. Under **clip to shape**, check **Enable** and click on **Specify shape**. Note that the polygon layer f16 is selected. Click OK. Click OK again. Note that the interpolation does not completely fill the boundary file. Right click on **Inverse Distance Weighting** and select **Properties**. Click on the **Extent** tab and set the extent to “the rectangular extent of f16.” Click

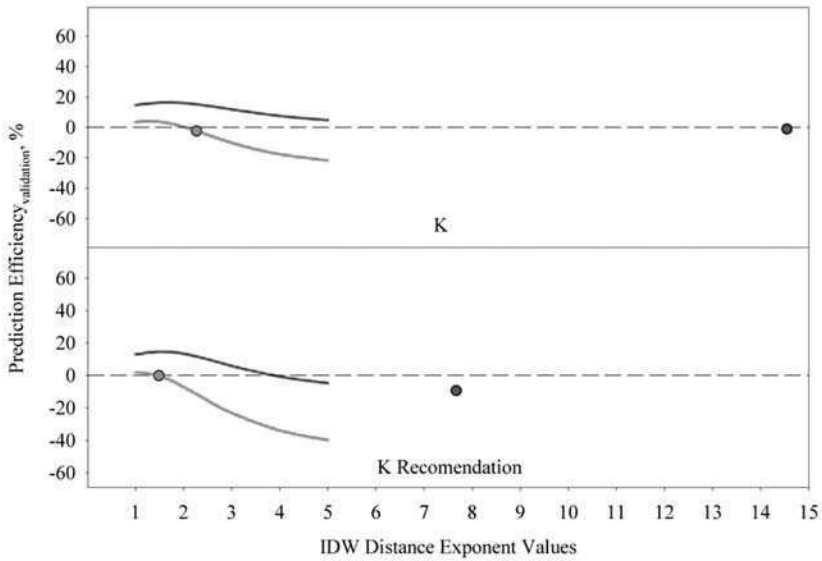
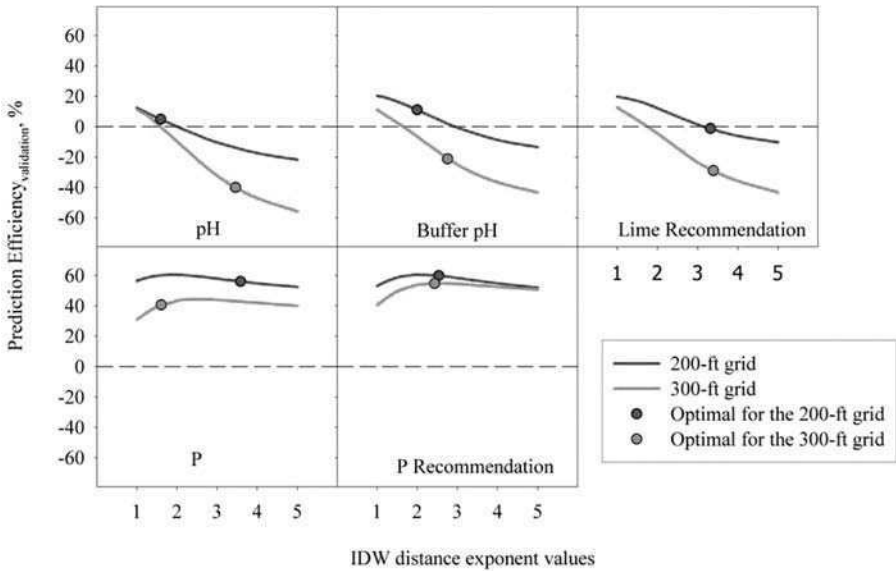


FIGURE 6.6 Prediction efficiency (validation analysis) versus IDW distance exponent values with optimal distance exponent values determined with cross validation.

on **Symbology** and then click on **Filled Contours**. Change the color ramp to the red to yellow to green ramp like before. Click OK. The screen should look like the graphic in Figure 6.11. Save your work.

Click off all the layers. Then click on the *xyfield16_val* and *Inverse distance weighting* map layers. Now put your cursor over the *xyfield16_val* layer and drag

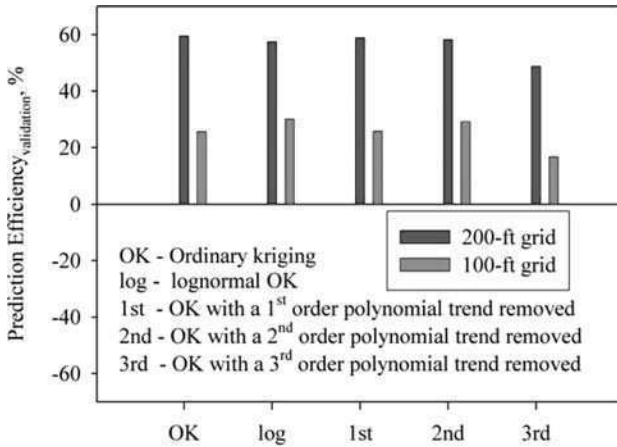


FIGURE 6.7 Prediction efficiency for ordinary kriging for soil test P.

this layer to the top. The validation points will be used to test the quality of the interpolated map. Right click on the inverse distance weighted map and click on **method properties**. Click **next**. These are the cross validation results. The Y axis represents the predicted value at each validation data point and the X value represents the measured values for each prediction point. If there is a 1:1 correspondence between predicted and measured, the data will fall along the dashed 1:1 line. A high-quality prediction will be clustered very close to this line. The blue line is the regression of the predicted as a function of measured. If the map is of high quality, the blue regression line should be along the dashed 1:1 line and the points should be scattered very close to the dashed line.

There are also quantitative values provided. Look under prediction errors. The mean (-0.012 pH units) is the bias of the map. Bias squared is accuracy. Bias in this map is very small (overall very accurate). The root mean squared error (RMSE, 0.32 pH units) is the square root of (precision + accuracy).

To view the validation results click **next**. Note that the slope of the regression line for cross validation is much greater than for validation analysis (0.33 compared to 0.14). The RMSE is also slightly greater for cross-validation than validation analysis (0.33 compared with 0.32). The above exercises can be repeated for each nutrient and with different variables in the data set.

ACKNOWLEDGMENT

This material is based upon work supported by the Cooperative State Research, Education and Extension Service, U.S. Department of Agriculture, under Agreement Numbers 99-34408-7561 and 00-34408-9287.

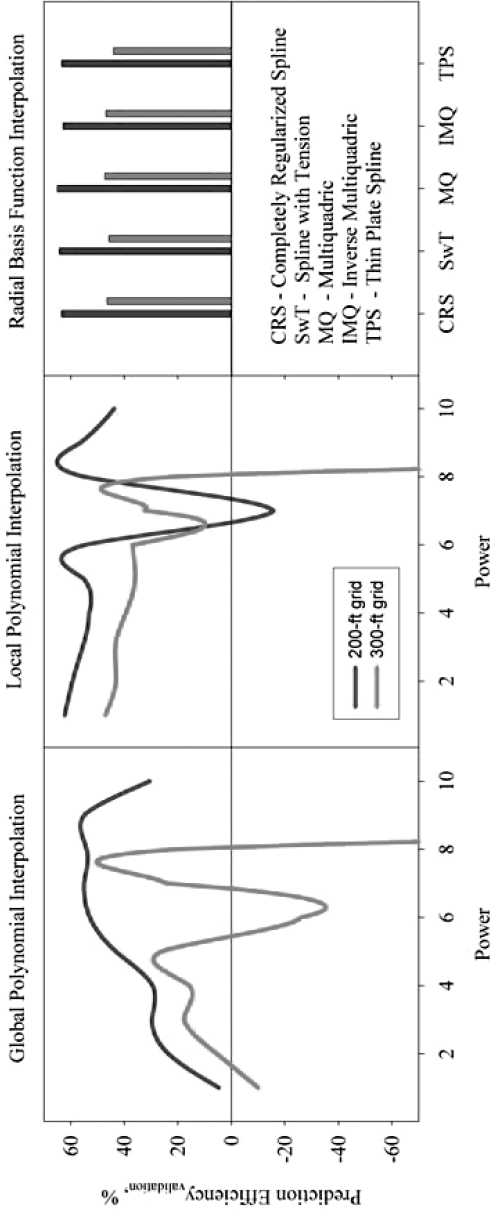
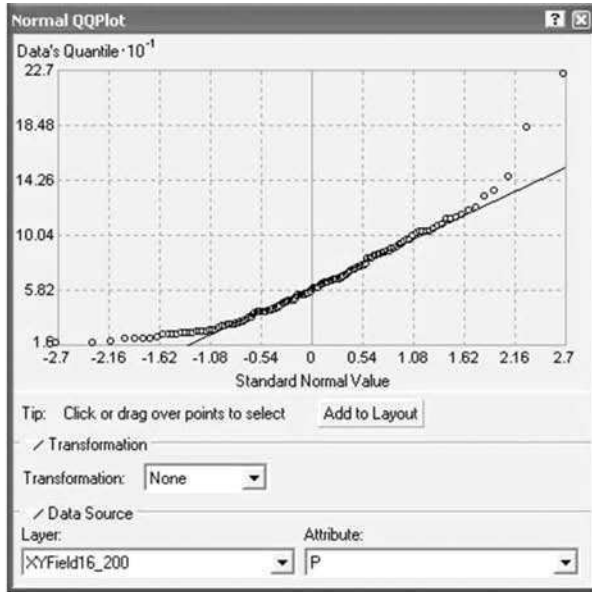


FIGURE 6.8 Prediction efficiency for global and local polynomial and radial basis function interpolation for soil test P.

a.



b.

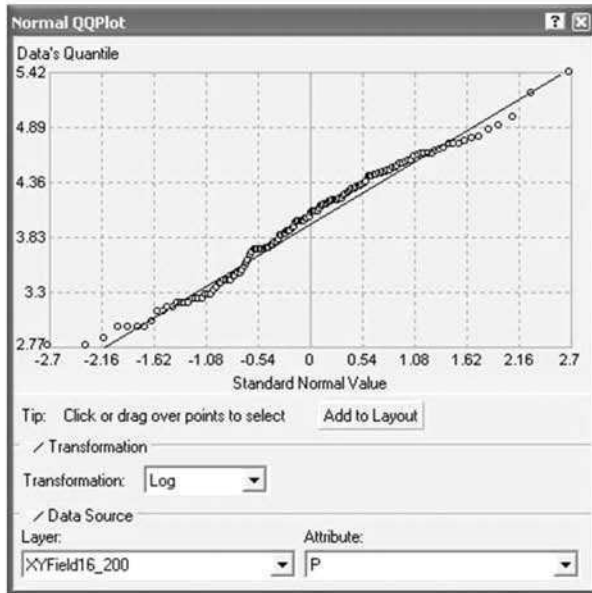


FIGURE 6.9 QQ plots for (a) raw and (b) log transformed soil P values.

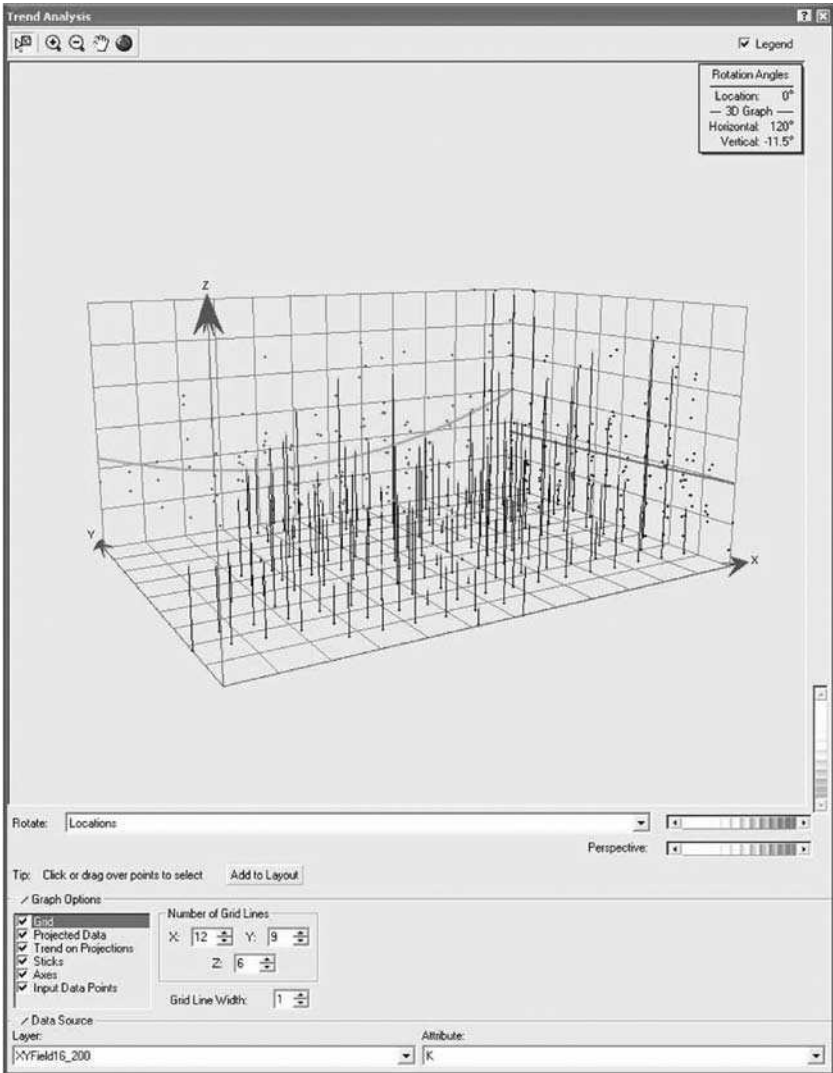


FIGURE 6.10 Trend analysis for soil test K values where the colored lines indicate the trends in the cardinal directions. The residuals in each direction are projected onto the sides of the graphs and are represented by the colored dots. The graph can be rotated to observe the trends in other directions.

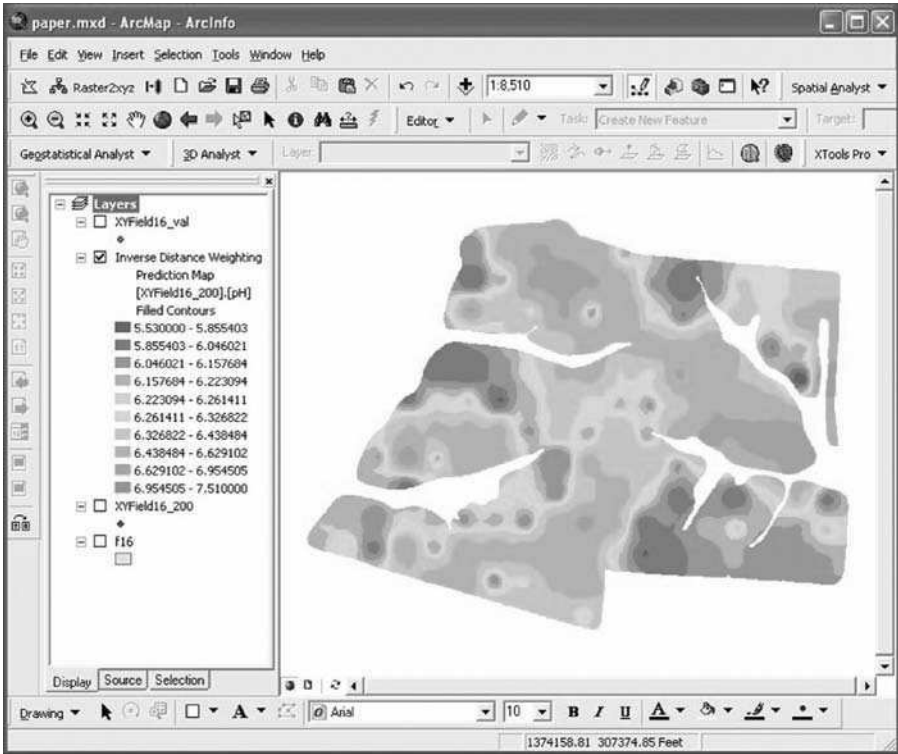


FIGURE 6.11 Interpolated soil pH values.

REFERENCES

1. Sawyer, J.E., Concepts of variable rate technology with considerations for fertilizer application, *J. Prod. Agric.*, 7, 195, 1994.
2. Johnston, K. et al., *Using ArcGIS Geostatistical Analyst*, ESRI Press, Redlands, CA, 2001.
3. Mueller, T.G. et al., Map quality for site-specific management, *Soil Sci. Soc. Am. J.*, 65, 1547, 2001.
4. Mueller, T.G. et al., Site-specific fertility management: a model for map quality, *Soil Sci. Soc. Am. J.*, 68, 2031, 2004.
5. Brouder, S.M., Hofmann, B.S., and Morris, D.K., Mapping soil pH: accuracy of common soil sampling strategies and estimation techniques, *Soil Sci. Soc. Am. J.*, 69, 427, 2005.
6. Deutsch, C.V. and Journel, A.G., *GSLIB: Geostatistical Software Library and User's Guide*, 2nd ed., Oxford University Press, New York, 1998.
7. Zhang, R., Myers, D.E., and Warrick, A.W., Estimation of the spatial distribution of soil chemicals using pseudo-cross-variograms, *Soil Sci. Soc. Am. J.*, 56, 1444, 1992.
8. Gotway, C.A. et al., Comparison of kriging and inverse-distance methods for mapping soil parameters, *Soil Sci. Am. J.*, 60, 1237, 1996.

9. Kravchenko, A. and Bullock D.G., A comparative study of interpolation methods for mapping soil properties, *Agron. J.*, 91, 393, 1999.
10. Schloeder, C.A., Zimmermann, N.E., and Jacobs, M.J., Comparison of methods for interpolating soil properties using limited data, *Soil Sci. Soc. Am. J.*, 65, 470, 2001.
11. Chiles, J.P. and Delfiner, P., *Geostatistics: Modeling Spatial Uncertainty*, Wiley, New York, 1999.
12. Cressie, N., *Statistics for Spatial Data, rev. ed.* John Wiley & Sons, New York, 1993.
13. Goovaerts, P., *Geostatistics for Natural Resource Evaluation*, Oxford University Press, New York, NY, 1997.
14. Issaks, E. and Srivastava, R., *An Introduction to Applied Geostatistics*, Oxford University Press, New York, NY, 1989.
15. Olea, R.A., *Geostatistics for Engineers and Earth Scientists*, Kluwer Academic Publishers, Norwell, MA, 1999.
16. Mueller, T.G. et al., Optimizing inverse distance weighted interpolation with cross-validation, *Soil Sci.*, 170, 504, 2005.
17. Shoemaker, H.E., McLean, E.O., and Pratt, P.F., Buffer methods for determining lime requirement of soils with appreciable amounts of extractable aluminum, *Soil Sci. Soc. Amer. Proc.*, 25, 274, 1961.
18. University of Kentucky, *2004–2005 Lime and Nutrient Recommendations*, Kentucky Agric. Exp. Stn. Bull. AGR-1, 2004.
19. Vitosh, M.L., Johnston, J.W., and Mengel, D.B., *Tri-state Fertilizer Recommendations for Corn, Soybeans, Wheat, and Alfalfa*, Michigan State University Ext. Bull E-2567, 1995.

7 Gleaning More Information from Yield Data

T.S. Murrell, Q.B. Rund and H.F. Reetz, Jr.

CONTENTS

7.1 Executive Summary.....	121
7.2 Introduction	122
7.3 Methods	124
7.3.1 Visualizing Profitability	124
7.3.2 Visualizing Production.....	126
7.3.3 Visualizing Partial Nutrient Budgets	126
7.4 Results	128
7.4.1 Visualizing Profitability	128
7.4.2 Visualizing Production.....	129
7.4.3 Visualizing Partial Nutrient Budgets	130
7.5 Conclusions	131
7.6 Step-by-Step Exercises Using ArcGIS 8.2	132
7.6.1 Visualizing Profitability	133
7.6.2 Categorizing Profitability.....	134
7.6.3 Visualizing Profit Consistency.....	135
Acknowledgments.....	139
References.....	139

7.1 EXECUTIVE SUMMARY

In production agriculture, geospatially referenced yield data are often collected but are many times underutilized. This chapter focuses on analytical techniques that are straightforward to perform and rely on concepts easily explained. Procedures are described for extracting profitability, production, and nutrient budget information from yield and other accompanying data commonly available in production settings.

Two fields, both managed in a maize (*Zea mays* L.)/soybean (*Glycine max* L. Merr.) rotation, were selected to demonstrate techniques discussed in this chapter. One field, in Minnesota, was used to show how profitability could be visualized if crop prices and total costs were known or could be reasonably estimated. Production

levels relative to yield goals were also evaluated. Coding techniques were explained that allowed profit and production consistency to be evaluated over time. The second field, in Illinois, was used to demonstrate how to estimate partial nutrient budgets from yield data, nutrient application rates, and soil test levels.

These analyses led to practical evaluations of current management practices. In the Minnesota field, soybean was found to be less consistently profitable than maize and maize yield goals should be increased. In the Illinois field it was found that phosphorus (P) and potassium (K) fertilizer rates should be reduced in a majority of the field.

7.2 INTRODUCTION

So often in production settings, maps of crop yield are the final products delivered in precision agriculture programs. While yield maps do provide valuable information, there is much practical information that can be further gleaned from them. Generating such information is not straightforward, however, and involves several steps.

The first step toward using yield data is to “clean” it. Raw yield data contain erroneous observations that need to be removed to improve the accuracy of analytical results. There are many techniques for cleaning yield data,¹⁻³ but these are not discussed here. In addition, software tools are available on the Internet that can help users identify and remove errors in raw yield data files.⁴⁻⁶ Data cleaning is discussed in Chapters 4 and 10.

Once cleaned, yield data are generally mapped using geographic information system (GIS) software. Maps of individual yield observations are the first maps generated; however, interpolation procedures are usually employed to “fill in” data gaps using estimates based on surrounding observations or accompanying data.⁷ The end result is a map of modeled yield for the whole field. Interpolation techniques include inverse distance weighting, ordinary kriging, block kriging, cokriging, simple kriging with varying local means, and kriging with external drift.⁸⁻¹⁴ The latter three methods have been examined when secondary spatial information is available for a field, such as aerial imagery.⁹ Accuracy of maps generated by various interpolation methods can be assessed and compared using cross-validation techniques.⁷

Once yield maps have been generated for a given cropping season, they must be combined with other information to answer practical questions posed by farmers and their advisors. Questions about causes of yield variability in the field may require extensive documentation, such as current and past management practices, historical land use, soil mapping units, and soil fertility, to name just a few.¹⁵ Even so, causes of yield variability can be elusive. Other information, however, can be more straightforward to generate. For instance, maps of profitability are created through simple mathematical manipulations of yield data.¹⁶

Once multiple years of yield data exist for a field, more analytical techniques become available. The focus of such methods is to quantify how yield changes over time at any given point in the field to delineate contiguous areas, or zones, where management practices can be varied. Statistical evaluations have been the thrust of most of the techniques developed to date. Their primary objective is to characterize, over time, production levels and their associated variability.

The statistical methods employed have been varied. Many use temporal variance as a basis for classifying stability, where less variable areas are classified as being more consistent.^{10,11,13,16,17} When delineating management zones, yield levels can be combined with variance estimates. Often, measured yields are transformed to a relative scale, a process termed normalization, as temporal trends are assessed. Cluster analysis techniques have also been employed as a means of delineating zones from yield data.^{10,12-14} This approach consists of a host of specific analyses, but in general it strives to divide data into separate classes, with each one being homogeneous internally yet distinct from other classes.¹⁸

Maps resulting from statistical classification approaches provide farmers and advisors with valuable information that can be used to change expectations about production levels in various regions within the field; however, they are only part of the information that these practitioners need and that can be generated from multiple years of yield data.

A complementary method of analyzing many years of yield data is to use a coding scheme to classify yield data into meaningful categories. Diker et al.⁸ introduced this method for delineating regions in the field that were either above (assigned a value of 1) or below (assigned a value of 0) the annual field average yield. An ArcView® (ESRI, Redlands, California) script was then used that calculated how many years a particular grid point had been marked with a 1. When this count was mapped, it demonstrated how many years various areas in the field exceeded the annual field average yield.

The strength of the coding approach is its simplicity, both in derivation and interpretation. Such a straightforward approach is important in production settings, where techniques are more readily adopted if they can be simply explained. Higher conceptual complexity is a shortcoming of statistical methods in such settings. The weakness of the coding approach is its lack of quantification. Knowing that an area in the field met or did not meet a specific criterion does not provide any information on the degree to which that area compared to the threshold value. Quantification, both of yield levels and their associated variability, is the strength of the statistical methods. Consequently, the two techniques are best used together.

The purpose of this chapter is to illustrate a few basic techniques that can be used to extract more information from yield data, for both single and multiple years. The target audience is the practitioner (farmer, advisor, government agent, university extension agent/educator) who wants to use yield data to evaluate management practices. Consequently, the emphasis in this chapter is on straightforward yet informative analyses that rely upon only the data that are readily and widely available in production settings. The techniques presented focus on three primary areas of interest: (1) profitability, (2) production levels, and (3) nutrient budgets. For multiple years of data, coding approaches were used because of their straightforward concepts. Readers desiring more quantitative assessments of yield trends and associated variability are referred to other chapters in this book. Exercises at the end of the chapter demonstrate essential steps in the analyses. While specific instructions and illustrations were developed for ArcGIS® v. 8.2. (ESRI, Redlands, California) with the Spatial Analyst extension, the general approaches are appropriate for a wide range of GIS software.

7.3 METHODS

The methods outlined below use grid, also termed raster, layers. These data layers have a grid structure composed of equally sized square cells. Each cell represents a discretely uniform unit of area. This type of data layer was used for two primary reasons. First, many GIS software packages have tools for incorporating raster layers into mathematical operations. Second, raster layers that have been created with consistent settings ensure the same spatial coordinates for each cell each year, allowing temporal changes to be evaluated. It is assumed that readers are familiar with the techniques needed to generate and manipulate these layers in their own GIS software. In the equations that follow, raster layers are denoted with square brackets and constants with parentheses.

7.3.1 VISUALIZING PROFITABILITY

The data in this section and the one that follows came from a 9.7-ha (24-acre) field at the Southwest Research and Outreach Center of the University of Minnesota, located near Lamberton in Redwood County, Minnesota. Maize was grown in 1998 and 2000 and soybean was grown in 1999 and 2001. Crops were harvested using a yield monitor coupled with a GPS receiver. Yield data were cleaned and interpolated using the inverse distance weighting method with a power of 2 and a variable search radius to include the nearest 12 points. Rasters of interpolated yield were created using a 9.144-m (30-ft) cell size. Whole-field production targets, termed yield goals, for this field were 8.8 and 3.0 Mg ha⁻¹ (140 and 45 bu acre⁻¹) for maize and soybean, respectively (Table 7.1). Since actual costs were not available, whole field costs of production for each year were estimated from profitability survey data from southwestern Minnesota.¹⁹⁻²² Additionally, historical average prices received by Minnesota farmers, as recorded by the National Agricultural Statistics Service (USDA-NASS),²³ were used instead of actual prices received for maize and soybean because these prices were not recorded.

Profit rasters were created for each crop (*i*) using Equation 7.1.

$$[\textit{profit}_i] = [\textit{yield}_i] \times (\textit{crop price}_i) - (\textit{total costs}_i) \quad (7.1)$$

Although crop price and total costs of production were constants in this example, they can vary across the field. When this is the case, those data layers can be converted to rasters and used instead of constants.

Rasters of production costs per unit were calculated for each crop year using Equation 7.2. These rasters allowed ready evaluations of profitability across the field under changing market conditions.

$$[\textit{per unit costs}_i] = \frac{(\textit{total costs}_i)}{[\textit{yield}_i]} \quad (7.2)$$

TABLE 7.1
Economic data for each crop year at the Minnesota location (S.I. and U.S. units provided)

Year	Commodity	Yield Goal		Total Costs ¹⁹⁻²²		Price ²³	
		(Mg ha ⁻¹)	(bu acre ⁻¹)	(\$ ha ⁻¹)	(\$ acre ⁻¹)	(\$ Mg ⁻¹)	(\$ bu ⁻¹)
1998	Maize	8.8	140	672.45	272.13	67.25	1.71
1999	Soybean	3.0	45	481.14	194.71	162.26	4.42
2000	Maize	8.8	140	624.95	252.91	67.25	1.71
2001	Soybean	3.0	45	456.38	184.69	158.59	4.32

Rasters of profitability averaged over years were created for each crop and across both crops. These averages were calculated according to Equation 7.3, where *n* is the total number of rasters.

$$[\textit{average profit}] = \frac{\sum_{i=1}^n [\textit{profit}_i]}{n} \tag{7.3}$$

In the same manner, average per-unit production costs for each crop were calculated using Equation 7.4.

$$[\textit{average per unit costs}_i] = \frac{\sum_{i=1}^n [\textit{per unit costs}_i]}{n} \tag{7.4}$$

To investigate temporal consistency in profit, binary rasters of profitability were created from each crop’s annual profit rasters. Cells were assigned a value of 0 if they were unprofitable or a 1 if they were profitable. Next, annual binary profit rasters were added across years for each crop to assess consistency of profitability for a given commodity (Equation 7.5).

$$[\textit{profit consistency}] = \sum_{i=1}^n [\textit{binary profit}_i] \tag{7.5}$$

Resulting values for each cell were counts of the number of profitable years. Possible values were 0, 1, or 2, since only 2 years’ data existed for each crop. Last, annual binary profit rasters were added across all years and crops to gain insight into profit consistency for the maize/soybean cropping system. The number of profitable years in this analysis ranged from 0 to 4.

7.3.2 VISUALIZING PRODUCTION

Yield rasters from each year were normalized on the basis of yield goals, using Equation 7.6 and the data in Table 7.1. The resulting rasters expressed yield as a percentage of yield goal.

$$[\textit{normalized yield}_i] = \frac{[\textit{yield}_i]}{(\textit{yield goal}_i)} \times 100 \quad (7.6)$$

This normalization accomplished two things. First, it provided a ready assessment of how yields compared to production goals. Second, it created a relative scale that allowed different crops to be included in a temporal analysis.

Like profit rasters, annual normalized yield rasters were converted to binary rasters. If an individual cell in the raster met or exceeded the yield goal (normalized yield $\geq 100\%$) it was coded to a 1. If it did not meet the yield goal (normalized yield $< 100\%$), it was coded to a 0. Rasters of production consistency were then created by adding individual years' binary rasters of normalized yield. Binary rasters were added over years for each crop and over all years for all crops, analogous to Equation 7.5.

7.3.3 VISUALIZING PARTIAL NUTRIENT BUDGETS

The data for this section came from a field in central Illinois. Maize was grown in 2001 and 2003 and soybean was grown in 2002. Variable rate applications of P and K were made in the fall of 2000, 2001, and 2002, prior to the subsequent cropping season. This field was used for evaluating P and K rates, so applications were made in rectangular areas (9.1 m \times 110 m or 30 ft \times 360 ft). As in the previous data set, rasters were created from yield data. Additionally, rasters were created from variable rate P and K application data as well as soil test data from the fall of 2002.

Partial nutrient budgets compare the quantity of nutrients applied to the amount removed by crop harvest, according to Equation 7.7.

$$[\textit{nutrient budget}_n] = \sum_{i=1}^n [\textit{nutrient additions}_i] - \sum_{i=1}^n [\textit{nutrient removal}_i] \quad (7.7)$$

They are used extensively in nutrient management planning to schedule manure applications and to manage soil test levels. The term "partial" is used because these budgets do not account for all mass inputs and outputs from the system. For example, additions from atmospheric deposition and losses to erosion are not considered. In Equation 7.7, n is the number of individual crops (i) considered in the partial budget. These budgets consider all nutrient applications made for a given crop, such as manure and commercial fertilizer. In this study, P and K applications were made each fall prior to the next season's crop, so the minimum amount of time spanned by the budget was one year. Longer time periods are considered in budgets when

nutrients are applied for more than one crop. An example common to the Midwest United States is a biennial P and/or K application made in the fall prior to the next season's maize crop. The rate applied is intended to satisfy the requirements of both maize and the succeeding soybean crop. In this case, the partial budget spans a minimum of two years to account for the quantity of nutrients removed by both crops. Budgets covering the minimum time periods are the most commonly used; however, longer-term partial budgets that consider multiple nutrient applications and crop seasons provide more insight into the long-term impacts of management practices on nutrient mass balance. For the Illinois field, budgets spanning all three years of yield and nutrient applications were generated.

Calculating P and K budgets required estimates of nutrient removal for each nutrient each year (Equation 7.8).

$$[\text{nutrient removal}_i] = [\text{yield}_i] \times (\text{removal coefficient}_i) \quad (7.8)$$

The removal coefficient in this equation is the amount of P or K removed per harvest unit, expressed on a dry matter (DM) basis in S.I. units or on a 15.5% or 13.0% moisture basis in U.S. units for maize and soybean, respectively. For maize, estimated removal rates were 4.0 kg P (Mg DM)⁻¹ and 4.9 kg K (Mg DM)⁻¹ (0.43 lb P₂O₅/bu and 0.28 lb K₂O/bu). For soybean, estimated nutrient removal estimates of 7.1 kg P (Mg DM)⁻¹ and 20.7 kg K (Mg DM)⁻¹ (0.85 lb P₂O₅/bu and 1.30 lb K₂O/bu) were used. These estimates were those provided by the state extension service where the study was located.²⁴

After calculating the nutrient removal rates for each crop, Equation 7.7 was used to create partial budget rasters. Rasters of variable nutrient application maps provided information on nutrient additions. The partial budgets spanned three crops (maize 2001, soybean 2002, and maize 2003) and three nutrient applications (each fall from 2000 to 2002).

Partial budget rasters were then coded into three categories (Table 7.2). Individual cells were assigned a value of 20 if their budgets were approximately balanced, indicated by a value of 0 ± 12 kg P ha⁻¹ or 0 ± 23 kg K ha⁻¹ (0 ± 25 lb P₂O₅ or K₂O acre⁻¹). Negative budgets, <-12 kg P ha⁻¹ or <-23 kg K ha⁻¹ (<-25 lb P₂O₅ or K₂O acre⁻¹) were coded to a 10. Positive budgets >12 kg P ha⁻¹ or >23 kg K ha⁻¹ (>25 lb P₂O₅ or K₂O acre⁻¹) were coded to a 30.

To be meaningful, partial budgets were combined with soil test levels. Whether or not a positive, negative, or balanced budget was appropriate depended upon how soil test levels compared to target ranges, described further in Table 7.2. Consequently, variable P and K application rasters were coded according to these soil test criteria. It was assumed that balanced nutrient budgets were equivalent to the rates needed to maintain soil test levels. Cells in soil test rasters were assigned a value of 1 if they were within an acceptable range of target levels. Acceptable ranges were 15–25 mg kg⁻¹ (ppm) for P and 120–150 mg kg⁻¹ for K. If soil test levels for cells were <15 mg kg⁻¹ or <120 mg kg⁻¹ for P and K, respectively, values of 0 were assigned. Finally, cells were assigned a 2 if their levels were >25 mg kg⁻¹ or >150 mg kg⁻¹ in soil test P or K, respectively.

TABLE 7.2
Codes and interpretations for partial budget and soil test rasters, considered alone and in combination

Partial Budget	Budget Code	Measured Soil Test Level Compared to the Target Soil Test Level	Soil Test Code	Combined Code: Budget Code + Soil Test Code	Management Correction Needed?	Type of Management Correction Needed
Negative	10	Below target	0	10	Yes	Increase inputs
Negative	10	At target	1	11	Yes	Increase inputs
Negative	10	Above target	2	12	No	–
Balanced	20	Below target	0	20	Yes	Increase inputs
Balanced	20	At target	1	21	No	–
Balanced	20	Above target	2	22	Yes	Decrease inputs
Positive	30	Below target	0	30	No	–
Positive	30	At target	1	31	Yes	Decrease inputs
Positive	30	Above target	2	32	Yes	Decrease inputs

Once both budgets and soil test levels had each been coded into three categories, they were added together to create nine new categories that combined both pieces of information. As demonstrated in Table 7.2, these nine categories led to three primary decisions about current management practices: (1) increase nutrient rates, (2) decrease nutrient rates, or (3) make no change. Consequently, the nine combined categories were represented in the legend by only three different symbols that represented each management decision.

7.4 RESULTS

7.4.1 VISUALIZING PROFITABILITY

Profit rasters generated from Equation 7.1 are shown for each crop year in Figure 7.1. Across all crops and years, estimated profit ranged from $-\$321$ to $\$282$ ha⁻¹ ($-\$130$ to $\$114$ acre⁻¹). Profitability averaged across two years for each crop (Figure 7.2), calculated according to Equation 7.3, showed that maize was profitable across a greater proportion of the field area (90.7%) than was soybean (42.9%). Also, average maize profitability exceeded soybean profitability by $\$81.16$ ha⁻¹ ($\$32.87$ acre⁻¹). The lower profitability of soybean brought down the average net returns across all years to $\$22.57$ ha⁻¹ ($\$9.14$ acre⁻¹), which was 64% lower than the average profitability for maize.

Production costs per unit, calculated by Equation 7.2, were averaged across years for each crop (Equation 7.4) and mapped in Figure 7.3. Average per unit costs of production for maize and soybean were $\$61.75$ and $\$172.91$ Mg⁻¹ ($\$1.57$ and $\$4.71$ bu⁻¹), respectively.

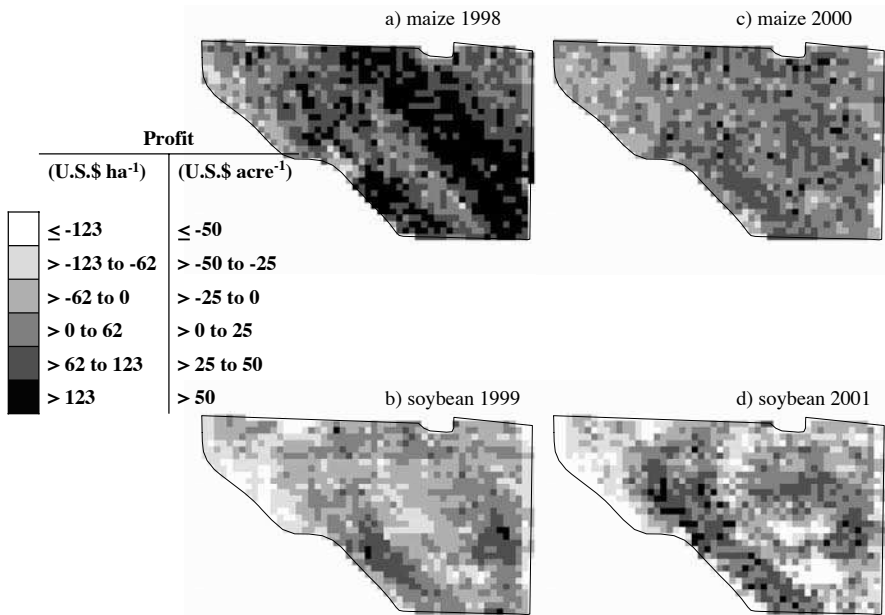


FIGURE 7.1 Profit rasters for each crop year: (a) maize 1998, (b) soybean 1999, (c) maize 2000, and (d) soybean 2001.

Figure 7.4 demonstrates how binary maps of profitability were created as precursors to maps of profit consistency over time. This coding scheme made the greater extent of maize profitability more readily discernable.

Consistency of profit over time is shown in Figure 7.5. Maize had 75.7% of the field area profitable in two of the last two years and 19.6% profitable in only one year. The northwest corner (top left) was the most inconsistent and poorest performing area of the field (Figure 7.5a). Soybean was much less consistent, with only 28.1% of the field profitable in both years and 30.6% profitable in only one year. The best performing areas of the field for soybean were two approximately parallel areas running northwest to southeast (Figure 7.5b). These areas corresponded to two ridges in the field. When analyzed over the entire rotation, these two ridges were the most consistently profitable, as shown in Figure 7.5c.

7.4.2 VISUALIZING PRODUCTION

How consistently production levels met or exceeded yield goals is shown in Figure 7.6. Approximately 93.8% of the field regularly exceeded (two out of two years) the 8.8 Mg ha⁻¹ (140 bu acre⁻¹) yield goal that had been set for maize production. This result indicated that production goals for maize should be increased for the field. For soybean only 20.7% of the field met or exceeded the production goal of 3.0 Mg ha⁻¹ (45 bu acre⁻¹) in both years. The target level was met or exceeded in one of the two years on 26.7% of the field. As shown in Figure 7.6b, production

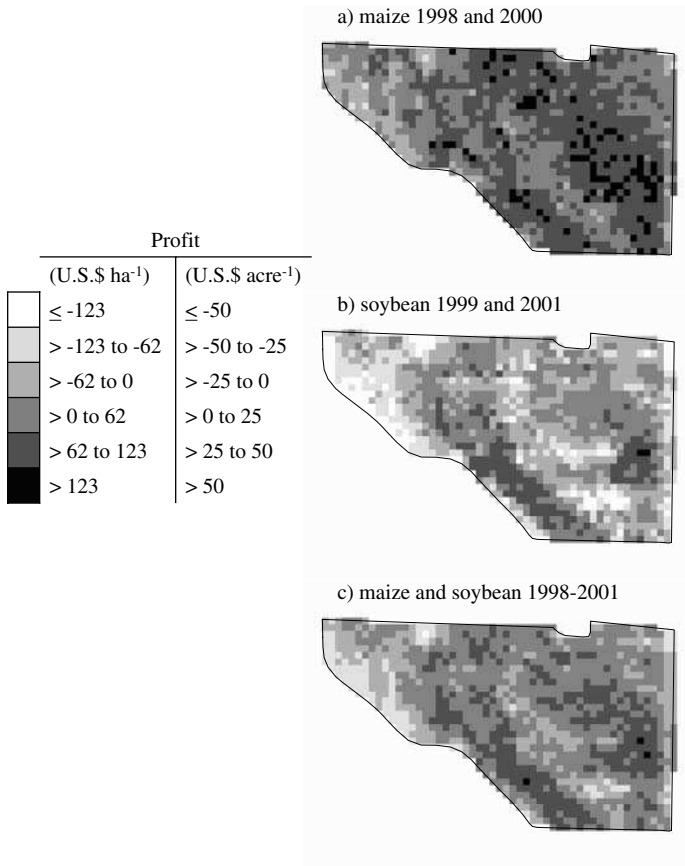


FIGURE 7.2 Average profit rasters for (a) maize 1998 and 2000, (b) soybean 1999 and 2001, and (c) maize and soybean 1998–2001.

was consistently higher along the ridges in the field. The poorer performance of soybean than maize across most of the field led to maps of production consistency (compare b and c in Figure 7.6).

7.4.3 VISUALIZING PARTIAL NUTRIENT BUDGETS

The Illinois field for which nutrient budgets were examined had been previously used for a P and K rate evaluation study. Consequently, applications had been made in rectangular strips that produced many of the spatial features in the P and K partial budgets in Figure 7.7a,b. The more natural-looking features in these maps originated from variability in nutrient removal, which was directly related to variability in yield. Positive partial budgets for P existed on 55.3% of the field and 31.9% of the area had a negative budget, meaning only 12.8% of the field was balanced (Figure 7.7a). For K, 58.6%, 35.3%, and 6.1% of the field area had a positive, negative, and balanced budget, respectively (Figure 7.7b).

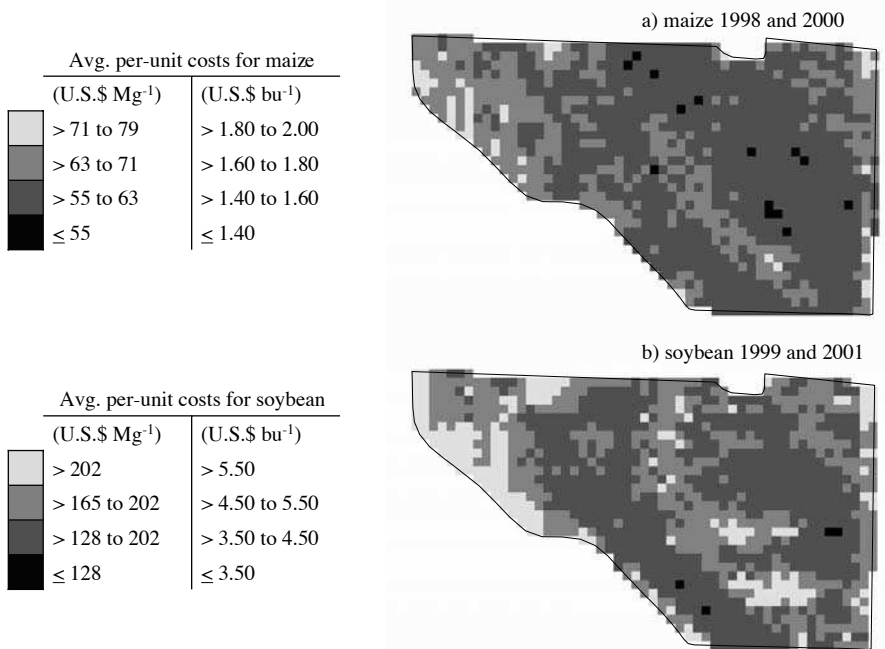


FIGURE 7.3 Average per-unit production rasters for (a) maize 1998 and 2000 and (b) soybean 1999 and 2001.

Soil test levels across the field were generally within target ranges. Desired P soil test levels were observed in 73.5% of the field. Only 4.9% of the field was below the target range, while 21.6% was higher (Figure 7.7c). Potassium was at desired levels on 64.8% of the field. Higher and lower levels were present on 4.8% and 30.4% of the field, respectively (Figure 7.7d).

Since the majority of the field had positive budgets of P and K and much of the field was at target soil test levels, rate reductions were called for on the majority of the field (Figure 7.8). Combined codes (Table 7.2) indicated that P reductions were needed on 56.3% of the field and lower K applications were appropriate for 56.9%. Applying rates needed to maintain P and K soil tests at their target levels was recommended for 17.8% and 15.9% of the field area, respectively. That left 25.9% of the field that needed higher rates of P while 27.2% needed increased rates of K.

7.5 CONCLUSIONS

The techniques used in this chapter were used to assess profitability, production, and nutrient budgets. For the Minnesota field studied, the techniques demonstrated that soybean was not as profitable as maize. In addition, target production levels of maize needed to be increased to reflect the yield attained in the last two seasons when maize was grown.

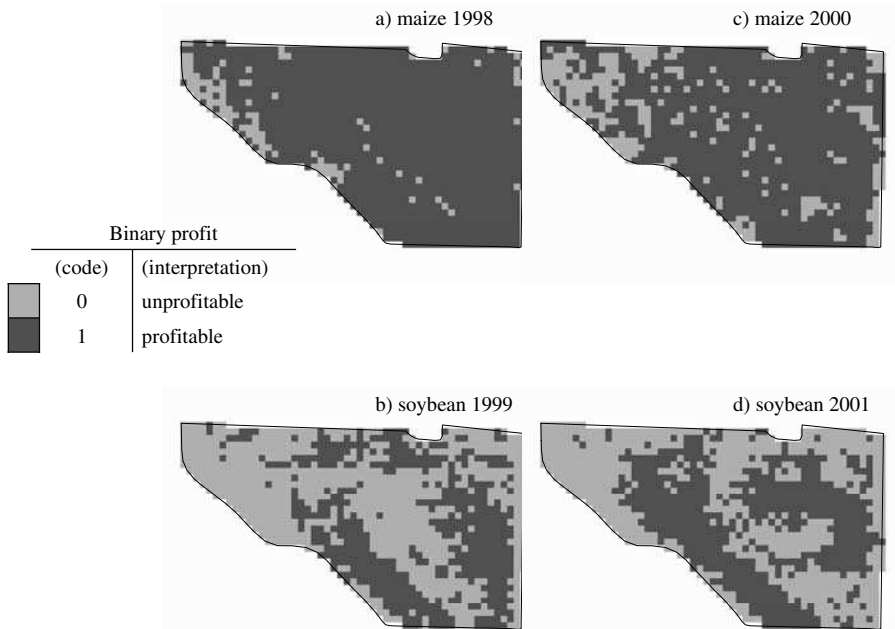


FIGURE 7.4 Binary rasters of annual profit for (a) maize 1998, (b) soybean 1999, (c) maize 2000, and (d) soybean 2001.

For the Illinois field, historical rates applied with the P and K rate studies dominated the nutrient budgets' spatial features. The majority of the field required rate reductions of both nutrients to help soil test levels stay at or return to desired ranges.

This chapter outlined straightforward procedures that are easily explained yet provide valuable assessments of management practices. The procedures do, however, lack quantification when deciding the degree to which practices need to be altered. Consequently, they are probably best combined with the types of statistical approaches discussed in other chapters of this book.

7.6 STEP-BY-STEP EXERCISES USING ARCGIS 8.2

These exercises require ArcGIS 8.2 with the Spatial Analyst extension activated. For system requirements or software information, visit www.esri.com. Data layers for these exercises are found on the compact disk (CD) under the folder for Chapter 7. Ensure that the Spatial Analyst toolbar is visible. If it is not, click **View > Toolbars > Spatial Analyst** on the standard toolbar. As a note, U.S. units are used in these exercises.

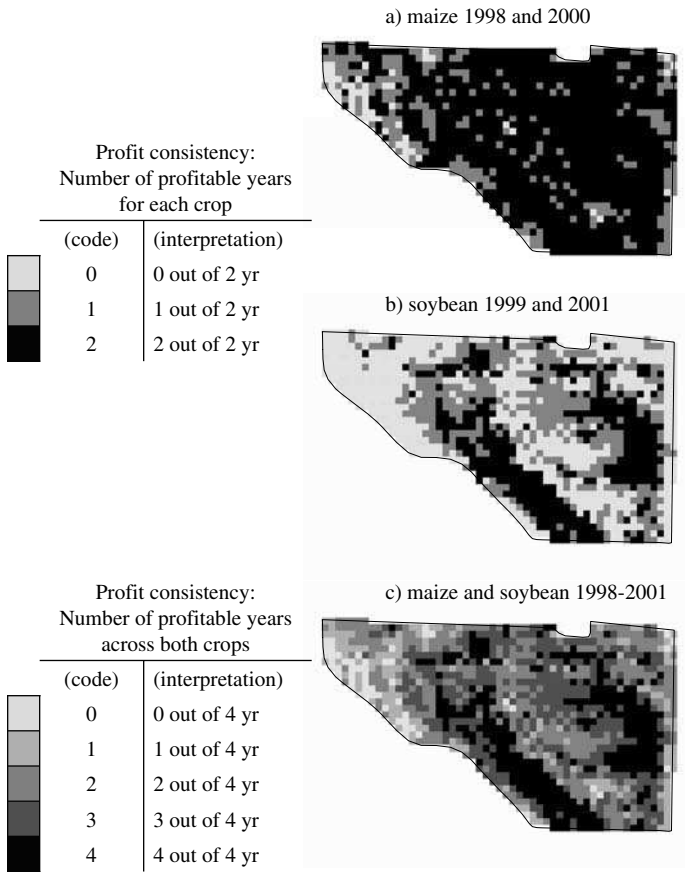


FIGURE 7.5 Profit consistency rasters for (a) maize 1998 and 2000, (b) soybean 1999 and 2001, and (c) maize and soybean 1998–2001.

7.6.1 VISUALIZING PROFITABILITY

In this exercise, you will generate a profit map from the 2001 soybean data, using Equation 7.1 and the crop price and total costs in Table 7.1.

1. Open ArcMap to a new, empty map.
2. Click **File > Add Data**. In the **Add Data** dialog box, navigate to Chapter7\ExerciseA\ on the CD accompanying this book and open file *ydsoy2001*. This is a raster of soybean yield from 2001.
3. Click **Spatial Analyst** on the **Spatial Analyst** toolbar and select **Raster Calculator**.
4. In the **Raster Calculator** dialog box, double click on *ydsoy2001* in the text box under the **Layers** label (Figure 7.9). Then click the multiplication (*) button on the calculator. Next, enter the unit price of soybeans, 4.32, click the minus button (-) on the calculator, and enter the total costs of

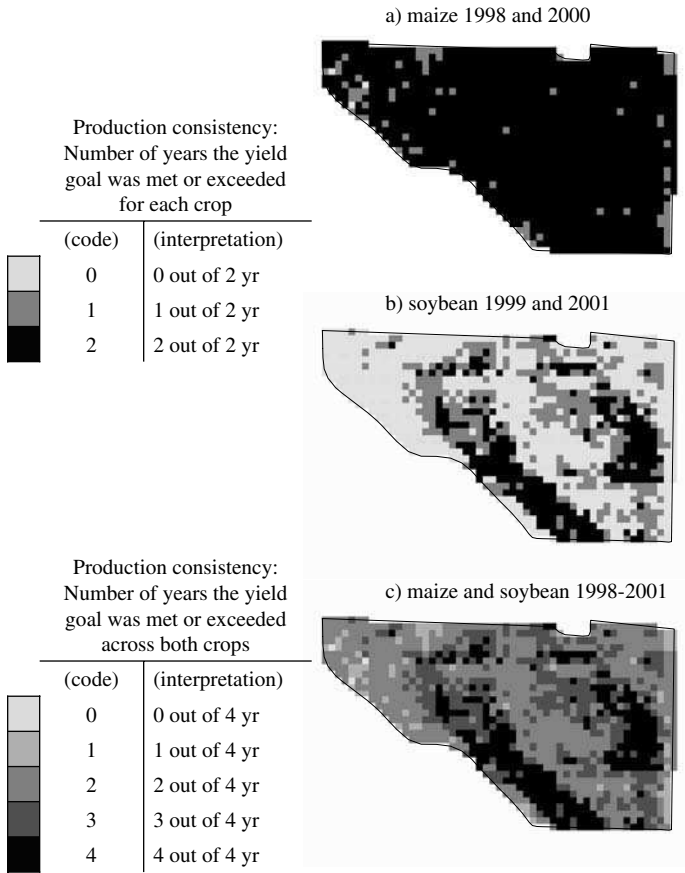


FIGURE 7.6 Production consistency rasters for (a) maize 1998 and 2000, (b) soybean 1999 and 2001, and (c) maize and soybean 1998–2001.

184.69. The **Raster Calculator** dialog box should look like the one in Figure 7.9. Once it does, click the **Evaluate** button.

5. A new layer appears with profit ranging from $-\$130.26$ to $\$76.31 \text{ acre}^{-1}$ (Figure 7.10). This is the newly created profit map. Once you have completed this exercise, close ArcMap.

7.6.2 CATEGORIZING PROFITABILITY

This exercise demonstrates how to create binary categorical maps of profit for a given crop year.

1. Open ArcMap to a new, empty map.
2. Click **File > Add Data**. In the **Add Data** dialog box, navigate to Chapter7\ExerciseB\ on the CD accompanying this book and open file *psoy2001*. This is a raster of soybean profitability from 2001.

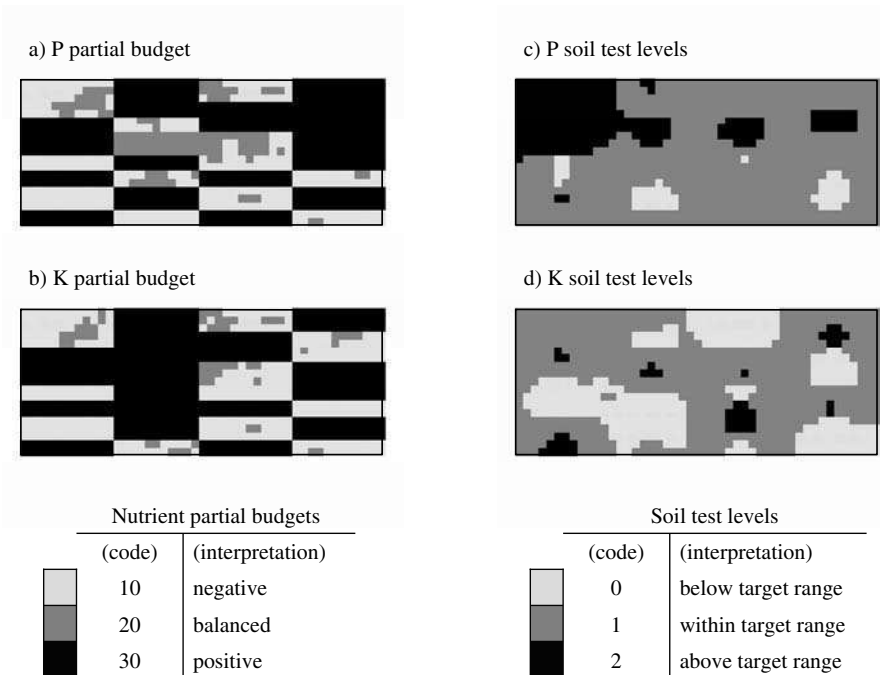


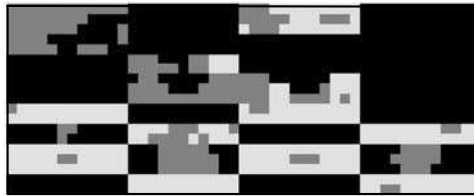
FIGURE 7.7 Coded rasters for (a) P partial budgets, (b) K partial budgets, (c) P soil test levels, and (d) K soil test levels.

3. Click **Spatial Analyst** on the **Spatial Analyst** toolbar and select **Raster Calculator**.
4. Type CON then press the left parentheses button. Double click on *psoy2001* under **Layers**. Next, press the less than or equal to button (\leq) then type 0, a comma, another 0, a comma, then a 1. Press the right parenthesis button on the calculator. The expression should be just like that in Figure 7.11. This expression uses the CON function, which has the form CON(condition, expression or value if true, expression or value if false). The expression entered in this exercise means that if a cell in the *psoy2001* raster is less than or equal to 0, it is unprofitable and therefore assigned a value of 0. If the value of the cell was greater than or equal to 0, then it was coded to a value of 1, denoting it was profitable. Once the expression has been correctly entered, press the **Evaluate** button.
5. A new layer appears with only 2 values, 0 and 1, denoting unprofitable and profitable areas, respectively (Figure 7.12). Such binary profit categorization maps form the basis of the profit consistency maps generated by Equation 7.5. Once you have completed this exercise, close ArcMap.

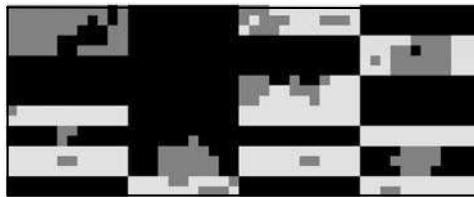
7.6.3 VISUALIZING PROFIT CONSISTENCY

In this exercise, you will create a map of profit consistency, based on Equation 7.5.

a) P



b) K



Combined categories:
Coded partial budgets
+ coded soil tests

(codes)	(interpretation)
10, 11, 20	increase nutrient rate
12, 21, 30	maintain nutrient rate
22, 31, 32	reduce nutrient rate

FIGURE 7.8 Combined partial budget and soil test categorical rasters for (a) P and (b) K, with legends coded to three tones to denote needed management changes.



FIGURE 7.9 Raster Calculator settings for generating a profit map from the 2001 soybean data.

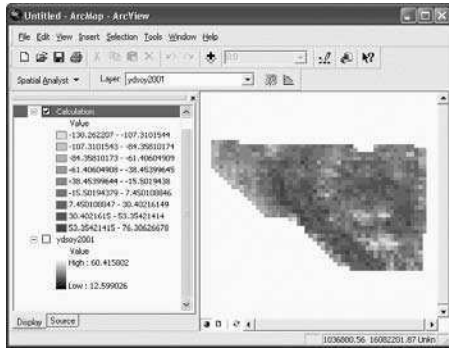


FIGURE 7.10 A raster of profit for the 2001 soybean year.



FIGURE 7.11 Raster Calculator settings for the CON function that generates a binary map of profit for the 2001 soybean year.

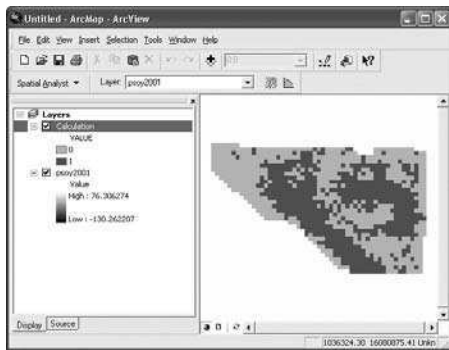


FIGURE 7.12 A binary raster of profit for the 2001 soybean year, with 0 and 1 denoting unprofitable and profitable areas, respectively.

1. Open ArcMap to a new, empty map.
2. Click **File > Add Data**. In the **Add Data** dialog box, navigate to Chapter7\ExerciseC\ on the CD accompanying this book and open file *cpcrn1998*. This is a binary raster of profitability for the 1998 maize crop. In the same manner, add the remaining three binary profit rasters named *cpcrn2000*, *cpsoy1999*, and *cpsoy2001*.
3. Click **Spatial Analyst** on the **Spatial Analyst** toolbar and select **Raster Calculator**.
4. Double click *cpcrn1998* under the label **Layers**. Press the plus (+) key on the calculator then double click *cpcrn2000*. Keep pressing the plus key and adding additional layers until all rasters have been added together and the expression matches that in Figure 7.13. Click the **Evaluate** button.
5. A new layer appears with five values, representing the number of years out of the last four that individual cells have been profitable, which is a measure of profit consistency (Figure 7.14). Once you have completed this exercise, close ArcMap.

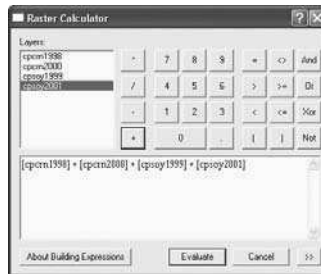


FIGURE 7.13 Raster Calculator expression that adds together binary profit rasters from all crop years to generate a map of profit consistency, according to Equation 7.5.

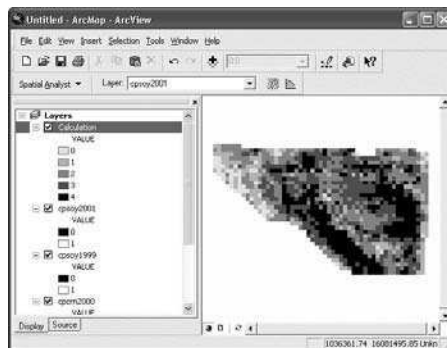


FIGURE 7.14 A consistency map of profitability, where each number represents the number of years, out of the last four, that a cell was profitable.

ACKNOWLEDGMENTS

This material is based upon work supported by the Cooperative State Research, Education, and Extension Service (CSREES), U.S. Department of Agriculture, under agreement No. 00-52103-9679 of the Initiative for Future Agriculture and Food Systems (IFAFS) program. Any opinions, findings, conclusions, or recommendations expressed in this publication are those of the authors and do not necessarily reflect the view of the U.S. Department of Agriculture. The authors would also like to acknowledge Mr. Max Crandall, formerly with ESRI, for extending his assistance and expertise to the Potash & Phosphate Institute and the Foundation for Agronomic Research.

REFERENCES

1. Reyniers, M. and De Baerdemaeker, J., Comparison of two filtering methods to improve yield data accuracy, *Trans. ASAE*, 48, 909, 2005.
2. Robinson, T.P. and Metternicht, G., Comparing the performance of techniques to improve the quality of yield maps, *Agric. Syst.*, 85, 19, 2005.
3. Simbahan, G.C., Dobermann, A., and Ping, J.L., Screening yield monitor data improves grain yield maps, *Agron. J.*, 96, 1091, 2004.
4. Drummond, S., Yield editor software, <http://www.ars.usda.gov/Services/docs.htm?docid=4776>, USDA-ARS, Columbia, MO, 2005.
5. Islam, M.M., Field analyst 1.1: A decision support system for agronomic management intensity, <http://plantsci.sdstate.edu/precisionfarm/paper/publicationSoftware.aspx>, South Dakota State Univ., Brookings, SD, 2005.
6. Simbahan, G.C. and Dobermann, A., Yield check — an algorithm for filtering of yield monitor data, <http://soilfertility.unl.edu>, University of Nebraska, Lincoln, NE, 2004.
7. Isaaks, E.H. and Srivastava, R.M., *Applied Geostatistics*, Oxford University Press, New York, NY, 1989.
8. Diker, K., Heermann, D.F., and Brodahl, M.K., Frequency analysis of yield for delineating yield response zones, *Precision Agric.*, 5, 435, 2004.
9. Dobermann, A. and Ping, J.L., Geostatistical integration of yield monitor data and remote sensing improves yield maps, *Agron. J.*, 96, 285, 2004.
10. Dobermann, A. et al., Classification of crop yield variability in irrigated production fields, *Agron. J.*, 95, 1105, 2003.
11. Lauzon, J.D. et al., Assessing the temporal stability of spatial patterns in crop yields using combine yield monitor data, *Can. J. Soil Sci.*, 85, 439, 2005.
12. Ping, J.L. and Dobermann, A., Creating spatially contiguous yield classes for site-specific management, *Agron. J.*, 95, 1121, 2003.
13. Roel, A. and Plant, R.E., Spatiotemporal analysis of rice yield variability in two California fields, *Agron. J.*, 96, 77, 2004.
14. Schepers, A.R. et al., Appropriateness of management zones for characterizing spatial variability of soil properties and irrigated maize yields across years, *Agron. J.*, 96, 195, 2004.
15. Doerge, T.A., Yield map interpretation, *J. Prod. Agric.*, 12, 54, 1999.
16. Blackmore, S., The interpretation of trends from multiple yield maps, *Comput. Electron. Agric.*, 26, 37, 2000.

17. Blackmore, S., Godwin, R.J., and Fountas, S., The analysis of spatial and temporal trends in yield map data over six years, *Biosyst. Eng.*, 84, 455, 2003.
18. Everitt, B.S., Landau, S., and Leese, M., *Cluster Analysis*, 4th ed., Arnold Publishers, London, 2001.
19. Southwestern Minnesota Farm Business Management Association, 2001 annual report, Staff paper P02-2, Department of Applied Economics, University of Minnesota, St. Paul, <http://www.cffm.umn.edu/Publications/MNAnRprtsPrv.aspx>, 2002.
20. Southwestern Minnesota Farm Business Management Association, 2000 annual report, Staff paper P01-2, Department of Applied Economics, University of Minnesota, St. Paul, <http://www.cffm.umn.edu/Publications/MNAnRprtsPrv.aspx>, 2001.
21. Southwestern Minnesota Farm Business Management Association, 1999 annual report, Staff paper P00-2, Department of Applied Economics, University of Minnesota, St. Paul, <http://www.cffm.umn.edu/Publications/MNAnRprtsPrv.aspx>, 2000.
22. Southwestern Minnesota Farm Business Management Association, 1998 annual report, Staff paper P99-2, Department of Applied Economics, University of Minnesota, St. Paul, <http://www.cffm.umn.edu/Publications/MNAnRprtsPrv.aspx>, 1999.
23. USDA-NASS, Data and statistics, http://www.nass.usda.gov/Data_and_Statistics/index.asp, 2005.
24. Hoefl, R.G. and Peck, T.R., Soil testing and fertility, in *Illinois Agronomy Handbook*, Hoefl, R. and Nafziger, E., Eds., University of Illinois, Champaign, 1995, chap. 11.

8 Soil Salinity Mapping Using ArcGIS

Florence Cassel S.

CONTENTS

8.1 Executive Summary.....	141
8.2 Introduction	142
8.3 Methods	143
8.3.1 Soil Salinity Assessment.....	143
8.3.2 Soil Salinity Mapping.....	144
8.3.2.1 Salinity Data	144
8.3.2.2 Field Boundary Data.....	145
8.3.2.3 Coordinate System.....	145
8.3.2.4 Correlating Soil Salinity Data with Other Soil and Crop Parameters.....	147
8.4 Results	147
8.4.1 Setting the Working Environment	147
8.4.2 Importing Data Into ArcGIS.....	148
8.4.2.1 Salinity Data	148
8.4.2.2 Field Boundary Data.....	150
8.4.2.3 Layer Properties	150
8.4.3 Spatial Analyses	152
8.4.3.1 Spatial Analyst Extension.....	152
8.4.3.2 Raster Interpolation.....	153
8.4.3.3 Contour Maps	156
8.4.3.4 Using the Salinity Map for Precision Agriculture	157
8.4.3.5 Correlating Soil Salinity Data with Other Soil Parameters.....	159
8.4.4 Map Layout.....	160
8.5 Conclusions	161
References.....	162

8.1 EXECUTIVE SUMMARY

Soil salinity is a critical problem in many arid and irrigated agricultural areas of the United States because of saline parent material, shallow water table, and inadequate

drainage that prevents the leaching of soluble salts. Excessive salinity negatively affects crop productivity. Therefore, it is important to evaluate soil salinity levels in agricultural fields in order to determine management methods that will help optimize crop production. Soil salinity can be measured remotely and very accurately using the electromagnetic induction (EM) methodology. When coupled with a GPS and data logging capabilities, a mobilized EM system can rapidly provide automated and georeferenced measurements of soil salinity over vast areas. This chapter describes the use of such technology for crop management practices in saline soils and details the methods to incorporate these remote-sensing data into a GIS environment for the development of soil salinity maps. The use of Spatial Analyst for the creation of surface maps is also described. In addition, this chapter explains how the salinity maps can be used to develop prescription maps for precision farming applications in cotton systems.

8.2 INTRODUCTION

Soil salinization is an agricultural and environmental concern in many arid and semi-arid regions of the United States. In California, salinity affects large areas because of the inherently clayey and saline nature of the soils, intensive irrigation that results in rising water tables, high evapotranspiration, and inadequate drainage.¹ Excessive soil salinity adversely impacts crop production, soil and water quality, and eventually results in soil erosion and land degradation. In these areas, characterizing the spatial and temporal changes in soil salinity is essential to sustain land quality, optimize crop and water management practices, and recommend adequate soil reclamation.

Over the past decade, electromagnetic induction (EM) has become a very useful and cost-effective technique for monitoring soil salinity over large areas.²⁻⁴ Compared to other methods, such as soil sampling and four-electrode probes, the EM technology provides quick, low-cost, and non-invasive measurements of soil salinity.^{5,6} Several researchers have demonstrated the usefulness of EM surveys as a rapid and economical technique to provide 3-D quantification of soil salinity levels^{7,8} as well as to predict potential crop yield reduction due to elevated salinity.⁹ Additionally, when used with a GPS and mobilized system, the EM technique allows detailed characterization of soil salinity variability across the surveyed area.

Electromagnetic induction is based on the principle that current can be applied to the soil through induction and that the magnitude of the induced current loops is directly proportional to the depth-weighted apparent electrical conductivity (EC) of the soil.^{10,11} The depth of measurement depends on the instrument length, frequency, and orientation relative to the soil surface. Since solid soil particles and rock material have very low EC, the instrument response is primarily influenced by the EC of soil water, which is dependent on the concentrations and types of ions in solution, the content and types of soil clays, the volumetric water content, and the soil water temperature. In saline soils, variations in EM measurements are primarily due to changes of ionic concentrations in the soil water. Details on the principle of the EM technology can be found in McNeill.¹⁰ In certain instances, EM instruments can also be used to indirectly characterize other soil physical and chemical properties, such as moisture, texture, and nitrate concentrations.

This chapter describes the use of a mobilized EM-GPS system to assess soil salinity in agricultural fields and details methods to incorporate remote-sensing data into a GIS environment to create soil salinity maps. These maps provide vital information to growers by identifying salt-affected areas and can be used to implement precision farming practices for variable seeding, fertilizer, or amendment applications. The use of Spatial Analyst for the creation of surface maps is also described. In addition, this chapter explains how the salinity maps can be used to develop prescription maps for precision farming applications in cotton systems. This chapter shows how to create soil surface maps in ArcGIS® v. 9.1 (ESRI, Redlands, California) using field data collected on the fly. The example presented here focuses on mapping soil salinity in agricultural fields but can be extended to any soil or plant parameters obtained experimentally in any grid pattern.

8.3 METHODS

8.3.1 SOIL SALINITY ASSESSMENT

The soil salinity assessment study was conducted in a 64-ha cotton field near Fresno, California. Soil salinity data were obtained by performing field surveys using a Mobile Conductivity Assessment (MCA) system. The MCA system, developed at the Center for Irrigation Technology, California State University, Fresno, comprised four basic components mounted on a Spra-Coupe tractor: (1) EM-38® sensor (Geonics Limited, Mississauga, Ontario, Canada), (2) global positioning system (AgGPS® 132, Trimble Navigation Limited, Sunnyvale, California), (3) computer, and (4) hydraulic soil sampler (Figure 8.1). The EM sensor was placed in a PVC carrier-sled attached 3 m behind the tractor to avoid any signal interference due to metallic objects. The GPS data were differentially corrected to sub-meter accuracy and collected as decimal degree coordinates. Two digital interfaces connected the EM sensor and GPS receiver to the on-board computer that instantaneously recorded the EM readings along with their GPS location. The ESAP statistical package¹² was used to analyze the EM data.

The MCA system was driven along transects (field rows) spaced 38 m apart. The EM and GPS data were obtained every 10 m approximately along each transect. The use of the motorized system allowed the survey to be completed in three hours. After the survey, the EM and GPS data were processed and saved into a text file; the GPS coordinates were projected to NAD 1983 UTM Zone 10. This file was imported into the ESAP statistical package to design an optimum sampling plan for calibrating the EM readings and predicting soil salinity values. The sampling plan encompassed 12 locations that were spatially representative of the EM measurements. Then, soil sampling was conducted at those selected locations using a hydraulic soil sampler. A navigational device was used with GPS to return to the selected field locations. Samples were collected to a depth of 0.5 m and analyzed for electrical conductivity, texture, and moisture. Based on the EM data and soil sample analyses, salinity was estimated at all surveyed locations using stochastic methods.¹² These estimated salinity data were used to generate the surface maps described below. Soil

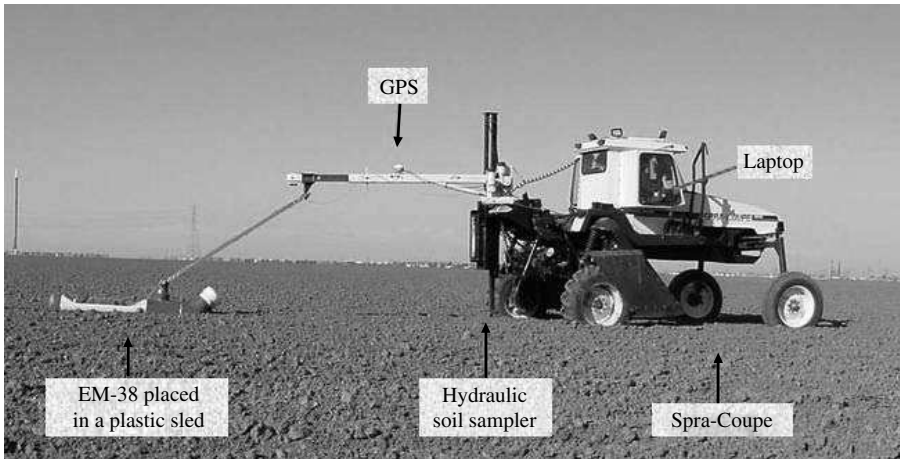


FIGURE 8.1 Mobile conductivity assessment system used to conduct the soil salinity surveys.

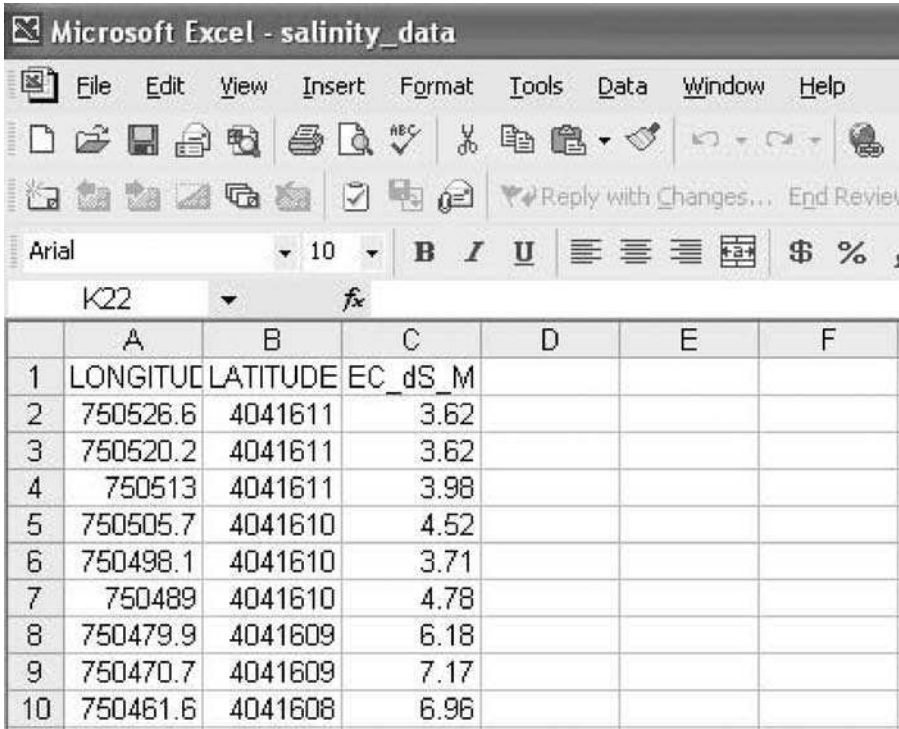
samples can also be collected at additional depths to obtain soil salinity estimates and maps at those depths. Depending on specific contamination or production problems encountered by the growers, other soil parameters, such as nitrate or boron, can also be analyzed and mapped.

8.3.2 SOIL SALINITY MAPPING

The following applications are needed to produce soil maps: ArcMap with Spatial Analyst extension, Arc Catalog, Arc Toolbox, and Excel (Microsoft Corp., Redmond, Washington). The Spatial Analyst extension is required to create continuous surface maps from discrete sample points. This extension also provides numerous analysis and spatial modeling tools, including converting features (points, lines, polygons) to rasters, performing neighborhood and zone analyses, and modeling and analyzing raster and vector data. Additional optional applications and extensions include ArcPad and Geostatistical Analyst. ArcPad is an application used to delineate and georeference the boundaries of the surveyed field via a handheld device integrated with a GPS. The Geostatistical Analyst extension can be used to define a spatial model that will be integrated in the kriging interpolation.

8.3.2.1 Salinity Data

The soil salinity and GPS data need to be saved as a text file that will be later imported into ArcMap. The file should be tab delimited with three columns: longitude (X), latitude (Y), and estimated salinity data (Z). The headings of each column should be written in the first row. The text file can be created easily in Excel or any text editor. Figure 8.2 shows the *salinity.txt* file created for this exercise.



The screenshot shows a Microsoft Excel window titled "salinity_data". The spreadsheet contains the following data:

	A	B	C	D	E	F
1	LONGITUDE	LATITUDE	EC_dS_M			
2	750526.6	4041611	3.62			
3	750520.2	4041611	3.62			
4	750513	4041611	3.98			
5	750505.7	4041610	4.52			
6	750498.1	4041610	3.71			
7	750489	4041610	4.78			
8	750479.9	4041609	6.18			
9	750470.7	4041609	7.17			
10	750461.6	4041608	6.96			

FIGURE 8.2 Screen shot of the *salinity.txt* file created for this soil salinity exercise.

8.3.2.2 Field Boundary Data

Field boundary data were also collected after the EM survey by driving the vehicle around the field using a pocket PC connected to a GPS receiver. Collection of such data is important to help visualize the experimental site and perform the spatial analyses. In this study, the ArcPad application was used to automatically create a shapefile of the field boundaries that can be imported into ArcMap and overlaid with the soil salinity map. Other applications, such as HGIS (Starpal, Inc., Fort Collins, Colorado), can also provide shapefiles of field boundaries.

Additionally, geographic maps representing the area where the study was conducted can be added to the soil salinity map to provide more information on the relative location of the field with respect to nearby town or streets, as well as counties and states. Such maps can be downloaded from various local and state agency websites.

8.3.2.3 Coordinate System

It is important to know the coordinate system parameters for the data sets you are collecting or downloading. To correctly position source data with respect to each

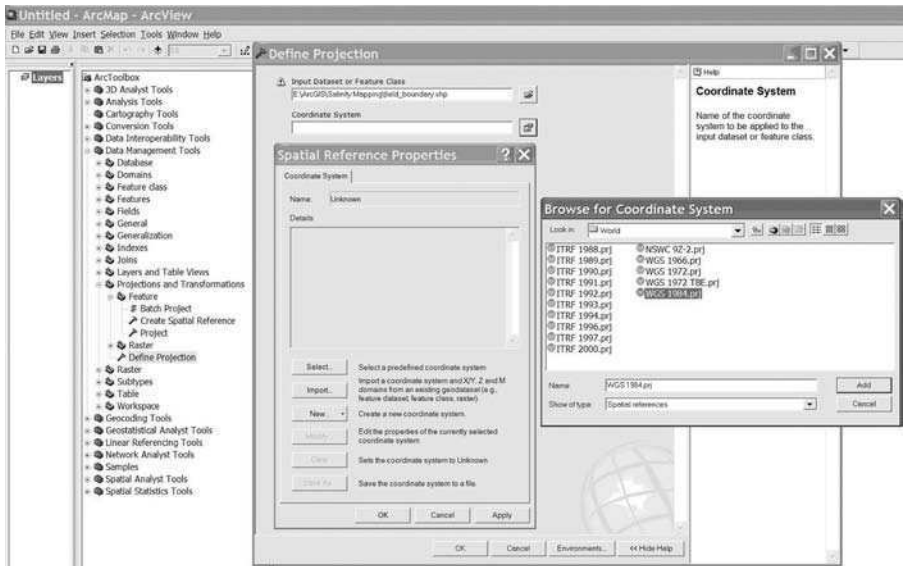


FIGURE 8.3 Screen shot of ArcMap window illustrating the field_boundary procedure for defining the coordinates of the shapefile.

other, all data must have the same coordinate system. However, if you have files with different coordinate systems, you can project them to one common system using ArcToolbox. Such conversion is performed in a two-step process: (1) define the current coordinate system and (2) project to a new coordinate system.

1. In the **ArcToolbox** window, click the + signs next to **Data Management Tools** and **Projections and Transformations** (Figure 8.3).
2. First, double-click on **Define Projection**. In the **Define Projection** window, select the input data set to define and then the *Coordinate system* using the **Open** and **Map Properties** buttons, respectively.
3. In the **Spatial Reference Properties** window, click on **Select a predefined coordinate system** and browse through the list to select the coordinate system corresponding to your file. Click **Add** and **OK** twice. Close the **Define Projection** window once the task has been completed successfully.
4. Second, project the coordinate system of your file by double-clicking on **Project** under **Data Management Tools > Projections and Transformations > Feature** (Figure 8.4).
5. Select the input data set you want to project and the output dataset location. Enter the name of the new output file and click **Save**.
6. Select the output coordinate system using the **Map Properties** button. Close the **Project** window when the task has been completed.

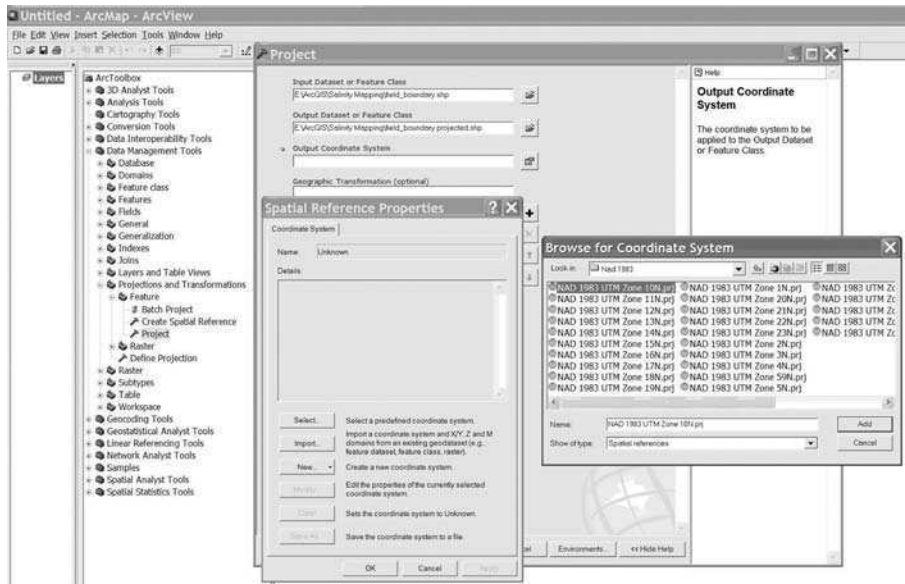


FIGURE 8.4 Screen shot of ArcMap window for projecting the coordinate system of the field_boundary shapefile.

Detailed information on projections and coordinate systems can be found in the *ESRI Guide to Map Projections*.

8.3.2.4 Correlating Soil Salinity Data with Other Soil and Crop Parameters

Soil salinity maps can be overlaid with other soil parameter maps to derive correlations among all measured parameters. Such correlations can be obtained with any other soil/crop/insect parameter of interest. For example, yield data collected with a yield monitor can provide valuable information for comparison with soil salinity. In our study, saturation percentage (SP) was used as an index of texture and data were estimated at all surveyed locations using the ESAP software.

To import the data into ArcMap, create a new text file with three columns containing the GPS coordinates and SP data (Figure 8.5). The format of the file should be identical to the one saved for the salinity data. Since the salinity and SP data were obtained for the same locations, you can also append the new data in the *salinity_data* file. For this chapter, another text file was created and saved as *SP_data*.

8.4 RESULTS

8.4.1 SETTING THE WORKING ENVIRONMENT

To set the working environment, perform the following:

	A	B	C	D	E
1	LONGITUDE	LATITUDE	SAT_PERC (%)		
2	750526.61	4041611.11	45.2		
3	750520.18	4041610.66	45.2		
4	750513.03	4041610.5	47.3		
5	750505.7	4041610.17	47.8		
6	750498.1	4041610.34	45.7		
7	750489.04	4041609.93	48.2		
8	750479.88	4041609.02	52.2		
9	750470.71	4041608.88	55.1		
10	750461.61	4041608.31	54.9		

FIGURE 8.5 Screen shot of Excel data file for import into ArcMap containing GPS coordinates and saturation percentage data.

1. After opening ArcMap, create a working directory where all your files will be saved. We set up a directory under C:\ArcGIS\ESRI. Copy all your text files and shapefiles to that directory using Arc Catalog.
2. In the ArcMap **View** menu, select **Data Frame Properties** in the drop-down menu to name the layer in the **General** tab and change the projection to UTM 83 Zone 10N in the **Coordinate System** tab. The map units will automatically be set as meters.

8.4.2 IMPORTING DATA INTO ARCGIS

8.4.2.1 Salinity Data

1. Choose **Tools > Add XY Data** from the menu to import your salinity data file (Figure 8.6). In the **Add XY Data** window, choose *salinity_data.txt*. The headings of the first two columns appear as X Field and Y Field coordinates; make sure X and Y represent the longitude and latitude data, respectively. Click on **Edit** and select the coordinate system of the soil data, Projected UTM NAD 83 Zone 10N. Then click OK twice. The XY data appear in the Data View and the name of the file is shown in the Table of Contents as *salinity_data.txt.Events*. The map shows the geographical locations where the experimental data were collected (Figure 8.7).
2. To convert the text file into a shapefile: right-click on the file name in the Table of Contents, point to **Data** and select **Export Data** (Figure 8.8). In

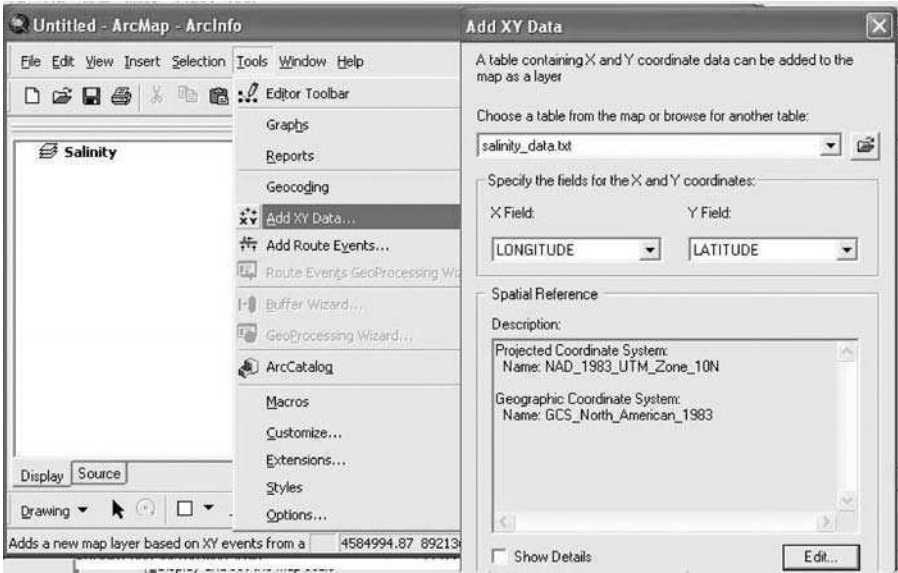


FIGURE 8.6 Screen shot of ArcMap window illustrating how to import the salinity_data file.

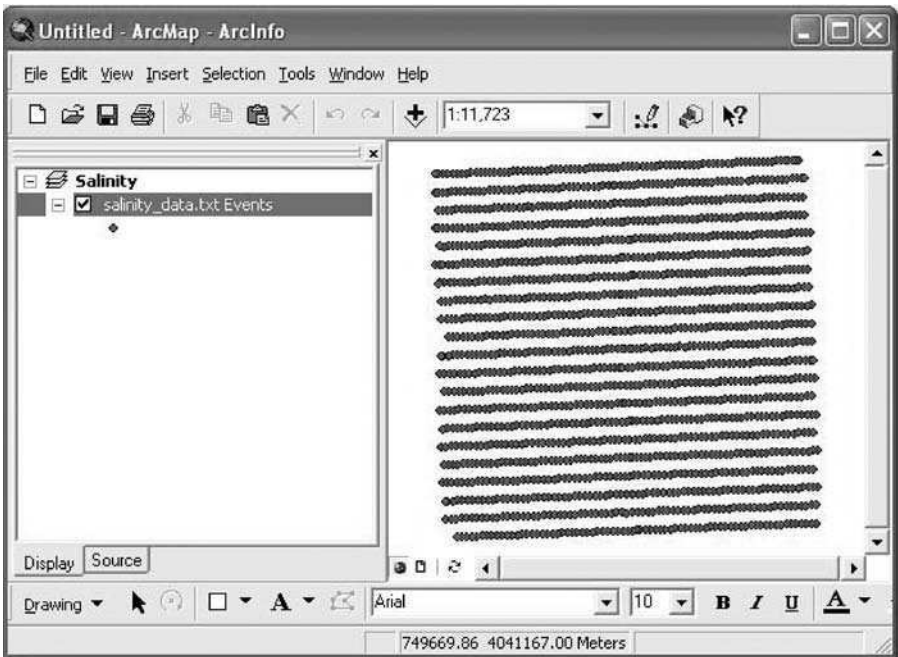


FIGURE 8.7 Screen shot of ArcMap window showing the geographical locations of the experimental data.

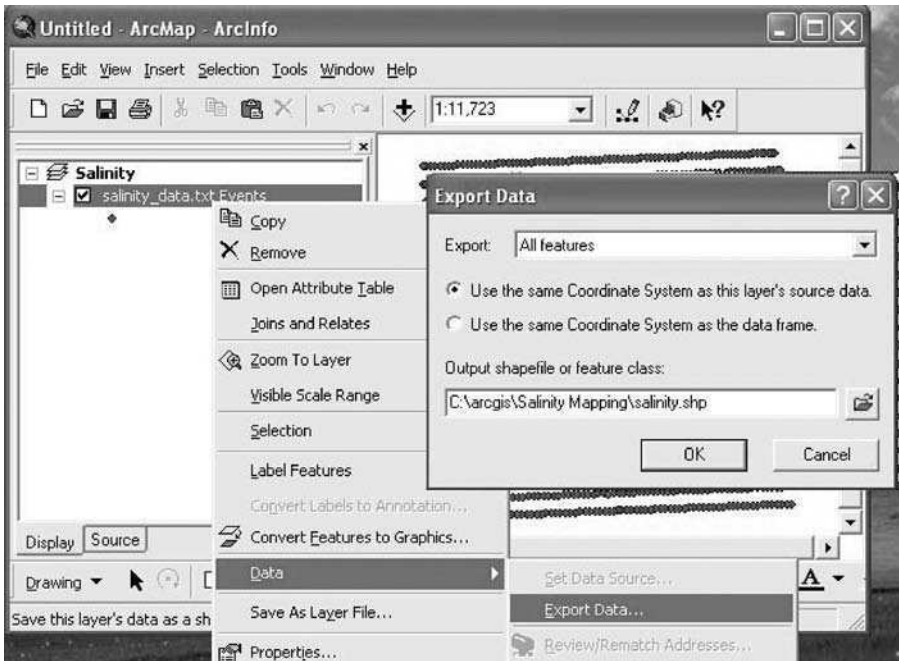


FIGURE 8.8 Screen shot of ArcMap window showing how to convert the text file into a shapefile.

the **Export Data** window, select **use the same coordinate system as this layer's source data** and enter the name of the output shapefile, *salinity.shp*. Click OK and then Yes to add the exported data to the map as a layer. The new shape file of the salinity data appears in the Data View and the name of the file is shown in the Table of Contents.

3. Save the map document as *salinity*.

8.4.2.2 Field Boundary Data

To import the field boundary shapefile, click on the **Add Data** button. Then, point to the file name (*field_boundary_projected.shp*) and click **Add**. The field boundary shapefile data appear in the Data View and the name of the file in the Table of Contents (Figure 8.9). Save the map document.

8.4.2.3 Layer Properties

You can change the layer properties (map colors, data intervals, etc.) by double-clicking on the layer name in the Table of Contents. You will now work on the salinity layer to improve the presentation of the map.

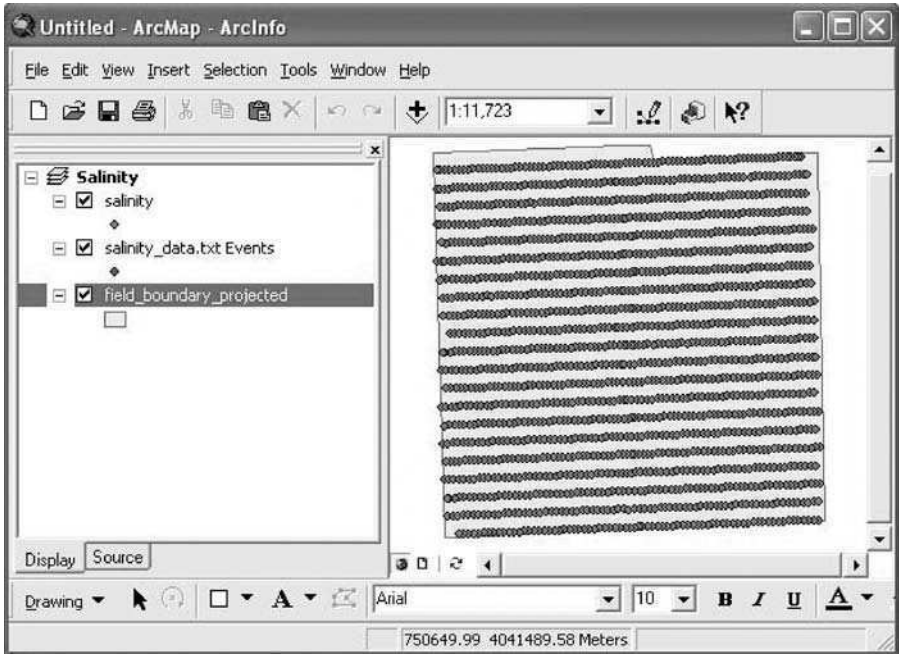


FIGURE 8.9 Screen shot of ArcMap window showing the field_boundary shapefile projected with the data point locations.

1. In the **Layer Properties** window (Figure 8.10), click on **General** tab and change the layer name to *soil salinity (dS/m)*.
2. In the **Symbology** tab, classify the salinity values into graduated color classes. In the **Show** section, choose **Quantities > Graduated colors**. Select **EC_dS_m** for the field value, and choose the green to red color ramp. In the **Classification** section, click on the **Classify** button. Then, select **Define Interval** using the drop-down arrow in the **Method** section and set the interval size to 1 (which refers to 1 dS m⁻¹); this will automatically create 11 intervals based on the salinity values. The break values of the classes will appear at the bottom right corner of the **Classification** window. Click **OK**. Double-click on **Label** to set the number formats (you should still be working under the **Symbology** tab). ArcMap will create a salinity map with colors gradually changing for each class as displayed in the color ramp. Click **OK**.

The map with the new graduated color classes will appear in the **Data View** (Figure 8.11). The legend is shown in the Table of Contents with the range values of the 11 classes and their corresponding color labels. The map shows areas of high salinity in the northern part of the field and areas of low salinity in the south part of the field.

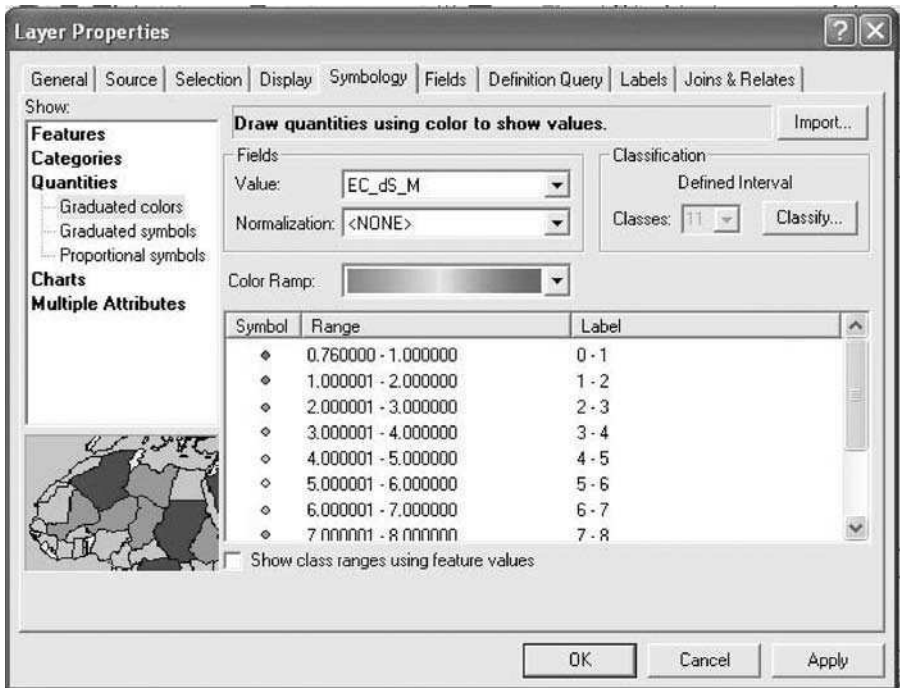


FIGURE 8.10 Screen shot of the layer properties window used to change the characteristics of the salinity layer.

8.4.3 SPATIAL ANALYSES

8.4.3.1 Spatial Analyst Extension

1. Enable the Spatial Analyst extension. Choose **Tools > Extensions** from the menu and check the **Spatial Analyst** box. This extension will enable you to create raster files in the ArcGIS environment. Spatial Analyst should then be active any time you start ArcMap. Next, choose **View > Toolbars** and check **Spatial Analyst**. The **Spatial Analyst** toolbar will appear on the ArcMap interface; you can dock it next to the Standard Toolbar.
2. When working with Spatial Analyst, it is important to set a few parameters to save all processing data and output files in the same directory, and speed up the analysis process. From the Spatial Analyst toolbar, select **Options**.
3. In the **Options** dialog box, click on the **General** tab and set the working directory to C:\ArcGIS\ESRI. Next to **Analysis Mask**, select the *field_boundary_projected.shp* from the drop-down box. This feature will limit all grid operations to the extent defined by the selected layer boundaries. In the **Analysis Coordinate System** section, select the option most

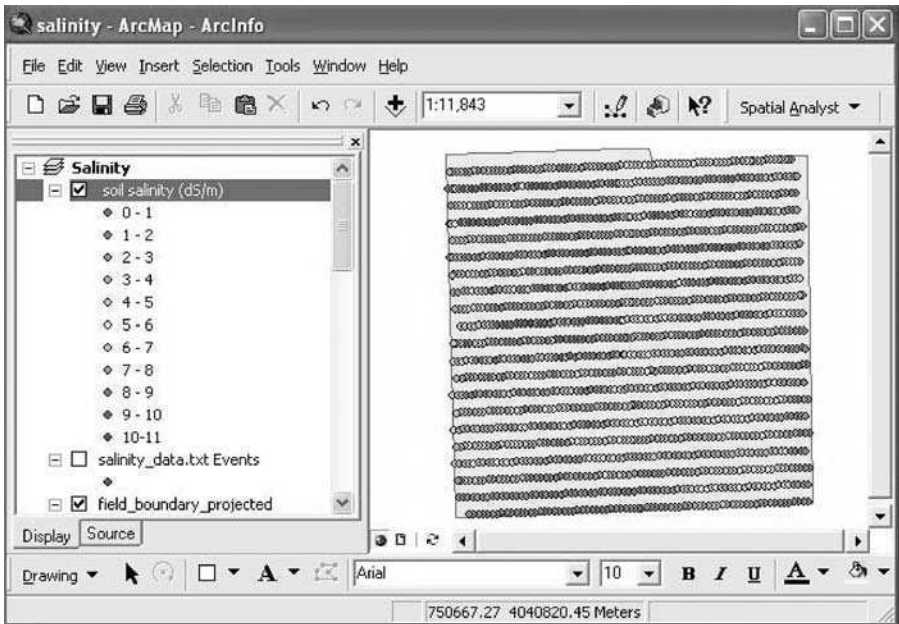


FIGURE 8.11 Screen shot of ArcMap window showing the salinity map with graduated color classes.

appropriate for you. In this exercise, we want to save the output files in the same coordinate systems as the input files.

4. Click on the **Extent** tab, select **Same as Layer field_boundary_projected** from the drop-down box.
5. Click on the **Cell size** tab and select **As Specified Below** from the drop-down box, then enter 10 in the **Cell Size** box. This number indicates the size of our output grid cell, i.e., 10 m. You can choose a smaller cell size if you want to generate a more precise map. Click OK to close the **Options** window. Save the map document.

8.4.3.2 Raster Interpolation

Spatial Analyst is used to create and analyze continuous raster data sets. These data sets are made of individual cells of identical size, each having a Z value, i.e., salinity. Spatial Analyst uses statistical methods to predict the Z values at non-surveyed locations. This procedure is called interpolation and the ArcGIS application provides several options to create surface raster maps: kriging, IDW (inverse-distance weighting), and spline. This chapter focuses on the kriging interpolation. The IDW technique is also chosen for certain agricultural studies. Kriging is a linear unbiased estimation method that provides estimates at unsampled points based on the surrounding data collected at precise locations.¹³ The intrinsic hypothesis is that the variogram depends on the distance between samples and not on the sampling location. Kriging will thus provide salinity information at any point in the field.

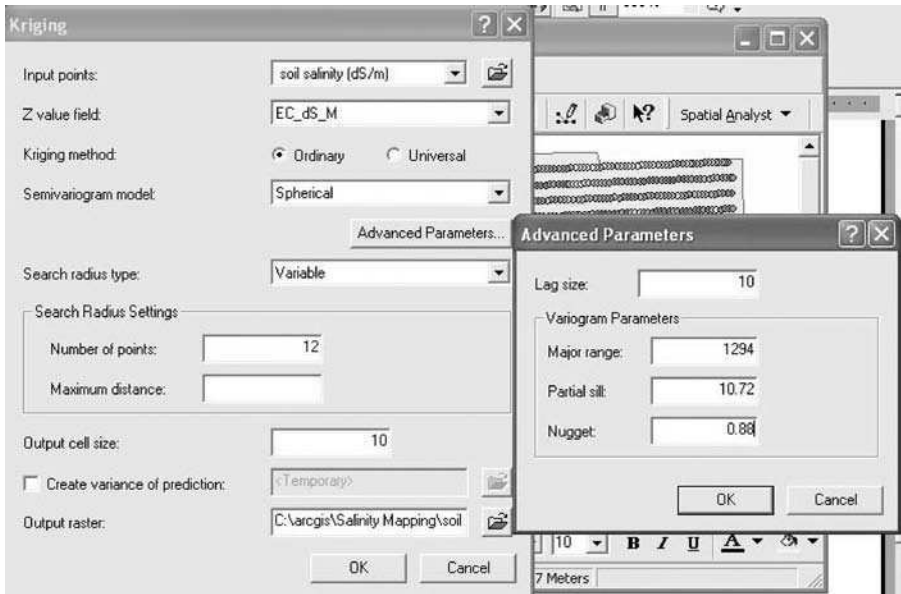


FIGURE 8.12 Screen shot of the kriging windows used by Spatial Analyst to create and analyze continuous raster data sets.

1. Activate the salinity layer in the Data Frame Table of contents.
2. In the Spatial Analysis toolbar, click on **Interpolate to Raster** and select **Kriging** (Figure 8.12).
3. In the **Kriging** window, select the soil salinity (dS/m) layer as the **Input points** and choose EC_dS_M as the **Z value field**. Select the **Ordinary Kriging method** and use the drop-down arrow to specify the semivariogram model. Such a model helps characterize the spatial structure of the salinity data and determine the spatial dependency between salinity measurements (i.e., the distance up to which the salinity data are auto-correlated and likely to be similar). The variogram models are obtained by performing geostatistical analyses using the ArcMap Geostatistical Analyst extension or other applications, such as GS+® (Gamma Design Software, Plainwell, Michigan). Detailed information on semivariogram models and geostatistical analyses can be found in Isaaks and Srivastava,¹³ Vieira et al.,¹⁴ Cambardella et al.,¹⁵ and Meirvenne and Hofman.¹⁶ For this chapter, we used the GS+ software to determine the semivariogram model that best characterized our salinity data.
4. The spatial structure of the salinity data was described by a spherical model with a range of 1294 m, a sill of 10.72, and a nugget of 0.88. Click **Advanced Parameters** and enter those values; click OK. In the **Search Radius Settings** section, enter 12 next to the **Number of points** and leave the **Maximum distance** box blank. These settings indicate that one grid cell will be interpolated using the data collected at 12 adjacent surveyed

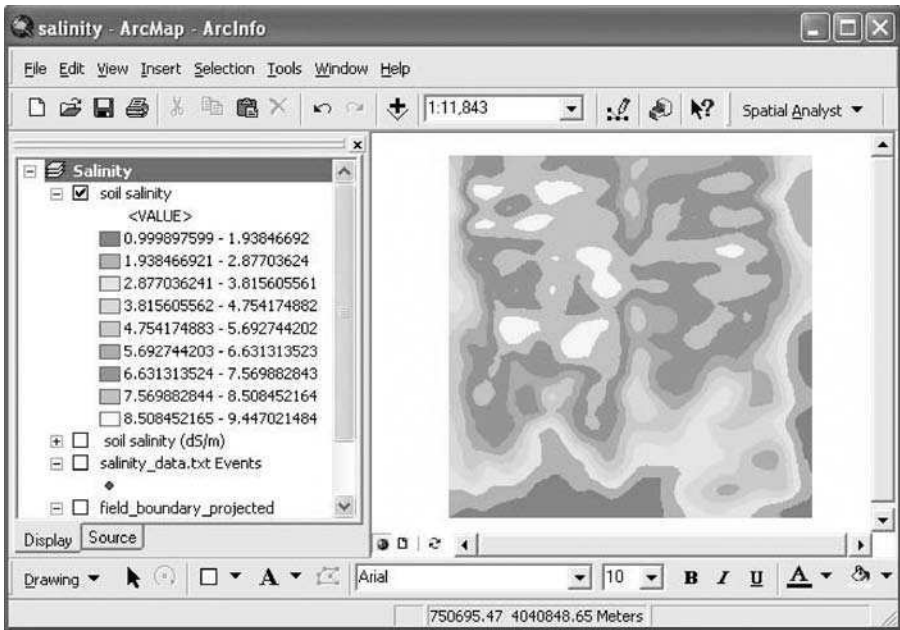


FIGURE 8.13 Screen shot of ArcMap window showing the raster map of soil salinity.

locations. The **Output cell size** should already be set at 10 m. Finally, enter the name of the output raster file: *soil_salinity*. Click OK. The new raster map appears in the Data View with its legend in the Table of Contents (Figure 8.13).

Notes: (1) The input kriging parameters will differ for other data sets depending on the spatial structure of the data, number of lag classes desired, etc. (2) When using the kriging interpolation, ArcGIS will not follow exactly the shape of *field_boundary_projected* shapefile; it will create a rectangular surface map. This problem will not appear if you use the IDW or spline interpolations. However, you can easily clip your surface map in Spatial Analyst by setting the analysis map to the *field_boundary_projected* shapefile and generating a new file (*soil_salinity_clipped*) using the Raster calculator as shown in Figure 8.14. (3) Using the kriging interpolation under Spatial Analyst is acceptable if you just want to display a surface map of your data. However, if you need to conduct further spatial analyses with your surface maps, it is recommended you use the Geostatistical Analyst extension, which provides more accurate interpolation results. Numerous kriging algorithms can be chosen in Geostatistical Analyst and comprehensive tools are available to analyze your data, including logarithmic transformation, error prediction and characterization, and detrending.

5. Open the **Layer Properties** window to modify the appearance of the new clipped map. The layer *soil_salinity_clipped* should be activated in the

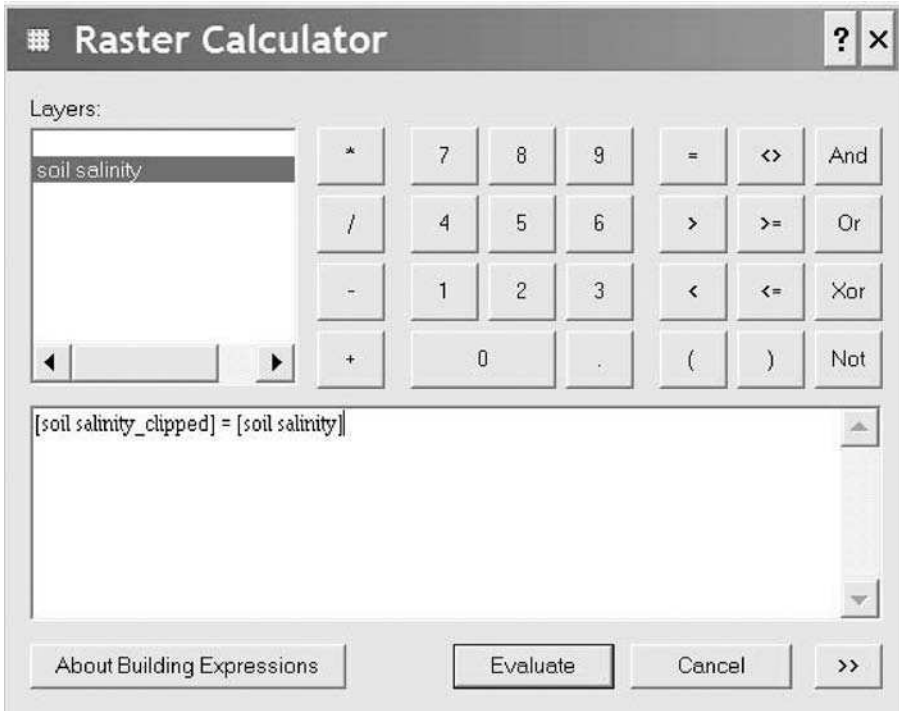


FIGURE 8.14 Screen shot of ArcMap window showing one method of clipping raster data.

Data Frame Table of contents. Click on the **Symbology** tab to classify the data into nine classes of **defined interval size 1** and choose the green to red color ramp. Click OK. Set the label format with no decimals. ArcMap will create a salinity map with colors gradually changing for each class as displayed in the color ramp. Click OK. The map with the new graduated color classes will appear in the Data View. The legend is shown in the Table of Contents with the range values of the nine classes and their corresponding color labels (Figure 8.15).

6. Activate the point and raster layers to verify that the interpolation resulted in correct estimation of the salinity levels across the field. Save the map document.

8.4.3.3 Contour Maps

We will create a contour map and layer it above the clipped raster salinity map to help visualize the salinity variability across the field.

1. In the Spatial Analyst toolbar, click on **Surface Analysis** and select **Contour**. In the **Contour** window, select the *input surface* layer name using the drop-down arrow. Set the contour interval at 1, base contour at 0, and Z factor at 1. Enter the name of the output file (*soil salinity_contour*)

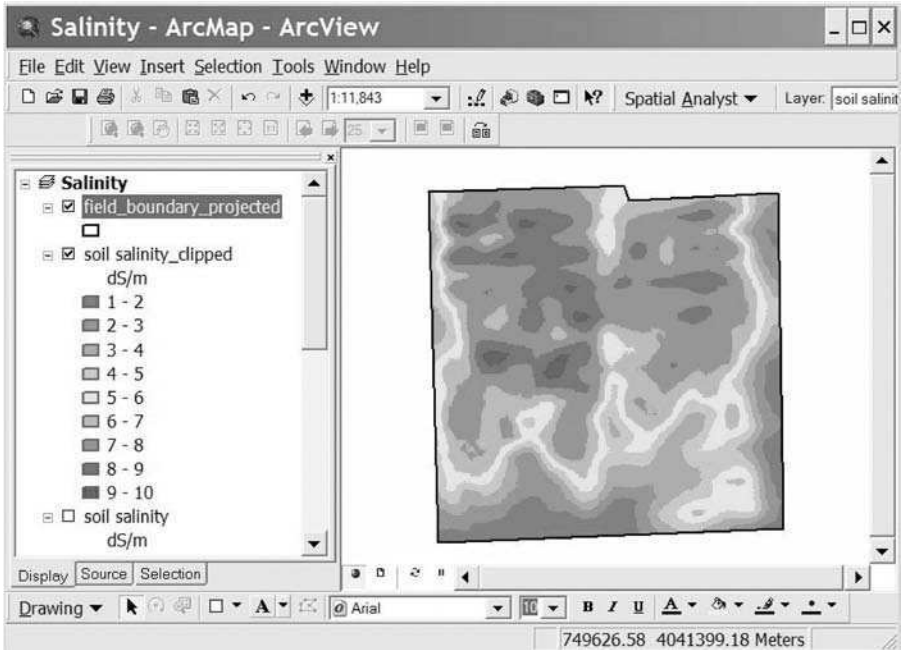


FIGURE 8.15 Screen shot of ArcMap window showing the new clipped raster map with graduated color classes.

- and click OK. The contour map now overlays the clipped salinity raster map.
2. Double-click on the name of the contour layer in the Table of Contents to change the Layer properties. Click on the **Symbology** tab to modify the size of the contour lines and the legend label. Click on the button in the **Symbol** section, and change the line size to 1. In the **Legend** section, enter the unit of the contour data, dS/m, as the **label appearing next to the symbol in table of contents**.
 3. In the **Labels** tab, check the **Label Features in this layer** box and choose to **Label all the features the same way**. In the **Text String** section, select **CONTOUR** as the **Label Field**. Click on the **Symbol** button in the **Text Symbol** section to change the font and size of the labels to Arial 9. Click OK. Hit the **PlacementProperties** button to place all the labels above the lines. A new layer of contours now appear in the Data View (Figure 8.16). Save the map document.

8.4.3.4 Using the Salinity Map for Precision Agriculture

Production of cotton is affected by elevated soil salinity levels. As we have seen on the salinity raster maps, high variability in salinity exists across the field. Therefore, certain farmers have started managing their fields as different sub-units instead of one homogeneous area. One important concern for growers is the low seed emer-

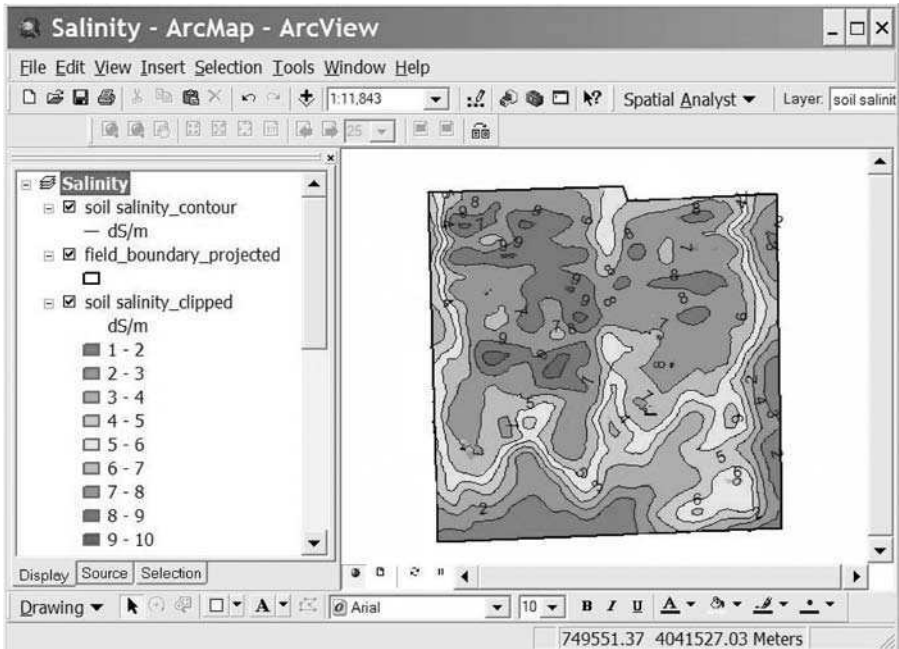


FIGURE 8.16 Screen shot of ArcMap window showing the new contour map of soil salinity with graduated color classes.

gence in saline areas. To reduce this problem, farmers are now using variable rate seeding technology to plant high seeding rates in saline areas and lower seeding rates in non-affected areas, because it is expected that plant emergence will be reduced in salt-affected soils. The Spatial Analyst application can be used to reclassify the salinity maps into seeding application rates. We selected three salinity level thresholds usually followed by cotton growers in California: <3 , $3-6$, and >6 dS m^{-1} and related these levels to seeding application rates of 10, 15, and 18 lbs ac^{-1} , respectively (Table 8.1).

1. Activate the *soil salinity_clipped* raster layer in the Table of Contents.
2. In the Spatial Analyst toolbar, click on **Reclassify**. Click on the **Classify** button, select the **Equal Interval** classification method and enter 3 in the **Classes** box. In the **Break Values** section, reset the first two values to 3 and 6. Click OK.
3. In the **Reclassify** window, enter the New Values as 10, 15, and 18; these values represent the seeding rates for each salinity zone. Enter the name of the Output raster file (*seed_VRT*). Click OK. You can use a smaller output cell size (i.e., 1 m) to obtain a smoother and more precise prescription seeding map.

TABLE 8.1
Reclassification values for seeding application rates

Old Values Salinity (dS m ⁻¹)	New Values Seeding Rates (lbs ac ⁻¹)
1–3	10
3–6	15
6–9.5	18

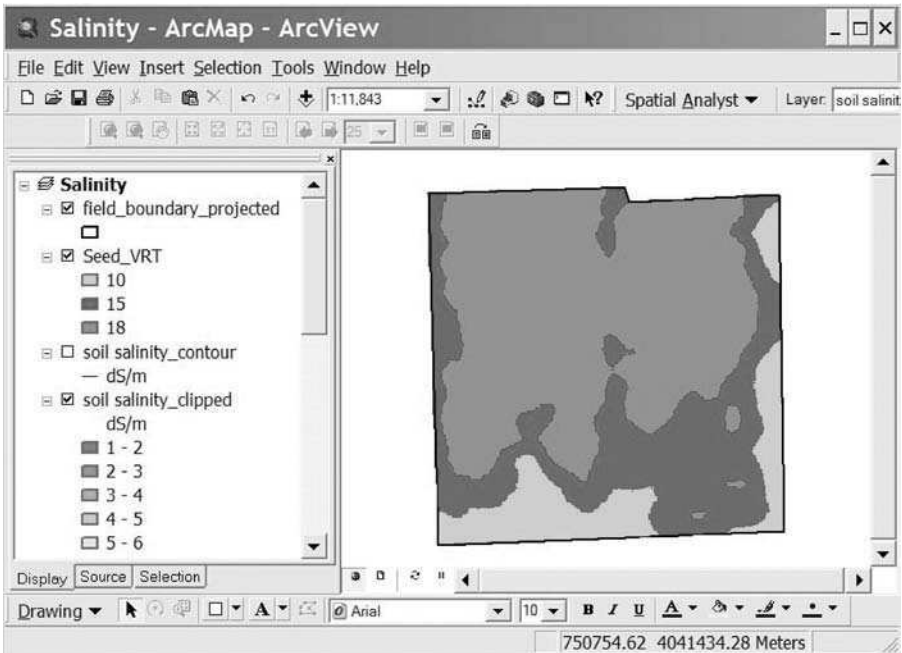


FIGURE 8.17 Screen shot of ArcMap window showing a prescription seeding map created using reclassification procedures.

Figure 8.17 illustrates the type of prescription map that can be given to the grower and used in conjunction with guidance and delivery systems to apply the prescribed seeding rates based on the salinity level at any particular location.

8.4.3.5 Correlating Soil Salinity Data with Other Soil Parameters

In this study, a soil SP map was also produced based on experimental SP data. The same steps presented for salinity were followed to create the SP map. The map in Figure 8.18 shows similar variability patterns to the salinity map. Areas of high SP, or high clay contents, are found in more saline areas. The salinity and SP data sets obtained from the interpolations can be exported for correlation analyses. Such

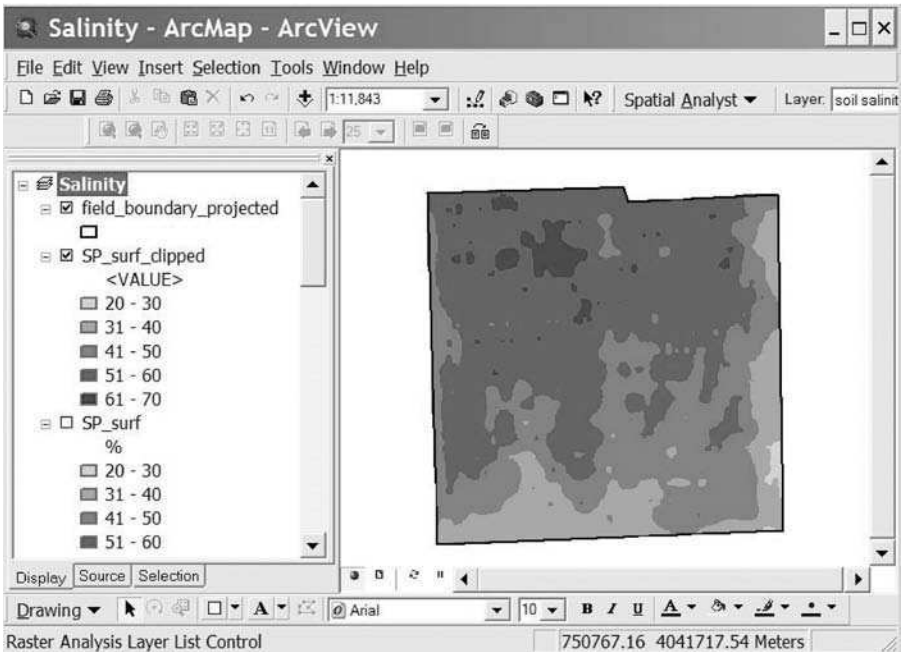


FIGURE 8.18 Screen shot of ArcMap window showing the saturation percentage map with graduated color classes.

comparative studies can be done for other soil/crop parameters collected in the field along with the salinity data.

8.4.4 MAP LAYOUT

The map layout view needs to be activated to create a layout for printing or exporting.

1. Highlight the map layer you want to print or export.
2. Click **View > Layout View**. The map appears on a page format (Figure 8.19).
3. Click the **Insert** menu to add cartographic elements, such as title, text, legend, north arrow, scale bar, picture, or object to the layout view. The font, size, and color of the title can be changed in the **Title** window.
4. Resize the map by clicking on the **Data Frame**, selecting the nodes, and dragging the frame nodes to the chosen size. The position of the map can also be changed by clicking on the **Data Frame** and moving it on the map with the mouse. Right-click on the **Data Frame** to obtain the **Data Frame Properties** window and change the color of the border frame to white. Each cartographic element can also be resized and positioned anywhere in the layout.

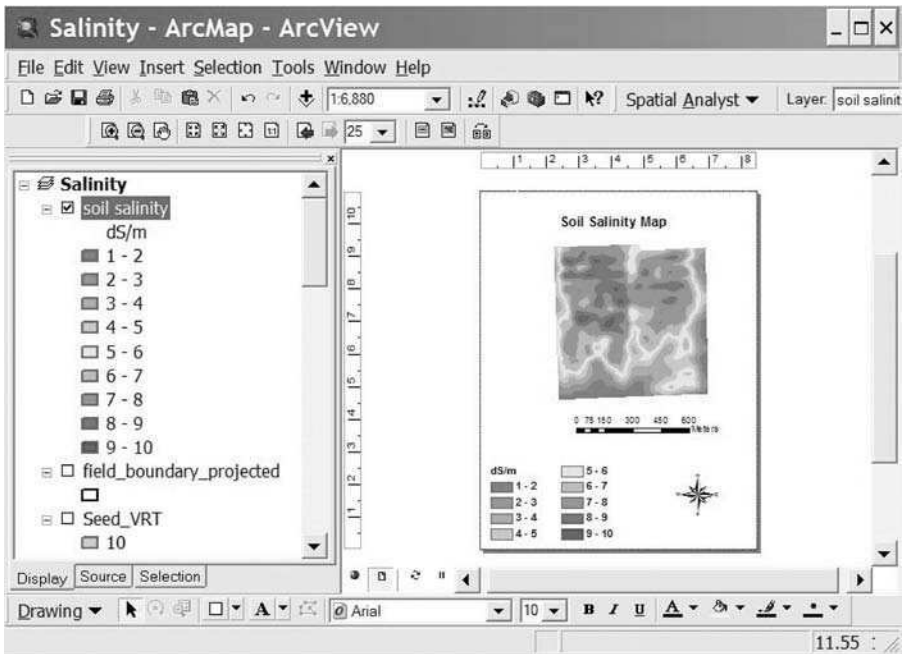


FIGURE 8.19 Screen shot of ArcMap window showing the map layout view for printing or exporting.

5. When satisfied with the layout, save the map.
6. Click on **File > Print** to print the map or **File > Export Map** to export the map as an image.

8.5 CONCLUSIONS

Assessment of soil properties and applications of precision farming practices are important for optimizing crop productivity in poor quality soils, such as those affected by salinity. Management of soil salinity problems has become easier to implement with the development of remote sensing techniques, GIS, and site-specific tools. In this chapter, you learned how soil salinity data can be collected remotely and integrated into a GIS environment for generating surface maps and developing prescription maps for precision farming applications in cropping systems. You should now be familiar with the use of Spatial Analyst for creating raster files and interpolating data into smoothed continuous maps, as well as reclassifying your raster data into new specified intervals for crop management practices. It should be emphasized that surface interpolations need to be conducted very scientifically as each interpolation method takes into account different assumptions of the data and therefore uses different calculations. Selection of the appropriate interpolation method should be based on the nature of your data. Geostatistical methods, such as kriging, usually provide better continuous (prediction) maps because they take into consideration the

spatial relationship among measured data points. These methods can also provide a measure of accuracy and certainty of the predictions. The example chosen for this exercise focused on soil salinity mapping in cotton fields but the same approach could be applied to any soil or plant parameters obtained experimentally in any ecosystem.

REFERENCES

1. Letey, J., Soil salinity poses challenges for sustainable agriculture and wildlife, *CA Agriculture*, 55, 2000.
2. Ceuppens, J., Wopereis, M.C.S., and Miézan, K.M., Soil salinization processes in rice irrigation schemes in the Senegal River Delta, *Soil Sci. Soc. Am. J.*, 61, 1122, 1997.
3. Davis, J.G. et al., Using electromagnetic induction to characterize soils, in *Applications of Electromagnetic Methods: Agriculture*, Geonics Limited, Mississauga, ON, Canada, 1999.
4. Sudduth, K.A., Kitchen, N.R., and Drummond, S.T., Soil conductivity sensing on clay pans: comparison of electromagnetic induction and direct methods, in *Applications of Electromagnetic Methods: Agriculture*, Geonics Limited, Mississauga, ON, Canada, 1999.
5. Lesch, S.M., Herrero, J., and Rhoades, J.D., Monitoring for temporal changes in soil salinity using electromagnetic induction techniques, *Soil Sci. Soc. Am. J.*, 62, 232, 1998.
6. McKenzie, R.C. et al., Use of the electromagnetic-induction meter (EM38) as a tool in managing salinisation, *Hydrogeol. J.*, 5, 37, 1997.
7. Hendrickx, J.M.H. et al., Soil salinity assessment by electromagnetic induction of irrigated lands. *Soil Sci. Soc. Am. J.*, 56, 1933, 1992.
8. Lesch, S.M. et al., Mapping soil salinity using calibrated electromagnetic measurements, *Soil Sci. Soc. Am. J.*, 56, 540, 1992.
9. Bennett, D.L. and George, R.J., Using the EM38 to measure the effect of soil salinity on *Eucalyptus globulus* in south-western Australia, *Agric. Water Mgmt.*, 27, 69, 1995.
10. McNeill, J.D., *Electrical conductivity of soils and rocks*, Tech. Note TN-5, Geonics Limited, Mississauga, ON, Canada, 1980.
11. Rhoades, J.D. and Corwin, D.L., Determining soil electrical conductivity-depth relations using an inductive electromagnetic soil conductivity meter, *Soil Sci. Soc. Am. J.*, 45, 255, 1981.
12. Lesch, S.M. and Rhoades, J.D., *ESAP-95 Software Package Version 2.01R*, USDA-ARS, George E. Brown Jr. Salinity Laboratory, Riverside, CA, 1999.
13. Isaaks, E.H. and Srivastava, R.M., *An Introduction to Applied Geostatistics*, Oxford Univ. Press, New York, 1989.
14. Vieira, S.R. et al., Geostatistical theory and application to variability of some agronomic properties, *Hilgardia*, 51, 1, 1983.
15. Cambardella, C.A. et al., Field-scale variability of soil properties in central Iowa soils, *Soil Sci. Soc. Am. J.*, 58, 1501, 1994.
16. Meirvenne, M.V. and Hofman, G., Spatial variability in topsoil micronutrients in a 1-ha cropland plot, *Comm. Soil Sci. Plant Anal.*, 120, 103, 1989.

9 Using GIS and On-the-Go Soil Strength Sensing Technology for Variable-Depth Tillage Assessment

*Pedro Andrade-Sanchez and
Shrinivasa K. Upadhyaya*

CONTENTS

9.1 Executive Summary.....	163
9.2 Introduction	164
9.3 Literature Review	164
9.4 Background Information	165
9.5 Methods	166
9.6 Results	167
9.6.1 Regression Analysis of UCD-SCPS Output and Cone Index Data...	167
9.6.2 Tutorial: Visualization of CI-Equivalent Quantities.....	167
9.7 Conclusions	178
Acknowledgments.....	179
References.....	179
Appendix 9.1 Campbell Scientific CR23X Data Logger Code.....	180

9.1 EXECUTIVE SUMMARY

In recent years, several soil dynamic research groups have been developing instrumented shanks (i.e., chisels/subsoilers) for the quantification of soil compaction in real-time. The goal of this research is to develop an alternative to standardized cone penetrometer technology commonly used for measuring soil resistance at selected points.¹⁻⁶ Compaction sensors are designed to record the mechanical resistance of soil to cutting at different depths of the soil profile. However, due to the complex nature of the soil-tool interaction, it has been difficult to establish sound relationships between standard measurements, primarily cone index (CI), and soil strength measurements

provided by these sensors. This limitation is a clear disadvantage for the new sensors since soil compaction has generally been assessed from standard cone penetrometer measurements. Extensive field tests at the University of California, Davis, have resulted in an empirical relationship that relates sensor-based soil strength measurements with standard CI values for multiple depths and the depth of these measurements within the soil profile.

This chapter reports on the development of the UC Davis soil compaction profile sensor (UCD-SCPS) and an empirical relationship found between the measurements obtained using the UCD-SCPS and standard cone penetrometer.^{2,7} A method is proposed to transform the sensor output into CI-equivalent quantities that improves soil compaction assessment and mapping. The real-time compaction measurement system consists of a soil compaction profile sensor (UCD-SCPS), a DGPS receiver, and a data logger. Techniques are presented to generate and visualize maps of CI-equivalent data and prescribed variable tillage depth for the case of a typical farm located in central Missouri. Data sets and code used for sensor-GPS interfacing are provided.

9.2 INTRODUCTION

In recent years, precision agriculture has generated widespread attention and increased interest in the use of real-time sensors for extracting soil and plant information. In the field of soil dynamics, this new trend has resulted in the development of sensors for measuring soil physical properties for the purpose of assessing and managing variability in soil management problems like soil compaction. Measuring soil-reaction forces to obtain soil properties for machine-control purposes, with a particular thrust toward hardpan detection and management, is a common approach adopted by several researchers.^{1,3,8,9} When these sensors are interfaced with Global Positioning Systems (GPS), they can be used to develop maps of soil strength.^{1,3,6,9} The within-field variability detected by these sensors indicates that in many situations only certain regions of a field may require corrective management such as site-specific tillage. However, a significant problem remains with the proper interpretation of the information generated with these devices. Ongoing research is focused on the analysis of data generated with these new technologies to address management problems like soil compaction.

This chapter is targeted to engineers, scientists, and students with particular interest in soil mechanics, power and machinery, and precision agriculture. The tutorial section is intended to serve as an example of interfacing sensors, GPS receivers, and data loggers for field measurements. Moreover, it presents a procedure for using ESRI® ArcGIS v. 9.1 (ESRI, Redlands, California) software for the interpretation of spatial variability of soil cutting resistance data within a field.

9.3 LITERATURE REVIEW

The variability in soil compaction can be assessed with the measurement of soil strength indices such as the cone index (CI), which is a composite soil parameter

that depends on several properties including bulk density, moisture content, and texture. Many plant functions are affected by the compaction state of soil,^{10–13} in particular, root growth, which gets impeded sharply when soil CI reaches or exceeds 300 psi (2 MPa).^{12–14} However, CI is a point measurement that exhibits significant variability,¹⁵ is tedious and time consuming to acquire, and may require significant amounts of labor to obtain sufficient spatial measurements. For these reasons, on-the-go soil compaction profile sensors are highly desirable to enable the rapid assessment of soil compaction within a field.

Several groups have developed systems that will measure soil compaction continuously and in real time using instrumented shanks designed to measure the resultant vertical and horizontal forces acting on the tillage tool to measure average soil compaction in the whole-soil profile.^{4,5,9,16} Others have explored the alternative of measuring soil strength along the tillage tool by using a rigid chisel instrumented with multiple sensors.^{8,17,18} However, this approach has potential problems in dealing with cross-sensitivity between the sensing elements. Newer developments, such as the UCD-SCPS, make use of shanks instrumented with an array of force transducers that are directly attached to cutting elements assembled in the front of the tillage tool.^{1–3,6,7} This approach results in fully independent sensing units capable of measuring soil cutting resistance directly ahead of the cutting elements.

Even for these improved profile sensors, interpreting the output in terms of soil physical properties has been a challenge. Raw measurement data have very limited application and a meaningful analysis procedure is needed to obtain useful information. Andrade et al.^{2,7} used a step-wise regression approach to show that a relationship exists between horizontal soil reaction forces on the cutting elements located at some depth and soil cone index values corresponding to the same depth provided the depth location of the sensing elements is properly taken into account.

9.4 BACKGROUND INFORMATION

The UCD-SCPS is a sensor with unique features in its geometry. The design goal was to develop a thin shank with sufficient structural rigidity, combined with a shape that could achieve self-penetration into the ground. The UCD-SCPS design included a 90° rake angle, a shank width of only 2.7 cm, and the use of five customized octagonal ring load-sensing units, resulting in an effective sensing range of 7.5–45.7 cm soil depth (Figure 9.1). These load-sensing units were custom-designed based on their relative location along the depth and expected load at that depth in order to maintain similar sensitivity levels among all five sensing units.

Four strain gauges were installed on each octagonal ring to measure the horizontal component of soil reaction force or draft. An overload protection mechanism consisting of disc springs arranged in series/parallel configurations was installed to become active when the total displacement of the force sensing assembly reached rated load capacity of the individual sensing unit.



FIGURE 9.1 CAD drawing of the UCD-SCPS.

9.5 METHODS

Prior to field testing, the sensing elements were individually calibrated using a loading machine I-1122[®] (Instron, Norwood, Massachusetts). The calibration procedure revealed that the association between the sensor output and the applied static loads was always linear with very high coefficients of determination. The compaction profile sensor was attached to a three-point hitch frame that was fitted with a pair of gauge wheels to keep constant depth of operation. The device was satisfactorily tested in an experimental field near the UC Davis campus. The sensor output at a given depth correlated with the cone index values obtained at the same depth.

The UCD-SCPS unit was evaluated in a 10-ha field located near Centralia in central-northern Missouri. Flags were installed on a 27.5-m square grid to mark CI measurement sites and to guide the path of the UCD-SCPS unit to ensure that sensor measurements intersected the grid points. Triplicate soil cone penetrometer readings were obtained at each grid point using an ASAE standard cone with a narrow-base (129 mm^2)¹⁹ and averaged. The UCD-SCPS was operated at an average speed of 1.02 m s^{-1} and at a constant soil depth of 40.6 cm. A Differential Global Positioning System (DGPS) receiver (AgGPS-130[®], Trimble, Sunnyvale, California) was interfaced to the UCD-SCPS using the RS232 port on the CR23X[®] (Campbell Scientific, Logan, Utah) data logger used to record data from the sensor at a frequency of 1 Hz.

The data logger code is provided in the appendix. A field boundary file was created using the UCD-SCPS system operated in the raised position.

Regression analyses were performed between the sensor output aggregated around each grid point and the cone index values obtained at grid points. Since each grid point represented CI and UCD-SCPS data separated at five levels of depth, the resulting aggregated data set consisted of 670 observations.⁷ The field boundary file and the UCD-SCPS continuous data file are provided with this book under Chapter 9.

The continuous data set of UCD-SCPS output was processed with ArcGIS v. 9.1 to obtain maps of soil cutting resistance for the nine transects tested. The procedure that is described in the tutorial section includes maps of raw data, as well as maps of data interpolated across the whole field. The purpose of presenting the data in these forms was to demonstrate the potential use of the UCD-SCPS as a sensor capable of providing real-time information that is needed for site-specific, variable-depth tillage.

9.6 RESULTS

9.6.1 REGRESSION ANALYSIS OF UCD-SCPS OUTPUT AND CONE INDEX DATA

An equation was derived relating the UCD-SCPS sensor, CI data, and depth values using a stepwise regression procedure as follows:

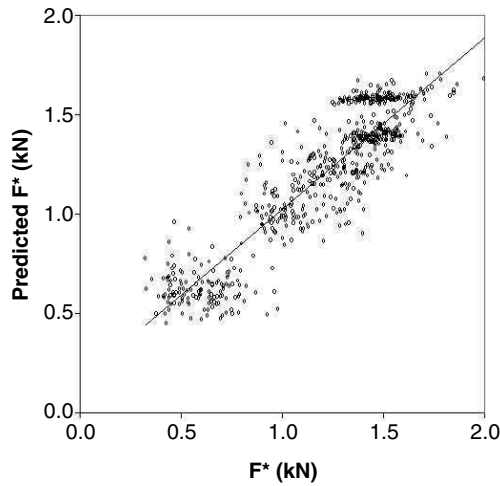
$$\sqrt{UCD - SCPS}_i = a_1 CI_i + a_2 d_i + a_3 (CI * d)_i \quad (9.1)$$

where $UCD - SCPS_i$ = sensor output of the i th layer (kN), CI_i = cone index of the i th layer (MPa), d_i = depth location of the i th layer (m), $a_1 = 0.449$, $a_2 = 3.642$, and $a_3 = -0.864$.

This relationship is illustrated in Figure 9.2. Equation 9.1 was used to compute CI-equivalent quantities by substituting discrete values of cone index (i.e., 1.0, 2.0, 3.0, 4.0, and 5.0 MPa.) as well as the recorded values of depth of the active cutting elements with respect to the surface (i.e., 10.0, 17.5, 25.0, 32.5, and 40.0 cm). The computed CI-equivalent quantities are presented in Table 9.1 and are presented in maps for further visual inspection and interpretation of the potential application of the UCD-SCPS to variable depth tillage. Detailed procedures are highlighted in the tutorial section.

9.6.2 TUTORIAL: VISUALIZATION OF CI-EQUIVALENT QUANTITIES

The tutorial section is based on an exercise using software package ArcGIS v. 9.1. You will be using utilities ArcCatalog, ArcMap, and ArcToolbox; along with extensions 3-D Analyst and Spatial Analyst. Two data files are provided for this tutorial section (*Boundary_MI.csv* and *UCDSCPS.csv*).



$$F^* = \sqrt{UCD-SCPS}_i = a_1 CI_i + a_2 d_i + a_3 (CI \cdot d)_i$$

FIGURE 9.2 Results of regression analysis of CI and UCD-SCPS data for a field in Centralia, Missouri.

TABLE 9.1
CI-equivalent quantities (kN) computed using Equation 9.1 for a field in Centralia, Missouri

Depth (d) (cm)	Cone Index (MPa)				
	1.0	2.0	3.0	4.0	5.0
10.0	0.528	1.187	2.108	3.293	4.740
17.5	0.875	1.520	2.343	3.344	4.521
25.0	1.308	1.895	2.590	3.395	4.308
32.5	1.827	2.311	2.850	3.446	4.099
40.0	2.434	2.768	3.122	3.498	3.896

1. Create a working folder in the hard drive of the computer where all files will be stored. Save the data files *Boundary_MI.csv* and *UCDSCPS.csv* in the working folder. Make sure to select this working folder to save any file created during the tutorial procedures.
2. Creating a boundary shapefile. Open ArcCatalog and select the working folder in the explorer window. Under the **File** menu select **New > Shapefile**. Give a name to the file to create (i.e., *Boundary*), select **Polygon** as the Feature type. In the **Spatial Reference** window select **Edit**. Press the **Select** button, and select **Geographic Coordinate Systems**. Press **Add** and select **World**. Press **Add** and select *WGS 1984.prj*. Press the **OK**

button in all open windows (Figure 9.3). The shapefile *Boundary.shp* has

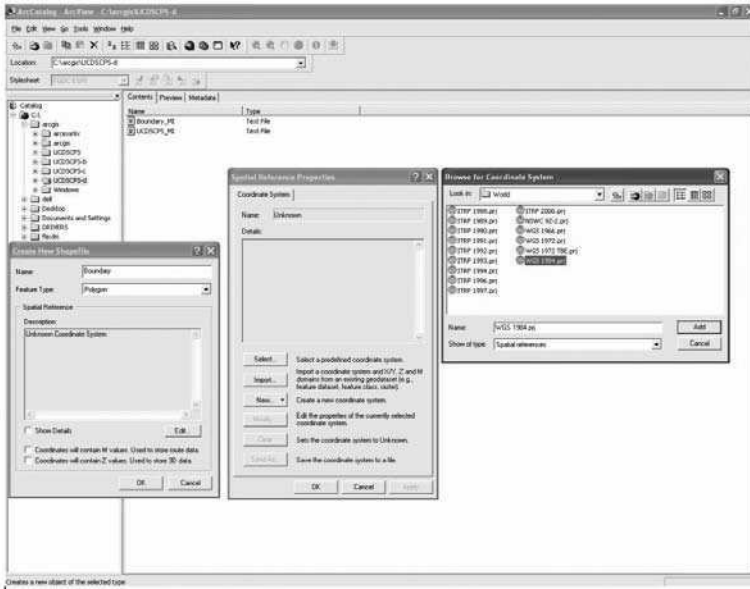


FIGURE 9.3 ArcCatalog windows to create a shapefile for boundary.

been created and appears listed in the explorer window, but it contains no data. It still needs to be edited. This will be done in ArcMap.

3. Editing the boundary shapefile.
 - a. Bringing the data in. Open ArcMap software. Press the **Add data** button (this is the button with the plus sign in the yellow background). Find the working folder in the browser. Select the text file *Boundary_MI* and press OK. A table with the name *Boundary_MI* will appear in the explorer window on the left. Select it with the mouse. Go to the **Tools** menu > **Add XY data**. On this window, make sure the table *Boundary_MI.csv* is selected in the browser. Also the X and Y fields should be set to Longitude and Latitude respectively (Figure 9.4). Repeat the same procedure detailed in section 2 above for projection selection of the data. Click OK. A new layer will be created with the name *Boundary_MI.csv Events*. A table right below this layer contains the data for the shape file (Figure 9.5).
 - b. Press the **Add data** (plus sign) button. Select the shapefile *Boundary*. This layer will appear on the explorer on the left. Enlarge the **Editor** tool bar, select **Start Editing**, and select the working folder with the boundary shapefile. Press OK. On the **Editor** tool bar under **Task** select **Create new feature**, and under **Target** select the *Boundary* shapefile. Select the marker tool (pencil-like icon) to draw the boundary following the points in the window (Figure 9.5). Double click the mouse's right

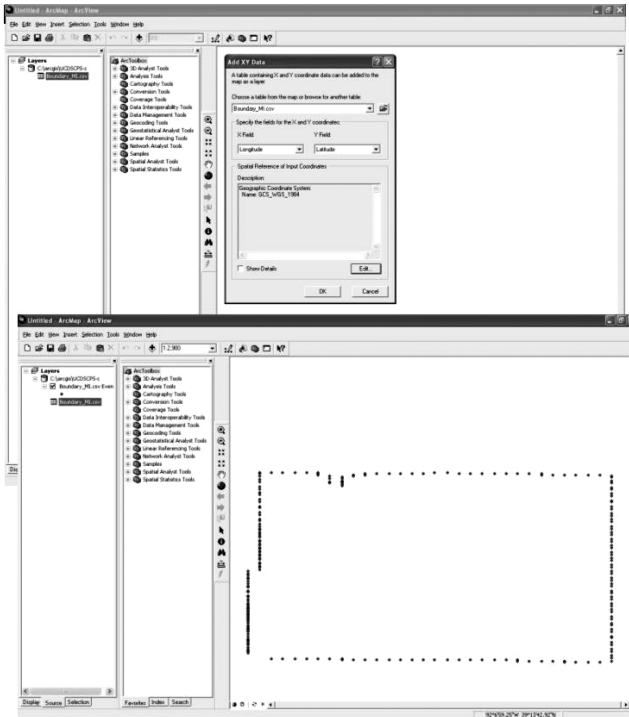


FIGURE 9.4 ArcMap functions for bringing in the boundary data table.

button to close the polygon. Go to the **Editor** tool bar and select **Stop Editing**. Click **Yes** to save your edits.

- c. Sometimes it is desirable to make appearance changes to the field boundary layer. Click on the colored rectangle below the boundary layer in the explorer on the left. Select the background **Crop**, increase the line width, and change line color to black (Figure 9.6).
4. Visualizing the UCD-SCPS raw data.
 - a. Bringing the data in. On the ArcMap main view, press the **Add data** button and select the text file UCDSCPS_MI and press OK. Select the table *UCDSCPS.csv* that will appear in the explorer window on the left. Go to **Tools > Add XY data**. In this window, make sure the table *UCDSCPS_MI.csv* is selected in the browser. Also the X and Y fields should be set to Longitude and Latitude, respectively. Repeat the same procedure detailed in section 3c for projection selection of the data. Click OK. A new layer will be created with the name *UCDSCPS_MI.csv Events*.
 - b. Creating a shapefile with UCD-SCPS data. Select the layer *UCDSCPS_MI.csv Events* and right click on it. Select **Data > Export Data** (Figure 9.7). In the window that will appear, choose to export All Features. For the option **Use the same coordinate system as:**

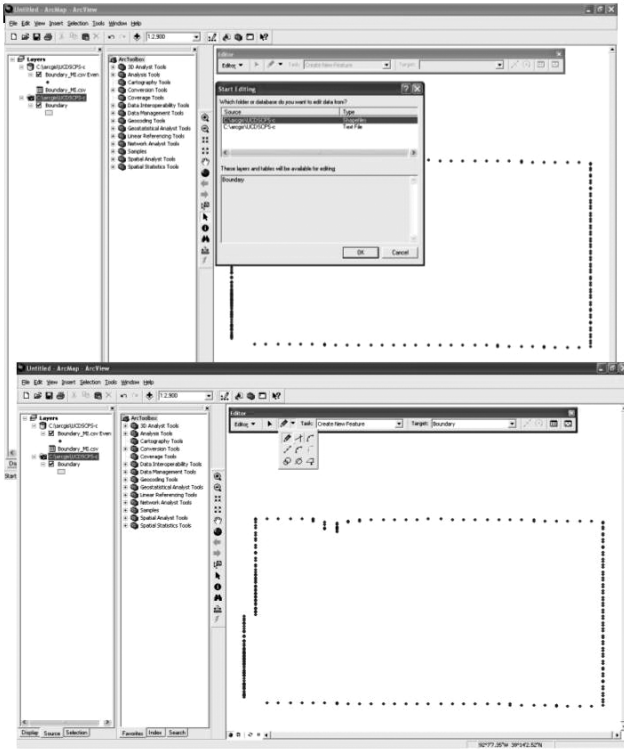


FIGURE 9.5 ArcMap functions for editing the boundary shapefile.

- select **this layer's source data**. Give a name to the output shapefile and make sure it will be stored in the working directory. Click OK and the new shapefile will appear as a new layer listed in the explorer on the left.
- c. Visualizing the UCD-SCPS data. Select the shapefile with the UCD-SCPS data and double click on it. Click on the **Symbology** tab. Select **Quantities > Graduated colors**. On the **Fields** frame, select **Value: D10** from the scroll-down list. This is the name for the data corresponding to 10 cm depth. On the **Classification** frame, select **5 Classes by Natural Breaks** (Figure 9.8). Click OK and Yes when asked **Do you want to add the expected data to the map as a layer?** Selecting this layer with a check mark on the square next to it will present the data as generated by the UCD-SCPS along the nine transects for the first portion of the soil profile (10 cm).
 - d. Changing the appearance of the UCD-SCPS data layer. Make changes to the range and label of each class, as well as the size of the markers. This is possible by clicking the name and marker of the UCD-SCPS layer in the explorer window (Figure 9.9).

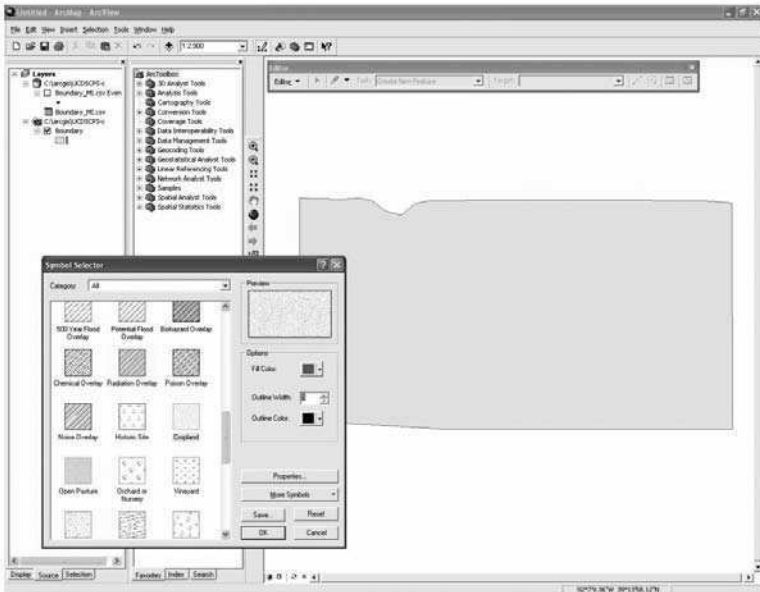


FIGURE 9.6 ArcMap functions to make appearance changes to field boundary layer.

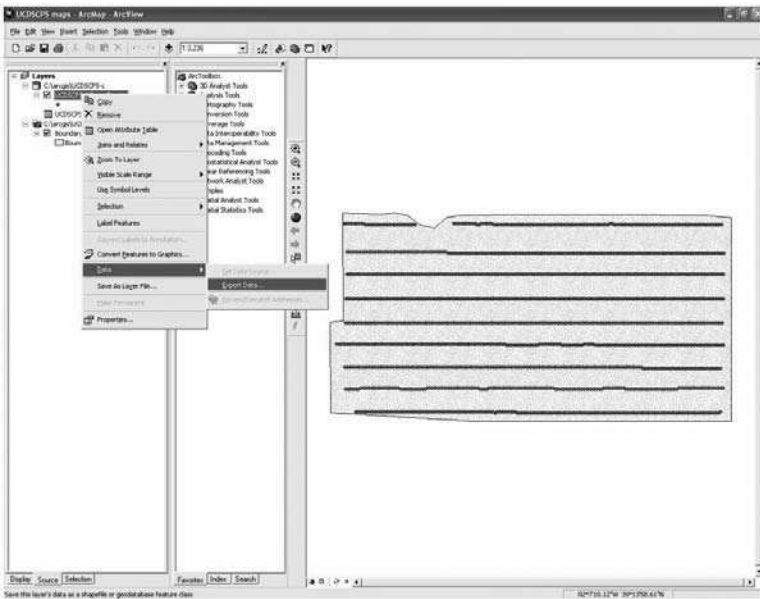


FIGURE 9.7 ArcMap functions to export UCD-SCPS data.

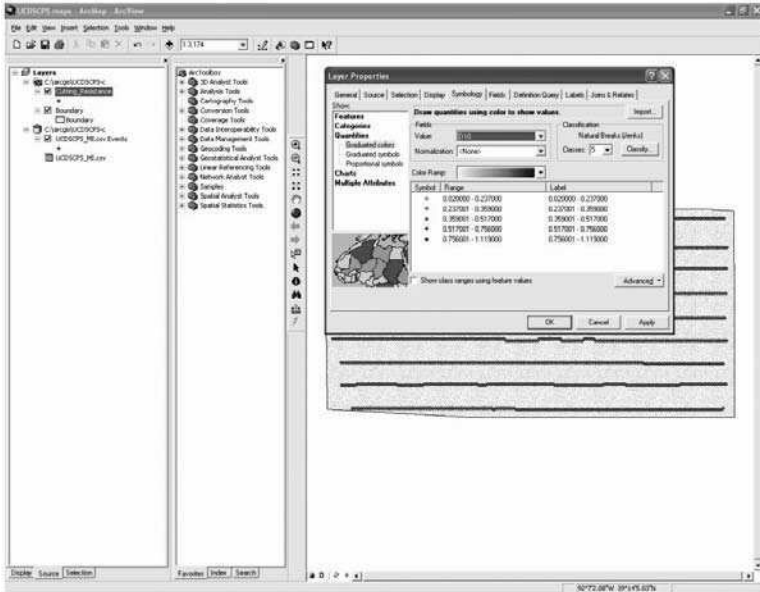


FIGURE 9.8 ArcMap functions to visualize UCD-SCPS data.

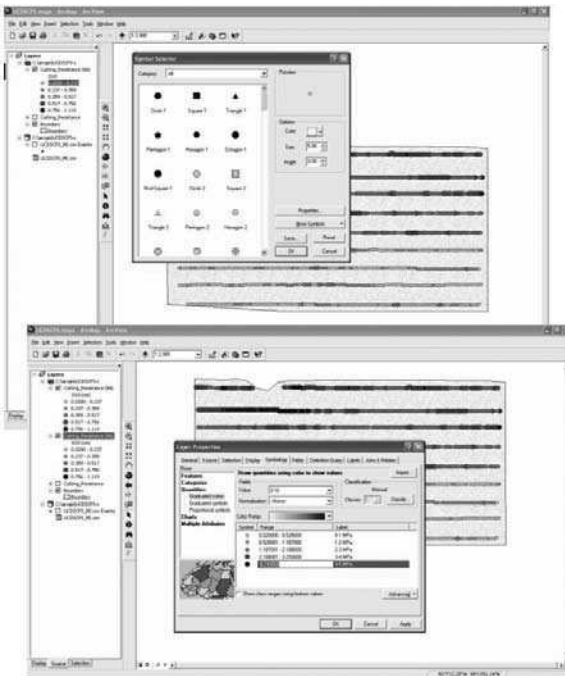


FIGURE 9.9 ArcMap functions to modify appearance of UCD-SCPS data layer.

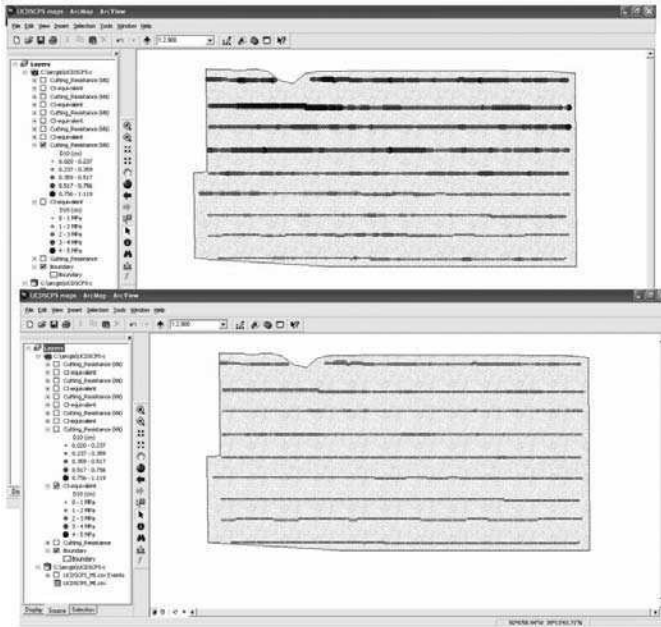


FIGURE 9.10 Maps of UCD-SCPS continuous raw data and CI-equivalent quantities for a depth of 10 cm.

- e. Mapping UCD-SCPS data and CI-equivalent quantities. Section 4d shows you how to view continuous UCD-SCPS data, but we are interested in visualizing another dimension of this sensor output. For the same UCD-SCPS layer, we will modify the ranges of the five classes according to the values of Table 9.1. We will change the name of each class to their corresponding CI-equivalent range (Figure 9.9). The two forms of UCD-SCPS data in the depth of 10 cm are presented in Figure 9.10.
 - f. Creating multiple layers of UCD-SCPS data. This can be achieved by selecting the first layer we created (**D10**) > **right-click** > **copy**. Then select **Paste** from the **Edit** menu. This copy can be modified to show another depth of information by double clicking on it. Click on the **Symbology** tab. Select **Quantities** > **Graduated colors**. On the **Fields** frame, select **Value: D18** from the scroll-down list. This procedure can be repeated for all five depths of the soil profile that were explored with the UCD-SCPS to generate maps of raw UCD-SCPS data and maps of CI-equivalent quantities as illustrated by a collection of CI-equivalent maps (Figure 9.11).
5. Interpolation of the UCD-SCPS data: Creating a prescription map for tillage depth.
 - a. Using Spatial Analyst extension in ArcMap. To activate this extension go to **Tools** > **Extensions** and check the box next to **Spatial Analyst**.

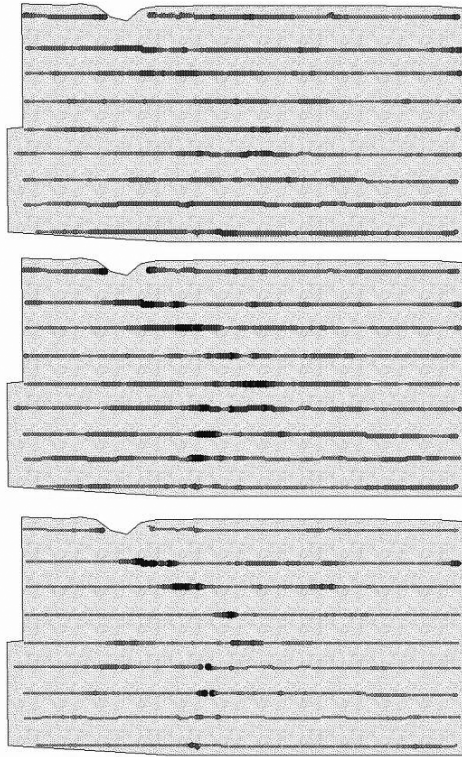


FIGURE 9.11 Maps of CI-equivalent quantities for depths 25, 32.5, and 40 cm (from top to bottom). Color scale is same for all maps.

There are different ways to perform interpolation functions. Expand the **ArcToolbox** menu > **3-D Analyst Tools** > **Raster Interpolation** > **Kriging** (see the Kriging window in Figure 9.12). Select a layer that contains all the UCD-SCPS data in **Input point features**, select one of the depths (i.e., D25 for data at depth 25 cm) in the **Z value field** and give a name to the raster to be created (i.e., *Kriging_25*) in **Output surface raster**. For the purposes of this tutorial we will select the default settings of kriging. Further geostatistical analyses can help us define more suitable parameter values. Press OK and a new raster layer should appear in the explorer on the left. This same procedure will be repeated for all five depths contained in the *UCD-SCPS* data set. The default maps generated by kriging can be edited for consistency to previous maps (Figure 9.13).

Note: Since kriging procedures create a rectangular surface map, you need to change some of the settings of Spatial Analyst. Make a tool bar for **Spatial Analyst** by selecting **View** > **Tool bars** > **Spatial Analyst**. Press the **Spatial Analyst** tab and select **Options**. Select the **General** tab and under **Analysis Mask** select a feature class or a

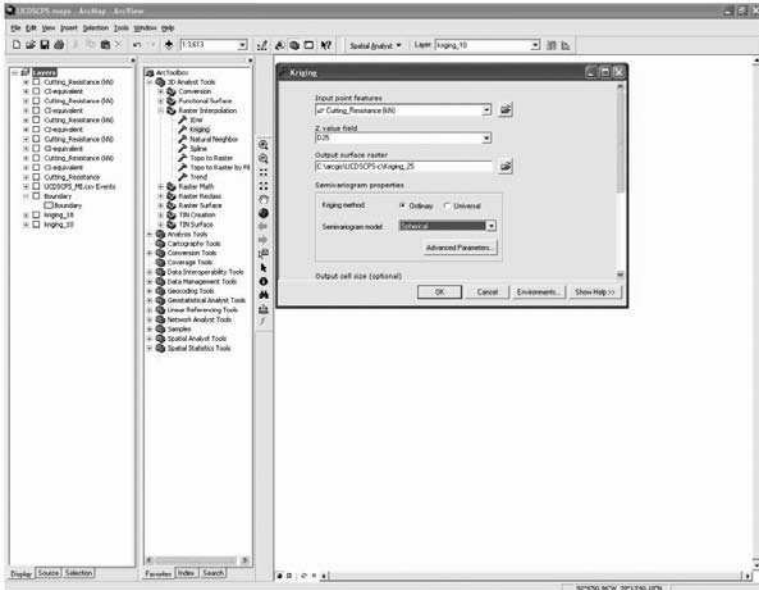


FIGURE 9.12 ArcMap functions to perform kriging interpolation of UCD-SCPS data.

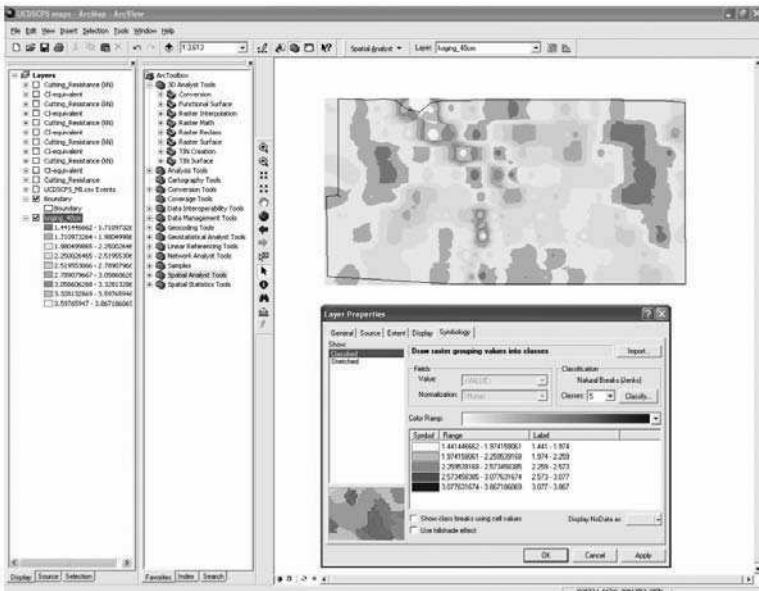


FIGURE 9.13 ArcMap functions to modify layer properties of UCD-SCPS rater surface.

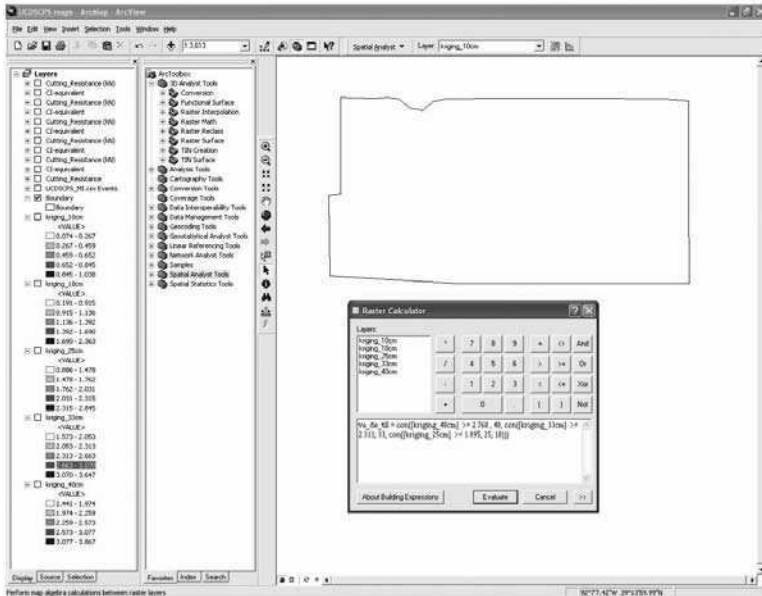


FIGURE 9.14 ArcMap functions to create a new raster surface using the raster calculator and conditional statements.

previous raster dataset that has data limited by the field boundary. In the **Extent** tab, under **Analysis Extent** select **As specified above** and make sure that the values for the four sides will cover (or slightly exceed) the field boundary.

- b. Creating a composite raster file. The last step of this tutorial is to create a raster surface in the form of a prescription map that will contain variable depth tillage information. This recommendation map is created by defining critical values of soil strength and combining data from different raster surfaces. From Table 9.1, use the set of CI-equivalent quantities corresponding to 2.0 MPa as threshold values. The purpose of this exercise was to define the most appropriate depth of operation during tillage for each cell in the raster set.

Press the **Spatial Analyst** tab and select **Raster calculator**. Write conditional statements to assign unique values to each cell in a new raster surface. The following statement is written in the Raster calculator (Figure 9.14):

```
Var_dep_till = con([kriging_40cm] >= 2.768, 40, con([kriging_33cm] >= 2.311, 33, con([kriging_25cm] >= 1.895, 25, 18)))
```

The above logical statement gives instructions to start analyzing the values of the cells at the deeper position (40 cm), all the cells with values equal or larger than the threshold value of 2.0 MPa for that depth will receive the value of 40; the remaining cells will be analyzed in terms of their values at the adjacent depth (33 cm). Again, the cells

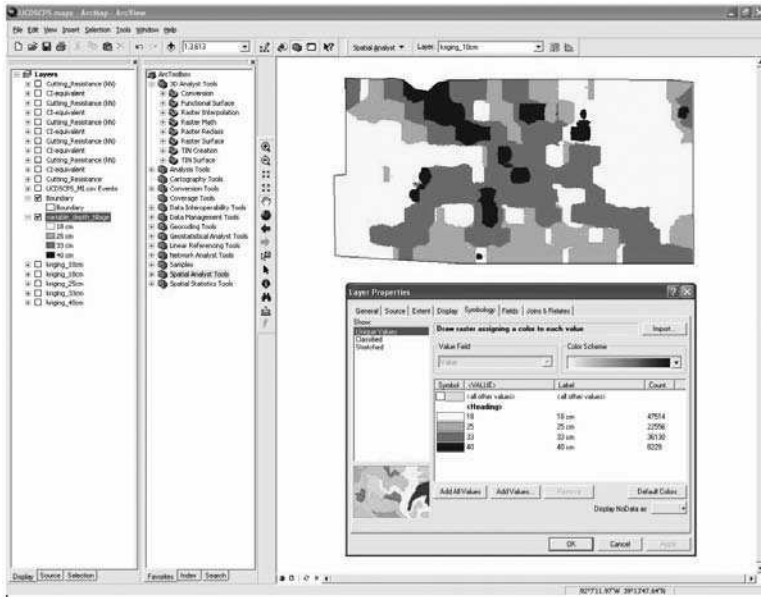


FIGURE 9.15 Prescription map for variable depth tillage in a field in Centralia, Missouri.

with values equal or greater than the threshold value at that depth will be assigned the value 33; the rest will be analyzed in the context of the next depth (25 cm). Due to practical implications, this exercise was run to define values of total depth of operation for 40, 33, and 25 cm. The remaining cells were assigned a value of 25 cm.

The new raster appears in the explorer window on the left, and can be edited for color scheme consistency by double clicking the layer (Figure 9.15). This map is the final step in this analysis. The number of cells fitting into each of the depths of tillage can be used to make an assessment of the potential energy savings if tillage is performed on a variable depth scheme.

9.7 CONCLUSIONS

The performance of the UCD-SCPS was enhanced by interfacing the sensor to a DGPS receiver and data logger to obtain georeferenced data. The UCD-SCPS operated satisfactorily under commercial field conditions. Including depth information in the empirical analyses increased the explanatory power of prediction models to the point that CI-equivalent quantities can be determined from the sensor output.

The overall interpretation of Figures 9.11 and 9.15 indicates that tillage depth should not be uniform, but should be varied on a site-specific basis depending on the variability of soil compaction along the soil profile. Only a reduced portion of the field requires deep tillage and the potential energy savings by implementing variable depth tillage will be most certainly significant.

The type of information generated by the UCD-SCPS is suitable for providing feedback to depth-control systems of power units so that variable-depth, site-specific tillage can be accomplished. We have provided simple guidelines in the tutorial section for visualizing continuously acquired data, as well as interpolated information across the whole field. Further understanding of the structure of soil strength data can be gained by applying additional analytical tools available in the GIS software.

ACKNOWLEDGMENTS

The financial support received from Deere and Co., The California Energy Commission (CEC), Mexico's National Council for Science and Technology (CONACYT), and The University of California Institute for Mexico and The United States (UCMEXUS) is greatly appreciated. Moreover, the authors want to express their gratitude to William Chancellor, Tom Anderson, Carol Plouffe, Benoit Poutre, Ken Sudduth, and Sun-Ok Chung for their technical assistance during the design, construction, and/or field evaluation of the UCD-SCPS.

REFERENCES

1. Adamchuk, V.I. et al., Instrumentation system for variable depth tillage, ASAE Paper No. 031078, presented at ASAE Annual International Meeting, Las Vegas, NV, 2003.
2. Andrade, P. et al., Soil profile measurements using an instrumented tine, ASAE Paper No. 011060, presented at ASAE Annual International Meeting, Sacramento, CA, 2001.
3. Khalilian, A. et al., A control system for variable depth tillage, ASAE Paper No. 021209, presented at ASAE Annual International Meeting, Chicago, IL, 2002.
4. Mouazen, A.M. et al., Two-dimensional prediction of spatial variation of a sandy loam field-based on measured horizontal force of compaction sensor, cutting depth, and moisture content, *Soil Till. Res.*, 74, 91, 2003.
5. Sirjacobs, D. et al., On-line soil mechanical resistance mapping and correlation with soil physical properties for precision agriculture, *Soil Till. Res.*, 64, 231, 2002.
6. Sun-Ok, C., Sudduth, K.A., and Hummel, J.W., On-the-go soil strength profile sensor using a load cell array, ASAE Paper No. 031071, presented at ASAE Annual International Meeting, Las Vegas, NV, 2003.
7. Andrade, P., Upadhyaya, S., and Jenkins, B., Evaluation of the UC Davis compaction profile sensor, ASAE Paper No. 021185, presented at ASAE Annual International Meeting, Chicago, IL, 2002.
8. Adamchuk, V.I., Morgan, M.T., and Sumali, H., Application of a strain gauge array to estimate soil mechanical impedance on-the-go, *Trans. of the ASAE*, 44, 1377, 2001.
9. Manor, G. and Clark, R.L., Development of an instrumented subsoiler to map soil hard-pans and real-time control for subsoil depth, ASAE Paper No. 011022, presented at ASAE Annual International Meeting, Sacramento, CA, 2001.
10. Busscher, W.J. and Bauer, P.J., Soil strength, cotton root growth and lint yield in a southeastern USA coastal loamy sand, *Soil Till. Res.*, 74, 151, 2003.

11. Duiker, S.W., Diagnosing soil compaction using a penetrometer (soil compaction tester), Agricultural Research and Cooperative Extension, Pennsylvania State University, Agronomy Facts Sheet 63, 2002.
12. Taylor, H.M. and Gardner, H.R., Penetration of cotton seedling taproots as influenced by bulk density, moisture content, and strength of soil, *J. Soil Sci.*, 96, 153, 1963.
13. Unger, P.W. and Kaspar, T.C., Soil compaction and root growth: a review, *Agron. J.*, 86, 759, 1994.
14. Schwab, E.B., et al., Conservation tillage systems for cotton in the Tennessee Valley, *Soil Sci. Soc. Am. J.*, 66, 569, 2002.
15. Sudduth, K.A., Bollero, G.A., and Sun-Ok, C., Soil strength sensing for quantifying within-field variability, ASAE Paper No. 021182, presented at ASAE Annual International Meeting, Chicago, IL, 2002.
16. Liu W. et al., Development of a texture/soil compaction sensor, in Proc. 3rd International Conference on Precision Agriculture, Precision Agriculture Center, University of Minnesota, Minneapolis, MN, 1996, 617.
17. Alihamsyah, T., Humphries, E.G., and Bowers Jr., C.G., A technique for horizontal measurement of soil mechanical impedance, *Trans. of the ASAE*, 33, 73, 1990.
18. Glancey, J.L. et al., An instrumented chisel for the study of soil-tillage dynamics, *Soil Till. Res.*, 14, 1, 1989.
19. ASAE Standards, *S313.3 Soil Cone Penetrometer*. St. Joseph, MI, ASAE, 2004.

APPENDIX 9.1 CAMPBELL SCIENTIFIC CR23X DATA LOGGER CODE

This program looks at the GPS (Table 1) and sensors (Table 2) and records the data as follows:

Location	Remarks	Location	Remarks
1	Test no.	9	Sensor 4
2	GPS latitude DD.MM (deg & min)	10	Sensor 5
3	GPS latitude DDDD (decimal deg)	11	Speed sensor (not used)
4	GPS longitude DD.MM (deg & min)	12	Depth sensor (not used)
5	GPS longitude DDDD (decimal deg)	13	Switch to control data recording
6	Sensor 1	14	Flag (1 or 0) to control test no.
7	Sensor 2	15	Output control (0 or 10)
8	Sensor 3		

```

/* Table 1 Program
01:1          /* Execution interval 1 sec

/* Instructions to read, switch, manage locations 14 and 15, and get GPS data

1:P1          /* Read switch and store in loc. 13
1:1
2:15
3:11
4:13
5:1
6:0

2:P30          /* Set loc 15 to 10. This makes sure that loc 15 is 10 only when Table 1 is
1:1          /* executed or GPS is read. In Table 2 loc 15 is checked and if it is 10,
2:1          /* output flag will be set and loc 10 will be set to 0. This secures that we
3:15          /* get an output every time the GPS is read

3:P15          /* Read GPS
1:1          /* 1 rep
2:03          /* 4800 baud rate
3:1          /* 0.01 sec. This should be non-zero to use serial port (i.e. Command 9)
4:9          /* Read serial port
5:1          /* Could be 1 or 0 –not used
6:0          /* Not used
7:42          /* Termination character "*"
8:512         /* Buffer. Should be large. For Trimble 128 or 256 is OK. Rockwell needs 512
9:100         /* CTS/Input wait
10:27         /* Location for storing data
11:1          /* Multiplier
12:0          /* Offset

4:P63          /* Analyze GPS string – Look for $GPGGA string
1:36          /* $
2:71          /* G
3:80          /* P
4:71          /* G
5:71          /* G
6:65          /* A
7:0          /* End of string
8:0          /* Must be zero if not looking for other strings

          /* Sparse data and store Latitude and Longitude
5:P45
1:28
2:2          /* Store Latitude degrees and minutes "DDmm" in loc 2

6:P44
1:28
2:2          /* Store Latitude decimal minutes ".mmmm" in loc 3

```

```

7:P45
1:28
2:2          /* Store Longitude degrees and minutes "DDmm" in loc 4

8:P44
1:28
2:2          /* Store Longitude decimal minutes ".mmmm" in loc 5
              /* End of GPS acquisition

              /* Look at switch manage loc 14 (test flag) and loc 5 (test no)
9: P89          /* If switch (loc 13) is on (>2000) then do
1:13
2:3
3:2000
4:30

10: P89          /* If flag (loc 14) = 0 then do
1:14
2:1
3:0
4:30

11:P32          /*Include test no. (loc 5)
1:1
12:P30          /* Set flag (loc 14) = 1
1:1
2:0
3:14

13:P95          /* End flag do loop

14:P94          /* If switch is not on

15:P30          /* Set flag (loc 14) = 0

16:P95          /*End switch do loop

```

```

/* Table 2 Program
01:D2          /* Execution interval 0.2 sec

/* Instructions to read sensors and write the data

1:P6          /* Repeat command P6 (full bridge) five times to read all five load cells
              /* and store the data in locations 6, 7, 8, 9, 10. Use offset and multiplier
              /* values from calibration equations to convert voltage to force units

              /* Output control – Look at loc 15 and manage output
6:P89        /* If switch (loc 13) is on (>2000) then do
1:13
2:3
3:2000
4:30

7:P89        /* If loc 15 = 10, then do
1:15
2:1
3:10
4:30

8:P86        /* Set output flag
1:10

9:P78        /* Write data with high precision

10:P30       /* Set loc 15 = 0
1:0
2:1
3:15

11:P95       /* End output control do loop

12:P70       /* Write first five input locations
1:5
2:1

13:P71       /* Write average values of all five sensors
1:5
2:6

14:P95       /* End switch do loop

```

10 Collocating Multiple Self-Generated Data Layers

Viacheslav I. Adamchuk and Chenguang Wang

CONTENTS

10.1 Executive Summary.....	185
10.2 Introduction	186
10.3 Methods	187
10.4 Results	191
10.5 Conclusions	196
10.6 Supplemental Files	196
References.....	196

10.1 EXECUTIVE SUMMARY

In many instances a single self-generated data layer does not provide information about an agricultural field sufficient for site-specific crop management. Therefore, an analysis of multiple data layers is important.¹ Based on geographic coordinates, collocated point measurements that belong to different data layers can be grouped to investigate relationships between alternative point estimates (e.g., crop yield versus a particular soil property). Unfortunately, this task cannot be accomplished using geographic information system (GIS) software packages available to crop producers.

As described in this chapter, DM_Comp software was developed as a stand-alone application suitable for performing primitive comparisons of several self-generated point data layers. Input data must be available in the form of delimited text files with unprojected geographic coordinates represented in decimal degrees. The output files will follow the same format and will be placed in the same directory as the input files. Further analysis of the output data can be performed using either a spreadsheet or an actual GIS software package.

The main function of the DM_Comp includes collocating multiple self-generated data layers in (1) points that belong to one of these layers (using user-defined fixed radius or nearest neighbor averaging) and (2) centers of rectangular grid cells (using grid cell averaging). In addition, a simple statistical filter has been included to remove

outlier points from yield data files available in AgLeader® (AgLeader Technology, Inc., Ames, Iowa) advanced text export format. A primitive graphic interface was added to observe the integrity of different data layers in terms of field coverage.

The supplemental example includes three years of soybean yield, laboratory analysis of soil sample results, a soil electrical conductivity map, and a map produced using a soil mechanical resistance on-the-go sensor. The software presented is an example of primitive stand-alone applications that can aid spatial data analysis when specific straight-forward processing is required and/or the access to high-level GIS software packages is not available.

10.2 INTRODUCTION

The majority of data layers generated through precision agriculture practices represents a one-dimensional array of qualitative values such as yield parameters or soil properties georeferenced to a common system of geographic coordinates (most likely WGS-84). In many instances, useful information pertaining to relationships between various data layers can be observed only if these data sets are related based on common coordinates. However, the process of defining these relationships is not trivial.

In the modern GIS environment, the most frequent comparison between different field data layers is done through generating, and then analyzing, surfaces (raster maps) representing spatial structure in a given sparse data set. For example, each data set (yield, on-the-go sensor, or soil laboratory analysis records) can be filtered and interpolated to the extent of the field boundaries using a common interpolation procedure (e.g., inverse distance weighting, kriging, etc.). Then, collocated cells that belong to several interpolated surfaces (with values predicted based on each data layer) can be included in a consistent numerical and/or logical computation. Therefore, quantitative determination of the relationship (correlation) between different data layers can be accomplished¹.

Unfortunately, many of the procedures involved are not available in many GIS software packages commonly used in production agriculture. Also, the inappropriate use of many existing surface interpolation methods can lead to significant errors due to low mapping density in combination with weak spatial structure. Therefore, there is a need for a stand-alone program (or module) to help combine various precision agriculture data sets into a single file with a simple data structure, which could be further analyzed using commonly available software.

The objective of this chapter is to report on an example of such a software application. The required functions were to (1) read and recognize various text-delimited data files with WGS-84 longitude and latitude columns (e.g., soil laboratory reports, on-the-go soil sensor, or yield data), (2) filter unprocessed yield files (AgLeader® advanced text export format) based on statistical limits for individual sensor outputs and overall yield estimates, (3) relate multiple data sets to a single sparse data set (typically with the smallest density) using the simplest procedures (averaging of nearest neighbor values and/or averaging of data points within a fixed radius area), (4) graphically display the data extent and generate rectangular grids with full coverage of data domain (adjust size to avoid split cells), (5) determine

average data values within each grid cell, and (6) output the combined data sets as a text-delimited file.

The described program, `DM_Comp.exe`, was developed using a C++ code to accommodate all of these requirements. The current version does not contain help and user guide options, and it may malfunction since all combinations of input parameters have not been tested. The main purpose of this software was to illustrate the functionality that could be pursued by future developers.

10.3 METHODS

`DM_Comp` (Data Management – Comparison) is a stand-alone program that can be used to combine various common sources of spatial data such as yield, soil laboratory analysis, topography, electrical conductivity or other on-the-go soil sensor measurements. This software includes two main utilities: (1) process yield and other spatial data files to determine values corresponding to a specific sparse data set (such as laboratory soil analysis) and (2) develop a rectangular grid pattern and determine corresponding average attributes from every input data file corresponding to each grid cell. `DM_Comp` should not be viewed as an alternative to GIS software in any way. Rather, it serves as an effective complementary program used to conduct multilayer analyses of spatial data. Such analyses can be performed in a spreadsheet or statistical software environment using delimited output text files, and may include, for example, regression analysis between different data layers (i.e., yield versus soil nutrients level or soil electrical conductivity versus selected soil properties) or development of crop response equations.

Every input data layer must be available as a delimited text file with two columns corresponding to geographic position (latitude and longitude) in decimal degrees with respect to WGS-84 datum (commonly used by Global Positioning System). The existence of a header row is optional. The type of data delimiter (comma or tab) is detected automatically.

There is no interpolation process involved. All data manipulations are accomplished solely by matching geographic coordinates from various data layers. Simple arithmetic averaging is done when more than one data point satisfies the requirements when searching across different layers. Unavailable matching data points result in incomplete rows within the output file that may be excluded from further statistical analysis.

Flexibility and simplicity are the biggest advantages of this program, which takes only 2.16 MB of storage space and requires no installation. To start the program, a user should simply double click on the program icon that appears in Windows Explorer or through the Run option of the Windows Start menu.

The main window of `DM_Comp` (Figure 10.1) appears right after the program is started. This window allows a user to (1) select a sparse data file and define the corresponding yield and other data files to be matched, (2) set the power for yield data filtering and a method for the multilayer data search, and (3) execute the data collocating routine and switch to the Graph View window mode. The most common Windows control options (e.g., closing the program, selecting multiple files, selecting/deselecting data columns, etc.) have been included to provide an intuitive user

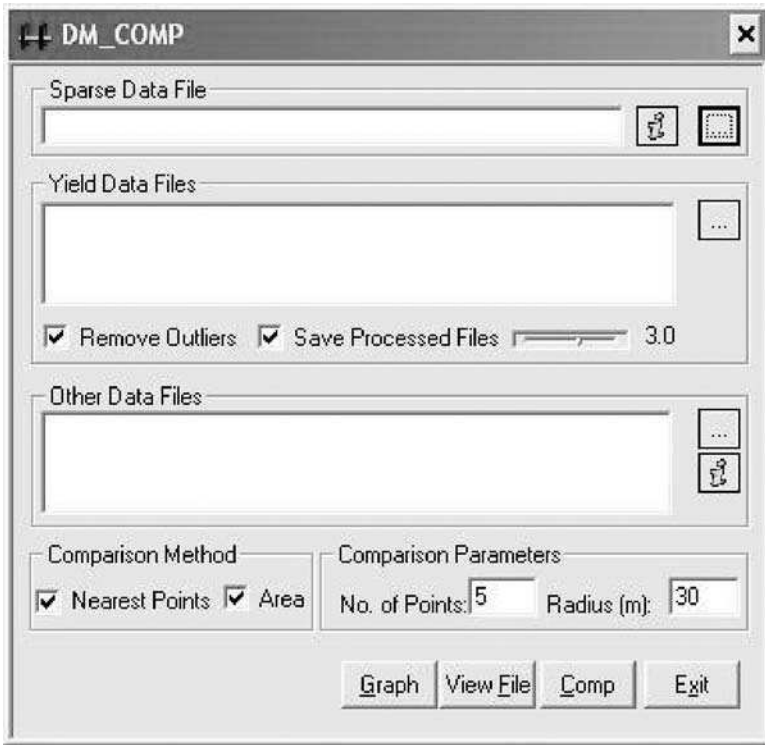


FIGURE 10.1 DM_Comp main window.

interface. Information about DM_Comp can be viewed when the program icon in the upper left corner is pressed and scrolled down to the About Comp menu option.

A **Sparse Data File** is any text-delimited spatial data file containing geographic longitude and latitude columns, in decimal degrees, followed by other attributes described in the header line, which are recommended but not necessary. This file is the basis for the output, and defines the number of rows (data points) for which corresponding values from other data layers are found.

The button symbolized by three dots opens the file selection dialog box (Figure 10.2). Names of files with .txt extension will appear first. If an input file has a different extension, the “all files” extension type should be used. Each button symbolized with an “i” opens the file information dialog box (Figure 10.3), which will also appear after making a sparse data file selection. In this box, the user can set the coordinate columns (if different than longitude and latitude) and select or unselect columns to be included or excluded from the output file. The output file will be written to the same directory as the original sparse data file. The original name will also be kept with “_comp” added before the extension in the output file name.

A **Yield Data File** is a raw file obtained from an AgLeader yield monitor using the **advanced text export** option. If processed, delimited text yield data files should be considered as “other data files” (described below). Similarly, the button with three dots should be used to open the dialog box for selecting the appropriate yield files

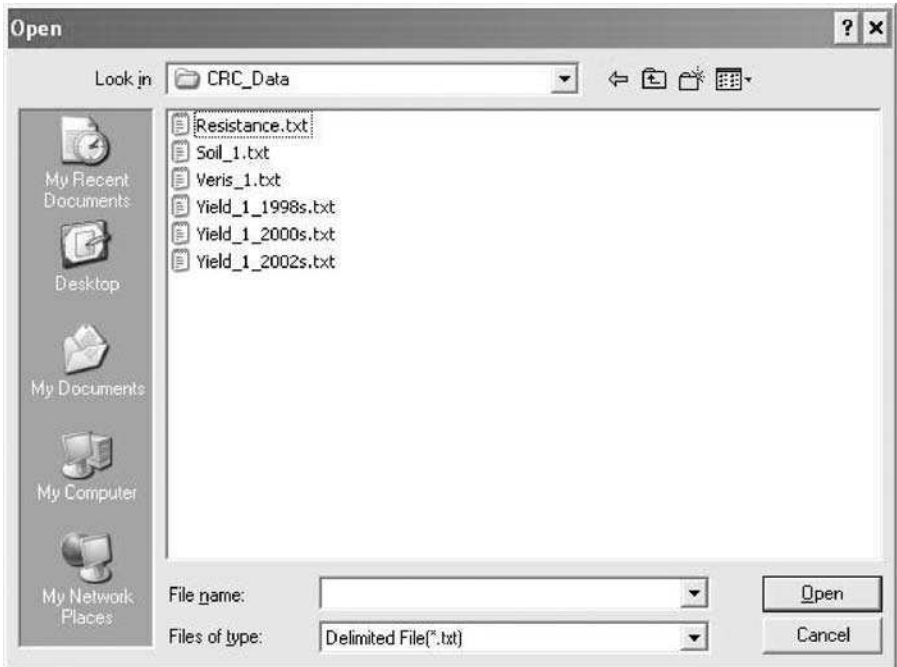


FIGURE 10.2 Open file dialog box.

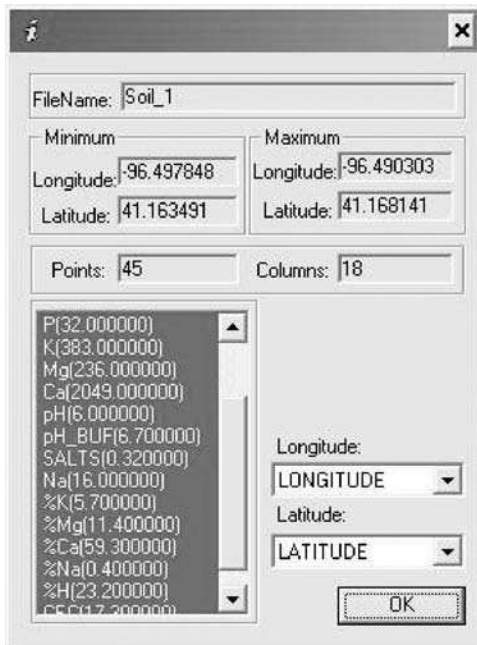


FIGURE 10.3 Data file information window.

(multiple selections can be made by holding the shift key down). The **Remove Outlier** box should be checked to enable a built-in filter that removes outlying data points from each yield data file. When the **Save Processed File** box is checked, yield files with outliers removed will be saved. The original yield file names will be used with “_out” added before the extension. Otherwise, the yield files with outliers removed will be erased when DM_Comp is closed. The horizontal sliding bar can be used to set the power of the built-in filter. The number indicated represents the multiplier for standard deviations to consider the values of individual sensor measurements or the calculated yield being erroneous. It ranges from 0 (almost all data points removed) to 5 (the most conservative filter). The default filter power is set at 3. Yield, moisture, and elevation values calculated from each input yield file are written to the output file. Blanks are used to substitute unavailable or corrupted values.

An **Other Data File** is any delimited text file with longitude and latitude columns. Those usually include processed yield files, soil electrical conductivity, and other on-the-go sensor recordings. The functions of the file selection and the information buttons are the same as described above, except that the files must be selected one at a time. Multiple columns in each file are allowed, and their order will be preserved when preparing the output file.

Combining Parameters contains two main settings of this program. The user has the ability to define a rule to distinguish collocated values. The values can be defined either as a certain number of nearest neighbors (5 by default), as all points located within a predefined area around individual sparse data points (within 30-m radius by default), or both combined. If neither box is checked, DM_Comp will search for the single nearest point. All distance calculations were conducted according to Adamchuk.²

The **View File** button can be used to open a text view window to review all input and generated output files (if available) in the text mode. The X button should be clicked to return to the main window. The **Comp** button starts combining (matching) all specified data files. After the work is completed, the output file is saved and a log message box appears (Figure 10.4). It provides information about program performance such as the number of points left without a qualified match. The **Exit** button or **Alt+F4** should be pressed to quit the program.

The **Graph** button opens a **Graphic View** window (Figure 10.5). Points from each file (sparse, yield, and other data files) can be viewed on the screen if selected. When ID is selected, a small square will appear in the middle of each grid cell (default 4×4). The user is able to specify both easting (X) and northing (Y) grid dimensions, or indicate the number of grid cells in each direction. The **Square Grid** option can also be used to ensure similar grid cell dimensions in both directions. Enabling the **Show Grid** option will display the lines of grid cells calculated for a given field using an optimized boundary rule (adjust grid size to avoid partial cells within data domain). If the **Save** button is pressed, the request to specify an output file name will appear. The output file will contain an ID column with the corresponding longitude and latitude for the center of each grid cell followed by the corresponding average values from all highlighted data files (all columns previously selected). If at least one selected data layer does not contain points within the specific

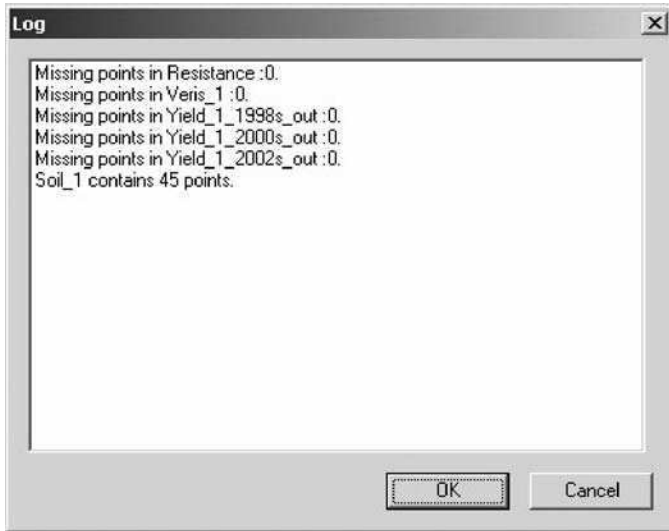


FIGURE 10.4 Spatial data matching log report.

grid cells, these cells are excluded from the output file. Therefore, data layers with different density and/or coverage should be saved separately. This option can be used to generate a center-point grid soil sampling map. Either OK or the X button can be used to return to the main window of the DM_Comp program.

10.4 RESULTS

Enclosed with the program is a typical data set consisting of three years of soybean yield, georeferenced analytical soil lab results, as well as soil electrical conductivity and mechanical resistance data. The following steps will guide the user through an example of complete data processing using DM_Comp.

1. Start the program by clicking the **DM_Comp** icon in Windows Explorer (the program will run better if copied to the hard disk first).
2. Press the **Open File** button in the **Sparse Data File** area and navigate to the *Soil_1.txt* file. This file contains a laboratory report from a soil analysis performed on 45 samples (2.5-acre grid sampling). Assuming that we do not want to include laboratory results on percent base saturation in the output, unselect the %K, %Mg, %Ca, %Na, and %H fields. Click OK to return to the main window.
3. Press the **Open File** button in the **Yield Data File** area and select *Yield_1998_s.txt*, *Yield_2000_s.txt*, and *Yield_2002_s.txt* yield files (press and hold the shift key to select multiple files). These are soybean yield files from the 1998, 2000, and 2002 growing seasons. Click OK to return to the main window.

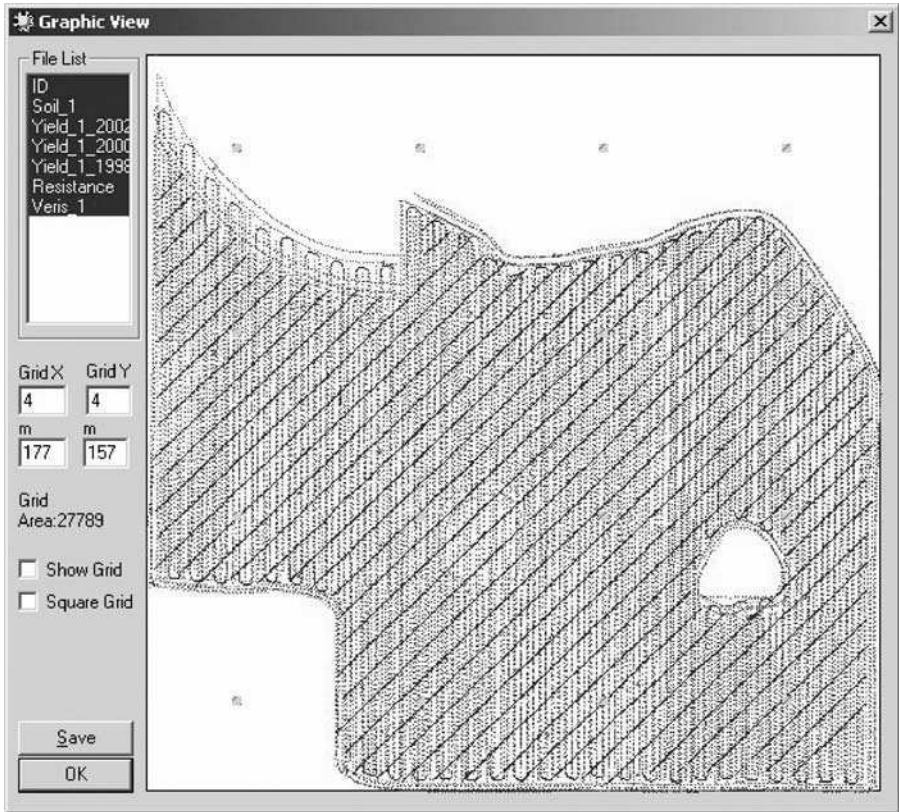


FIGURE 10.5 DM_Comp graphical view window.

4. Use the default filter settings. However, you can also change the power of the filter by dragging (or clicking) the scroll bar to the left or right.
5. Press the **Open File** button in the **Other Data Files** area and select the *Veris_1.txt* file. This is the output from the Veris® 3100 (Veris Technologies, Inc., Salina, Kansas) electrical conductivity mapping system. After pressing OK, you can select columns of interest (SHALLOW and DEEP). These data represent two depths of electrical conductivity measurements. Press OK.
6. Press the **Open File** button in the **Other Data Files** area again and select the *Resistance_1.txt* file. This is the output from an experimental soil mechanical resistance mapping tool.³ After pressing OK, select three depth layers representing mechanical resistance (in units of pressure MPa) at 0–4-in, 4–8-in, and 8–12-in depth intervals. Press OK.
7. Set the comparing method to all the points within a 30-m radius (only the **Area** checkbox should be on). Press **Comp** to perform the calculations. This may take a few minutes.

8. Observe the log message and press OK. The output file named *Soil_I_comp.txt* will be written to the drive. It will include columns from the *Soil_I.txt* file as well as the matched values from all other files.
9. Click the **View File** button and review the input and output text files (use the pull-down menu at the top). Press X in the upper right corner to close the **File View** window.
10. Press the **Graph** button to open the **Graphic View** window. Examine the map by selecting and unselecting different fields in the upper left selection window. When done, select all fields except *Soil_I* (to avoid data with density much smaller than the size grid cells to be defined). Click **Show Grid** to see the boundaries of the default (4 × 4) grid. Enter 40 m to define the easting grid interval (X). To make the grid square, check the **Square Grid** option. In this case, both dimensions will be automatically adjusted and each grid cell will represent an approximate 0.4-acre area.
11. Click **Save** to record the output file with coordinates for the center of each grid cell and averages of all previously selected data for each cell. The user must specify a descriptive file name (for example: *0.4_acre_grid.txt*). Click OK to return to the main window and exit the program.

The two output files can be processed further using common software packages. The resulting *Soil_I_comp.txt* can be used to determine correlations between specific soil properties and each additional data layer (Table 10.1), and to further study specific relationships. For example, one could explore dependency between (1) soil pH and soybean yield, (2) cation exchange capacity and soil electrical conductivity, or (3) soil organic matter content and soil mechanical resistance (Figure 10.6). Yield

TABLE 10.1
Pearson coefficients of correlation summary

Soil Property	Soybean Yield			Electrical Conductivity		Soil Mechanical Resistance		
	2002	2000	1998	0–30 cm	0–90 cm	0–10 cm	10–20 cm	20–30 cm
OM	-0.02	0.03	-0.02	0.11	0.16	-0.18	-0.01	0.21
P	-0.48	-0.45	-0.23	-0.43	-0.46	0.25	-0.29	-0.38
K	-0.07	-0.18	0.10	-0.02	-0.01	-0.12	-0.37	-0.25
Mg	0.37	0.27	0.16	0.68	0.59	-0.14	0.42	0.45
Ca	0.15	0.08	0.03	0.39	0.28	0.03	0.24	0.26
Soil pH	0.00	-0.04	0.01	0.11	0.05	0.07	0.07	0.04
Buffer pH	0.15	0.18	-0.06	0.29	0.29	0.09	0.20	0.26
Salts	0.21	0.30	0.29	0.42	0.37	-0.18	0.14	0.28
Na	0.02	0.08	-0.29	-0.01	0.00	-0.21	0.07	0.22
CEC	0.23	0.11	0.05	0.45	0.35	-0.09	0.26	0.26

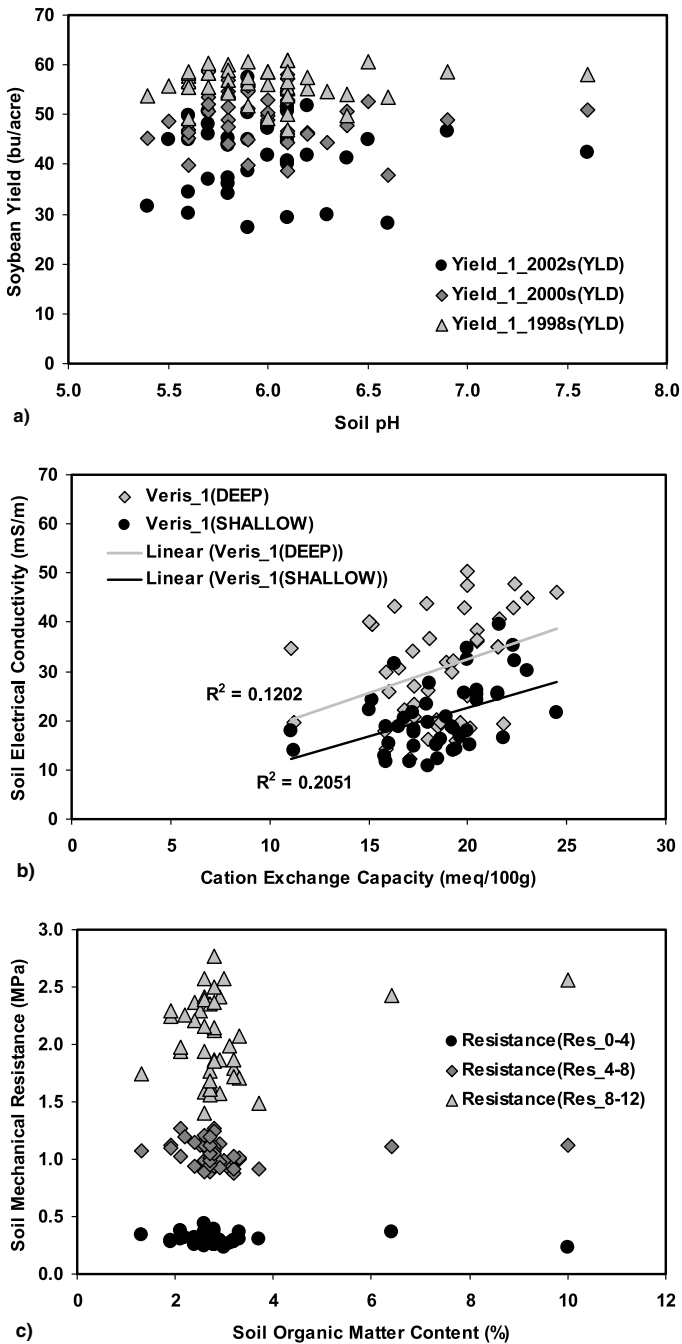


FIGURE 10.6 Example of relationships between (a) soil pH and soybean yield, (b) cation exchange capacity and soil electrical conductivity, and (c) soil organic matter content and soil mechanical resistance using 45 soil sampling points as processed with DM_Comp software.

response and other important relationships can be defined when similar output files from different fields are combined.

The other output file, *0.4_acre_grid.txt*, can be illustrated by creating original and processed deep electrical conductivity maps using a simple GIS software package (Figure 10.7). In the case of 0.4-acre averaging, each data point includes an ID number as well as the grid cell average for selected attributes. Missing points mean that the corresponding grid cells did not contain at least one original data point from at least one selected data layer.

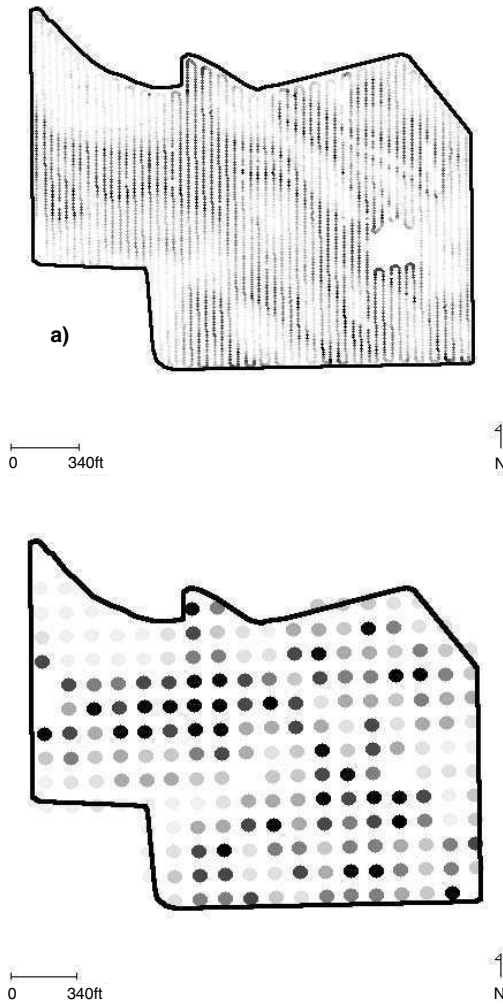


FIGURE 10.7 Deep soil electrical conductivity maps produced using (a) the original data and (b) 0.4-acre square grid averaging option.

10.5 CONCLUSIONS

The DM_Comp software was developed as a stand-alone application capable of collocating multiple self-generated point data layers. It illustrates the concept of task-oriented spatial data handling without the need for the actual GIS software. A similar approach can be pursued to facilitate other specific data management routines (e.g., filtering, primitive geostatistical analysis or management zone delineation).

In this example, DM_Comp was used to compare several common self-generated data layers. Analysis of relationships between different data layers can be pursued through a decision-making process. For example, the user could identify soil properties to be considered as yield limiting factors. An ability to relate laboratory analysis of the limited number of soil samples and high-density soil sensor measurements can help calibrate the sensor to better delineate field areas with potential nutrient deficiency. Grid cell averaging can be pursued when either simply defining a rectangular grid cell pattern for a follow-up soil sampling, or when analyzing spatial data files with measurement spacing different with respect to northing and easting directions. More advanced analytical methods will certainly require a GIS software package with data smoothing, interpolation, or raster computation capabilities.

10.6 SUPPLEMENTAL FILES

The following files should be copied to the same folder to follow the example above:

1. *DM_Comp.exe* is a program itself.
2. *Soil_1.txt* is a georeferenced soil laboratory analysis report.
3. *Yield_1_1998s.txt* is the 1998 soybean yield data saved using the AgLeader advanced text export format.
4. *Yield_1_2000s.txt* is the same for 2000 growing season.
5. *Yield_1_2002s.txt* is the same for 2002 growing season.
6. *Veris_1.txt* is a Veris® 3100 EC Surveyor output file.
7. *Resistance_1.txt* is a logging file with on-the-go soil mechanical resistance measurements.

REFERENCES

1. Adamchuk, V.I., Dobermann, A., and Ping, J., Listening to the story told by yield maps, Precision Agriculture extension circular EC 04-704, University of Nebraska, Lincoln, Nebraska, 2004.
2. Adamchuk, V.I., Untangling the GPS data string, Precision Agriculture extension circular EC 01-157, University of Nebraska, Lincoln, Nebraska, 2001.
3. Siefken, R.J., Adamchuk, V.I., Eisenhauer, D.E., and Bashford, L.L., Mapping soil mechanical resistance with a multiple blade system, *Appl. Eng. Agr.*, 21, 15, 2005.

Index

A

- Adamchuk, V.I., 163–165, 185–186, 190, 192
- Algerbo, P.A., 67
- Alihamsyah, T., 165
- Andrade, P., 163–165, 167
- ArcGIS
- fertility management, 104–105, 108, 111–112
 - soil salinity mapping, 141–162
 - yield data, 133–138
- ArcView
- historical management, soil sampling, 49–64
 - GIS application, 53–62
 - homesteads, impact of, 51–53
 - nutrient variability, impact of human factors, 51–53
 - nitrogen management, sugar beets, 35–48
 - ground-based sensor, 44–46
 - satellite images, 41–44
 - pest management, 1–34
 - delivery potential factors, 22–28
 - land-use data, 19
 - pesticide application/properties, 22
 - proximity data, 20–22
 - soils data, 12–19
 - productivity zones, 65–79
 - cleaning yield monitor data, 67
 - exercise, 77–78
 - file formats, 77
 - gridding data, 67
 - identifying productivity zones, 69–74
 - statistical calculations, 67–69
 - yield variability, zone impacts, 74
 - yield data, 65–79, 123
 - exercises, 132–138

- partial nutrient budgets, 126–128, 130–131
- production, 126, 129–130
- profit consistency, 135–138
- profitability, 124–125, 128–129, 133–135

B

- Baker, J.L., 3, 7
- Bashford, L.L., 192
- Bauer, P.J., 165
- Beck, K.G., 88
- Beet, sugar, remote sensing, nitrogen management, 35–48
 - ground-based sensor, 44–46
 - satellite images, 41–44
- Benefits variability, 83
 - hand-drawn map predictions, site-specific weed management, 83
 - WeedSite, 83
- Bennett, D.L., 142
- Bernard, C., 6
- Beyerlein, D.C., 6
- Blackmer, A.M., 50
- Blackmore, S., 67, 122–123
- Bollero, G.A., 165
- Bosley, D.B., 82
- Bowers Jr., C.G., 165
- Boydell, B.C., 83, 93
- Brodahl, M.K., 122–123
- Brouder, S.M., 104, 108, 110
- Brown
- J.R., 50
 - R.B., 83, 93, 96
- Buchholz, D.D., 50
- Bullock D.G., 104
- Buschena, D., 83
- Bussan, A.J., 83
- Busscher, W.J., 165

C

- Cambardella, C.A., 154
 Canner, S.R., 82
 Cardina, J., 82–83
 Carlson, C.G., 50
 Caro, H.J., 3–4, 7
 Chang, J., 50, 66
 Chiles, J.P., 104
 Christensen
 B., 3, 7
 S., 83, 93, 96
 Christy, C.D., 51
 Cihacek, L.J., 50
 Clark, R.L., 164–165
 Clay, D.E., 50
 Cleaning yield monitor data, productivity zones, yield monitor data, 67
 Coble, H.D., 96
 Colbach, N., 82
 Colliver, C.T., 83, 93
 Collocation, multiple self-generated data layers, 185–197
 Contour maps, soil salinity mapping, 156–157
 Coordinate system, soil salinity mapping, 145–147
 Correlating salinity data, soil salinity mapping, 147, 159–160
 Correll, D.L., 3, 7
 Corwin, D.L., 142
 Coulton, M.R., 39
 Cressie, N., 104, 108
 Crohain, A., 37
 Cussans, G.W., 83, 93

D

- Data management comparison. *See* DM_COMP
 Davis, J.G., 142
 Day, W., 83
 De Baerdemaeker, J., 122
 Dean, J.D., 4
 Decision algorithms
 hand-drawn map predictions, site-specific weed management, 88–89

- WeedSite, 88–89
 Delfiner, P., 104
 Delivery potential factors, pest management, ArcView, 22–28
 Deutsch, C.V., 104
 Diker, K., 122–123
 DM_COMP, 185–197
 Dobermann, A., 122–123, 185–186
 Doerge, T.A., 122
 Donigian, A.S., 6
 Drummond
 P.E., 51
 S., 122
 Duiker, S.W., 165

E

- Eisenhauer, D.E., 192
 Environment, working, soil salinity mapping, 147–148
 Everitt, B.S., 123

F

- Ferguson, R.B., 50
 Field boundary data, soil salinity mapping, 145, 150
 File formats
 ArcView, 77
 productivity zones, yield monitor data, 77
 Fish and Wildlife Service land, pest management, 1–34. *See also* U.S. Fish and Wildlife Service
 Fleming, K.L., 50, 69
 Forcella, F., 82–83, 93, 96
 Franzen, D., 41, 50

G

- Gardner, H.R., 165
 Gaussoin, R.E., 88
 George, R.J., 142
 Geostatistical Analyst, fertility management, 105, 111–113
 Gerhards, R., 83, 93
 Giles, J.F., 37, 45

Glancey, J.L., 165
 Goodman, D.
 Goovaerts, P., 104
 Gotway, C.A., 82, 104
 Green, H.M., 83, 93
 Gridding data
 ArcView, 67
 productivity zones, yield monitor data,
 67
 Groeneveld, R.W.M., 83, 93
 Ground-based sensor, nitrogen
 management, sugar beets,
 44–46
 Gunsolus, J.L., 82–83, 93, 96

H

Hand-drawn map predictions, weed
 management, 81–101
 accuracy, 96
 benefits variability, 83
 decision algorithms, 88–89
 evaluation, 85–90
 examples, 90–96
 limitations, 96
 polygons, identifying, 88
 predictions, 92–96
 program overview, 84–85
 simulation polygons, predicting
 outcomes for, 88
 speed, 96
 viewing results, 89–90
 Havlin, J.L., 50
 Headden, W.P., 37
 Heerman, D.F., 122–123
 Heisel, T., 83, 93
 Hendrickx, J.M.H., 142
 Hergert, G.W., 50
 Herrero, J., 142
 Historical management, soil sampling
 error reduction, 49–64
 GIS application, 53–62
 homesteads, impact of, 51–53
 nutrient variability, impact of human
 factors, 51–53
 Hoef, R.G., 127
 Hofman, G., 154
 Hofmann, B.S., 104, 108, 110

Homesteads, impact of, historical
 management, soil sampling
 error reduction, 51–53
 Hummel, J.W., 163–165
 Humphries, E.G., 165

I

Identifying polygons, hand-drawn maps,
 site-specific weed
 management in field, 88
 Identifying productivity zones,
 productivity zones, yield
 monitor data, 69–74
 ArcView, 69–74
 Importing data, soil salinity mapping,
 148–152
 Information from yield data, 121–140
 exercises, 132–138
 partial nutrient budgets, 126–128,
 130–131
 production, 126, 129–130
 profit consistency, 135–138
 profitability, 124–125, 128–129,
 134–135
 Isaaks, E., 104, 122, 153–154
 Islam, M.M., 122

J

Jacobs, M.J., 104
 Jenkins, B., 164–165, 167
 Jenks, G.F., 39
 Johansen, D.P., 51
 Johnson
 G., 82–83, 93
 H.P., 3
 Johnston
 J.W., 105
 K., 104–105, 108, 112
 Journel, A.G., 104

K

Kachman, S.D., 50
 Kappler, B.F., 88
 Kaspar, T.C., 165
 Khalilian, A., 163–165

King, R.P., 82–83, 88, 93, 99
 Kitchen, N., 50–51, 69, 142
 Klein, R.N., 88
 Knezevic, S.Z., 88
 Kravchenko, A., 104
 Kristensen, K., 83, 99
 Kvien, C.K., 83, 93

L

Land-use data, pest management, 1–34
 delivery potential factors, 22–28
 Fish and Wildlife Service land, 1–34
 land-use data, 19
 pesticide application/properties, 22
 proximity data, 20–22
 soils data, 12–19
 Landau, S., 123
 Lauzon, J.D., 122–123
 Layer properties, soil salinity mapping,
 150–152
 Leese, M., 123
 Leonard, R.A., 3–4, 7
 Lesch, S.M., 142–143
 Letey, J., 142
 Limitations of hand-drawn map
 predictions in weed
 management, 96
 Liu W., 165
 Long, D.S., 83, 93
 Lotz, L.A.P., 83, 93
 Ludwick, A.E., 37, 45
 Lund, E.D., 51
 Luschei, E.C., 83
 Lybecker, D.W., 88, 99
 Lyon, D.J., 88

M

Mac, M. J., 3
 Manor, G., 164–165
 Map layout, soil salinity mapping,
 160–161
 Map quality assessment, site-specific
 fertility management, 103–120
 Mapping soil salinity, 141–162
 contour maps, 156–157
 coordinate system, 145–147

 correlating salinity data, 147, 159–160
 field boundary data, 145, 150
 importing data, 148–152
 layer properties, 150–152
 map layout, 160–161
 precision agriculture, salinity map,
 157–159
 raster interpolation, 153–156
 salinity data, 144–145, 148–150
 soil salinity assessment, 143–144
 spatial analyses, 152–160
 spatial analyst extension, 152–153
 working environment, 147–148
 Maps, hand-drawn, in weed management,
 81–101
 accuracy, 96
 benefits variability, 83
 decision algorithms, 88–89
 evaluation, 85–90
 examples, 90–96
 limitations, 96
 polygons, identifying, 88
 predictions, 92–96
 program overview, 84–85
 simulation polygons, predicting
 outcomes for, 88
 site-specific strategies, 83
 speed, 96
 viewing results, 89–90
 Martin, A.R., 88, 96
 Masson, F.X., 6
 Maxwell, B.D., 83, 93
 McDonald, S.K., 88
 McKenzie, R.C., 142
 McLean, E.O., 105
 McNeill, J.D., 142
 Medlin, C.R., 83, 96–99
 Meirvenne, M.V., 154
 Metternicht, G., 122
 Miller, P.C.H., 83, 93
 Moore, M., 67
 Moraghan, J.T., 37
 Morgan, M.T., 164–165
 Morris, D.K., 104, 108, 110
 Mortensen, D.A., 82–83, 93, 99
 Mouazen, A.M., 163, 165
 Mueller, T.G., 104, 108, 110
 Muggleston, M.A., 83, 93

Muleer, T.G., 104–105
 Mulla, D.J., 83
 Multiple self-generated data layers,
 collocation, 185–197
 Myers, D.E., 104

N

Ng, H.Y.F., 3, 7
 Nissen, S.J., 88
 Nitrogen management, remote sensing,
 sugar beets, 35–48
 ground-based sensor, 44–46
 satellite images, 41–44
 Nordbo, E., 83, 99
 Nutrient variability, impact of human
 factors, 51–53

O

Olea, R.A., 104
 Oman, C.C., 88
 On-the-go soil strength sensing
 technology, variable-depth
 tillage assessment,
 163–183
 Oriade, C.A., 82–83, 93, 99

P

Paice, M.E.R., 83, 93
 Partial nutrient budgets, yield data,
 126–128, 130–131
 Peck, T.R., 127
 Pest management, U.S. Fish and Wildlife
 Service land, 1–34
 delivery potential factors, 22–28
 land-use data, 19
 pesticide application/properties, 22
 proximity data, 20–22
 soils data, 12–19
 Ping, J., 122–123, 185–186
 Plant, R.E., 122–123
 Pocknee, S., 83, 93
 Polygon, identification, weed
 management, 88
 Polygone, simulation, weed management,
 88

Precision agriculture, salinity maps, soil
 salinity mapping, 157–159

Predictions

 hand-drawn map predictions, site-
 specific weed management,
 92–96
 WeedSite, 92–96
 Production, yield data, information from,
 126, 129–130
 Productivity zones
 cleaning yield monitor data, 67
 exercise, 77–78
 file formats, 77
 gridding data, 67
 identifying, 69–74
 statistical calculations, 67–69
 yield monitor data, 65–79
 yield variability, zone impacts, 74

Profit consistency, information from yield
 data, 135–138

Profitability information from yield data,
 124–125, 128–129, 133–135

Program overview, WeedSite, 84–85

Proximity data, pest management,
 ArcView, 20–22

R

Rao, P.S.C., 3–4
 Raster interpolation, soil salinity
 mapping, 153–156
 Remenapp, H.E.H., 3, 7
 Remote sensing, nitrogen management,
 sugar beets, 35–48
 ground-based sensor, 44–46
 satellite images, 41–44
 Reuss, J.O., 37, 45
 Rew, L.J., 83, 93
 Reyniers, M., 122
 Rhoades, J.D., 142–143
 Rhode, W.A., 3
 Rixhon, L., 37
 Roberts, D.W., 83, 93
 Robinson, T.P., 122
 Rodriguez, R.R., 50
 Roel, A., 122–123
 Roeth, F.W., 88, 96
 Roose, E.J., 6

S

- Salinity mapping, 141–162. *See also* Soil salinity mapping
- Satellite images, nitrogen management, ArcView, sugar beets, 41–44
- Sawyer, J.E., 104
- Schepers, A.R., 122–123
- Schloeder, C.A., 104
- Schwab, E.B., 165
- Schweizer, E.E., 82, 88, 99
- Seelig, B.D., 3
- Shanahan, J., 45
- Sharpley, A.N., 6
- Shaw, D.R., 83, 96–99
- Shoemaker, H.E., 105
- Siefken, R.J., 192
- Simbahan, G.C., 122
- Sims, A.L., 37
- Simulation polygons, hand-drawn map predictions, site-specific weed management, 88
- Sirjacobs, D., 163, 165
- Site-specific weed management, hand-drawn map predictions, 81–101
 - accuracy, 96
 - benefits variability, 83
 - decision algorithms, 88–89
 - evaluation, 85–90
 - examples, 90–96
 - limitations, 96
 - polygons, identifying, 88
 - predictions, 92–96
 - program overview, 84–85
 - simulation polygons, predicting outcomes for, 88
 - site-specific strategies, 83
 - speed, 96
 - viewing results, 89–90
- Skopp, J., 50
- Smith
 - D.D., 5–7
 - L.J., 37
 - S.J., 6
- Soil salinity mapping, 141–162
 - ArcGIS, 141–162
 - contour maps, 156–157
 - coordinate system, 145–147
 - correlating salinity data, 147, 159–160
 - field boundary data, 145, 150
 - importing data, 148–152
 - layer properties, 150–152
 - map layout, 160–161
 - precision agriculture, using salinity map for, 157–159
 - raster interpolation, 153–156
 - salinity data, 144–145, 148–150
 - soil salinity assessment, 143–144
 - spatial analyses, 152–160
 - spatial analyst extension, 152–153
 - working environment, 147–148
- Soil sampling error reduction, historical management, 49–64
 - GIS application, 53–62
 - homesteads, impact of, 51–53
 - nutrient variability, impact of human factors, 51–53
- Soils data, pest management, ArcView, 12–19
- Southwestern Minnesota Farm Business Management Association, 124
- Sparrow, D.H., 82
- Spatial analyses, soil salinity mapping, 152–160
- Spatial analyst extension, soil salinity mapping, 152–153
- Speed
 - hand-drawn map predictions, site-specific weed management, 96
 - WeedSite, 96
- Srivastava, R., 104, 122, 153–154
- Statistical calculations, productivity zones, yield monitor data, 67–69
- Steckler, J.-P.G.A., 83, 93, 99
- Stewart, B.A., 5
- Sudduth, K.A., 142, 163–165
- Sugar beets, remote sensing, nitrogen management, 35–48
 - ground-based sensor, 44–46
 - satellite images, 41–44
- Sumali, H., 164–165
- Sun-Ok, C., 163–165
- Swinton, S.M., 88, 99

T

Taylor, H.M., 165
 Thylen, L., 67
 Tyler, D.A., 83, 93

U

UCD-SCPS, variable-depth tillage
 assessment, 163–183
 Unger, P.W., 165
 Upadhyaya, S., 164–165, 167
 U.S. Fish and Wildlife Service land, pest
 management, 1–34
 delivery potential factors, 22–28
 land-use data, 19
 pesticide application/properties, 22
 proximity data, 20–22
 soils data, 12–19

V

Van Wychen, L.R., 83
 Variability of nutrients, impact of human
 factors, 51–53
 Variable-depth tillage assessment
 on-the-go soil strength sensing
 technology, 163–183
 UCD-SCPS, 163–183
 Vencill, W.K., 83, 93
 Vieira, S.R., 154
 Viewing results, WeedSite, 89–90
 Vitosh, M.L., 105

W

Walker, T., 69
 Wallinga, J., 83, 93
 Walter, A.M., 83, 93, 99
 Warrick, A.W., 104
 Wauchope, R.D., 3
 WeedSite, 81–101
 accuracy, 96
 benefits variability, 83
 decision algorithms, 88–89
 evaluation, 85–90
 examples, 90–96
 limitations, 96

polygon identification, 88
 predictions, 92–96
 program overview, 84–85
 simulation polygones, predicting
 outcomes, 88
 site-specific strategies, 83
 speed, 96
 viewing results, 89–90
 Westfall, D.G., 50, 69
 Westra, P., 82, 88, 99
 Wicherek, S.P., 6
 Wicks, G.A., 88
 Wiens, D.W., 50, 69
 Wiles, L.J., 82, 88, 99
 Williams II, M.M., 83, 93, 99
 Wilson, R.G., 88
 Wischmeier
 D.A., 5–7
 W.H., 5, 7
 Working environment, soil salinity
 mapping, 147–148
 Wu, T.L., 3, 7
 Wyse-Pester, D.Y., 82–83, 93

Y

Yield data, 121–140
 cleaning yield monitor data, 67
 file formats, 77exercise, 77–78
 gridding data, 67
 identifying productivity zones, 69–74
 partial nutrient budgets, 126–128,
 130–131
 production, 126, 129–130
 productivity zones, 65–79
 profit consistency, 135–138
 profitability, 124–125, 128–129,
 134–135
 statistical calculations, 67–69
 yield variability, zone impacts, 74
 Yield variability, zone impacts
 productivity zones, yield monitor data,
 74

Z

Zhang, R., 104
 Zimmermann, N.E., 104

GIS Applications in Agriculture

GIS APPLICATIONS IN AGRICULTURE SERIES

The increased efficiency and profitability that the proper application of technology can provide has made precision agriculture the hottest developing area within traditional agriculture. The first single-source volume to cover GIS applications in agronomy, *GIS Applications in Agriculture* examines ways that this powerful technology can help farmers produce a greater abundance of crops with more efficiency and at lower costs.

Each chapter describes the nature of a problem, examines the purpose and scope of a GIS application, presents the methods used to develop the application, and then goes on to provide results and offer a conclusion as well as supporting information. When appropriate, the chapters present the underlying statistical approach for the GIS software that is used. The text also includes a CD-ROM featuring data sets and color maps produced by the use of GIS.

Concentrating more on the approach and less on the specific software, the authors describe the methods used to develop an application and discuss limitations to the algorithms and the programming code used. They then summarize the application in terms of what it does, how it works, its limitations, and its potential uses. The book provides a toolkit for the acquisition, management, and analysis of spatial data throughout the agriculture value chain.

7526

ISBN 0-8493-7526-6



9 780849 375262

**CRC Press**Taylor & Francis Group
an informa businesswww.taylorandfrancisgroup.com6000 Broken Sound Parkway, NW
Suite 300, Boca Raton, FL 33487270 Madison Avenue
New York, NY 100162 Park Square, Milton Park
Abingdon, Oxon OX14 4RN, UKwww.crcpress.com